Multimodality ImAging of Cardiovascular Dysfunction

Risk factors, diagnostics and treatment options

Bibi van Thiel

Multimodality ImAging of Cardiovascular Dysfunction

Risk factors, diagnostics and treatment options

Bibi van Thiel

To access the ePub, scan the following QR-code:
https://reader.ogc.nl/52705f8b-00bf-48d5-b22f-cc266ebd03ee.epub
wachtwoord = ImAgingCVD

Multimodality ImAging of cardiovascular dysfunction
Risk factors, diagnostics and treatment options

ISBN: 978-94-92683-56-4
Cover design: Heart watercolor art painting by Genefy Art ©
Layout and printed by: Optima Grafische Communicatie, Rotterdam, The Netherlands

Multimodality ImAging of Cardiovascular Dysfunction

Risk factors, diagnostics and treatment options

Multimodality ImAging
van Hart- en Vaat Dysfunctie
Risicofactoren, diagnostiek en behandelingsmogelijkheden

Proefschrift

ter verkrijging van de graad van doctor aan de
Erasmus Universiteit Rotterdam
op gezag van de rector magnificus
Prof.dr. H.A.P. Pols
en volgens besluit van het College voor Promoties.

De openbare verdediging zal plaatsvinden op
Dinsdag 4 Juli 2017 om 15.30 uur

door

Bibi Sherise van Thiel
geboren te Rotterdam

Erasmus University Rotterdam

PROMOTIECOMISSIE

Promotoren:	Prof.dr. R. Kanaar
	Prof.dr. A.H.J. Danser
Overige leden:	Prof.dr. H.J.M. Verhagen
	Prof.dr. D.J.G.M. Duncker
	Prof.dr. C.G. Schalkwijk
Copromotoren:	Dr. J. Essers
	Dr. I. van der Pluijm

Financial support by the Dutch Heart Foundation and the Dutch Kidney Foundation for the publication of this thesis is gratefully acknowledged.
Additional financial support for publication of this thesis was generously provided by the Erasmus MC

TABLE OF CONTENTS

PART I

INTRODUCTION

CHAPTER I

GENERAL INTRODUCTION AND SCOPE OF THIS THESIS

GENERAL INTRODUCTION AND SCOPE OF THIS THESIS

Cardiovascular diseases are a major cause of mortality worldwide.[1] Cardiovascular disease includes all diseases of the heart and circulation, including coronary diseases, such as angina and myocardial infarction and other diseases like stroke, heart failure, hypertension (high blood pressure), and aortic aneurysm formation. The underlying mechanisms vary depending on the disease in question. In this thesis, the role of DNA damage, atherosclerosis and the renin angiotensin system, factors that modulate cardiovascular damage and disease, are investigated and discussed.

DNA damage and aging

Aging is an inevitable part of life and unfortunately also a major risk factor for health complications and disease. As such, the prevalence of cardiovascular disease increases tremendously with age.[2] During aging, diverse detrimental changes in cells and tissues occur and manifest differently in each cell type. These series of structural, architectural and compositional modifications also take place in the heart and the vasculature with age, which will eventually affect cardiovascular performance and sets the stage for the onset of cardiovascular disease including heart failure, myocardial infarction, hypertension, stroke and aneurysm formation.

One of the principal causes of aging is the accumulation of DNA damages over time. Both endogenous (internal) and exogenous (external) agents can affect our DNA, resulting in irreversible DNA damage. Normally, these damages are recognized and can be repaired by different DNA repair systems. However, if DNA repair is hampered this can have serious consequences for cells such as cell cycle arrest, cellular senescence and apoptosis, processes which are known to be involved in the development of cardiovascular disease. One of these DNA repair systems is the Nucleotide Excision Repair (NER) pathway.[3] Four important steps in this system are damage recognition, helix unwinding, dual incision, and repair ligation. Key proteins that are involved in the dual incision step are the DNA endonucleases ERCC1/XPF and XPG.

Ercc1 mouse model of accelerated aging

The ERCC1 (Excision Repair Cross Complementation group 1) protein, along with its binding partner XPF (Xeroderma Pigmentosum group F), forms an endonuclease that is involved in different DNA pathways; NER, interstand crosslink repair and homologous recombination repair. The ERCC1-XPF protein complex is responsible for excision of various types of DNA lesions at the 5'end of the damage. The XPF protein contains the endonuclease catalytic activity, and ERCC1 is necessary for DNA binding. Human patients and mouse mutants with mutations in the ERCC1-XPF complex can exhibit xeroderma

pigmentosum, severe Cockayne syndrome, XFE progeroid syndrome, Cerebro-oculo-facio-skeletal syndrome and/or Fanconi anaemia features.[4]

The *Ercc1*$^{d/-}$ mutant mouse is one of the most widely studied mouse models of accelerated aging, containing one knockout allele and one protein truncating mutation, via which the last seven amino acids at the C-terminus of the Ercc1 protein are deleted. These mice have a severely compromised, but not completely inactive, DNA repair capacity and exhibit premature death (with a lifespan of ~24 weeks).[5] During their life they experience a remarkably wide range of pathological, physiological and behavioral features related to accelerated aging such as progressive neurodegeneration (e.g. dementia, ataxia, priapism, hearing and vision loss), osteoporosis, kyphosis, sarcopenia and retarded growth. Moreover, *Ercc1*$^{d/-}$ mutant display accelerated age-dependent vasodilator dysfunction, increased vascular stiffness, increased blood pressure and vascular cell senescence.[6] Thus, the *Ercc1*$^{d/-}$ mouse model can be used to study the aging process due to endogenous DNA damage and its effects on the heart and vessels.

Fat deposition (e.g. atherosclerosis)

A fatty streak is the first, by eye, visible lesion in the development of atherosclerotic disease. These fatty streaks, also called plaques, are caused by accumulation of fat, cholesterol and other substances. The build-up of these plaques in and around the vasculature is called atherosclerosis. These plaques can cause thickening and stiffening of the vessel wall. Over time, these plaques can become so thick that they can block the inside of the artery and interfere with normal blood flow. Some of the diseases that could develop as a result of this plaque build-up include coronary heart disease, carotid artery disease, peripheral artery disease and chronic kidney disease. Moreover, it is thought that atherosclerosis and aneurysms are highly associated, as atherosclerosis is frequently observed in the aortic wall of patients with abdominal aortic aneurysms. It should be noted that many of the risk factors for aortic aneurysms are similar to those for atherosclerosis, including smoking, hypertension, inflammation and family history. However, in some patients atherosclerosis leads to aortic narrowing, while in others it leads to aortic dilatation; consequently, there is much debate as to whether atherosclerosis is a causative factor in aneurysm formation.

Aneurysmal Fibulin-4 mouse model

One of the mouse models that can be used to study the relation between atherosclerosis and aneurysms formation is the Fibulin-4 mouse model. Fibulin-4 is one of the seven members of extracellular matrix proteins that play an important role in elastic fiber and collagen assembly and function. Mice with a reduced expression of Fibulin-4 (indicated as 'Fibulin-4^{R}', where R stands for reduced expression) display defects in the aortic wall, which could lead to aneurysm formation. Hence, mice with only 25% expression of Fibuline-4 (homozygous Fibulin-4$^{R/R}$ mice) develop aortic aneurysms, while mice with a 50%

expression of Fibulin-4 (heterozygous Fibulin-$4^{+/R}$ mice) develop minor aortic abnormalities.[7] These heterozygous Fibulin-$4^{+/R}$ mice do not yet develop aneurysms spontaneously but are susceptible to develop aneurysms upon exposure to different stressors such as age and high fat diet, and thus are a good model to test the effect of risk factors on aneurysm formation.

The renin-angiotensin system

The renin angiotensin system (RAS) has emerged as one of the most important links in the pathophysiology of many types of cardiovascular diseases.[8] Besides its classical regulatory effects on blood pressure and sodium homeostasis, the RAS is involved in the regulation of vascular tone and remodeling of the vessel wall. Dysregulation and overproduction of the RAS hormone angiotensin II (Ang II), the main peptide of the RAS, is believed to contribute to the initiation and progression of several cardiovascular diseases. Historically, Ang II in circulating blood was seen as a regulatory hormone involved in the regulation of blood pressure, aldosterone release and sodium reabsorption. Yet, now there is also ample evidence that locally produced Ang II promotes cell proliferation, apoptosis, fibrosis, oxidative stress and inflammation, processes known to contribute to remodeling of the vasculature.[9] It is generally believed that the local production of Ang II is involved in the pathogenesis and progression of atherosclerosis and aneurysm disease, and that inhibition of the RAS has beneficial therapeutic effects on the vasculature, possibly even on aortic aneurysms. Moreover, since Ang II signaling affects the aging process, while many vascular diseases are age-related, it is important to understand how the RAS is regulated during normal aging. Although we know that the systemic RAS is suppressed during aging, the activity of tissue RAS in the elderly is not fully understood yet and needs to be further explored.

Scope of this thesis

Cardiovascular diseases are life-threatening and their occurrence increases with age. Most often there is not one cause for disease, but instead several risk factors are involved that increase the risk of development and progression of disease. In this thesis, important factors are explored that play a role in cardiovascular damage and disease, such as DNA damage, atherosclerosis and the RAS. **Chapter 2**, part I, starts with describing the general structure and cell biology of the vessel wall. In **Chapter 3** the focus lies on the components that are under the influence of the RAS and that contribute to the development and progression of vascular disease; e.g. extracellular matrix defects, atherosclerosis and aging.

In part II, we studied the effect of two risk factors, atherosclerosis and increased RAS signaling, on the development and progression of aortic aneurysms. In the clinic it is known that in some patients atherosclerosis leads to aortic narrowing, while in others it leads to

aortic dilatation. Hence, a better understanding on the differences in pathogenesis leading to both atherosclerosis and aneurysm formation is required. Therefore, in **Chapter 4** the relation between atherosclerosis and aortic aneurysms formation was investigated, with the intention to find molecular pathways and markers that differentiate these two diseases. Furthermore, it has been well established that activation of the RAS plays an important role in the physiology and pathophysiology of the cardiovascular system and it has been suggested that over activation of the RAS promotes the development of aortic aneurysms. In **Chapter 5** the therapeutic potential of the RAS blocker losartan, an angiotensin II type 1 (AT_1) receptor, on aneurysm progression was examined.

In part III, the effect of defective DNA repair and the consequential aging process on the development of cardiovascular damage is investigated. **Chapter 6** discusses the effect of accelerated aging on vascular function and morphology, as well as the effect of dietary restriction, known to induce an anti-aging response, on the vasculature. In **Chapter 7**, the effect of aging on the heart was characterized and the use of fluorescent molecular markers for the early detection of cardiovascular disease was tested.

In part IV, the role of the RAS was investigate under various conditions. Though it is suggested that changes in the reactivity and/or responsiveness of the systemic RAS occur with aging, little is known about the regulation and activity of the RAS within local tissues during aging. Yet, this knowledge is required to successively treat and/or prevent renal disease in the elderly. In **Chapter 8** the use of the renin activatable near-infrared fluorescent probe ReninSense680™ was tested to facilitate non-invasive imaging of renin activity *in vivo*. In addition, the intrarenal renin activity was determined in accelerated aging *Ercc1*$^{d/-}$ mice with age-related kidney pathology. Besides the traditional role of the RAS in blood pressure regulation, it is hypothesized that certain RAS components are synthesized in the brain and that this so-called brain RAS is relevant in the regulation of the cardiovascular system. However, the concept of a brain RAS has been controversial and this controversy continues to this day. Therefore, in **Chapter 9** the occurrence of (pro) renin in the brain was re-evaluated. Inhibition of the RAS with aliskiren, a potent renin inhibitor, is hampered by diarrhea at high doses and thus no maximum effect of renin inhibition in humans has been established. Accordingly, in **Chapter 10** the use of VTP-27999, a novel renin inhibitor -without major side-effects at high doses- was examined in order to establish the maximum effect of renin inhibition, focusing on the kidney.

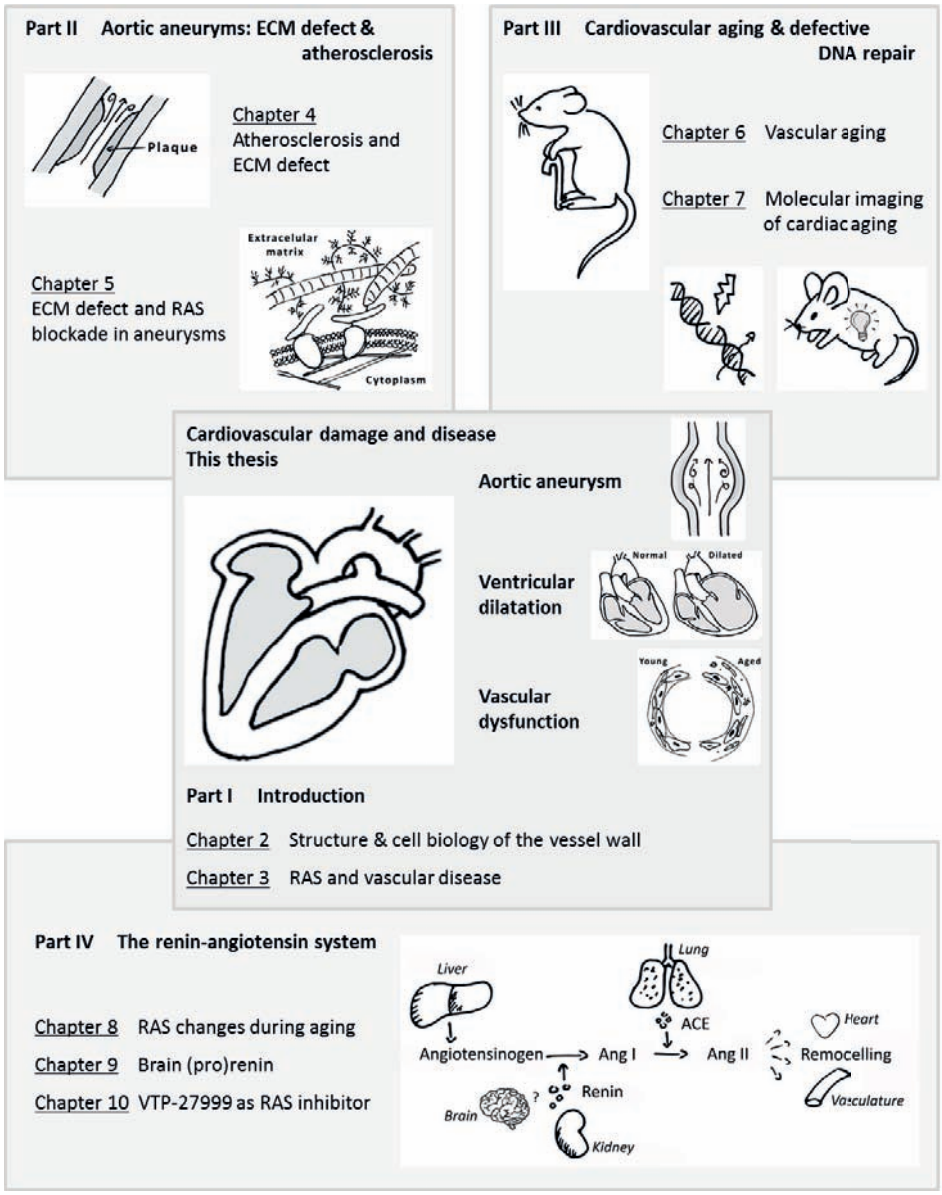

Figure 1. Schematic overview of topics and relationship discussed in this thesis.

REFERENCES

1. World Health Organisation. Cardiovascular diseases (cvds). Sept. 2016
2. Niccoli T, Partridge L. Ageing as a risk factor for disease. *Curr Biol*. 2012;22:R741-752
3. Marteijn JA, Lans H, Vermeulen W, Hoeijmakers JH. Understanding nucleotide excision repair its roles in cancer and ageing. *Nat Rev Mol Cell Biol*. 2014;15:465-481
4. Niedernhofer LJ, Garinis GA, Raams A, Lalai AS, Robinson AR, Appeldoorn E, Odijk H, Oostendorp R, Ahmad A, van Leeuwen W, Theil AF, Vermeulen W, van der Horst GT, Meinecke P, Kleijer WJ, Vijg J, Jaspers NG, Hoeijmakers JH. A new progeroid syndrome reveals that genotoxic stress suppresses the somatotroph axis. *Nature*. 2006;444:1038-1043
5. Dolle ME, Kuiper RV, Roodbergen M, Robinson J, de Vlugt S, Wijnhoven SW, Beems RB, de la Fonteyne L, de With P, van der Pluijm I, Niedernhofer LJ, Hasty P, Vijg J, Hoeijmakers JH, van Steeg H. Broad segmental progeroid changes in short-lived ercc1(-/delta7) mice. *Pathobiol Aging Age Relat Dis*. 2011;1
6. Durik M, Kavousi M, van der Pluijm I, Isaacs A, Cheng C, Verdonk K, Loot AE, Oeseburg H, Bhaggoe UM, Leijten F, van Veghel R, de Vries R, Rudez G, Brandt R, Ridwan YR, van Deel ED, de Boer M, Tempel D, Fleming I, Mitchell GF, Verwoert GC, Tarasov KV, Uitterlinden AG, Hofman A, Duckers HJ, van Duijn CM, Oostra BA, Witteman JC, Duncker DJ, Danser AH, Hoeijmakers JH, Roks AJ. Nucleotide excision DNA repair is associated with age-related vascular dysfunction. *Circulation*. 2012;126:468-478
7. Hanada K, Vermeij M, Garinis GA, de Waard MC, Kunen MG, Myers L, Maas A, Duncker DJ, Meijers C, Dietz HC, Kanaar R, Essers J. Perturbations of vascular homeostasis and aortic valve abnormalities in fibulin-4 deficient mice. *Circ Res*. 2007;100:738-746
8. Ferrario CM. Role of angiotensin ii in cardiovascular disease therapeutic implications of more than a century of research. *J Renin Angiotensin Aldosterone Syst*. 2006;7:3-14
9. van Thiel BS, van der Pluijm I, te Riet L, Essers J, Danser AH. The renin-angiotensin system and its involvement in vascular disease. *Eur J Pharmacol*. 2015;763:3-14

CHAPTER 2

STRUCTURE AND CELL BIOLOGY OF THE VESSEL WALL

Bibi S. van Thiel[1,2,3], Ingrid van der Pluijm[1,2], Roland Kanaar[1,4], A.H. Jan Danser[3], Jeroen Essers[1,2,4]

[1]Department of Molecular Genetics, Cancer Genomics Center Netherlands, [2]Department of Internal Medicine, Division of Vascular Medicine and Pharmacology, Department of Vascular Surgery, [3]Department of Pharmacology, [4]Department of Radiation Oncology, Erasmus Medical Center, Rotterdam, The Netherlands.

(ESC Textbook of Vascular Biology; Section 1: Foundation of the vascular wall; Chapter 1)

INTRODUCTION

A healthy heart pumps about 6000-8000 liters of blood around the body each day. Blood is carried through the body via blood vessels. The blood vessels form a closed system that begins and ends at the heart. In mammals blood circulates through two separate circuits: the pulmonary circuit and the systemic circuit (Fig. 1.1).

- Pulmonary circuit: the right ventricle of the heart pumps blood into the lungs, where waste gases are exchanged for oxygen, after which the blood is transported back to the left atrium of the heart.
- Systemic circuit: the left ventricle pumps oxygenated blood to all tissues and organs of the body via the aorta after which deoxygenated blood is transported back to the right atrium of the heart.

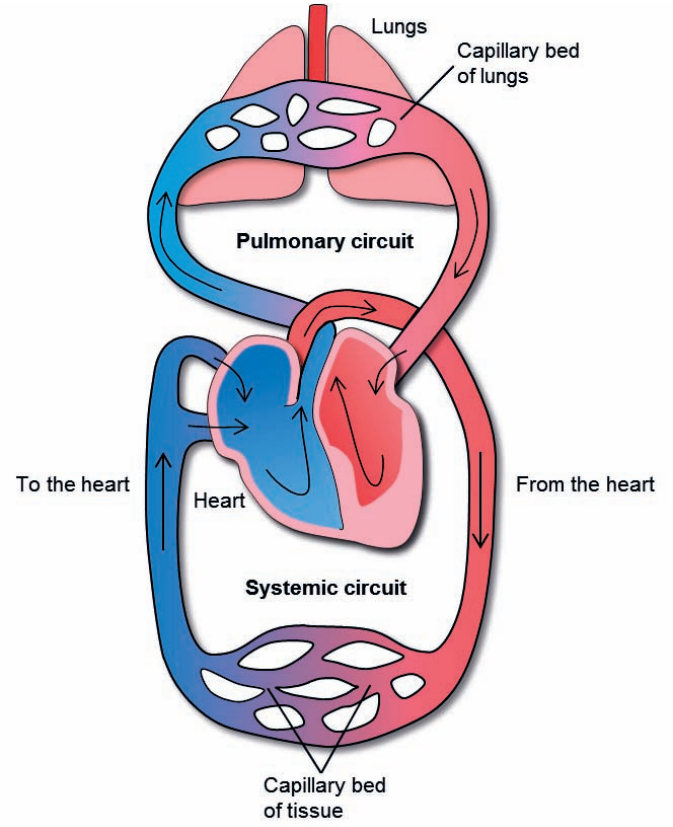

Figure 1.1: Schematic overview of the cardiovascular circulatory system. Note that arteries and oxygenated blood are depicted in red and veins and deoxygenated blood are depicted in blue.

Figure 1.1 gives a simplified overview of the blood flow through the body, where deoxygenated blood is depicted in blue and oxygenated blood is depicted in red. Note that somewhat counterintuitively, deoxygenated blood does not refer to blood without oxygen. Rather, it refers to a lower oxygenation grade than that of oxygenated blood because a certain amount of oxygen has been delivered to tissues. As a result, deoxygenated blood still contains about 75% of oxygen compared to oxygenated blood.

A well-functioning cardiovascular system is essential for all vertebrates. The blood vessels are a conduit for a variety of molecules, such as nutrients, oxygen and waste products, to and from all parts of the body. Blood vessels have several main functions:

1. Distribution of blood containing nutrients (e.g. glucose and amino acids), oxygen (O_2), water and hormones to all the tissues and organs of the body.
2. Removal of metabolic waste products and carbon dioxide (CO_2) from the tissues to the excretory organs and the lungs, respectively.
3. Regulation of blood pressure.
4. Maintenance of constant body temperature (thermoregulation).

Distribution of nutrients, gases and removal of waste products

The primary function of blood vessels is to transport blood around the body, thereby supplying organs with the necessary O_2 and nutrients. At the same time, the vessels remove waste products and CO_2 to be processed or removed from the body.

Regulation of blood pressure

Blood vessels control blood pressure by changing the diameter of the vessel through either constriction (vasoconstriction) or dilation (vasodilation). Variations in blood pressure occur in various parts of the circulation depending on the diameter of the vessel.

Maintenance of constant body temperature (thermoregulation)

Blood vessels help maintain a stable body temperature by controlling the blood flow to the surface area of the skin. To prevent overheating, blood vessels near the surface of the skin can dilate, allowing excessive heat of the blood to be released to the surroundings. In contrast, blood vessels near the skin's surface can constrict, reducing heat loss through the skin when needed under cold circumstances.

STRUCTURE OF THE VESSEL WALL

Blood vessels need to be well-constructed, as they have to withstand the pressure of circulating blood through the body every day. The vessel wall is arranged in three distinct layers,

termed tunica: an inner layer (tunica intima), a middle layer (tunica media) and an outer layer (tunica adventitia) (Fig. 1.2). These layers mainly contain endothelial cells, vascular smooth muscle cells and extracellular matrix, including collagen and elastic fibers.

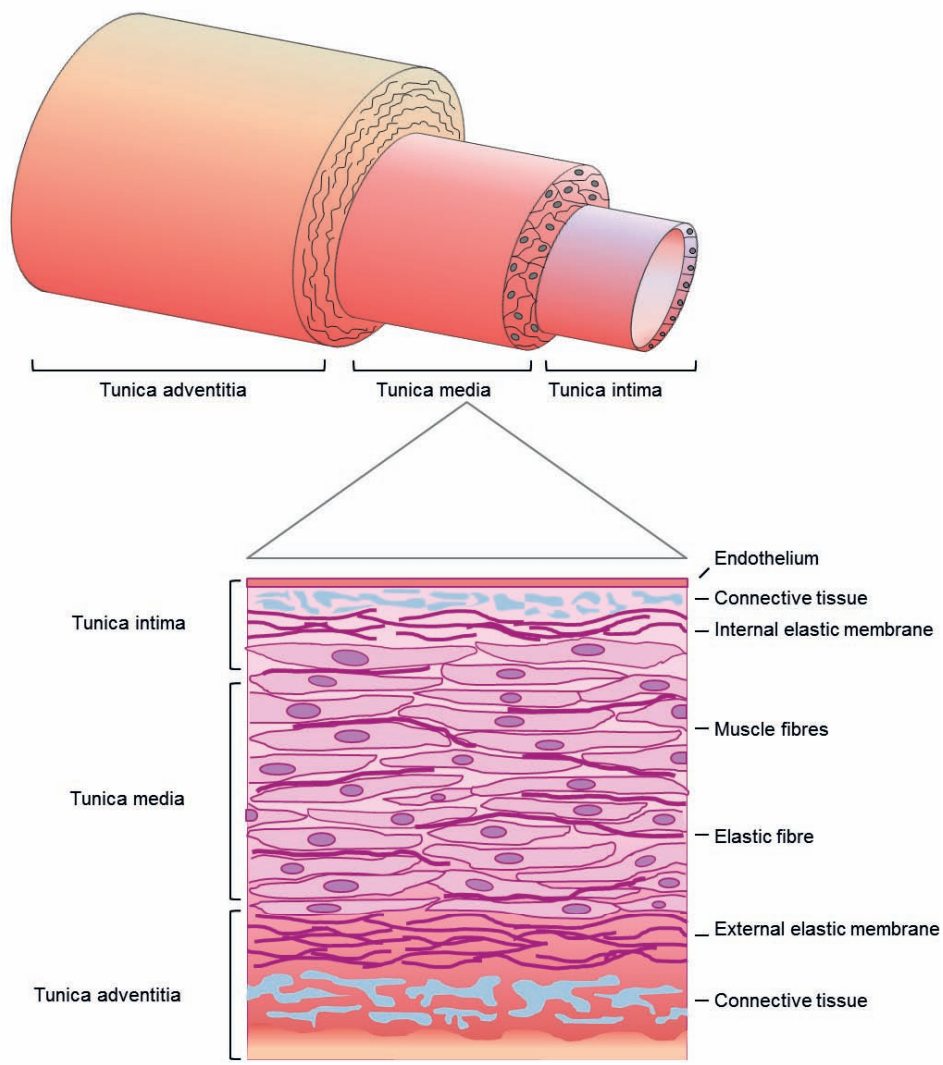

Figure 1.2: General structure of the vessel wall, showing the tunica intima, tunica media and tunica adventitia and a close-up depicting the different structures within these layers.

Tunica intima

The tunica intima ('inner coat') is the innermost layer of a blood vessel. In healthy vessels, it consists of a thin single layer of endothelial cells, which are in direct contact with the blood in the lumen, as well as a subendothelial layer made-up mostly by connective tissue. The single layer of endothelial cells, called endothelium, has a smooth surface that minimizes the friction of the blood as it moves through the lumen. The endothelium plays a role in vascular permeability, inflammation, coagulation and vascular tone, which refers to the maximal degree of contraction by vascular smooth muscle cell relative to its maximally dilated state. The subendothelial layer, also called basal lamina, provides a physical support base for the endothelial cells and flexibility of the vessel for stretching and recoil. Moreover, it guides cell and molecular movement during tissue repair of the vessel wall. The tunica intima is the thinnest layer of the blood vessel and minimally contributes to the thickness of the vessel wall. In arteries and arterioles, the outer margin of the tunica intima is separated from the surrounding tunica media by the *internal elastic membrane*, a thick layer of elastic fibers. The internal elastic membrane provides structure and elasticity to the vessel and allows diffusion of materials through the tunica intima to the tunica media. Microscopically, the lumen and the tunica intima of an artery appear wavy because of the partial constriction of the vascular smooth muscle cells in the tunica media, the middle layer of the blood vessel, whereas the tunica intima of a vein appears smooth.

Tunica media

The middle layer, tunica media, is considered to be the muscular layer of the blood vessel as it primarily contains circularly arranged smooth muscle fibers together with extracellular matrix, mostly elastin sheets. It is often the thickest layer of the arterial wall and much thicker in arteries than in veins. The tunica media provides structural support as well as vasoreactivity (the ability of blood vessels to contract or to relax in response to stimuli) and elasticity to the blood vessel. The primary role of the vascular smooth muscle cells is to regulate the diameter of the vessel lumen. Concerning blood pressure regulation, the vascular smooth muscle cells in the tunica media can either contract causing vasoconstriction, or relax causing vasodilation. During vasoconstriction, the lumen of the vessel narrows, leading to an increase in blood pressure, whereas vasodilation widens the lumen allowing blood pressure to drop. Both vasoconstriction and vasodilation are partially regulated by nerves (nervi vasorum). The tunica media is separated from the tunica adventitia by a dense elastic lamina called the *external elastic membrane*. Under the microscope, these laminae appear as wavy lines. This structure is usually not apparent in small arteries and veins.

Tunica adventitia

The tunica adventitia (also known as tunica externa) is the outermost layer of the vessel wall, surrounding the tunica media. The adventitia is predominantly made-up by extracel-

lular matrix (collagen and elastic fibers), nutrient vessels (vasa vasorum) and autonomic nerves (nervi vasorum). Fibroblasts and numerous macrophages are also present in this layer. The tunica adventitia is often the thickest layer in veins, sometimes even thicker than the tunica media in larger arteries. The tunica adventitia helps to anchor the vessel to the surrounding tissue and provides strength to the vessels as it protects the vessel from overexpansion.

Vasa vasorum

Characteristic of the adventitial layer is the presence of small blood vessels, called the vasa vasorum. The vasa vasorum supplies blood and nourishment to the tunica adventitia and outer parts of the tunica media, as these layers are too thick to be nourished merely by diffusion from blood in the lumen, and removes 'waste' products. Because of the thick and muscular walls of the arteries, the vasa vasorum are more frequent in the wall of arteries than in the wall of veins.

COMPONENTS OF THE VASCULAR WALL

The vascular wall is composed of many cell types and constituents that influence the diameter and functional control of the vessel wall. Several main cell types include endothelial cells, vascular smooth muscle cells and immune cells (Fig. 1.3). Interaction between these

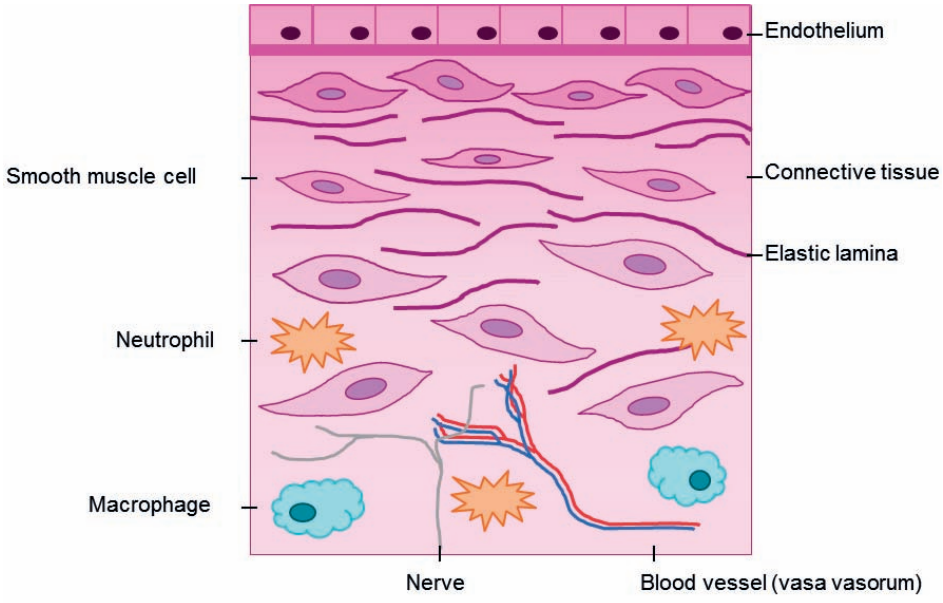

Figure 1.3. Summary of the major components of the vessel wall.

cell types allows the vessel to adapt to alterations in pressure and various physical stimuli by either dilation or contraction.

Endothelium

Vascular endothelial cells lining the entire circulatory system, from the heart and arteries to the small capillary beds, are in direct contact with blood. They form a single-cell layer (monolayer) called the endothelium, which has been estimated to cover a surface area of more than 1000 m^2 in humans. The morphological shape of endothelial cells varies across the circulatory system (Flaherty et al. 2012). In large arteries, endothelial cells are aligned and elongated in the direction of the blood flow, whereas in region of disturbed flow, e.g. near bifurcations, endothelial cells are more round and do not align in a specific direction. Varying among the vascular tree, endothelial cells are between 0.2 to 2.0 µm thick and 1 to 20 µm long. They are joined together by tight junctions, which restrict the transportation of large molecules across the endothelium. Endothelial cells are active contributors to a variety of vessel-related activities, including permeability, vascular tone and hemostasis. Vascular endothelial cells have several important functions (Box 1.1).

Box 1.1 Vascular endothelial cell function

1. Providing a semi-permeable barrier between the vessel lumen, containing the blood, and the surrounding tissues. Selective material, electrolytes, macromolecules, fluid and cells can pass the barrier entering or leaving the bloodstream.
2. Regulating vascular tone, by secreting vasoactive substances that stimulate the smooth muscle cells of the tunica media to relax or contract, thus widening or narrowing the vessel.
3. Modulating cellular adhesion and inflammation of the vasculature, as endothelial cells regulate lymphocyte and leucocyte adhesion and transendothelial migration, from the bloodstream across the barrier into the vessel wall, by expression of surface adhesion molecules.
4. Modulating haemostasis and coagulation. Under normal conditions, endothelial cells express a wide variety of non-thrombogenic factors that maintain blood fluidity and help prevent inappropriate blood clotting.
5. Involved in the formation of new blood vessels (angiogenesis). Angiogenesis is in part regulated by the endothelial cell, which is important in wound healing.

The endothelium has a strategic position in the vessel wall, right between the circulating blood and the vascular smooth muscle cell. From this position, the endothelium plays a vital role in controlling vascular function, as it is able to respond to mechanical and hormonal signals and receive information from cellular constituents of the vessel wall. Endothelial cells are highly dynamic as they need to interpret changes in blood composition and mechanical changes, and respond properly to several stimuli, either physical or chemical, by producing a variety of factors that contribute to the control of vascular tone, vascular inflammation, cellular adhesion, hemostasis and coagulation. For instance, the endothelium serves as a semi-permeable barrier, restricting and controlling the move-

ment of fluids, molecules and cells across the blood vessel wall. This movement across the endothelial lining can occur via different mechanisms, either through the endothelial cells (transcellular) or by passing the junction between two adjacent endothelial cells (paracellular). The permeability of the barrier can be altered in response to specific stimuli that act on endothelial cells. Also, endothelial cells themselves can secrete different vasoactive substances that influence the activity of the underlying vascular smooth muscle cell, and thereby the contractile state of the vessel. For instance, endothelial cells can secrete nitric oxide which causes the vascular smooth muscle cells to relax, consequently leading to vasodilation. Moreover, endothelial cells tightly regulate the expression of adhesion molecules on their surface. These adhesion molecules not only modulate cell migration but are also important in response to local injury, as platelets and other inflammatory cells are recruited to the site of damage in need of defense or repair. Furthermore, endothelial cells are required to maintain blood fluidity and prevent thrombus formation. They bind and display tissue factors that have anti-coagulant properties thereby preventing the initiation of coagulation.

Injury and dysfunction of the endothelium directly or indirectly plays a vital role in the initiation and development of most of human vascular diseases. Endothelial dysfunction not only leads to an imbalance between vasoconstriction and vasodilation but also causes coagulation disorders and can be involved in the malignant growth of tumors. It is also involved in numerous other physiological and pathological conditions such as hypertension, septic shock, diabetes and hypercholesterolemia. Moreover, endothelial dysfunction is seen as the initial step in the atherosclerotic process.

Vascular smooth muscle cells

Vascular smooth muscle cells are the most prominent cell type of an artery and, depending on the size of the artery, may comprise several layers. Vascular smooth muscle cells are typically 2 to 5 µm in diameter, and vary from 100 to 500 µm in length. Yet, as the vascular smooth muscle cells can either relax or contract, their actual length depends on the physiological conditions and functioning of the cell. The vascular smooth muscle cells exert different functions, which translates into two different phenotypes of the vascular smooth muscle: contractile or synthetic. The contractile smooth muscle cells are long spindle-shaped cells that contain a single centrally positioned elongated nucleus, whereas the synthetic vascular smooth muscle cell are less elongated and have a more cobblestone morphology. Each smooth muscle cell is enclosed by a variable amount of extracellular matrix, containing collagen, elastin and various proteoglycans. Smooth muscle cells are arranged in different orientations, either circumferentially or helically, along the longitudinal axis of the vessel. Smooth muscle cells are connected to each other by tight- and gap-junctions. These junctions permit the transfer of signaling molecules between cells and increase the tensile strength of the medial layer, respectively, allowing the control

of the diameter of the vessel. Smooth muscle cell are normally quiescent cells that do not divide. However, damage to the vessel wall can drive the smooth muscle cells into a proliferative state in which they will divide and migrate.

In the artery, almost all smooth muscle cells are present in the tunica media. The primary function of smooth muscle cells is to regulate the diameter of the vessel lumen, as it directly controls vessel tone and regulates blood pressure by either contraction or relaxation. In the small arteries (less than 300 μm in diameter) and veins, contraction of the vascular smooth muscle cell is responsible for the regional distribution of the blood flow as it gives a reduction in lumen diameter and thereby increases vascular resistance, leading to a higher blood pressure. Vasoconstriction in the larger arteries has a different hemodynamic effect and mostly affects the stiffness (compliance) of the blood vessel, increasing the impedance to move blood through the artery.

Regulation of the vascular diameter by activation/deactivation of vascular smooth muscle cells is primarily under control by the autonomic nerves in the adventitial layer that act on specific receptors present on the outside of vascular smooth muscle cell. Yet, other locally produced and blood-borne factors can also act directly on the vascular smooth muscle cell and thus play an important role in its function. Smooth muscle cell contraction can be initiated by electrical, chemical or mechanical stimuli. Contractility of smooth muscle cells is controlled by actin and myosin filaments of the cytoskeleton, which make up a substantial portion of the cytoplasm of smooth muscle cells. Besides contractility, vascular smooth muscle cells also perform other functions such as migration, proliferation, proinflammatory and secretory, responses that become progressively important during vessel remodeling, injury and disease. For example, the smooth muscle cells produce a variety of extracellular matrix components, including collagen and elastin. Activated vascular smooth muscle cells also secrete matrix metalloproteinases (MMPs), which facilitate extracellular matrix remodeling. The ratio between vascular smooth muscle cells and the amount of extracellular matrix determines the overall mechanical properties and structural integrity of the vessel. The phenotype of the vascular smooth muscle cell can range from contractile to synthetic. These two phenotypes of smooth muscle cells not only differ in morphology but also in expression levels of different genes and their proliferative and migratory properties. Contractile smooth muscle cells are most often quiescent whereas synthetic smooth muscle cells have a high proliferation and migratory rate. The vascular smooth muscle cells can switch between these two phenotypes in response to changes in environmental cues, therefore these cells are not only important in short-term regulation of the lumen diameter but also in long-term adaptation of the vessel through structural remodeling.

There is clear evidence that vascular smooth muscle cells are involved in the pathogenesis of several vascular diseases, including atherosclerosis, restenosis, hypertension,

asthma and vascular aneurysms. Upon vascular injury, the smooth muscle cells undergo a phenotypic switch from contractile to synthetic, which most often includes increased proliferation, migration to the site of damage and increased excretion of extracellular matrix proteins. These characteristics play an important role in vascular repair, however, when occurring in high degrees, it predisposes the cell to acquire characteristics that contribute to the development of vascular diseases. The most acknowledged disease, in which smooth muscle cells play a key role, is atherosclerosis. However, the precise role of smooth muscle cells in atherosclerotic disease progression most likely depends on disease stage, as smooth muscle cells play a disadvantageous role in lesion development and progression, whereas they have a beneficial role in stabilizing the fibrous cap and consequently prevent plaque rupture.

Pericytes

Pericytes are the contractile cells of the capillaries and venules, whereas vascular smooth muscle cells are the contractile cells of other blood vessels (arteries, arterioles and veins). The size and morphology of pericytes greatly depends on location and type of vessel, and may be irregular in a single vessel. Generally, they have an elongated shape with a prominent round nucleus, and are surrounded by basal lamina material that is continuous with the basement membrane of the tunica intima. These pericytes are wrapped around the endothelial cells on the luminal side of the basement membrane. Pericytes have been associated with regulating capillary blood flow and stabilization of microvessels.

Cytoskeleton proteins

Cytoskeletal proteins are structural elements surrounding the cell membrane and are important to maintain cellular shape and integrity. These proteins play an active role in the interaction between blood vessels and the surrounding environment. Key cytoskeleton proteins include actin filaments, microtubules and intermediate filaments. Actin filaments are important in cell-cell control and cell-matrix interactions as they can bind to plasma membrane proteins. Actin filaments surrounding the endothelial cell are therefore involved in fluid and molecule exchange between the tissue and the circulating blood, by tightly regulating the vascular barrier. Furthermore, actin filaments are involved in cell motility, particular in the contraction of the vessel wall through association with the motor protein myosin. As such, when vascular smooth muscle cells become activated, the cytoskeleton proteins actin and myosin rapidly reorganize, creating membrane bound, parallel-organized units termed 'stress fibers'. In this complex, myosin slides along the actin filaments, which produces an increased intracellular tension leading to contraction of the cell. The microtubules not only support the cellular structure, but also are involved in cell division, as they facilitate the formation of spindles during mitosis. Intermediate

filaments appear to have a structural role in maintaining cellular integrity but might also provide an anchoring for contractile proteins.

Vascular extracellular matrix

The extracellular matrix is a highly-organized network of proteins containing collagen and elastin fibers and a loose network of proteoglycans. Foremost, the extracellular matrix provides structural support and elasticity to the vessel wall, keeping cells in place and allowing adaptation of the vessel wall to high blood pressure. Endothelial cells of the tunica intima, vascular smooth muscle cells of the tunica media and fibroblasts of the tunica adventitia all produce extracellular matrix proteins that have a different function in each tunica. The extracellular matrix proteins of the tunica intima make up the sub-endothelial basement membrane, which provides flexibility of vessels for stretching and recoil, whereas the extracellular matrix of the tunica media is responsible for strength and stretch of the vessel wall, as well as for transmission of muscle contraction. The tunica adventitia is made up principally by extracellular matrix, and contains a limited number of cells. This layer adds further strength to the vessels wall. Additionally, the extracellular matrix provides specific informational cues to vascular cells, thereby regulating cellular adhesion, proliferation, differentiation and migration.

Collagen

Physical properties of the blood vessel wall largely depend on collagen fibers. These collagen fibers provide a supporting framework that anchors smooth muscle cells in place. When internal pressures are high, the collagen network becomes rigid, limiting elasticity of the vessel wall. Collagen types I, III, and IV are present in the adventitia, tunica media and basement membranes, respectively. Veins tend to have a higher collagen content than arteries. Once blood vessels start to lose their collagen, tiny ruptures can occur in the vessel wall.

Elastin

Elastin provides vessels with the ability to stretch and recoil in response to hemodynamic forces resulting from alterations in blood pressure. Many elastin molecules are cross-linked and connected to each other and other molecules, including microfibrils, fibulins and collagen, to form an elastic fiber. These elastic fibers allow the vessels to expand during the contractile phase of the heart and then recoil during the filling phase of the heart, keeping the blood flowing forward. These elastic fibers are mainly found in the tunica media of arteries, where smooth muscle cells and collagen fibers are present between these elastic layers. Depletion of elastin is often due to destruction rather than reduced production.

Integrity of the extracellular matrix is essential to maintain both physical and biological properties of the vessel, as changes in the extracellular matrix affect the local environment that vascular cells are embedded in. As a result, cellular adhesion, prolif-

eration, migration, differentiation, and gene expression of several vascular cells will be affected. Moreover, disruption and/or deletion of these extracellular matrix proteins has deleterious effects on the structure and function of vessels, as it contributes to weakening of the vessel wall. Maintaining a proper balance between the different matrix components depends on new synthesis of matrix proteins and on matrix degradation by enzymes, such as MMPs. An imbalance of extracellular matrix proteins in favor of matrix degradation is for instance seen in vascular diseases like aneurysms, where it leads to vessel wall rupture, and atherosclerosis, where it is involved in plaque destabilization.

Infiltrating immune cells

Endothelial cells and vascular smooth muscle cells are able to produce a variety of immune and inflammatory mediators, such as tumor necrosis factor-α (TNF-α), interleukins (IL), platelet-derived growth factors (PDGF). These factors stimulate migration of immune cells and inflammatory cells from the blood into the tissue. As a result, different immune cells can be found in the vessel wall, including macrophages and lymphocytes. For instance, activated endothelial cells can express adhesion molecules that allow mononuclear leucocytes, such as monocytes and T-cells, to attach to the endothelium and penetrate into the tunica intima. Penetration of these cells into the tunica media by endothelial cells is seen as one of the early steps in the development of atherosclerotic lesions.

TYPES OF BLOOD VESSELS

Blood vessels are found throughout the body and can be categorized by function and by composition of the wall. There are five general types of blood vessels: arteries, arterioles, capillaries, venules and veins (Fig. 1.4). As these types of blood vessels have to withstand different degrees of blood pressure, the composition of the wall varies among these types (see Table 1.1).

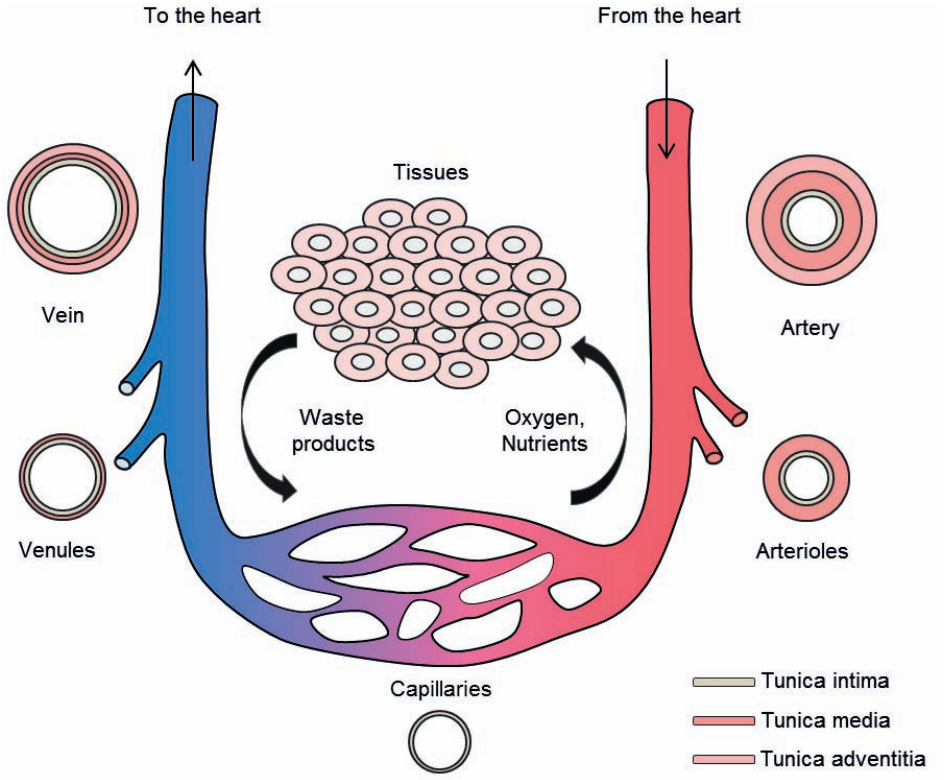

Figure 1.4: Schematic drawing showing major structural characteristics of the different types of blood vessels.

Arteries

Arteries carry highly pressurized oxygen rich blood away from the heart to other organs of the body. Because arteries experience high blood pressure and pulsatile flow as blood is ejected from the heart, they must be strong, elastic and flexible and therefore have a much thicker wall than veins. Arteries consist of three layers, tunica intima, media and adventitia. The tunica media of an artery is very thick and contains more smooth muscle cells and elastic fibers than that of veins, allowing the arteries to be more contractile and elastic, respectively. The large arteries of the body contain a lot of elastic laminae that allows the artery to stretch and accommodate to high blood pressure. The arteries branch repeatedly into smaller and smaller vessels, eventually becoming arterioles. According to size and function, arteries can be divided into two groups.

Table 1: Summary of the characteristics of different blood vessels.

Type of vessel	Actions	Structure vessel wall	Structure fits function
Artery	Carries blood away from the heart to the arterioles at high pressure	Three-layer thick wall (endothelial lining, middle smooth muscle and elastic tissue layer, outer connective tissue layer; strong, elastic and flexible; narrow lumen	Strong, elastic walls and narrow lumen help to maintain high blood pressure
Arteriole	Helps control blood flow from arteries to capillaries	Similar three layers as arteries but thinner; very narrow lumen	Vessel wall helps control blood flow by constricting or dilating
Capillary	Supply tissue with nutrients and gases and removal of waste products	Single thin layer of endothelium	Thin wall brings blood into close contact with tissue; allowing diffusion
Venule	Connects capillaries to veins	Thinner wall than arterioles, less smooth muscle and elastic tissue; extremely porous wall	Porous wall makes it easy for fluids and blood cells to pass through
Vein	Carries relatively low-pressure blood from venules to the heart	Similar layers as arteries but thinner; thin middle layer but thicker outer layer; contains valves; wide lumen	Thin wall and wide lumen allow housing of a large volume of blood and offers less resistance to blood flow

1. Elastic arteries

Elastic arteries are found close to the heart and receive blood directly from the heart. These arteries are called elastic because the tunica media is dominated by elastic laminae that give the vessel wall great elasticity, helping the artery to stretch in response to high pulsatile blood pressures during each heartbeat. The aorta, pulmonary trunk and the larger arteries that originate from them, are types of elastic arteries. Their tunica intima is thicker than that of muscular arteries and is surrounded by an internal elastic lamina, which is less well defined because of the abundance of elastic laminae. The tunica media of elastic arteries is much thicker compared to other arteries. It is primarily made up of multiple elastic laminae alternating with thin layers of smooth muscle cells and collagen fibers, which together form a lamellar unit. The external elastic lamina is difficult to distinguish from other elastic lamellar units in the tunica media. The tunica adventitia appears thinner than the tunica media and contains vasa vasorum, as the walls of these arteries are too thick to receive enough oxygen and nutrients from blood flow in the vessel lumen. The vasa vasorum supplies both the tunica media and the tunica adventitia with oxygen.

2. Muscular arteries

Muscular arteries are medium-sized arteries, which distribute the blood to various tissues and organs. These types of arteries include the femoral, brachial and coronary arteries. The diameter of the muscular artery lumen is on average 0.1 mm to 10 mm. The tunica intima of muscular arteries is thinner than those of elastic arteries. The tunica media

consists mostly of multiple layers of smooth muscle cells and less of elastic laminae. The elastic laminae are confined to two circumscribed rings: the internal elastic laminae and the external elastic laminae. The thickness and appearance of the tunica adventitia is variable. The greater amount of smooth muscle cells combined with less elastic laminae results in less elasticity but a better ability to constrict and dilate.

Arterioles

Arterioles are the smallest arteries of the body and have the same three layers as the larger arteries. The critical endothelial lining of the tunica intima is intact, and it still rests on the internal elastic laminae, which is not always well defined in histological sections. The tunica media generally consists of less than six layers of smooth muscle cells and there is no external elastic lamina. The tunica adventitia is about the same size as the tunica media. The arteriole lumen is around 10-100 μm in diameter. As arterioles have a small diameter, they generate a great resistance to blood flow and are critically involved in slowing down blood flow. Smooth muscle cells of the tunica media form concentric rings that control distribution of blood flow by either contracting or dilating lumen size. Normally, smooth muscle cells are slightly contracted, causing the arterioles to maintain a consistent vascular tone.

Capillaries

Blood moves from the arterioles into the capillaries, which are tiny, narrow, thin-walled vessels that connect arteries with veins. Capillaries are the smallest of all blood vessels, about 5-8 μm in diameter, and blood pressure further drops as it encounters extra resistance flowing through the capillaries. Their walls consist of a single layer of endothelial cells and an underlying basement membrane, often accompanied by pericytes. The basement membrane keeps cells in place and is largely made up of proteins. Capillaries have no tunica media or tunica adventitia. The diameter of a capillary is just wide enough to allow single red blood cells (erythrocytes) to pass through. The thin wall of the capillaries facilitates its primary function: exchange of oxygen, nutrients and other substances, between blood and the underlying tissue. Most capillaries are organized into a network called capillary bed. Based on the morphology of their endothelial layer, capillaries can be classified into three different types.

1. *Continuous capillaries* consist of an uninterrupted, continuous lining of endothelial cells, which are joined by tight non-permeable junctions, and a complete basement membrane. The continuous capillaries have a low permeability to molecules; it only allows small molecules, like water and ions, to diffuse through the tight junctions, which have gaps of unjointed membrane called intercellular clefts. They are commonly found in skin, muscles, lung and central nervous tissue.

2. *Fenestrated capillaries* have leakier intracellular junctions and perforations in the endothelial cell body, called fenestrae or pores. The fenestrae are present at both the luminal and basal surface of the cell, and the endothelial cells are surrounded by a continuous basement membrane. Fenestrated capillaries are much more permeable compared to continuous capillaries, and allow larger molecules and a limited amount of proteins to bypass the endothelial cells. The extent of fenestra may depend on the physiological state of the surrounding tissue, as their numbers may depend on the need to absorb or secrete. They are found in tissues that participate in fluid exchange including endocrine glands, intestinal villi and kidney glomeruli.
3. *Discontinuous capillaries,* also called sinusoids, are the largest of all capillaries and have larger, open spaces in the endothelium, containing a lot more intracellular clefts. They are very permeable (leaky) and allow large molecules, including red and white blood cells and various serum proteins, to pass through the intracellular spaces of the endothelium. Discontinuous capillaries contain a basement membrane that is often incomplete. These discontinuous capillaries are found in areas where the exchange of substances is advantageous, i.e. in the liver, hematopoietic organs (spleen and bone marrow) and some endocrine organs.

Venules

Blood flows from the capillary beds into very small veins called venules (10-200 μm in diameter). Venules allow deoxygenated blood to return from the capillary beds to the larger blood vessels called veins. Venules consist of a tunica intima, a thin tunica media and a tunica adventitia. The vessel wall of venules is thinner than arterioles and is extremely porous, making it easy for fluids and blood cells to pass through their walls. Venules can be further subclassified into muscular (50-200 μm) and post-capillary venules (10-50 μm). The post-capillary venule starts where two capillaries from the capillary bed come together. It is a non-muscular vessel, as the tunica media consists of an incomplete layer of pericytes and scattered smooth muscle cells. Instead, the post-capillary venule has a thin very permeable endothelial layer, making them the preferred site of white blood cell (leucocyte) adhesion and transmigration. Hence, the response of the vasculature to inflammation is generally localized in the post-capillary venules. During inflammatory responses, vasoactive substances act on the endothelium which results in extravasation of fluid and the migration of leucocytes into the tissue. Post-capillary venules join together, forming larger muscular venules. In the muscular venules, the pericytes are replaced by one or two layers of smooth muscle cells.

Veins

Multiple venules unite to form veins. Veins carry deoxygenated blood back from tissues and organs towards the heart. One difference between veins and arteries is the direction of

blood flow. As in arteries, veins have three layers. However, veins have much thinner walls than arteries as they are distant from the heart and subsequently experience less pressure from the blood flow. The tunica intima and tunica adventitia are similar in structure to arteries though the tunica media is much thinner. The tunica intima consists of the endothelial lining with its basement membrane, and surrounding internal elastic laminae. The tunica media of veins is thin and only contains a few smooth muscle cells and elastic laminae, whereas the tunica adventitia is much thicker, containing collagen and occasionally some smooth muscle cells and elastic fibers. In general, veins are larger in diameter (varying from 1 mm to 15 mm), containing a wide lumen, which together with the thin walls allows the accommodation of a large blood volume. Most of the blood volume of the body, around 60%, is contained within veins at any time. Because of these thin walls and a small medial layer, veins do not have the same elasticity and vasoconstriction capacities as arteries. Blood is displaced through veins by contraction of the surrounding muscles and pressure gradients that are created during inhalation and exhalation. Compared to arteries, veins are frequently irregular of shape and softer. Some veins also contain valves, particularly veins in the legs, which prevent backflow of blood as it travels back to the heart. Veins can be classified into four main types as shown in Box 1.2.

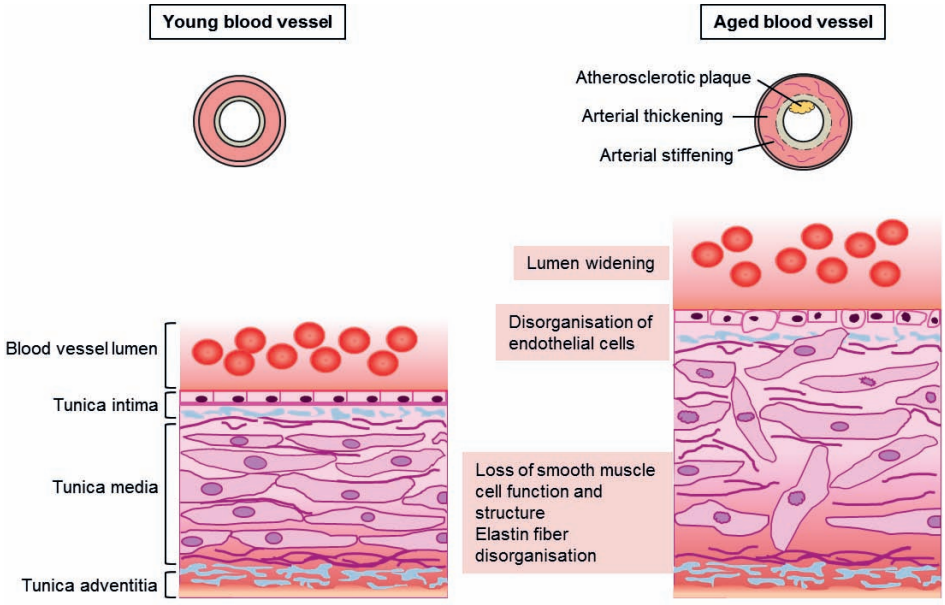

Figure 1.5. Schematic view of the structural changes of the vessel wall during aging.

Box 1.2 Classification of veins

1. *Pulmonary veins* carry oxygenated blood from the lungs to the left atrium of the heart
2. *Systemic veins* return deoxygenated blood from the rest of the body to the right atrium of the heart.
3. *Superficial veins* are located close to the surface of the skin and are not located near a corresponding artery.
4. *Deep veins* are located within muscle tissue and typically near a corresponding artery.

Lymphatic vessels: secondary drainage system

The general structure of lymphatic vessels is based on the three tunica described above. Lymphatic vessels are lined by endothelial cells and have a thin layer of smooth muscle cells followed by the adventitia. They are part of the lymphatic system that transports fluid away from tissues and plays an important role in the body's defense system. The fluid that lymphatic vessels carry is not blood, but is clear fluid, called lymph, that comes from blood plasma that exits blood vessels at the site of the capillaries.

AGING AND THE VASCULAR WALL

The prevalence of cardiovascular disease increases progressively with age. To understand why aging is closely linked to cardiovascular disease, it is essential to know what happens to our vessels during normal aging. Aging is a natural biological process that begins as soon as adulthood is reached and it causes diverse detrimental changes in cells and tissues. A series of structural, architectural and compositional modification take place in the vasculature during aging (Fig. 1.5). As such, with increasing age, blood vessels lose their flexibility and structural integrity, which diminishes the ability of blood vessels to expand and contract efficiently. In addition, age-related vascular alterations lead to loss of adequate tissue perfusion (ischemia), insufficient vascular growth or excessive remodeling. Eventually these changes affect cardiovascular performance and set the stage for the onset of several cardiovascular diseases including hypertension (high blood pressure), atherosclerosis, stroke and aneurysm formation.

Age-related structural changes

At a microscopic level, principal age-related structural changes of the vasculature include an increase in vessel lumen size and thickening and stiffening of the intimal and medial layer. Important structural changes causally related to vessel wall thickening and stiffening include vascular smooth muscle enlargement and relocation to the subendothelial space, increased extracellular matrix accumulation (particularly rich in glycosaminoglycans), and increased deposition of lipids and calcium salts. While the content of collagen increases, elastin fibers become disorganized, thinner and fragmented.

As an individual grows older, the endothelial barrier of the tunica intima becomes damaged and some of its specialized functions are blunted. The endothelial barrier becomes porous (leaky), the self-renewal process weakens and endothelial signaling is modified. For example, with increasing age endothelial cells produce substances that signal blood cells to adhere to the endothelial layer of the tunica media instead of smoothly flowing through the blood vessel lumen. Additionally, endothelial cells transmit signals to the underlying vascular smooth muscle cells in the tunica media that prompt these cells to change. These changes result in vascular smooth muscle cells to translocate and move towards the site of injury, where they reposition in the tunica intima just beneath the endothelial layer. At this site, the vascular smooth muscle cells multiply and produce matrix proteins, which eventually results in thickening of the tunica intima. Moreover, with age, some of the vascular smooth muscles of the tunica media die, increasing the workload of the remaining vascular smooth muscle cells and causing them to grow larger. Some changes cause vascular smooth muscle cells to switch from a contractile state to a state in which they produce excessive amounts of collagen proteins and other matrix substances, thereby creating imbalance between the elastin and collagen content of the tunica media. The ratio of collagen to elastin increases in favor of collagen, which is a 100 to 1000 times stiffer than elastin, resulting in a stiffer wall and a less compliant blood vessel. Moreover, vessel wall stiffening has been associated with the formation of cross-links between glucose and collagen. Growing levels of cross-links reduce elasticity of the vessel wall, as these cross-links glue together important proteins of the extracellular matrix thereby degrading its primary structure, preventing it from functioning correctly. Aging also affects elastin, as it becomes overloaded with calcium, stretches out, and eventually becomes fragmentized and disorganized.

Related diseases

Due to structural changes in the vessel wall with age, many of the arteries are less able to withstand the forces of pulsating blood. High systolic blood pressure, which is commonly observed in the elderly, may exacerbate this problem. As a result, the vessel wall becomes weakened and more prone to develop several vascular diseases, including aneurysms. Moreover, aging increases incidence and severity of atherosclerosis, as the age-related changes of the vessel wall make it easier for fatty substances to accumulate inside of the blood vessel. Several studies suggest that exercise, good nutrition and therapeutic interventions can slow down the aging process occurring within blood vessels. For example, it in elderly who regularly exercise arterial stiffening is less pronounced.

SUMMARY

The vessel wall consists of three different layers termed tunica intima, tunica media and tunica adventitia. The main components of these layers include endothelial cells, vascular smooth muscle cells, cytoskeleton proteins and extracellular matrix proteins. Interaction between these components of the different layers determines the biological and physical properties of the blood vessel. Changes and damage to these components and cellular constituents contribute to the pathogenesis and progression of several vascular diseases, as well as to aging of the vasculature. The subsequent chapters in this book will cover, in greater detail, related diseases of the vasculature.

REFERENCES

1. Flaherty JT, Pierce JE, Ferrans VJ, Patel DJ, Tucker WK, Fry DL. Endothelial nuclear patterns in the canine arterial tree with particular reference to hemodynamic events. Circ Res. 1972; 30:23–33.

FURTHER READING

Alberts B, Johnson A, Lewis J, Morgan D, Raff M, Roberts K, Walter P. (2104). Molecular Biology of the Cell, 6th edition. New York, Garland Science.

Saladin K. (2014). Anatomy and Physiology: The Unity of Form and Function, 7th edition. New York, McGraw Hill Education.

Marieb EN, Hoehn KN. (2015). Human Anatomy & Physiology 10th edition. New York, Pearson Education.

CHAPTER 3

THE RENIN–ANGIOTENSIN SYSTEM AND ITS INVOLVEMENT IN VASCULAR DISEASE

Bibi S. van Thiel[1,2,3], Ingrid van der Pluijm[2,3], Luuk te Riet[1,3], Jeroen Essers[2,3,4], A.H. Jan Danser[1]

[1]Department of Internal Medicine, Division of Pharmacology and Vascular Medicine, [2]Department of Molecular Genetics, Cancer Genomics Center, [3]Department of Vascular Surgery, [4]Department of Radiation Oncology, Erasmus MC, Rotterdam, The Netherlands

(European Journal of Pharmacology 2015 Sep 15;763(Pt A):3-14)

ABSTRACT

The renin-angiotensin system (RAS) plays a critical role in the pathogenesis of many types of cardiovascular diseases including cardiomyopathy, valvular heart disease, aneurysms, stroke, coronary artery disease and vascular injury. Besides the classical regulatory effects on blood pressure and sodium homeostasis, the RAS is involved in the regulation of contractility and remodeling of the vessel wall. Numerous studies have shown beneficial effect of inhibition of this system in the pathogenesis of cardiovascular diseases. However, dysregulation and overexpression of the RAS, through different molecular mechanisms, also induces, the initiation of vascular damage. The key effector peptide of the RAS, angiotensin II (Ang II) promotes cell proliferation, apoptosis, fibrosis, oxidative stress and inflammation, processes known to contribute to remodeling of the vasculature. In this review, we focus on the components that are under the influence of the RAS and contribute to the development and progression of vascular disease; extracellular matrix defects, atherosclerosis and aging. Furthermore, the beneficial therapeutic effects of inhibition of the RAS on the vasculature are discussed, as well as the need for additive effects on top of RAS inhibition.

1. GENERAL FUNCTION OF THE RENIN-ANGIOTENSIN SYSTEM

The renin-angiotensin system (RAS) is a peptide cascade well known for its critical role in the regulation of arterial blood pressure and sodium homeostasis, as well as cardiovascular regulation and remodeling. It regulates fluid and electrolyte balance through coordinated effects on the heart, blood vessels and kidneys. Angiotensin II (Ang II) is the primary effector hormone of this system that can act either as a systemic hormone or as a locally produced factor. Ang II is generated in two sequential steps: renin, secreted from the juxtaglomerular apparatus of the kidney, cleaves angiotensin I (Ang I) from liver-derived angiotensinogen, and Ang I is subsequently hydrolyzed by endothelial angiotensin-converting enzyme (ACE) to form Ang II. Ang II stimulates the adrenals to produce aldosterone and acts on cardiovascular and other tissues to regulate blood pressure and remodeling (Fig. 1). The recent identification of angiotensin-converting enzyme 2 (ACE2), which is responsible for the conversion of Ang II to angiotensin (1-7), suggest that this enzyme is a negative regulator of Ang II production, and thus the balance between ACE and ACE2 is important in the regulation of Ang II levels, as depicted in Figure 1. In addition to

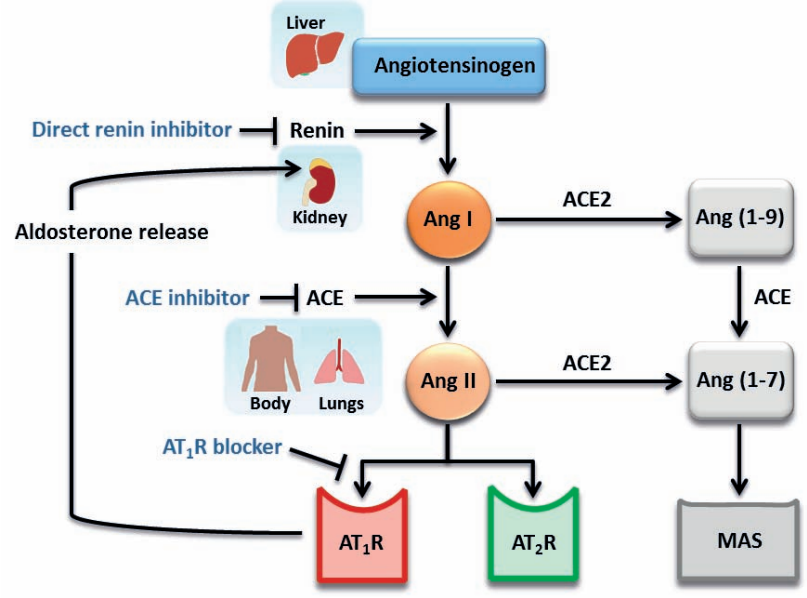

Figure 1. Schematic overview of the renin-angiotensin system (RAS) and its intervening compounds. Liver-derived angiotensinogen is cleaved into angiotensin I (Ang I) by renin that is secreted from the kidney. Ang I is subsequently hydrolyzed by endothelial angiotensin-converting enzyme (ACE) to form angiotensin II (Ang II). Ang II stimulates the adrenals, via the angiotensin type 1 receptor (AT_1R), to produce aldosterone and acts on cardiovascular and other tissues to regulate blood pressure and remodeling via the AT_1R and angiotensin type 2 receptor (AT_2R). Parts indicated in grey are only briefly discussed in the review.

the circulating RAS, there is increasing evidence for the existence of local or tissue RAS, which generate the Ang II that is involved in paracrine and/or autocrine signaling within organs and tissues. Tissue RAS is thought to be present in all major organs, including brain, heart, blood vessels, adrenals and the kidney.[1] The exact function of vascular tissue RAS remains elusive, but it most likely contributes to the fine-tuning of Ang II actions on vascular tone and remodeling. A schematic representation of the RAS, based on what is currently known, is depicted in Figure 1.

Ang II mediates its physiological actions mainly via two distinct receptors: angiotensin II type 1 (AT_1) and type 2 (AT_2) receptors. The majority of the functions of Ang II are mediated through AT_1 receptor binding, while the role and biological function of the AT_2 receptor is less well-defined. Binding of Ang II to the AT_1 receptor activates a series of signaling cascades leading to tissue remodeling and acute vasoconstriction, whereas binding to the AT_2 receptor is believed to have counteractive effects, as it has been reported to inhibit and antagonize the AT_1 receptor-mediated functions.[2, 3]

1.1 Role of the RAS in the pathogenesis of vascular disease

Cardiovascular diseases are a major cause of mortality worldwide. It is well established that RAS dysregulation and/or overexpression leads to a variety of harmful vascular effects, thereby contributing to the pathophysiology of cardiovascular diseases including hypertension, aneurysms, congestive heart failure, stroke, coronary artery disease and vascular injury.[4] Besides the classical regulatory effects on blood pressure and sodium homeostasis, the RAS is involved in the regulation of vascular tone and remodeling of the vessel wall. Activation of the AT_1 receptor by Ang II induces its well-known actions such as vasoconstriction, aldosterone and vasopressin release, renal tubular sodium reabsorption, renal blood flow reduction, and production of reactive oxygen species. The signal transduction pathway for vasoconstriction is established by stimulation of the AT_1 receptor which in turn activates phospholipase C, which cleaves the phospholipid phosphatidylinositol 4,5-bisphosphate into inositol-1,4,5-trisphosphate and diacylglycerol. Inositol-1,4,5-trisphosphate induces Ca^{2+} release into the cytosol, thereby activating myosin light chain kinase which phosphorylates myosin. Diacylglycerol activates protein kinase C, which phosphorylates C-kinase potentiated protein phosphatase-1 which directly inhibits the activity of myosin light chain phosphatase.[5] Both processes result in phosphorylation of myosin and thereby induce smooth muscle contraction. Moreover, AT_1 receptor stimulation has been implicated to mediate tissue remodeling as it promotes vascular smooth muscle cell migration and senescence, vascular hypertrophy, endothelial dysfunction, oxidative stress and the synthesis and release of extracellular matrix protein.[6] Multiple signal transduction cascades with complex interactions are activated by the AT_1 receptor (Fig. 2), including the mitogen activated protein kinase (MAPK) and the janus kinase/signal transducers and activators of transcription pathway[7], which together induce

cell growth, migration, proliferation and other processes linked to vascular remodeling. In addition, it is reported that Ang II acts pro-inflammatory and pro-atherogenic, both contributing to vascular remodeling and damage. Accordingly, overstimulation of the AT_1 receptor has been linked to various cardiovascular and renal pathologies such as left ventricular hypertrophy, vascular media hypertrophy, cardiac arrhythmias, atherosclerosis and glomerusclerosis.[6]

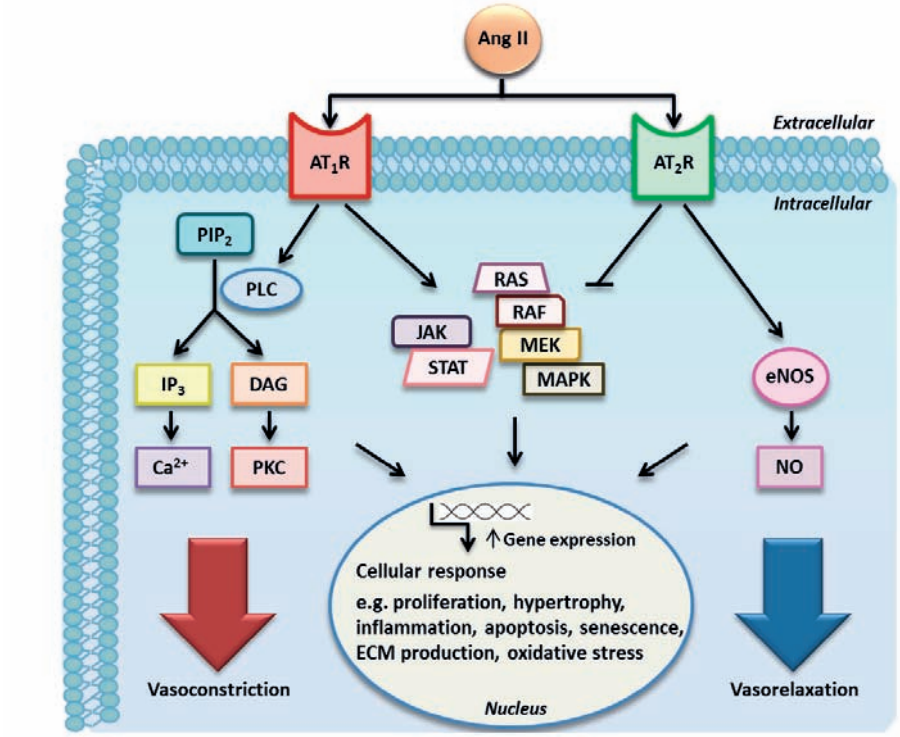

Figure 2. Effect of angiotensin II (Ang II) signaling on vascular tone and remodeling of the vessel wall, via the angiotensin type 1 and 2 receptors (AT_1R and AT_2R). AT_1 receptor activation induces vasoconstriction, mediated by the inositol trisphosphate (IP_3)-Ca^{2+} and diacylglycerol (DAG)-protein kinase C (PKC) pathways. This effect is counteracted by AT_2 receptor-induced activation of nitric oxide synthase (NOS) leading to vasorelaxation. AT_1 receptor stimulation also activates several signal transduction pathways which regulate the expression of target genes promoting cell proliferation, migration and senescence, vascular hypertrophy, inflammation, apoptosis, oxidative stress and the synthesis and release of extracellular matrix (ECM) proteins. Stimulation of the AT_2 receptor inhibits these processes by blocking the mitogen-activated protein kinase (MAPK) signaling pathway. Abbreviations: janus kinase (JAK), nitric oxide (NO), phospholipid phosphatidylinositol 4,5-bisphosphate (PIP2), phospholipase C (PLC), signal transducers and activators of transcription (STAT)

As mentioned above, besides the AT_1 receptor, Ang II can also mediate its effect via the AT_2 receptor. Generally, the counteractive effects of the AT_2 receptors, opposing those of AT_1 receptors, lead to vasodilatation[8], and suppression of growth, fibrosis and inflammation (Fig. 2). However, the latter is not a uniform finding, because it has been shown that under certain conditions, e.g. in the spontaneously hypertensive rat, AT_2 receptors may become AT_1 receptor-like.[9, 10] The mechanism behind this phenotypic change is unclear, but most likely involves a difference in location of endothelial cell versus vascular smooth muscle cell and/or heterodimerization with AT_1 receptor.[3] Therefore, whether upregulation of AT_2 receptors under pathological conditions is always beneficial, should be questioned.[11] Similar opposing findings are found in the heart; upregulation of AT_2 receptors in the post-myocardial infarction area has beneficial effects, but a massive increase of 9-fold overexpression of AT_2 receptors did not yield a positive effect anymore.[12] Thus, the balance between the AT_1/AT_2 receptors in traumatized tissue will probably determine whether the net effect is adaptive or maladaptive.

2. COMPONENTS CONTRIBUTING TO THE DEVELOPMENT AND PROGRESSION OF VASCULAR DISEASE

Several components which are under the influence of the RAS contribute to the development and progression of vascular disease (Fig. 3). The key components oxidative stress, extracellular matrix defects, atherosclerosis and aging and their effect on the vasculature will be discussed in this review.

2.1 Oxidative stress leading to vascular damage

It is well established that reactive oxygen species play a fundamental role in vascular damage and the development of cardiovascular disease.[13, 14] Reactive oxygen species include free radicals, mainly superoxide anions and hydroxyl radicals, and other molecules such as hydrogen peroxide and ozone. They are generated during cellular metabolism, in the vessel wall by all vascular cells, including endothelial cells, smooth muscle cells and adventitial fibroblasts. Several cellular sources are known to produce reactive oxygen species, with mitochondria as a major site of production. In general, reactive oxygen species are essential in the functioning of cells as they modulate many downstream signaling molecules regulating cell growth and vascular contraction and relaxation. However, an imbalance between reactive oxygen species generation and antioxidant protection, resulting in increased bioavailability of reactive oxygen species, leads to a state of oxidative stress. Oxidative stress contributes to vascular remodeling and dysfunction as it activates a series of signaling pathways involving MAPK, tyrosine kinases, protein tyrosine phosphatases, calcium channels and redox-sensitive transcription factors. Activation of all these factors

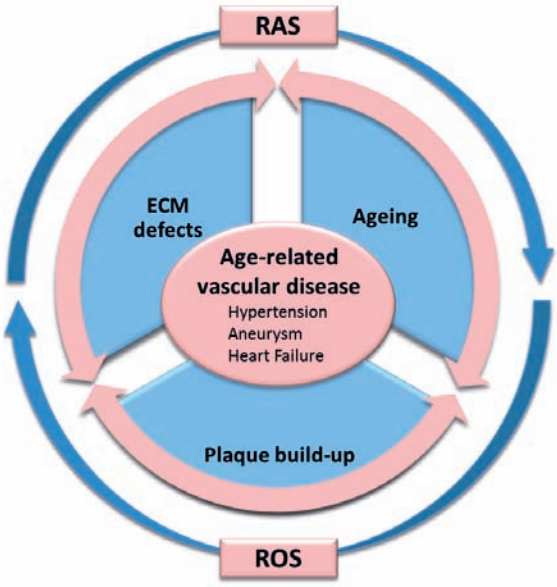

Figure 3. Interplay between the renin angiotensin system (RAS) and reactive oxygen species on three important components; extracellular matrix (ECM) defects, plaque build-up and aging, together contributing to the development and progression of age-related vascular disease. Abbreviations: reactive oxygen species (ROS).

results in increased cell migration and proliferation, expression of pro-inflammatory genes, extracellular matrix production and apoptosis in the vessel wall, which all play an important role in vascular injury.[15, 16] In addition, oxidative stress induces enhanced oxidation of low-density lipoproteins and inactivation of endothelial derived nitric oxide, processes known to be involved in atherosclerotic disease. Moreover, oxidative stress is known to induce DNA damage. As such, reactive oxygen species are the most likely trigger of DNA damage in atherosclerosis[17], where DNA damage is present in both plaques of patients with atherosclerosis as well as in the circulating blood cells of these patients.[18] Multiple lines of evidence indicate that the RAS contributes to reactive oxygen species generation and its deleterious effects. One of the effects of AT_1 receptor activation in cardiovascular tissue is the generation of reactive oxygen species[19], as Ang II stimulates the expression and activation of nicotinamide adenine dinucleotide phosphate-oxidase (NAD(P)H) in various cells (Fig. 4).[20, 21] In several Ang II-associated vascular diseases the occurrence of oxidative stress has been shown to be the result of activation of NAD(P)H oxidase, mitochondrial dysfunction, inflammation and the reduction of endogenous antioxidant enzymes.[22] In various pathological conditions it was found that elevated Ang II levels lead to upregulation of the NAD(P)H oxidase subunits in endothelial, adventitial and vascular smooth muscle cells, resulting in increased levels of reactive oxygen species in the vessel wall.[15]

Of note, reactive oxygen species in turn have been shown to cause increased expression of the AT_1 receptor, thereby modulating the generation of reactive oxygen species, creating a vicious circle.[23, 24] Moreover, in recent years it has become evident that Ang II not only activates NAD(P)H but also stimulates mitochondrial reactive oxygen species production and induces mitochondrial dysfunction, presented as increased mitochondrial hydrogen peroxide production, and decreased mitochondrial glutathione, state 3 respiration and membrane potential.[25, 26] Molecular mechanisms that are involved in Ang II-induced mitochondrial dysfunction include protein kinase C activation, which in turn activates NAD(P)H and stimulates peroxinitrite formation.[25] Moreover, Ang II-derived reactive oxygen species production triggers mitochondrial ATP-dependent potassium ($mitoK_{ATP}$) channel opening, which further promotes mitochondrial reactive oxygen species generation.[27] Research has shown that mitochondria-derived reactive oxygen species play an important role in the development of cardiovascular disease, and therapeutic targeting of mitochondrial reactive oxygen species by using a mitochondria-targeted antioxidant, significantly decreased blood pressure in Ang II-induced hypertension, and improved endothelial dysfunction.[28, 29] Moreover, it is suggested that mitochondrial dysfunction initiated by reactive oxygen species is one of the causes of aging, implying an important role of Ang II in aging and age-related diseases (Fig. 4).

2.2 Extracellular matrix defects and vascular disease

The extracellular matrix is composed of numerous macromolecules, including collagens, elastin and proteoglycans. These extracellular matrix molecules not only provide structural support to cells and tissues, but also exhibit important functional roles that control the behavior of cells such as adhesion, migration, proliferation and differentiation. Moreover, the extracellular matrix provides mechanical properties required for the functioning of the vasculature.[30] Minor alterations in extracellular matrix composition of the vasculature can lead to changes in cellular phenotype and function, which can ultimately lead to development of vascular disease. Diseases that are associated with an extracellular matrix defect include cutis laxa, osteogenesis imperfecta, Ehlers-Danlos and Marfan syndrome.[31] Moreover, it is suggested that alterations towards the breakdown of the extracellular matrix contributes to the progression of atherosclerosis and plaque instability[32], and to the formation of aortic aneurysms.[33, 34] It is suggested that the RAS plays a role in the alteration of extracellular matrix components as numerous studies have shown that blockade of the RAS reduces the incidence and progression of aortic aneurysms (which is discussed in section 3 of this review), although the precise role of the RAS in the onset of extracellular matrix defects is not well-understood yet.

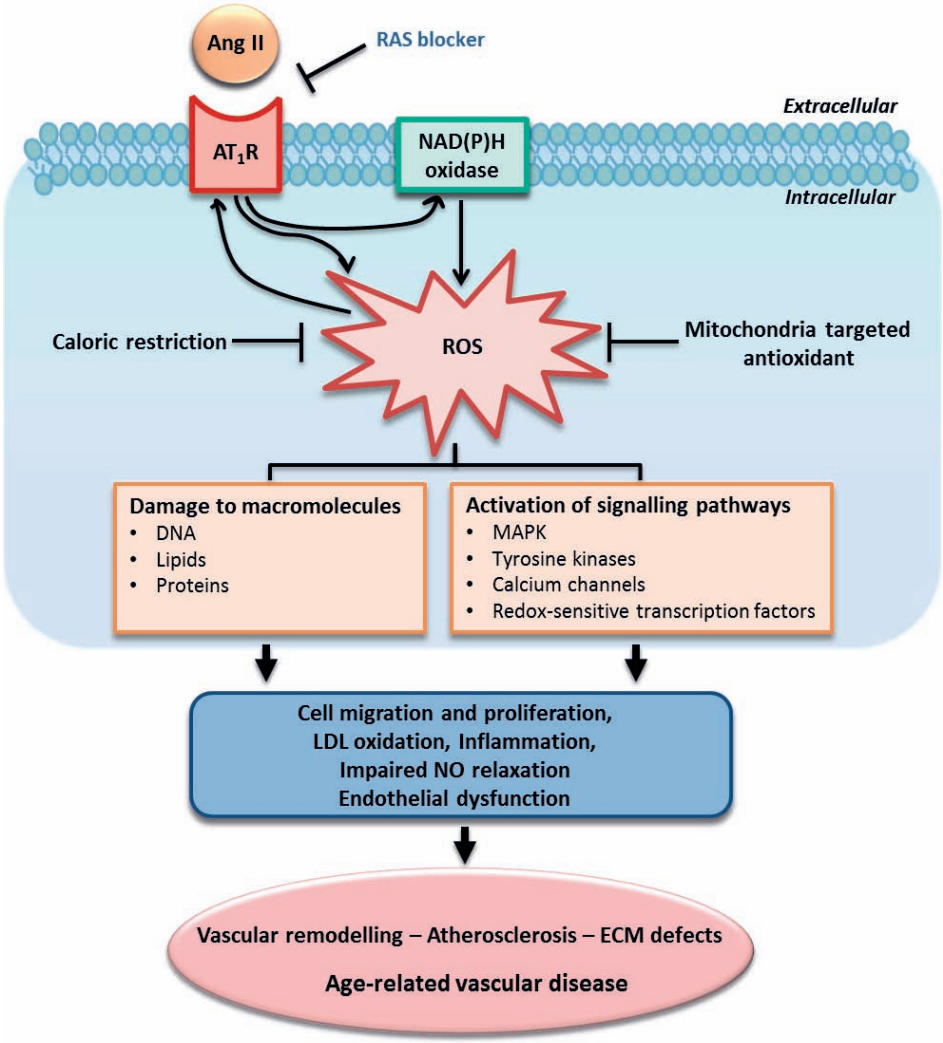

Figure 4. Effects of angiotensin type 1 receptor (AT_1R) activation -via angiotensin II (Ang II) receptor binding- on reactive oxygen species generation, leading to age-related vascular diseases. AT_1R stimulation upregulates nicotinamide adenine dinucleotide phosphate-oxidase (NAD(P)H), thereby increasing the formation of reactive oxygen species. Reactive oxygen species in turn activates several signaling pathways and induces damage to macromolecules, eventually contributing to the pathogenesis of age-related vascular disease. Abbreviations: extracellular matrix (ECM), low density lipoprotein (LDL), mitogen-activated protein kinase (MAPK), nitric oxide (NO), renin angiotensin system (RAS), reactive oxygen species (ROS).

2.2.1 The involvement of RAS in alterations of the extracellular matrix

Accumulating evidence indicates that increased Ang II signaling in the vessel wall results in the release of inflammatory and pro-fibrotic factors, and regulate the genetic expres-

sion of extracellular matrix proteins, which might lead to defects in the build-up of the extracellular matrix. As such, Ang II has been shown to promote vascular smooth muscle cells to synthesize extracellular matrix components.[35] For instance, Ang II-induced cultured rat vascular smooth muscle cells display increased levels of collagen, fibronectin, laminin and tenascin mRNA and protein.[36-38] Additionally, *in vivo* Ang II infusion results in increased fibronectin mRNA and protein.[39] Furthermore, Ang II stimulates the induction of various growth factors, inflammatory and pro-fibrotic factors including transforming growth factor beta (TGF-β)[40], platelet-derived growth factor[41], basic fibroblast growth factor[40], vascular endothelial growth factor[42] and insulin-like growth factor.[43] Ang II-induced TGF-β mRNA expression in vascular smooth muscle cells is mediated by activation of extracellular-signal-regulated kinase (ERK) and activator protein-1.[44] Ang II stimulates mRNA expression and activity of plasminogen activator inhibitor-1 and -2 in rat aortic smooth muscle cell.[45] It is intriguing that all these factors could play an important role in Ang II-mediated vascular disease.

2.2.2 Effect of Ang II induced TGF-β activation in extracellular matrix disruption and vascular disease

TGF-β production by Ang II has a pivotal role in vascular disease and fibrosis. TGF-β is a pleiotropic cytokine that regulates diverse functions such as proliferation, differentiation and apoptosis. Increased TGF-β-signaling results in increased pSmad2/3 signaling, the canonical pathway, and recent work has also shown an increase in pERK1/2 signaling, the so-called non-canonical pathway.[46-48] Activation of these pathways leads to changes in adhesion, proliferation, migration and differentiation. Moreover, TGF-β signaling plays a crucial role in the regulation of the extracellular matrix, mainly by stimulating the expression of collagens, fibronectin and proteoglycans. Furthermore, it induces the production of metalloproteinases that affect extracellular matrix breakdown. Thus, persistent activation of TGF-β receptors leads to an abnormal deposition of connective tissue, which is associated with fibrotic disease and vascular disease.[49, 50]

2.2.3 Involvement of Ang II-mediated extracellular matrix defects in aortic aneurysms

The strength and elasticity of our blood vessels is mainly established by the extracellular matrix components elastin and collagen, which originate in the medial layer of the vessel wall. Degeneration of the medial layer of the aorta allows the development of an aneurysm, which is characterized by elastic fiber fragmentation, loss of smooth muscle cells, and accumulation of amorphous extracellular matrix.[51] Two main types of aortic aneurysms can be distinguished; abdominal aortic aneurysm and thoracic aortic aneurysm. Abdominal aortic aneurysms are usually caused by multiple environmental factors, such as smoking, high blood pressure and inflammation, while the development of thoracic aortic aneurysms often has a genetic origin. Different experimental mouse models for abdominal

aortic aneurysms exist, for instance the well-recognized mouse models with infusion of Ang II in atherosclerotic apolipoprotein E - or low density lipoproteins (LDL) receptor knock out mice resulting in abdominal aneurysm formation. In contrast, most mouse models for thoracic aortic aneurysms are genetically engineered, containing mutations in for example extracellular matrix proteins and TGF-β receptors. A well-known genetic disease characterized by thoracic aortic aneurysms is Marfan syndrome, which is caused by a mutation in the extracellular matrix protein fibrillin-1.[52] Accumulating evidence in different thoracic aortic aneurysms mouse models has shown that increased TGF-β-signaling in the vasculature is responsible for the development of aneurysms, which will be discussed in more detail below. It is suggested that this increase in TGF-β-signaling leading to aortic aneurysm development is initiated by Ang II.[48, 53, 54] Moreover, recently it has been shown that blockade of the RAS downregulates pSmad2/3 and pERK1/2 signaling in aortic aneurysm, which gave rise to a new proposed signaling mechanism in which the AT_1/AT_2 receptors are directly involved in Smad2/3 and ERK1/2 activation.[46, 47]

2.3 Involvement of the RAS in atherosclerosis

Atherosclerosis refers to the build-up of fat, cholesterol and other substances in and around the vasculature. Over time this build-up, so-called plaques, causes thickening and stiffening of the vessel wall. Moreover, as these plaques grow larger and larger, they eventually partially or totally block the blood flow through an artery. Numerous cardiovascular diseases are a direct consequence of the atherosclerotic process. Diseases that could develop as a result of this plaque build-up include coronary heart disease, carotid artery disease, peripheral artery disease and chronic kidney disease. Two types of plaques are described in literature; stable and unstable/vulnerable plaques, the latter having a high risk of rupture.[55] Plaque rupture and subsequent thrombus formation are among the main causes of acute cardiovascular events like unstable angina, acute myocardial infarction and sudden cardiac death.[56] It is suggested that loss of vascular function together with oxidation and accumulation of low-density lipoprotein and endothelial damage promotes an inflammatory vascular response, which plays an essential role in the development of atherosclerotic plaques. Several risk factors are strongly associated with the onset of plaque build-up such as aging, smoking, lack of physical activity, unhealthy diet, hypercholesterolemia, hypertension and genetic background. In addition, it is proposed that the RAS, and particularly Ang II, is involved in the initiation and progression of atherosclerotic plaques, since various atherogenic stimuli are mediated by RAS activity.[57] Ang II stimulates the atherogenic process not only through its hemodynamic effects but also through various effects on the vessel wall itself.[58] In particular, Ang II promotes the generation of oxidative stress in the vasculature, which plays a pivotal role in endothelial dysfunction and lipoprotein oxidation. Furthermore, Ang II induces the expression of cellular adhesion molecules and pro-inflammatory cytokines, which contribute to the induc-

tion of the inflammatory process in the vessel wall. Ang II also triggers vascular smooth muscle cells to proliferate and migrate, subsequently leading them to produce growth factors and extracellular matrix components. It was also reported that overexpression of ACE2, which converts Ang II to Ang-(1-7), improves endothelial function and decreases plaque formation in atherosclerotic mice.[59, 60] Moreover, several studies suggest that Ang II may be involved in the acute complications of atherosclerosis by promoting plaque vulnerability, eventually resulting in plaque rupture.[61-64]

2.3.1 Evidence for the contribution of the RAS in atherosclerotic plaque build-up

The initial steps of the atherogenic process include endothelial damage and dysfunction, which allows the migration of inflammatory cells and lipid particles into the damaged part of the vessel wall, where they accumulate and form a 'fatty streak'. These lipid particles are taken up by macrophages and smooth muscle cells, which become fat-laden foam cells and release substances which trigger a greater inflammatory response. Next, smooth muscle cells migrate to the inner layer of the vessel wall, where they proliferate, produce extracellular matrix components and contribute to the formation of the fibrous cap covering the plaque. These processes together result in growth of the plaque.[65] Over time the plaque may become destabilized, resulting in plaque rupture which manifests as acute cardiovascular events.

It has become apparent that one of the most important mechanisms whereby Ang II exerts vascular damage, is the production and release of reactive oxygen species via stimulation of NAD(P)H.[19] Oxidative stress, which is caused by an imbalance between reactive oxygen species and antioxidants, induces nitric oxide inactivation, lipid oxidation, modifications in DNA and proteins, and activation of adhesion molecules, pro-inflammatory cytokines and matrix metalloproteinases. As discussed, Ang II induces reactive oxygen species generation in various vascular cells including smooth muscle cells, endothelial cells and adventitial fibroblasts by binding to the AT_1 receptor, expressed by these cells.[66] Enhanced levels of reactive oxygen species are an important feature of atherosclerosis. Reactive oxygen species are detected in all layers of the atherosclerotic vessel wall, particularly at pathophysiological relevant locations of the atherogenic process, such as the shoulder region of coronary atherosclerotic plaques where they co-localize with Ang II.[67-69]

An additional mechanism by which Ang II promotes atherosclerosis is endothelial dysfunction, which is considered one of the earliest steps in the atherosclerotic process. Several animal studies show that Ang II causes endothelial dysfunction, measured by impaired vasorelaxation in response to acetylcholine, which is a endothelium-dependent vasodilator.[20, 70, 71] Endothelial cells are the major regulators of vascular homeostasis and anticoagulant properties of the vessel. Endothelial dysfunction and/or apoptosis is considered to be an initial step in the development and progression of atherosclerotic plaques as it promotes abnormal vasomotion, a procoagulant state, and infiltration of inflammatory

cells into the vessel wall.[72] Oxidative stress is recognized as one of the main factors that promotes vascular endothelial dysfunction, as elevated levels of reactive oxygen species caused by Ang II induce impaired endothelial relaxation and vascular function. Nitric oxide, which is a potent vasodilator produced by endothelial cells, is inactivated in response to reactive oxygen species. Additionally, it is suggested that a more direct effect of Ang II on endothelial cells exist, as Ang II stimulates them to express various adhesion molecules and atherogenic genes. For instance, Ang II stimulates the mRNA and protein expression of vascular cell adhesion molecule-1, which leads to the recruitment of inflammatory cells to the site of plaque formation.[73, 74] Furthermore, Ang II was shown to regulate the expression of plasminogen activator inhibitor-1[75, 76] and stimulate endothelial cell apoptosis[77], resulting in an alteration in fibrinolytic balance which could lead to a highly thrombogenic state.

Another phase in the atherosclerotic process is fatty streak formation, characterized by oxidation of LDL, which Ang II facilitates by promoting reactive oxygen species formation. Oxidized LDL particles have important atherogenic properties as they can penetrate the endothelial layer after which they are taken up by macrophages and vascular smooth muscle cells, contributing to the creation of so-called foam cells. Moreover, Ang II increases the uptake of oxidized LDL by endothelial cells and macrophages, as it upregulates the expression of receptors that take up oxidized LDL, in the end leading to endothelial dysfunction.[78] Furthermore, oxidized LDL also triggers an inflammatory process that accelerates the formation of atherosclerotic plaques.

In atherosclerosis, vascular smooth muscle cells are involved in the stability of the plaque as they contribute to the formation of the fibrous cap. It is reported that Ang II triggers vascular smooth muscle cells to proliferate and migrate to the outer layer of the atherosclerotic plaques, where they produce growth factors and extracellular matrix proteins.[21, 79] With the secretion of extracellular matrix components by smooth muscle cells, the plaques increase in size and eventually become occlusive resulting in the occurrence of acute complications. Thus, inhibition of smooth muscle cell migration and proliferation may be beneficial to prevent early lesion formation, though, it might influence the stability of the plaque at the same time.

The progression of atherosclerosis is considered to be inflammation-driven, as advanced lesions of atherosclerosis are predominantly constituted of macrophages and lymphocytes. As mentioned, activation of the RAS increases the expression of adhesion molecules and pro-inflammatory chemokines and cytokines, leading to the recruitment and activation of various inflammatory cells into the vessel wall.[80] For example, Ang II activates nuclear factor κB (NFκB) which promotes the expression of adhesion molecules such as vascular cell adhesion molecule-1, intercellular adhesion molecule-1, E-selectin, and chemoattractant proteins such as monocyte chemoattractant protein-1.[81] Moreover, a study by Daugherty et al. shows that Ang II infusion in mice promoted rapid formation

of atherosclerotic plaques, and that these lesions were mainly dominated by lipid-laden macrophages and lymphocytes.[82] In addition, transiently heightened levels of Ang II in apolipoprotein E-deficient mice already caused a profound increase in atherosclerosis, attributable to stimulated expression of various immunological markers, including monocyte chemoattractant protein-1.[83] Ang II was also found to induce interleukin-6 expression in cultured vascular smooth muscle cells[84] and in advanced atherosclerotic lesions Ang II stimulates the expression of matrix metalloproteinase and plasminogen activator inhibitor-1, which leads to the destabilization of these plaques.[76, 85] Thus, Ang II stimulates the interaction between vascular cells and leukocytes contributing to the pathophysiology of atherosclerosis.

2.4 Aging: a key player in vascular damage

Aging is a natural biological process that is associated with diverse detrimental changes in cells and tissues resulting in an increased risk of health complications and disease with increasing age. As such, with age, various cardiovascular diseases including heart failure, myocardial infarction, atherosclerosis and hypertension increase tremendously.[86] During aging, a general decline in organ function occurs, and alterations in structure and function of the heart and the vasculature will eventually affect cardiovascular performance. For instance, elderly people are more affected by cardiac rhythm disturbances such as atrial fibrillation and most often have a reduced cardiac output. Additionally, age-related changes in the vasculature often relate to arterial stiffening, atherosclerosis, as well as an increased blood pressure. Whether the prevalence of cardiovascular disorders in the elderly is due to the aging process or whether these disorders occur more frequently because of longer exposure to risk factors is not well-defined yet. Research has shown that age-associated changes in structure and function of the vasculature share similarities with vascular changes seen in early stages of cardiovascular disease.[87, 88] With aging, the vessel wall gradually thickens and becomes stiffer, accompanied by impairment of vascular tone due to endothelial dysfunction. Moreover, age-related vascular damage is associated with increased extracellular matrix deposition, apoptosis, cell senescence and fibrosis.[89-91] The mechanisms underlying age-related vascular disease involve multiple factors and pathways, including oxidative stress, mechanical fatigue and environmental factors (e.g. food intake and diet). Further, it is reported that the systemic RAS is suppressed during normal aging. However, the activity of tissue RAS is not well defined yet. Research has shown that during aging, ACE is increased in vascular smooth muscle cells as well as vascular endothelial cells.[92-94] Additionally, upregulation of chymase is observed in the vessel wall during aging.[93] Although chymase is capable of converting Ang I to Ang II *in vitro*, its role *in vivo* is still controversial.[95, 96] Microarray analysis confirmed the upregulation of several genes within the RAS pathway in the vessel wall of aged mice.[97] Consequently, Ang II

is increased in the vasculature during advanced aging and was found to induce arterial remodeling in young animals, which mimicked features of vascular aging.[98]

2.4.1 The involvement of RAS components in aging and the effect on vascular damage

During aging, dysfunction of both endothelial cells as well as vascular smooth muscle cells occurs. Advanced aging leads to impaired endothelial nitric oxide synthesis resulting in a decline in endothelium-dependent vascular dilatation and eventually vascular stiffness.[99, 100] Additionally, the endothelial barrier becomes porous allowing the migration of vascular smooth muscle cells into the intima layer of the vessel wall where they proliferate and deposit extracellular matrix proteins resulting in vessel wall thickening. It is demonstrated that Ang II induces expression and activation of matrix metalloproteinase 2 and calpain-1 in the arterial wall, which has been linked to an age-related increase in migration capacity of vascular smooth muscle cells.[98, 101] The migration of these vascular smooth muscle cells is accompanied by Ang II-mediated increase in TGF-β-1 activity and collagen deposition, leading to thickening of the vessel wall mimicking features of the aging vasculature.[98] Furthermore, Kunieda and co-workers showed that Ang II signaling promotes a vascular aging phenotype by inducing vascular cell senescence.[102]

It has been proposed that a prominent cause of aging is the accumulation of unrepaired DNA damage[103-105], and considerable evidence supports a crucial role of DNA damage in the development of vascular disease, especially atherosclerosis.[106] DNA damage can be induced by exogenous and endogenous sources, including reactive oxygen species. It has been widely postulated that oxidative stress is a major determinant of lifespan, as it triggers mitochondrial dysfunction and cellular injury by targeting DNA, protein, lipids and other components of the cell, and thus is causatively involved in the aging process.[25, 107, 108] Oxidative stress not only leads to accumulation of reactive oxygen species but can also modify or damage DNA, processes known to be involved in aging. Research has linked enhanced reactive oxygen species to many age-related degenerative diseases including atherosclerosis, stroke and heart disease. Locally, an unbalance in reactive oxygen species can have deleterious effects as it can disturb cell signaling and can trigger apoptosis, cellular senescence and inflammation. It has been demonstrated that the RAS plays a role in age-related upregulation of reactive oxygen species, as increased Ang II/AT_1 receptor signaling activates NAD(P)H, leading to increased reactive oxygen species production in both vascular endothelial cells and vascular smooth muscle cells.[109] Benigni et al. reported that disruption of the AT_1 receptor in mice promotes longevity, probably through reduced oxidative stress and overexpression of pro-survival genes.[110] During aging, these mice also develop less atherosclerotic plaques and cardiac injury. As mentioned, oxidative stress also modifies and/or damages DNA, leading to altered gene expression which contributes to the aging process. As such, it was shown that Ang II induces DNA damage in epithelial human and porcine kidney cell lines, as well as in isolated mouse kidneys.[111, 112] In addition,

Ang II-induced reactive oxygen species results in DNA damage, leading to senescence and an accelerated aging phenotype of vascular smooth muscle cells.[102, 113] Thus, Ang II increases oxidative stress in the vasculature which leads to cell and organ deterioration, thereby accelerating the aging process resulting in an increased risk for vascular disease.

Moreover, mitochondrial dysfunction represents a common feature of the aging process. Mitochondria itself are a major source of reactive oxygen species during aging, and age-related mitochondrial dysfunction closely correlates with enhanced mitochondrial reactive oxygen species production reviewed by.[114, 115] reactive oxygen species production by mitochondria contributes to Ang II-induced vascular alterations and dysfunction[116] and Ang II blockade can protect against age-related mitochondrial dysfunction.[117] A schematic representation of this interaction is given in Figure 4. Furthermore, transgenic mice over-expressing mitochondrial superoxide dismutase 2, the critical scavenger of mitochondrial reactive oxygen species, demonstrated attenuated Ang II-induced hypertension and vascular oxidative stress.[28]

2.4.2 The role of RAS and aging in atherosclerosis

Especially atherosclerosis is an age-related disease as the prevalence and severity of atherosclerosis strikingly increase with age. There is evidence of accelerated cellular aging in atherosclerosis which includes impaired proliferation, cell senescence and DNA damage.[118] It was also found by Wang et al. that age-associated arterial remodeling and the development and progression of experimental atherosclerosis in young animals share common mechanisms, such as increased matrix metalloproteinase activity and Ang II signaling.[93] Moreover, it is suggested that aging prolongs the exposure to risk factors, which can cause increased production of reactive oxygen species within the vessel wall and the atherosclerotic plaque.

2.5 The role of RAS in age-associated gender differences in vascular disease

Growing evidence suggests that the development of vascular disease in women is different from that in men. Sex hormones play a key role in the gender-associated difference in pathophysiology of cardiovascular diseases.[119] Young, premenopausal women have a lower cardiovascular risk compared to men, which points to estrogen as a protective factor. For instance, blood pressure is found to be higher in men compared to age-matched women, while after menopause blood pressure rises sharply in women, again suggestive for a role of estrogen.[120] Furthermore, in menopausal and aged female rats, age-related vascular dysfunction is increased due to lack of estrogen.[121, 122] Moreover, studies have shown that estrogen is involved in regulation of the RAS: estrogens increase angiotensinogen and AT_2 receptor density, while they decrease renin, ACE and AT_1 receptor density.[123] In animal models of menopause, chronic replacement of estrogen reduces ACE activity in the aorta.[124, 125] Hence, as estrogen inhibits ACE expression in the vasculature[124], it subsequently reduces

the production of Ang II. Additionally, estrogen weakens the response and expression of the AT_1 receptor in the heart and the aorta.[126, 127] Thus, loss of estrogen production with menopause is associated with increased RAS signaling, leading to an increased risk for developing vascular disease.

Research has shown that the systemic RAS is suppressed during normal aging, which could be related to an increase in systolic blood pressure as described in the elderly.[128, 129] An increase in blood pressure during aging may suppress renin release from the kidney due to a higher perfusion pressure at the juxtaglomerular cells, contributing to the decline in circulating RAS. However, the activity of tissue RAS during aging is not yet well-defined. In humans, increased levels of Ang II, AT_1 receptor, ACE and adventitial chymase are found in the aortic wall of older donors.[94] Activation of these components not only leads to elevated blood pressure, but also results in harmful effect on the vasculature. These results are consistent with findings in postmenopausal women, and in men mentioned above, when compared to premenopausal women. Though it is known that aging exerts different effects on males compared to females, the precise actions of aging on the RAS and gender in different tissues are not well-established yet, and should be further elucidated.

3. THERAPEUTIC APPROACHES TO TARGET RAS IN VASCULAR DISEASE

Current medical therapies for managing Ang II-associated vascular diseases include β–blockers, statins, diuretics, calcium channel blockers and RAS inhibitors. In recent years, components of the RAS have become important targets in cardiovascular disease. Inhibition of the RAS is recommended for managing most of the cardiovascular diseases, such as hypertension, heart failure, acute myocardial infarction and stroke. Therapeutic interventions that control the effects of the RAS are often used for treatment of high blood pressure, particularly in young patients. In addition to their blood pressure-lowering effects, RAS inhibitors are also suggested to have additional cardioprotective effects. Both animal and human studies show that RAS blockade not only lowers blood pressure but may also prevent age-related structural and functional alterations in several organs.[130]

3.1 Current RAS-related therapeutic interventions for age-related vascular disease

There are several classes of RAS inhibitors available, including ACE inhibitors, angiotensin receptor blockers, direct renin inhibitors and mineralocorticoid receptor antagonists. All four of these inhibitors interrupt the formation or block the effect of Ang II and/or aldosterone. Monotherapy using ACE inhibitors cannot completely block the persistent activation of the RAS, due to either renin upregulation and/or the existence of ACE-independent pathways that convert Ang I to Ang II. Therefore, dual RAS blockade, in particular by combining ACE inhibitors and angiotensin receptor blockers, has been proposed in patients

with cardiovascular and renal disease, to obtain a more complete blockade of the RAS. Because of the reported deleterious effects of Ang II on cardiovascular tissue, it seems logical to target the RAS and thereby reduce the development of cardiovascular damage.

Several studies already demonstrated that ACE inhibitors might inhibit atherosclerosis in animal models independent of blood pressure lowering.[131-133] Additionally, renin inhibition and angiotensin receptor blockers reduced atherosclerotic lesion size in cholesterol fed mice susceptible for atherosclerosis.[134-137] Moreover, research in aneurysmal mouse models has shown that inhibition of the RAS reduces the formation and progression of aortic aneurysms. Inhibition and/or blockade of the RAS reduces the incidence, progression and mortality in mouse models of abdominal aortic aneurysms.[138, 139] Especially in mouse models of thoracic aortic aneurysms, inhibition of the RAS by AT_1 receptor blockade (by losartan) or TGF-β-signaling (by TGF-β-neutralizing antibodies) effectively blocks the production of downstream TGF-β and thereby inhibits aortic root dilatation and aneurysm formation.[46-48] This new mechanism of decreased TGF-β-signaling by blocking the RAS has initiated numerous clinical trials and different aneurysmal mouse model studies to investigate the potency of RAS blockade.[140, 141] Yet, the efficacy of several Ang II receptor blockers varies between different animal models and patients with aneurysm disease[142, 143], indicating that further investigation into the role of RAS targeting in cardiovascular disease is warranted.

Controversy remains as research has shown that dual RAS blockade gave conflicting results in different patient populations and was associated with adverse side effects. Combination of ACE inhibitors with angiotensin receptor blockers in the elderly with cardiovascular complications, is linked to an increased risk of adverse renal outcomes with higher rate of hyperkalemia, renal dysfunction and no observed benefit with respect to overall mortality.[144-147] Additionally, several clinical studies on dual RAS blockade were terminated early due to adverse side effects, implying that dual RAS blockade is not recommended. This might relate to the fact that a certain level of RAS activity is still required for proper physiological functioning of tissues, e.g., in the kidney[148], and that blockade of the RAS should be optimal rather than maximal. Moreover, some patients fail to respond positively to these treatments. As described above, variation exists in RAS between men and women but also at different ages, which complicates the prediction of how elderly will react to therapeutic intervention strategies for vascular disease. Thus, blocking and/or inhibiting the RAS should take disease, age and gender into account.[149]

Although the standard therapeutic interventions to control the effects of RAS activation, i.e. ACE inhibitors, angiotensin receptor blockers, direct renin inhibitors and mineralocorticoid receptor antagonists, are effective in controlling the progression of vascular disease in some patients, they are not effective in preventing the onset of new cardiovascular diseases, and vascular disease still persists as a leading cause of illness and death. Moreover, many RAS inhibiting therapies are not 100 percent effective in all patients and additionally give adverse side effects. Thus, it is necessary to identify bet-

ter therapeutic targets and strategies, which more successfully prevent and/or slow the progression of age-related vascular disease.

3.2 Indirect modulation of RAS in vascular disease: caloric restriction and anti-oxidants

One of the best anti-aging strategies so far has been shown to be associated with diet intake. Research has discovered that our diet has a great impact on life span and age-related diseases. Caloric restriction, defined as a reduction of 70% in calorie intake without malnutrition, has been shown to be the most potent strategy to slow the aging process and it extends life span in different short lived species, such as mice and rats. Moreover, caloric restriction has as number of beneficial effects on the aging cardiovascular system (reviewed by Weiss and Fontana).[150] In rhesus monkeys it has been shown that caloric restriction delays the onset of age-associated pathologies, which not only prolongs lifespan but also protects against the onset of cardiovascular disease.[151] The biological mechanisms that induce the beneficial effects include modifications in energy metabolism and insulin sensitivity, increased oxidative stress resistance, reduced production of mitochondria-derived reactive oxygen species and reduced inflammation.[152-154] In the vasculature, caloric restriction also enhances endothelial function and reduces the size and progression of atherosclerotic plaque formation in apolipoprotein E-deficient mice.[155] Furthermore, in the aorta it was shown that caloric restriction not only attenuates the production of reactive oxygen species and oxidative damage, but it also increases levels of the endogenous antioxidant glutathione and ascorbate.[156] Additionally, Finckenberg et al. showed that caloric restriction effectively ameliorates Ang II-induced mitochondrial remodeling and cardiac hypertrophy in transgenic rats expressing human renin and angiotensin genes, leading to a reduction in overall mortality.[157] This study also showed that caloric restriction attenuates fibrosis and cardiomyocyte apoptosis. Even though not much is known about the effect of caloric restriction on Ang II-induced vascular damage, it is suggested that caloric restriction may have beneficial effects as it attenuates oxidative damage, enhances endothelial function and preserves mitochondrial function, processes known to be negatively influenced by Ang II signaling.

Still, a caloric restriction diet does not have the same impact on life span in humans, possibly due to the fact that most people would not submit to such a rigorous dietary program. Therefore, research is aimed at determining the feasibility and efficacy of caloric restriction mimetics, both drugs and natural compounds, without lowering caloric intake. Resveratrol is one of the compounds that mimics the cardiovascular protective effects of calorie restriction, including the attenuation of mitochondrial oxidative stress in coronary arterial endothelial cells.[158, 159] Currently, several studies are in progress investigating the effect of caloric restriction and different caloric restriction mimetics in humans.[160, 161] Regardless of the results of these studies, a healthy, balanced and sensible diet combined with enough physical activity, is still very important to maintain overall health.[162]

Additionally, to improve current medical therapies for managing Ang II-associated cardiovascular disease, attention has been placed on antioxidant-based therapies and reactive oxygen species scavenging molecules to decrease oxidative stress associated with vascular damage. Overproduction of reactive oxygen species has been shown to be an important factor in the development of age-related cardiovascular diseases. As mentioned, reactive oxygen species plays a central role in cellular signaling when maintained at normal tissue levels, while during times of cell stress, excessive amounts of reactive oxygen species cause harmful effects on the vasculature. Increased levels of reactive oxygen species have been implicated in the pathogenesis of diverse diseases including cancer, diabetes mellitus, atherosclerosis and aging. During aging, the production of reactive oxygen species is increased, while some of the endogenous defense mechanisms decrease, leading to progressive damage of cellular structures and eventually an aging phenotype. As mentioned, especially mitochondrial-derived reactive oxygen species play an important role in aging and age-related cardiovascular disease.[163, 164] Therefore, it is logical to suggest that application of antioxidants or reactive oxygen species scavengers could be useful in the treatment of age-related vascular disease. Research already demonstrated that several RAS inhibitors have an antioxidant effect. In clinical studies, it is shown that administration of AT_1 receptor blocker candesartan mediates an antioxidant effect, resulting in less oxidative stress and inflammation, independent from its effect on blood pressure.[165]

Antioxidant therapies or reactive oxygen species scavengers may have an additional advantage over the current RAS therapies, because they can prevent vascular damage by direct interaction with reactive oxygen species, not only those produced by Ang II, but also by inflammatory cells or through the regulation of reactive oxygen species-dependent molecular signaling cascades. Several clinical trials and animal models of cardiovascular diseases have focused on antioxidant-based therapies to decrease oxidative stress. Strategies to deliver antioxidants include gene therapy, dietary sources, low-molecular-weight free radical scavengers, polyethylene glycol conjugation, and nanomedicine-based technologies, as reviewed recently by.[22] Although many studies have shown therapeutic benefits for monotherapy with antioxidant use on vascular disease, others have failed to show any beneficial effects. This might be because of incorrect dosing, the lack of interaction between the antioxidant and reactive oxygen species or due to the fact that a state of 'antioxidative' stress can occur, in which the antioxidants attenuate or block adaptive stress responses.[166] Thus, specific targeting of cells and locations where oxidative stress occurs might improve the efficacy of antioxidant therapies.

3.3 Combining RAS blockade with reactive oxygen species inhibition

Considering the above, combined inhibition of reactive oxygen species and RAS would be expected to have further beneficial effects on vascular damage, to a greater degree than RAS inhibition alone. Not only reactive oxygen species produced by Ang II signaling

via the AT_1 receptor will be reduced, but also reactive oxygen species produced by other sources which are independent of RAS signaling, including inflammatory cells and high pressure-derived reactive oxygen species. Indeed, recently it was shown that combining a mitochondria-targeted antioxidant, $MitoQ_{10}$, with an angiotensin receptor blocker, losartan, has an additive therapeutic benefit on attenuating development of hypertension and reducing left ventricular hypertrophy in stroke-prone spontaneously hypertensive rats.[167] Thus, combined RAS/reactive oxygen species blocking therapy might be a new strategy to prevent cardiovascular events.

4. CONCLUSION

Clearly, the RAS plays a critical role in the pathogenesis of many types of age-related vascular diseases. This review discussed that the RAS is involved in components that contribute to the development and progression of vascular disease; i.e. extracellular matrix defects, atherosclerosis and aging. Oxidative stress seems to be related to all of these components, subsequently contributing to the onset of vascular disease. Though, the precise mechanisms by which these components induce vascular damage still need further study.

Yet, it is not entirely clear which pathogenic mechanism should be targeted and which treatments should be used in prevention of cardiovascular events. Although numerous RAS inhibiting therapies have been developed and used in clinical settings for treatment of cardiovascular disease, they are not 100 percent effective in all patients and, particularly when given in combination, give rise to adverse side effects, including hyperkalemia and renal dysfunction. Moreover, the regulation of the RAS in the elderly is not fully understood yet and should be further explored, as many vascular diseases are age-related. Thus, it is necessary to further explore optimal strategies of (combined) RAS blockade to prevent or stop the progression of vascular disease. It would be particularly interesting to test the efficacy of combined RAS/reactive oxygen species suppressing therapy on cardiovascular disease in animal models of aging, as it might give further beneficial effects on the vasculature.

ACKNOWLEDGEMENT

This work was supported by the 'Lijf en Leven' grant (2011-2015): 'Dilating versus stenosing arterial disease' (to BvT, IvdP, JE).

REFERENCES

1. Gibbons GH. The pathophysiology of hypertension - the importance of angiotensin ii in cardiovascular remodeling. *Am J Hypertens*. 1998;11:177s-181s
2. AbdAlla S, Lother H, Abdel-tawab AM, Quitterer U. The angiotensin ii at(2) receptor is an at(1) receptor antagonist. *J Biol Chem*. 2001;276:39721-39726
3. Verdonk K, Danser AHJ, van Esch JHM. Angiotensin ii type 2 receptor agonists: Where should they be applied? *Expert Opin Inv Drug*. 2012;21:501-513
4. Dzau VJ. Tissue angiotensin and pathobiology of vascular disease - a unifying hypothesis. *Hypertension*. 2001;37:1047-1052
5. Kanaide H, Ichiki T, Nishimura J, Hirano K. Cellular mechanism of vasoconstriction induced by angiotensin ii - it remains to be determined. *Circ Res*. 2003;93:1015-1017
6. Unger T. The role of the renin-angiotensin system in the development of cardiovascular disease. *Am J Cardiol*. 2002;89:3A-9A
7. Hunyady L, Catt KJ. Pleiotropic at1 receptor signaling pathways mediating physiological and pathogenic actions of angiotensin ii. *Molecular Endocrinology*. 2006;20:953-970
8. Batenburg WW, Garrelds IM, Bernasconi CC, Juillerat-Jeanneret L, van Kats JP, Saxena PR, Danser AHJ. Angiotensin ii type 2 receptor - mediated vasodilation in human coronary microarteries. *Circulation*. 2004;109:2296-2301
9. Moltzer E, Verkuil AVA, van Veghel R, Danser AHJ, van Esch JHM. Effects of angiotensin metabolites in the coronary vascular bed of the spontaneously hypertensive rat loss of angiotensin ii type 2 receptor-mediated vasodilation. *Hypertension*. 2010;55:516-522
10. You D, Loufrani L, Baron C, Levy BI, Widdop RE, Henrion D. High blood pressure reduction reverses angiotensin ii type 2 receptor-mediated vasoconstriction into vasodilation in spontaneously hypertensive rats. *Circulation*. 2005;111:1006-1011
11. Busche S, Gallinat S, Bohle RM, Reinecke A, Seebeck J, Franke F, Fink L, Zhu MY, Sumners C, Unger T. Expression of angiotensin at(1) and at(2) receptors in adult rat cardiomyocytes after myocardial infarction - a single-cell reverse transcriptase-polymerase chain reaction study. *Am J Pathol*. 2000;157:605-611
12. Xu J, Sun Y, Carretero OA, Zhu LP, Harding P, Shesely EG, Dai XG, Rhaleb NE, Peterson E, Yang XP. Effects of cardiac overexpression of the angiotensin ii type 2 receptor on remodeling and dysfunction in mice post-myocardial infarction. *Hypertension*. 2014;63:1251-1259
13. Madamanchi NR, Vendrov A, Runge MS. Oxidative stress and vascular disease. *Arterioscl Throm Vas*. 2005;25:29-38
14. Sugamura K, Keaney JF. Reactive oxygen species in cardiovascular disease. *Free Radical Bio Med*. 2011;51:978-992
15. Montezano AC, Touyz RM. Reactive oxygen species, vascular noxs, and hypertension: Focus on translational and clinical research. *Antioxid Redox Sign*. 2014;20:164-182
16. Virdis A, Neves MF, Amiri F, Touyz RM, Schiffrin EL. Role of nad(p)h oxidase on vascular alterations in angiotensin ii-infused mice. *J Hypertens*. 2004;22:535-542
17. Madamanchi NR, Runge MS. Mitochondrial dysfunction in atherosclerosis. *Circ Res*. 2007;100:460-473
18. Mahmoudi M, Mercer J, Bennett M. DNA damage and repair in atherosclerosis. *Cardiovasc Res*. 2006;71:259-268
19. Nickenig G, Harrison DG. The at(1)-type angiotensin receptor in oxidative stress and atherogenesis - part ii: At(1) receptor regulation. *Circulation*. 2002;105:530-536

20. Rajagopalan S, Kurz S, Munzel T, Tarpey M, Freeman BA, Griendling KK, Harrison DG. Angiotensin ii-mediated hypertension in the rat increases vascular superoxide production via membrane nadh/nadph oxidase activation - contribution to alterations of vasomotor tone. *J Clin Invest*. 1996;97:1916-1923
21. Touyz RM, Schiffrin EL. Signal transduction mechanisms mediating the physiological and pathophysiological actions of angiotensin ii in vascular smooth muscle cells. *Pharmacol Rev*. 2000;52:639-672
22. Rosenbaugh EG, Savalia KK, Manickam DS, Zimmerman MC. Antioxidant-based therapies for angiotensin ii-associated cardiovascular diseases. *Am J Physiol-Reg I*. 2013;304:R917-R928
23. Nickenig G, Strehlow K, Baumer AT, Baudler S, Wassmann S, Sauer H, Bohm M. Negative feedback regulation of reactive oxygen species on at1 receptor gene expression. *Brit J Pharmacol*. 2000;131:795-803
24. Wassmann S, Nickenig G. Pathophysiological regulation of the at(1)-receptor and implications for vascular disease. *J Hypertens*. 2006;24:S15-S21
25. Doughan AK, Harrison DG, Dikalov SI. Molecular mechanisms of angiotensin ii-mediated mitochondrial dysfunction - linking mitochondrial oxidative damage and vascular endothelial dysfunction. *Circ Res*. 2008;102:488-496
26. de Cavanagh EM, Ferder M, Inserra F, Ferder L. Angiotensin ii, mitochondria, cytoskeletal, and extracellular matrix connections: An integrating viewpoint. *American Journal of Physiology - Heart & Circulatory Physiology*. 2009;296:H550-558
27. Kimura S, Zhang GX, Nishiyama A, Shokoji T, Yao L, Fan YY, Rahman M, Abe Y. Mitochondria-derived reactive oxygen species and vascular map kinases: Comparison of angiotensin ii and diazoxide. *Hypertension*. 2005;45:438-444
28. Dikalova AE, Bikineyeva AT, Budzyn K, Nazarewicz RR, McCann L, Lewis W, Harrison DG, Dikalov SI. Therapeutic targeting of mitochondrial superoxide in hypertension. *Circ Res*. 2010;107:106-U221
29. Gutierrez J, Ballinger SW, Darley-Usmar VM, Landar A. Free radicals, mitochondria, and oxidized lipids - the emerging role in signal transduction in vascular cells. *Circ Res*. 2006;99:924-932
30. Wagenseil JE, Mecham RP. Vascular extracellular matrix and arterial mechanics. *Physiological Reviews*. 2009;89:957-989
31. Bateman JF, Boot-Handford RP, Lamande SR. Genetic diseases of connective tissues: Cellular and extracellular effects of ecm mutations. *Nature Reviews Genetics*. 2009;10:173-183
32. Newby AC. Do metalloproteinases destabilize vulnerable atherosclerotic plaques? *Current Opinion in Lipidology*. 2006;17:556-561
33. Jeremy RW, Huang H, Hwa J, McCarron H, Hughes CF, Richards JG. Relation between age, arterial distensibility, and aortic dilatation in the marfan syndrome. *Am J Cardiol*. 1994;74:369-373
34. Hanada K, Vermeij M, Garinis GA, de Waard MC, Kunen MG, Myers L, Maas A, Duncker DJ, Meijers C, Dietz HC, Kanaar R, Essers J. Perturbations of vascular homeostasis and aortic valve abnormalities in fibulin-4 deficient mice. *Circ Res*. 2007;100:738-746
35. Lacolley P, Regnault V, Nicoletti A, Li ZL, Michel JB. The vascular smooth muscle cell in arterial pathology: A cell that can take on multiple roles. *Cardiovasc Res*. 2012;95:194-204
36. Kato H, Suzuki H, Tajima S, Ogata Y, Tominaga T, Sato A, Saruta T. Angiotensin ii stimulates collagen synthesis in cultured vascular smooth muscle cells. *J Hypertens*. 1991;9:17-22

37. Sharifi BG, LaFleur DW, Pirola CJ, Forrester JS, Fagin JA. Angiotensin ii regulates tenascin gene expression in vascular smooth muscle cells. *J Biol Chem*. 1992;267:23910-23915
38. Tamura K, Nyui N, Tamura N, Fujita T, Kihara M, Toya Y, Takasaki I, Takagi N, Ishii M, Oda K, Horiuchi M, Umemura S. Mechanism of angiotensin ii-mediated regulation of fibronectin gene in rat vascular smooth muscle cells. *J Biol Chem*. 1998;273:26487-26496
39. Kim S, Ohta K, Hamaguchi A, Omura T, Tominaga K, Yukimura T, Miura K, Tanaka M, Iwao H. At1 receptor-mediated stimulation by angiotensin ii of rat aortic fibronectin gene expression in vivo. *Br J Pharmacol*. 1994;113:662-663
40. Gibbons GH, Pratt RE, Dzau VJ. Vascular smooth muscle cell hypertrophy vs. Hyperplasia. Autocrine transforming growth factor-beta 1 expression determines growth response to angiotensin ii. *J Clin Invest*. 1992;90:456-461
41. Naftilan AJ, Pratt RE, Eldridge CS, Lin HL, Dzau VJ. Angiotensin ii induces c-fos expression in smooth muscle via transcriptional control. *Hypertension*. 1989;13:706-711
42. Williams B, Baker AQ, Gallacher B, Lodwick D. Angiotensin ii increases vascular permeability factor gene expression by human vascular smooth muscle cells. *Hypertension*. 1995;25:913-917
43. Delafontaine P, Lou H. Angiotensin ii regulates insulin-like growth factor i gene expression in vascular smooth muscle cells. *J Biol Chem*. 1993;268:16866-16870
44. Hamaguchi A, Kim S, Izumi Y, Zhan Y, Yamanaka S, Iwao H. Contribution of extracellular signal-regulated kinase to angiotensin ii-induced transforming growth factor-beta1 expression in vascular smooth muscle cells. *Hypertension*. 1999;34:126-131
45. Feener EP, Northrup JM, Aiello LP, King GL. Angiotensin ii induces plasminogen activator inhibitor-1 and -2 expression in vascular endothelial and smooth muscle cells. *J Clin Invest*. 1995;95:1353-1362
46. Habashi JP, Doyle JJ, Holm TM, Aziz H, Schoenhoff F, Bedja D, Chen YC, Modiri AN, Judge DP, Dietz HC. Angiotensin ii type 2 receptor signaling attenuates aortic aneurysm in mice through erk antagonism. *Science*. 2011;332:361-365
47. Habashi JP, Judge DP, Holm TM, Cohn RD, Loeys BL, Cooper TK, Myers L, Klein EC, Liu GS, Calvi C, Podowski M, Neptune ER, Halushka MK, Bedja D, Gabrielson K, Rifkin DB, Carta L, Ramirez F, Huso DL, Dietz HC. Losartan, an at1 antagonist, prevents aortic aneurysm in a mouse model of marfan syndrome. *Science*. 2006;312:117-121
48. Moltzer E, Riet LT, Swagemakers SMA, van Heijningen PM, Vermeij M, van Veghel R, Bouhuizen AM, van Esch JHM, Lankhorst S, Ramnath NWM, de Waard MC, Duncker DJ, van der Spek PJ, Rouwet EV, Danser AHJ, Essers J. Impaired vascular contractility and aortic wall degeneration in fibulin-4 deficient mice: Effect of angiotensin ii type 1 (at(1)) receptor blockade. *Plos One*. 2011;6
49. Verrecchia F, Mauviel A. Transforming growth factor-beta and fibrosis. *World J Gastroentero*. 2007;13:3056-3062
50. Intengan HD, Schiffrin EL. Vascular remodeling in hypertension - roles of apoptosis, inflammation, and fibrosis. *Hypertension*. 2001;38:581-587
51. Isselbacher EM. Thoracic and abdominal aortic aneurysms. *Circulation*. 2005;111:816-828
52. Dietz HC, Cutting GR, Pyeritz RE, Maslen CL, Sakai LY, Corson GM, Puffenberger EG, Hamosh A, Nanthakumar EJ, Curristin SM, Stetten G, Meyers DA, Francomano CA. Marfan-syndrome caused by a recurrent denovo missense mutation in the fibrillin gene. *Nature*. 1991;352:337-339
53. Daugherty A, Cassis LA, Lu H. Complex pathologies of angiotensin ii-induced abdominal aortic aneurysms. *J Zhejiang Univ-Sc B*. 2011;12:624-628

54. Lu H, Rateri DL, Bruemmer D, Cassis LA, Daugherty A. Involvement of the renin-angiotensin system in abdominal and thoracic aortic aneurysms. *Clin Sci*. 2012;123:531-543
55. Virmani R, Burke AP, Farb A, Kolodgie FD. Pathology of the unstable plaque. Progress in Cardiovascular Diseases. 2002;44:349-356
56. Libby P, Theroux P. Pathophysiology of coronary artery disease. *Circulation*. 2005;111:3481-3488
57. Sata M, Fukuda D. Crucial role of renin-angiotensin system in the pathogenesis of atherosclerosis. *J Med Invest*. 2010;57:12-25
58. Schmidt-Ott KM, Kagiyama S, Phillips MI. The multiple actions of angiotensin ii in atherosclerosis. *Regul Peptides*. 2000;93:65-77
59. Fraga-Silva RA, Costa-Fraga FP, Murca TM, Moraes PL, Lima AM, Lautner RQ, Castro CH, Soares CMA, Borges CL, Nadu AP, Oliveira ML, Shenoy V, Katovich MJ, Santos RAS, Raizada MK, Ferreira AJ. Angiotensin-converting enzyme 2 activation improves endothelial function. *Hypertension*. 2013;61:1233-+
60. Lovren F, Pan Y, Quan A, Teoh H, Wang GL, Shukla PC, Levitt KS, Oudit GY, Al-Omran M, Stewart DJ, Slutsky AS, Peterson MD, Backx PH, Penninger JM, Verma S. Angiotensin converting enzyme-2 confers endothelial protection and attenuates atherosclerosis. *Am J Physiol-Heart C*. 2008;295:H1377-H1384
61. Aono J. Deletion of the angiotensin ii type 1a receptor prevents atherosclerotic plaque rupture in apolipoprotein e-/- mice (vol 32, pg 1453, 2012). *Arterioscl Throm Vas*. 2014;34:E18-E18
62. Cheng C, Tempel D, van Haperen R, van Damme L, Algur M, Krams R, de Crom R. Activation of mmp8 and mmp13 by angiotensin ii correlates to severe intra-plaque hemorrhages and collagen breakdown in atherosclerotic lesions with a vulnerable phenotype. *Atherosclerosis*. 2009;204:26-33
63. Mazzolai L, Duchosal MA, Korber M, Bouzourene K, Aubert JF, Hao H, Vallet V, Brunner HR, Nussberger J, Gabbiani G, Hayoz D. Endogenous angiotensin ii induces atherosclerotic plaque vulnerability and elicits a th1 response in apoe(-/-) mice. *Hypertension*. 2004;44:277-282
64. da Cunha V, Martin-McNulty B, Vincelette J, Choy DF, Li WW, Schroeder M, Mahmoudi M, Halks-Miller M, Wilson DW, Vergona R, Sullivan ME, Wang YX. Anglotensin ii induces histomorphologic features of unstable plaque in a murine model of accelerated atherosclerosis. *J Vasc Surg*. 2006;44:364-371
65. Libby P, Ridker PM, Hansson GK. Progress and challenges in translating the biology of atherosclerosis. *Nature*. 2011;473:317-325
66. Touyz RM. Reactive oxygen species and angiotensin ii signaling in vascular cells - implications in cardiovascular disease. *Braz J Med Biol Res*. 2004;37:1263-1273
67. Schieffer B, Schieffer E, Hilfiker-Kleiner D, Hilfiker A, Kovanen PT, Kaartinen M, Nussberger J, Harringer W, Drexler H. Expression of angiotensin ii and interleukin 6 in human coronary atherosclerotic plaques - potential implications for inflammation and plaque instability. *Circulation*. 2000;101:1372-1378
68. Warnholtz A, Nickenig G, Schulz E, Macharzina R, Brasen JH, Skatchkov M, Heitzer T, Stasch JP, Griendling KK, Harrison DG, Bohm M, Meinertz T, Munzel T. Increased nadh-oxidase-mediated superoxide production in the early stages of atherosclerosis - evidence for involvement of the renin-angiotensin system. *Circulation*. 1999;99:2027-2033
69. Sorescu D, Weiss D, Lassegue B, Clempus RE, Szocs K, Sorescu GP, Valppu L, Quinn MT, Lambeth JD, Vega JD, Taylor WR, Griendling KK. Superoxide production and expression of nox family proteins in human atherosclerosis. *Circulation*. 2002;105:1429-1435

70. Seto SW, Krishna SM, Yu HY, Liu D, Khosla S, Golledge J. Impaired acetylcholine-induced endothelium-dependent aortic relaxation by caveolin-1 in angiotensin ii-infused apolipoprotein-e (apoe(-/-)) knockout mice. *Plos One*. 2013;8
71. Shatanawi A, Romero MJ, Iddings JA, Chandra S, Umapathy NS, Verin AD, Caldwell RB, Caldwell RW. Angiotensin ii-induced vascular endothelial dysfunction through rhoa/rho kinase/p38 mitogen-activated protein kinase/arginase pathway. *Am J Physiol-Cell Ph*. 2011;300:C1181-C1192
72. Weiss D, Sorescu D, Taylor WR. Angiotensin ii and atherosclerosis. *Am J Cardiol*. 2001;87:25c-32c
73. Pueyo ME, Gonzalez W, Nicoletti A, Savoie F, Arnal JF, Michel JB. Angiotensin ii stimulates endothelial vascular cell adhesion molecule-1 via nuclear factor-kappa b activation induced by intracellular oxidative stress. *Arterioscl Throm Vas*. 2000;20:645-651
74. Tummala PE, Chen XL, Sundell CL, Laursen JB, Hammes CP, Alexander RW, Harrison DG, Medford RM. Angiotensin ii induces vascular cell adhesion molecule-1 expression in rat vasculature - a potential link between the renin-angiotensin system and atherosclerosis. *Circulation*. 1999;100:1223-1229
75. Ridker PM, Gaboury CL, Conlin PR, Seely EW, Williams GH, Vaughan DE. Stimulation of plasminogen-activator inhibitor invivo by infusion of angiotensin-ii - evidence of a potential interaction between the renin-angiotensin system and fibrinolytic function. *Circulation*. 1993;87:1969-1973
76. Vaughan DE, Lazos SA, Tong K. Angiotensin-ii regulates the expression of plasminogen-activator inhibitor-1 in cultured endothelial-cells - a potential link between the renin-angiotensin system and thrombosis. *J Clin Invest*. 1995;95:995-1001
77. Dimmeler S, Rippmann V, Weiland U, Haendeler J, Zeiher AM. Angiotensin ii induces apoptosis of human endothelial cells - protective effect of nitric oxide. *Circ Res*. 1997;81:970-976
78. Li DY, Zhang YC, Philips MI, Sawamura T, Mehta JL. Upregulation of endothelial receptor for oxidized low-density lipoprotein (lox-1) in cultured human coronary artery endothelial cells by angiotensin ii type 1 receptor activation. *Circ Res*. 1999;84:1043-1049
79. Zhang F, Hu YH, Xu QB, Ye S. Different effects of angiotensin ii and angiotensin-(1-7) on vascular smooth muscle cell proliferation and migration. *Plos One*. 2010;5
80. Mazzolai L, Hayoz D. The renin-angiotensin system and atherosclerosis. *Curr Hypertens Rep*. 2006;8:47-53
81. Tham DM, Martin-McNulty B, Wang YX, Wilson DW, Vergona R, Sullivan ME, Dole W, Rutledge JC. Angiotensin ii is associated with activation of nf-kappa b-mediated genes and downregulation of ppars. *Physiol Genomics*. 2002;11:21-30
82. Daugherty A, Manning MW, Cassis LA. Angiotensin ii promotes atherosclerotic lesions and aneurysms in apolipoprotein e-deficient mice. *J Clin Invest*. 2000;105:1605-1612
83. Ayabe N, Babaev VR, Tang YW, Tanizawa T, Fogo AB, Linton MF, Ichikawaa I, Fazio S, Kon V. Transiently heightened angiotensin ii has distinct effects on atherosclerosis and aneurysm formation in hyperlipidemic mice. *Atherosclerosis*. 2006;184:312-321
84. Funakoshi Y, Ichiki T, Ito K, Takeshita A. Induction of interleukin-6 expression by angiotensin ii in rat vascular smooth muscle cells. *Hypertension*. 1999;34:118-125
85. Galis ZS, Khatri JJ. Matrix metalloproteinases in vascular remodeling and atherogenesis - the good, the bad, and the ugly. *Circ Res*. 2002;90:251-262
86. Niccoli T, Partridge L. Aging as a risk factor for disease. *Curr Biol*. 2012;22:R741-R752

87. Lakatta EG. Arterial and cardiac aging: Major shareholders in cardiovascular disease enterprises - part iii: Cellular and molecular clues to heart and arterial aging. *Circulation*. 2003;107:490-497
88. Lakatta EG, Levy D. Arterial and cardiac aging: Major shareholders in cardiovascular disease enterprises part i: Aging arteries: A "set up" for vascular disease. *Circulation*. 2003;107:139-146
89. Bachschmid MM, Schildknecht S, Matsui R, Zee R, Haeussler D, Cohen RA, Pimental D, van der Loo B. Vascular aging: Chronic oxidative stress and impairment of redox signaling-consequences for vascular homeostasis and disease. *Ann Med*. 2013;45:17-36
90. North BJ, Sinclair DA. The intersection between aging and cardiovascular disease. *Circ Res*. 2012;110:1097-1108
91. Oudot A, Martin C, Busseuil D, Vergely C, Demaison L, Rochette L. Nadph oxidases are in part responsible for increased cardiovascular superoxide production during aging. *Free Radical Bio Med*. 2006;40:2214-2222
92. Challah M, Nadaud S, Philippe M, Battle T, Soubrier F, Corman B, Michel JB. Circulating and cellular markers of endothelial dysfunction with aging in rats. *Am J Physiol-Heart C*. 1997;273:H1941-H1948
93. Wang MY, Takagi G, Asai K, Resuello RG, Natividad FF, Vatner DE, Vatner SF, Lakatta EG. Aging increases aortic mmp-2 activity and angiotensin ii in nonhuman primates. *Hypertension*. 2003;41:1308-1316
94. Wang M, Zhang J, Jiang LQ, Spinetti G, Pintus G, Monticone R, Kolodgie FD, Virmani R, Lakatta EG. Proinflammatory profile within the grossly normal aged human aortic wall. *Hypertension*. 2007;50:219-227
95. Tom B, Garrelds IM, Scalbert E, Stegmann AP, Boomsma F, Saxena PR, Danser AH. Ace-versus chymase-dependent angiotensin ii generation in human coronary arteries: A matter of efficiency? *Arteriosclerosis, Thrombosis & Vascular Biology*. 2003;23:251-256
96. Saris JJ, van Dijk MA, Kroon I, Schalekamp MA, Danser AH. Functional importance of angiotensin-converting enzyme-dependent in situ angiotensin ii generation in the human forearm. *Hypertension*. 2000;35:764-768
97. Rammos C, Hendgen-Cotta UB, Deenen R, Pohl J, Stock P, Hinzmann C, Kelm M, Rassaf T. Age-related vascular gene expression profiling in mice. *Mech Aging Dev*. 2014;135:15-23
98. Wang MY, Zhang J, Spinetti G, Jiang LQ, Monticone R, Zhao D, Cheng L, Krawczyk M, Talan M, Pintus G, Lakatta EG. Angiotensin ii activates matrix metalloproteinase type ii and mimics age-associated carotid arterial remodeling in young rats. *Am J Pathol*. 2005;167:1429-1442
99. Donato AJ, Eskurza I, Silver AE, Levy AS, Pierce GL, Gates PE, Seals DR. Direct evidence of endothelial oxidative stress with aging in humans - relation to impaired endothelium-dependent dilation and upregulation of nuclear factor-kappa b. *Circ Res*. 2007;100:1659-1666
100. Yavuz BB, Yavuz B, Sener DD, Cankurtaran M, Halil M, Ulger Z, Nazli N, Kabakci G, Aytemir K, Tokgozoglu L, Oto A, Ariogul S. Advanced age is associated with endothelial dysfunction in healthy elderly subjects. *Gerontology*. 2008;54:153-156
101. Jiang M, Bujo H, Ohwaki K, Unoki H, Yarnazaki H, Kanaki T, Shibasaki M, Azuma K, Harigaya K, Schneider WJ, Saito Y. Ang ii-stimulated migration of vascular smooth muscle cells is dependent on lr11 in mice. *J Clin Invest*. 2008;118:2733-2746
102. Kunieda T, Minamino T, Nishi JI, Tateno K, Oyama T, Katsuno T, Miyauchi H, Orimo M, Okada S, Takamura M, Nagai T, Kaneko S, Komuro I. Angiotensin ii induces premature senescence of vascular smooth muscle cells and accelerates the development of atherosclerosis via a p21-dependent pathway. *Circulation*. 2006;114:953-960

103. Lopez-Otin C, Blasco MA, Partridge L, Serrano M, Kroemer G. The hallmarks of aging. *Cell*. 2013;153:1194-1217
104. Marteijn JA, Lans H, Vermeulen W, Hoeijmakers JH. Understanding nucleotide excision repair and its roles in cancer and aging. *Nature Reviews Molecular Cell Biology*. 2014;15:465-481
105. Hoeijmakers JH. DNA damage, aging, and cancer. *N Engl J Med*. 2009;361:1475-1485
106. Mercer J, Mahmoudi M, Bennett M. DNA damage, p53, apoptosis and vascular disease. *Mutat Res-Fund Mol M*. 2007;621:75-86
107. Liochev SI. Reactive oxygen species and the free radical theory of aging. *Free Radical Bio Med*. 2013;60:1-4
108. Harman D. Aging: A theory based on free radical and radiation chemistry. *J Gerontol*. 1956;11:298-300
109. Min LJ, Mogi M, Iwai M, Horiuchi M. Signaling mechanisms of angiotensin ii in regulating vascular senescence. *Aging Res Rev*. 2009;8:113-121
110. Benigni A, Corna D, Zoja C, Sonzogni A, Latini R, Salio M, Conti S, Rottoli D, Longaretti L, Cassis P, Morigi M, Coffman TM, Remuzzi G. Disruption of the ang ii type 1 receptor promotes longevity in mice. *J Clin Invest*. 2009;119:524-530
111. Schmid U, Stopper H, Schweda F, Queisser N, Schupp N. Angiotensin ii induces DNA damage in the kidney. *Cancer Res*. 2008;68:9239-9246
112. Fazeli G, Stopper H, Schinzel R, Ni CW, Jo H, Schupp N. Angiotensin ii induces DNA damage via at1 receptor and nadph oxidase isoform nox4. *Mutagenesis*. 2012;27:673-681
113. Herbert KE, Mistry Y, Hastings R, Poolman T, Niklason L, Williams B. Angiotensin ii-mediated oxidative DNA damage accelerates cellular senescence in cultured human vascular smooth muscle cells via telomere-dependent and independent pathways. *Circ Res*. 2008;102:201-208
114. Mammucari C, Rizzuto R. Signaling pathways in mitochondrial dysfunction and aging. *Mech Aging Dev*. 2010;131:536-543
115. Trifunovic A, Larsson NG. Mitochondrial dysfunction as a cause of aging. *J Intern Med*. 2008;263:167-178
116. Widder JD, Fraccarollo D, Galuppo P, Hansen JM, Jones DP, Ertl G, Bauersachs J. Attenuation of angiotensin ii-induced vascular dysfunction and hypertension by overexpression of thioredoxin 2. *Hypertension*. 2009;54:338-344
117. de Cavanagh EMV, Inserra F, Ferder L. Angiotensin ii blockade: A strategy to slow aging by protecting mitochondria? *Cardiovasc Res*. 2011;89:31-40
118. Costopoulos C, Liew TV, Bennett M. Aging and atherosclerosis: Mechanisms and therapeutic options. *Biochem Pharmacol*. 2008;75:1251-1261
119. Fischer M, Baessler A, Schunkert H. Renin angiotensin system and gender differences in the cardiovascular system. *Cardiovasc Res*. 2002;53:672-677
120. Reckelhoff JF. Gender differences in the regulation of blood pressure. *Hypertension*. 2001;37:1199-1208
121. Novensa L, Novella S, Medina P, Segarra G, Castillo N, Heras M, Hermenegildo C, Dantas AP. Aging negatively affects estrogens-mediated effects on nitric oxide bioavailability by shifting er alpha/er beta balance in female mice. *Plos One*. 2011;6
122. Stice JP, Eiserich JP, Knowlton AA. Role of aging versus the loss of estrogens in the reduction in vascular function in female rats. *Endocrinology*. 2009;150:212-219
123. Hilliard LM, Sampson AK, Brown RD, Denton KM. The "his and hers" of the renin-angiotensin system. *Curr Hypertens Rep*. 2013;15:71-79

124. Brosnihan KB, Senanayake PS, Li P, Ferrario CM. Bi-directional actions of estrogen on the renin-angiotensin system. *Braz J Med Biol Res*. 1999;32:373-381
125. Novella S, Heras M, Hermenegildo C, Dantas AP. Effects of estrogen on vascular inflammation a matter of timing. *Arterioscl Throm Vas*. 2012;32:2035-U2670
126. Silva-Antonialli MM, Fortes ZB, Carvalho MHC, Scivoletto R, Nigro D. Sexual dimorphism in the response of thoracic aorta from shrs to losartan. *Gen Pharmacol-Vasc S*. 2000;34:329-335
127. Wu Z, Maric C, Roesch DM, Zheng W, Verbalis JG, Sandberg K. Estrogen regulates adrenal angiotensin at(1) receptors by modulating at(1) receptor translation. *Endocrinology*. 2003;144:3251-3261
128. Noth RH, Lassman MN, Tan SY, Fernandez-Cruz A, Jr., Mulrow PJ. Age and the renin-aldosterone system. *Arch Intern Med*. 1977;137:1414-1417
129. Weidmann P, De Myttenaere-Bursztein S, Maxwell MH, de Lima J. Effect on aging on plasma renin and aldosterone in normal man. *Kidney Int*. 1975;8:325-333
130. Iwanami J, Mogi M, Iwai M, Horiuchi M. Inhibition of the renin-angiotensin system and target organ protection. *Hypertens Res*. 2009;32:229-237
131. Charpiot P, Rolland PH, Friggi A, Piquet P, Scalbert E, Bodard H, Barlatier A, Latrille V, Tranier P, Mercier C, Luccioni R, Calaf R, Garcon D. Ace-inhibition with perindopril and atherogenesis-induced structural and functional-changes in minipig arteries. *Arterioscler Thromb*. 1993;13:1125-1138
132. Hayek T, Attias J, Coleman R, Brodsky S, Smith J, Breslow JL, Keidar S. The angiotensin-converting enzyme inhibitor, fosinopril, and the angiotensin ii receptor antagonist, losartan, inhibit ldl oxidation and attenuate atherosclerosis independent of lowering blood pressure in apolipoprotein e deficient mice. *Cardiovasc Res*. 1999;44:579-587
133. Kowala MC, Grove RI, Aberg G. Inhibitors of angiotensin-converting enzyme decrease early atherosclerosis in hyperlipidemic hamsters - fosinopril reduces plasma-cholesterol and captopril inhibits macrophage foam cell accumulation independently of blood-pressure and plasma-lipids. *Atherosclerosis*. 1994;108:61-72
134. Daugherty A, Rateri DL, Lu H, Inagami T, Cassis LA. Hyperch olesterolemia stimulates angiotensin peptide synthesis and contributes to atherosclerosis through the at(1a) receptor. *Circulation*. 2004;110:3849-3857
135. Lu H, Cassis LA, Daugherty A. Atherosclerosis and arterial blood pressure in mice. *Curr Drug Targets*. 2007;8:1181-1189
136. Lu H, Rateri DL, Feldman DL, Charnigo RJ, Fukamizu A, Ishida JJ, Oesterling EG, Cassis LA, Daugherty A. Renin inhibition reduces hypercholesterolemia-induced atherosclerosis in mice. *J Clin Invest*. 2008;118:984-993
137. Nussberger J, Aubert JF, Bouzourene K, Pellegrin M, Hayoz D, Mazzolai L. Renin inhibition by aliskiren prevents atherosclerosis progression - comparison with irbesartan, atenolol, and amlodipine. *Hypertension*. 2008;51:1306-1311
138. Iida Y, Xu BH, Schultz GM, Chow V, White JJ, Sulaimon S, Hezi-Yamit A, Peterson SR, Dalman RL. Efficacy and mechanism of angiotensin ii receptor blocker treatment in experimental abdominal aortic aneurysms. *Plos One*. 2012;7
139. Liao SX, Miralles M, Kelley BJ, Curci JA, Borhani M, Thompson RW. Suppression of experimental abdominal aortic aneurysms in the rat by treatment with angiotensin-converting enzyme inhibitors. *J Vasc Surg*. 2001;33:1057-1064

140. Moltzer E, Essers J, van Esch JHM, Roos-Hesselink JW, Danser AHJ. The role of the renin-angiotensin system in thoracic aortic aneurysms: Clinical implications. *Pharmacol Therapeut*. 2011;131:50-60
141. Groenink M, den Hartog AW, Franken R, Radonic T, de Waard V, Timmermans J, Scholte AJ, van den Berg MP, Spijkerboer AM, Marquering HA, Zwinderman AH, Mulder BJ. Losartan reduces aortic dilatation rate in adults with marfan syndrome: A randomized controlled trial. *European Heart Journal*. 2013;34:3491-3500
142. Sweeting MJ, Thompson SG, Brown LC, Greenhalgh RM, Powell JT. Use of angiotensin converting enzyme inhibitors is associated with increased growth rate of abdominal aortic aneurysms. *J Vasc Surg*. 2010;52:1-4
143. Thompson A, Cooper JA, Fabricius M, Humphries SE, Ashton HA, Hafez H. An analysis of drug modulation of abdominal aortic aneurysm growth through 25 years of surveillance. *J Vasc Surg*. 2010;52:55-61
144. Kuenzli A, Bucher HC, Anand I, Arutiunov G, Kum LC, McKelvie R, Afzal R, White M, Nordmann AJ. Meta-analysis of combined therapy with angiotensin receptor antagonists versus ace inhibitors alone in patients with heart failure. *Plos One*. 2010;5
145. Mallat SG. Dual renin-angiotensin system inhibition for prevention of renal and cardiovascular events: Do the latest trials challenge existing evidence? *Cardiovasc Diabetol*. 2013;12
146. McAlister FA, Zhang JG, Tonelli M, Klarenbach S, Manns BJ, Hemmelgarn BR, Network AKD. The safety of combining angiotensin-converting-enzyme inhibitors with angiotensin-receptor blockers in elderly patients: A population-based longitudinal analysis. *Can Med Assoc J*. 2011;183:655-662
147. Phillips CO, Kashani A, Ko DK, Francis G, Krumholz HM. Adverse effects of combination angiotensin ii receptor blockers plus angiotensin-converting enzyme inhibitors for left ventricular dysfunction - a quantitative review of data from randomized clinical trials. *Arch Intern Med*. 2007;167:1930-1936
148. Balcarek J, Seva Pessoa B, Bryson C, Azizi M, Menard J, Garrelds IM, McGeehan G, Reeves RA, Griffith SG, Danser AH, Gregg R. Multiple ascending dose study with the new renin inhibitor vtp-27999: Nephrocentric consequences of too much renin inhibition. *Hypertension*. 2014;63:942-950
149. Schilders JE, Wu H, Boomsma F, van den Meiracker AH, Danser AH. Renin-angiotensin system phenotyping as a guidance toward personalized medicine for ace inhibitors: Can the response to ace inhibition be predicted on the basis of plasma renin or ace? *Cardiovasc Drugs Ther*. 2014;28:335-345
150. Weiss EP, Fontana L. Caloric restriction: Powerful protection for the aging heart and vasculature. *American Journal of Physiology - Heart & Circulatory Physiology*. 2011;301:H1205-1219
151. Colman RJ, Anderson RM, Johnson SC, Kastman EK, Kosmatka KJ, Beasley TM, Allison DB, Cruzen C, Simmons HA, Kemnitz JW, Weindruch R. Caloric restriction delays disease onset and mortality in rhesus monkeys. *Science*. 2009;325:201-204
152. Rippe C, Lesniewski L, Connell M, LaRocca T, Donato A, Seals D. Short-term calorie restriction reverses vascular endothelial dysfunction in old mice by increasing nitric oxide and reducing oxidative stress. Aging Cell. 2010;9:304-312
153. Gredilla R, Sanz A, Lopez-Torres M, Barja G. Caloric restriction decreases mitochondrial free radical generation at complex i and lowers oxidative damage to mitochondrial DNA in the rat heart. *FASEB Journal*. 2001;15:1589-1591

154. Pamplona R, Portero-Otin M, Requena J, Gredilla R, Barja G. Oxidative, glycoxidative and lipoxidative damage to rat heart mitochondrial proteins is lower after 4 months of caloric restriction than in age-matched controls. *Mech Aging Dev*. 2002;123:1437-1446
155. Guo Z, Mitchell-Raymundo F, Yang H, Ikeno Y, Nelson J, Diaz V, Richardson A, Reddick R. Dietary restriction reduces atherosclerosis and oxidative stress in the aorta of apolipoprotein e-deficient mice. *Mech Aging Dev*. 2002;123:1121-1131
156. Csiszar A, Labinskyy N, Jimenez R, Pinto JT, Ballabh P, Losonczy G, Pearson KJ, de Cabo R, Ungvari Z. Anti-oxidative and anti-inflammatory vasoprotective effects of caloric restriction in aging: Role of circulating factors and sirt1. *Mech Aging Dev*. 2009;130:518-527
157. Finckenberg P, Eriksson O, Baumann M, Merasto S, Lalowski MM, Levijoki J, Haasio K, Kyto V, Muller DN, Luft FC, Oresic M, Mervaala E. Caloric restriction ameliorates angiotensin ii-induced mitochondrial remodeling and cardiac hypertrophy. *Hypertension*. 2012;59:76-84
158. Baur JA, Pearson KJ, Price NL, Jamieson HA, Lerin C, Kalra A, Prabhu VV, Allard JS, Lopez-Lluch G, Lewis K, Pistell PJ, Poosala S, Becker KG, Boss O, Gwinn D, Wang MY, Ramaswamy S, Fishbein KW, Spencer RG, Lakatta EG, Le Couteur D, Shaw RJ, Navas P, Puigserver P, Ingram DK, de Cabo R, Sinclair DA. Resveratrol improves health and survival of mice on a high-calorie diet. *Nature*. 2006;444:337-342
159. Ungvari Z, Labinskyy N, Mukhopadhyay P, Pinto JT, Bagi Z, Ballabh P, Zhang CH, Pacher P, Csiszar A. Resveratrol attenuates mitochondrial oxidative stress in coronary arterial endothelial cells. *Am J Physiol-Heart C*. 2009;297:H1876-H1881
160. Rickman AD, Williamson DA, Martin CK, Gilhooly CH, Stein RI, Bales CW, Roberts S, Das SK, Grp CS. The calerie study: Design and methods of an innovative 25% caloric restriction intervention. *Contemp Clin Trials*. 2011;32:874-881
161. Willcox BJ, Willcox DC. Caloric restriction, caloric restriction mimetics, and healthy aging in okinawa: Controversies and clinical implications. *Curr Opin Clin Nutr*. 2014;17:51-58
162. Anderson RM, Weindruch R. The caloric restriction paradigm: Implications for healthy human aging. *Am J Hum Biol*. 2012;24:101-106
163. Dai DF, Johnson SC, Villarin JJ, Chin MT, Nieves-Cintron M, Chen T, Marcinek DJ, Dorn GW, Kang YJ, Prolla TA, Santana LF, Rabinovitch PS. Mitochondrial oxidative stress mediates angiotensin ii-induced cardiac hypertrophy and g alpha q overexpression-induced heart failure. *Circ Res*. 2011;108:837-U173
164. Dai DF, Rabinovitch PS, Ungvari Z. Mitochondria and cardiovascular aging. *Circ Res*. 2012;110:1109-1124
165. Dohi Y, Ohashi M, Sugiyama M, Takase H, Sato K, Ueda R. Candesartan reduces oxidative stress and inflammation in patients with essential hypertension. *Hypertens Res*. 2003;26:691-697
166. Poljsak B, Milisav I. The neglected significance of "antioxidative stress". *Oxid Med Cell Longev*. 2012
167. McLachlan J, Beattie E, Murphy MP, Koh-Tan CHH, Olson E, Beattie W, Dominiczak AF, Nicklin SA, Graham D. Combined therapeutic benefit of mitochondria-targeted antioxidant, mitoq(10), and angiotensin receptor blocker, losartan, on cardiovascular function. *J Hypertens*. 2014;32:555-564

PART II

AORTIC ANEURYSMS

CHAPTER 4

FIBULIN-4 DEFICIENCY INDUCES THORACIC AND ABDOMINAL AORTIC WALL DILATION AND ALTERED PLAQUE MORPHOLOGY IN APOLIPOPROTEIN E-DEFICIENT MICE

N.W.M. Ramnath[1,2]*, B.S. van Thiel[1,2,4]*, K. Van der Heiden[3]*, L. Speelman[3], R.Y. Ridwan[1,2,4], P.M. van Heijningen[1], M. Vermeij[5], E.V. Rouwet[2], R. Kanaar[1,6], I. van der Pluijm[1,2], J. Essers[1,2,6]

* Equal contributors

[1]Department of Molecular Genetics, Cancer Genomics Center Netherlands, [2]Department of Vascular Surgery, [3]Department of Biomedical Engineering, [4]Department of Pharmacology, [5]Department of Pathology, [6]Department of Radiation Oncology, Erasmus Medical Center, Rotterdam, The Netherlands

(Manuscript in preparation)

ABSTRACT

Objective: Extracellular matrix degradation plays an important role in aortic aneurysm formation. In Fibulin-$4^{R/R}$ mice, deficiency of the extracellular matrix protein Fibulin-4 induces upregulation of matrix metalloproteinases (MMP) and elastin irregularities, resulting in early thoracic aortic aneurysms. In humans, aneurysms usually develop in the abdominal aorta with increasing age and are often associated with atherosclerosis. To investigate the molecular mechanisms of the interaction between aneurysm formation and atherosclerotic disease we crossbred Fibulin-$4^{+/R}$ mice, with minor extracellular matrix (ECM) abnormalities such as increased ECM deposition and slight MMP activation in the thoracic aorta, but without aortic dilation yet, onto an atherosclerotic Apolipoprotein E knockout (ApoE$^{-/-}$) background.

Approach: Double ApoE$^{-/-}$/Fibulin-$4^{+/R}$ mutant mice were fed a high fat diet (HFD) for 10, 20 or 30 weeks and compared to ApoE$^{-/-}$Fibulin-$4^{+/+}$ control mice. MMP activity in the aorta was determined using protease-activatable near-infrared fluorescent probes. Thoracic and abdominal aortic diameters were assessed using high-frequency ultrasound. After sacrifice, atherosclerotic burden in the aorta was evaluated.

Results: Interestingly, after 10 weeks of HFD, ApoE$^{-/-}$Fibulin-$4^{+/R}$ mice displayed increased MMP activity in the abdominal aorta and after 20 weeks of diet thoracic and abdominal aortic dilations were observed as compared to ApoE$^{-/-}$Fibulin-$4^{+/+}$ mice. In addition, ApoE$^{-/-}$Fibulin-$4^{+/R}$ mice showed increased plaque formation after 10 weeks of HFD and histological plaque analysis showed a distinct plaque architecture. Moreover, part of the ApoE$^{-/-}$Fibulin-$4^{+/R}$ mice developed symptoms of paralysis between 20 and 30 weeks of HFD and 30% did not survive beyond 30 weeks.

Conclusions: These results indicate that a subtle defect in the extracellular matrix of the aortic wall predisposes to the development of thoracic and abdominal aortic dilation upon atherosclerosis, and induces altered plaque morphology.

INTRODUCTION

Aortic aneurysm and dissections account for 1-2% of all deaths in the developed countries.[1] According to their location, aneurysms can be categorized in two main groups: thoracic aortic aneurysms (TAA) and abdominal aortic aneurysms (AAA). Aneurysms of the thoracic aorta, in particular the aortic arch, are characterized by necrosis of the medial layer of the aortic wall, also called cystic medial necrosis. TAAs usually occur due to a genetic mutation, for example aneurysms in Marfan's disease. Aneurysms of the distal aorta, in particular AAAs, are much more common and are thought to be caused by a multifactorial process.[2] Interestingly, recent clinical studies report a high frequency of TAAs in patients with aneurysms of the abdominal aorta.[3, 4] Important risk factors for aortic aneurysm formation are age and atherosclerosis, and these risk factors are similar for patients with aneurysms and those with arterial occlusive disease, which is characterized by narrowing of the arteries due to atherosclerosis.[5] However, the molecular mechanisms underlying aneurysm formation and the relation with atherosclerosis are largely unknown.

It is known that extracellular matrix degeneration plays an important role in TAA formation. Elastin is a crucial component of the extracellular matrix that is responsible for maintaining vessel wall elasticity.[6] Fibulin-4 is an extracellular matrix protein, which plays an important role in elastic fiber assembly and function and is a regulatory factor in elastogenesis.[7, 8] Indeed, Fibulin-4 deficient patients described so far present with TAAs, due to homozygous or compound heterozygous mutations, which usually develop to a severe stage of the disease within the first months or years of their life.[9-15] A proportion of these patients also presented with abdominal tortuosity and/or dilation on further examination.[12, 15]

Similar to Fibulin-4 deficient patients, previously developed mutant mice with a systemic 4-fold (Fibulin-$4^{R/R}$) reduced expression of Fibulin-4 present with aortic wall degeneration and thoracic aortic aneurysm.[16-18] Additionally, they develop impaired vascular contractility and increased arterial stiffness. Interestingly, a 2-fold reduced expression of Fibulin-4, in Fibulin-$4^{+/R}$ mice, also induces aortic disease but in a milder form. Although they do not develop aortic aneurysms spontaneously at adult age, they present with aortic wall degeneration, including elastic fiber fragmentation and slightly increased TGF-β signaling.[17, 19] Additionally, destruction of the extracellular matrix in the aortic wall of these Fibulin-4 mice is associated with increased expression and activation of matrix metalloprotease (MMPs), which are involved in degradation of the extracellular matrix.[17, 19] Molecular imaging using a near-infrared *in vivo* imaging probe for MMP activity (MMPsense680™) shows a graded increase in MMP activity in aneurysmal lesions of the aortic arch of Fibulin-$4^{+/R}$ and Fibulin-$4^{R/R}$ mice, showing that MMP activity is a leading indicator in these hypomorfic Fibulin-4 mice for aneurysm formation.[19]

To study whether and how a primary extracellular matrix defect can be involved in aortic dilation and atherosclerosis, we developed a mouse model in which we combined the subtle defect in the extracellular matrix of the Fibulin-$4^{+/R}$ mouse with the most commonly used model for atherosclerosis, the apolipoprotein E knockout (ApoE$^{-/-}$) mouse. At the age of 9 weeks, the double mutant mice were fed a high fat diet (HFD) to induce atherosclerotic plaque formation. Since MMP-induced elastin and collagen degradation are known to affect atherosclerotic plaque morphology[20, 21], we additionally analyzed whether plaque morphology in ApoE$^{-/-}$ mice is affected by Fibulin-4 deficiency. This model mimics the human situation as it combines the clinically observed association between (thoracic and abdominal) aortic dilation and atherosclerosis by combining an atherosclerosis mouse model (ApoE) and a subtle inherited defect present in the aortic wall (Fibulin-$4^{+/R}$) that might predispose these animals for the development of atherosclerosis associated aortic disease.

MATERIAL AND METHODS

Mouse model

Mice containing the Fibulin-4^{R} allele were generated as previously described.[2] All mice used were bred in a C57Bl/6J background and were kept in individually ventilated cages to keep them consistently micro-flora and disease free. Fibulin-4^{R} mice were crossbred with ApoE$^{-/-}$ mice (C57Bl/6J background) to obtain ApoE$^{-/-}$Fibulin-$4^{+/+}$ and ApoE$^{-/-}$Fibulin-$4^{+/R}$ mice. Female and male ApoE$^{-/-}$Fibulin-$4^{+/+}$ and ApoE$^{-/-}$Fibulin-$4^{+/R}$ mice were fed either a normal chow diet (Standard CRM (P), Special Diets Services, UK), a HFD containing 16% fat (Purified diet W 4021.06, AB diets Animal Nutrition, Woerden, the Netherlands) or a control fat diet (CFD) containing 5% fat (Purified diet W control 4021.69, AB diets Animal Nutrition, Woerden, the Netherlands) starting at the age of 9 weeks. Hind limb paralyses was observed by dragging of the limbs, and facial paralyses by loss of eye blink reflects, a bulging eye and abnormal vibrissae orientation with fibers flattened posterior against the head. Animals were housed at the Animal Resource Center (Erasmus University Medical Center), which operates in compliance with the "Animal Welfare Act" of the Dutch government, using the "Guide for the Care and Use of Laboratory Animals" as its standard. As required by Dutch law, formal permission to generate and use genetically modified animals was obtained from the responsible local and national authorities. All animal studied were approved by an independent Animal Ethical Committee (Dutch equivalent of the IACUC).

MMP imaging

Per 25 grams of body weight 2 nmol specific MMP activatable NIRF probes, MMPSense680™ (Perkin Elmer Inc., Akron, Ohio, USA), was injected into the tail vein of anesthetized mice

after 10 and 20 weeks of HFD or normal chow diet. Intact aortas were harvested 24 hours after injection for *ex vivo* fluorescence imaging, and analyzed using the Odyssey Imaging system (LI-COR® Biosciences, Lincoln, Nebraska, USA). Near-infrared images were obtained in the 700 nm channel.

Ultrasound imaging

Animals were sedated with 4% isoflurane and maintained on 1-3% isoflurane for anaesthesia, adjusted to the vital parameters of the mouse (heart rate > 400 bpm, breath rate 30 strokes/min). Mice were placed on a heating pad to maintain body temperature at 37°C. *In vivo* ultrasound imaging of the aortic arch, abdominal aorta and left ventricle (LV) was performed with a Vevo2100 (Visualsonics Inc., Toronto, Canada) using a 40-MHz linear interfaced array transducer (MS550S). B-mode and M-mode images of the aorta were captured. Diameters of the aortic arch were measured from the parasternal window at the level of the ascending aorta. Distensibility of the aortic arch was measured as the systolic to diastolic aortic diameter ratio in M-mode image data (calculated as systolic diameter minus diastolic diameter, divided by the diastolic diameter).

Analysis of plaque area and composition

To quantify the surface area affected by atherosclerosis, aortas were stained with Oil-red-O after 10 and 20 weeks of HFD and macro photographs of *en face* preparations were made (n=minimal 5 mice in each group). The Oil-red-O stained surface areas in the aortic arch, descending and abdominal aorta were quantified using ImageJ (Fiji). Additionally, plaque size and morphology were histologically analyzed after 10 and 20 weeks of HFD (n=minimal 5 mice in each group). The aortas with the branching brachiocephalic artery, left carotid artery and left subclavian artery of mice on 10 weeks of HFD were perfusion fixed with 1% paraformaldehyde after PBS flush, dehydrated and embedded in paraffin. Serial longitudinal sections of the aortic arch and cross sections of the abdominal aorta (5 µm) were prepared for histological analysis. Total plaque size in the inner curvature of the aortic arch and in the brachiocephalic artery was measured on haematoxylin-eosin stained slides using BioPix iQ 2.0 imaging software (BioPix, Göteborg, Sweden). Aortic wall structure and plaque morphology were additionally analyzed by histochemical staining with Resorcin-Fuchsin (elastin). Elastin content was analyzed on elastin stained slides with ImageJ (Fiji).

To further determine differences in plaque phenotype, including lipid content, cryosections were made of mice on 20 weeks HFD. After PBS flush aortic arches were embedded in Tissue-Tek (O.C.T. compound) and serial longitudinal cryosections were made (5 µm). Plaque size in the aortic arch and brachiocephalic artery was quantified on haematoxylin-eosin stained slides using Biopix. Oil-red-O staining was used to determine lipid content of the plaques.

Statistical analysis

All results are expressed as mean ± SEM (continuous results) or median (lower to upper limit) (aortic arch diameters). The unpaired 2-tailed Student t-test was performed to analyze the specific sample groups for significant differences. A p-value <0.05 was considered to indicate a significant difference between groups. All analyses were performed using IBM SPSS Statistics version 20.0 (SPSS Inc., Chicago, IL, USA).

RESULTS

Abdominal aorta of ApoE$^{-/-}$Fibulin-4$^{+/R}$ mice shows increased MMP activity

We have previously shown that extracellular matrix degeneration in Fibulin-4$^{+/R}$ and Fibulin-4$^{R/R}$ mice is associated with increased MMP activity in the thoracic aorta.[19] In this study, we tested whether extracellular matrix degeneration in the aortic wall of Fibulin-4 deficient mice could contribute to abdominal aortic lesions. Measurements of MMP activity in the abdominal aorta using the MMPsense probe indeed revealed a mild increased activity of 1.2 fold in Fibulin-4$^{+/R}$ abdominal aortas as compared to Fibulin-4$^{+/+}$ mice (Fig. 1A). However, these Fibulin-4$^{+/R}$ mice do not yet develop abdominal aortic dilations.

As atherosclerosis can be associated with aortic aneurysms, we next tested whether the induction of atherosclerosis in Fibulin-4^{R} heterozygous mice, which have minor extracellular matrix defects in the aortic wall, could lead not only to thoracic, but also abdominal aortic dilation. To induce atherosclerosis, Fibulin-4$^{+/R}$ mice were crossbred with ApoE$^{-/-}$ mice, which develop atherosclerosis spontaneously after 12 weeks.[22-24] Starting from the age of 9 weeks the double mutant ApoE$^{-/-}$Fibulin-4$^{+/R}$ and ApoE$^{-/-}$Fibulin-4$^{+/+}$ littermate controls were fed a HFD for 10 or 20 weeks to accelerate atherosclerotic plaque formation. ApoE$^{+/+}$Fibulin-4$^{+/+}$ and ApoE$^{+/+}$Fibulin-4$^{+/R}$ mice on a HFD for 10 or 20 weeks did not develop atherosclerosis and did not show additional vascular abnormalities as compared to Fibulin-4$^{+/+}$ and Fibulin-4$^{+/R}$ mice.

Interestingly, after 10 weeks of HFD, MMP activity measurement on whole aortas revealed a strongly increased MMP activity in the abdominal aortas of ApoE$^{-/-}$Fibulin-4$^{+/R}$ mice of 2.7 fold as compared to ApoE$^{-/-}$Fibulin-4$^{+/+}$ mice, and also compared to ApoE$^{-/-}$Fibulin-4$^{+/R}$ mice on a chow diet, which had a 1.6 fold increase compared to ApoE$^{-/-}$Fibulin-4$^{+/+}$ mice on chow diet (Fig.1B). This highly increased MMP activity in the abdominal aortas of ApoE$^{-/-}$Fibulin-4$^{+/R}$ mice was further increased after 20 weeks of HFD. ApoE$^{-/-}$Fibulin-4$^{+/R}$ mice on 20 weeks of HFD had a 13 fold increase as compared to ApoE$^{-/-}$Fibulin-4$^{+/+}$ mice. This indicates that induction of atherosclerosis in ApoE$^{-/-}$Fibulin-4$^{+/R}$ mice enhanced the already slightly increased MMP activity observed in the abdominal aorta of Fibulin-4$^{+/R}$ mice, which suggests that abdominal aortic wall lesions worsened progressively in ApoE$^{-/-}$Fibulin-4$^{+/R}$ mice on a HFD.

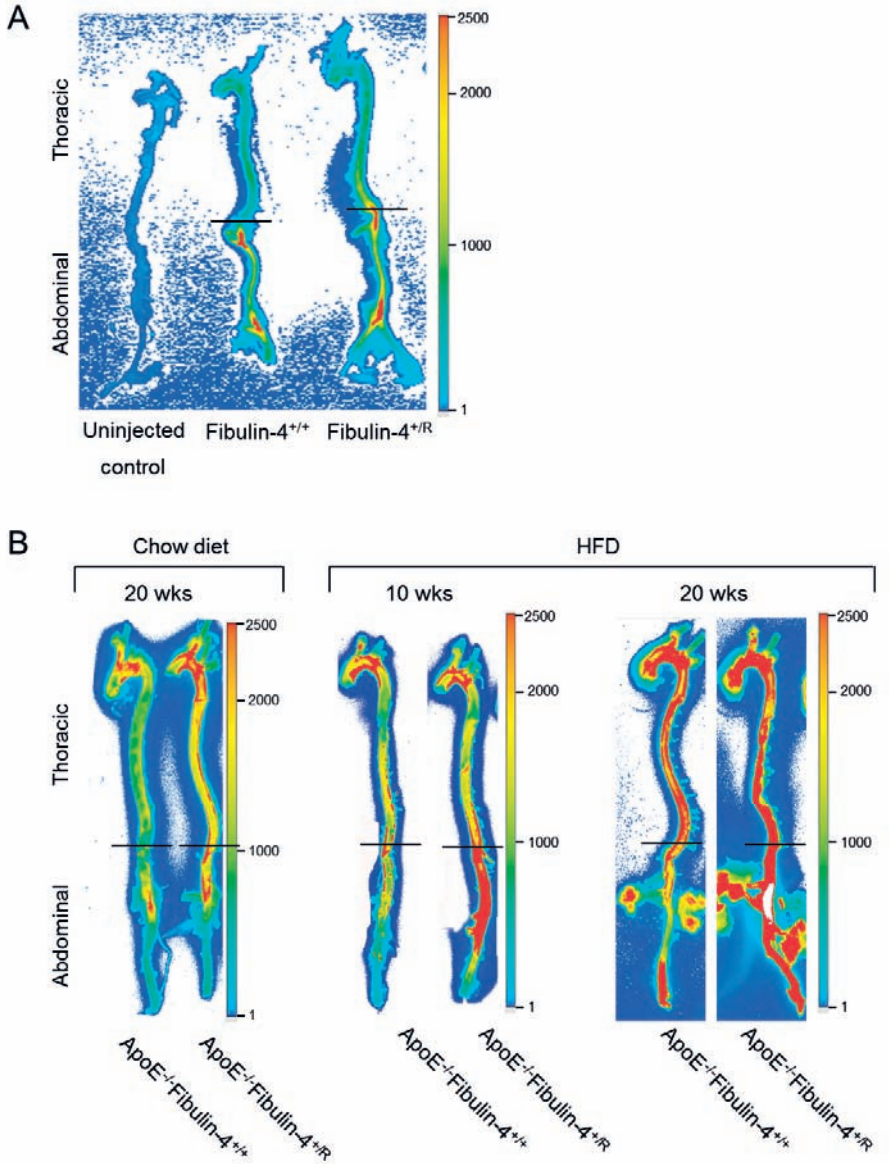

Figure 1. Increased MMP activity in ApoE$^{-/-}$Fibulin-4$^{+/R}$ abdominal aortas after 10 and 20 weeks of HFD. (A) E*x vivo* imaging of isolated aortas shows 1.2 fold higher MMP activity in the abdominal aortas of Fibulin-4$^{+/R}$ mice (n=6) as compared to Fibulin-4$^{+/+}$ abdominal aortas (n=4). (B) *Ex vivo* imaging of aortas after 10 and 20 weeks of HFD and chow diet shows a further increase in MMP activity in the abdominal aorta of ApoE$^{-/-}$Fibulin-4$^{+/R}$ mice (n=3) with a 2.7 fold increase after 10 weeks of HFD as compared to ApoE$^{-/-}$Fibulin-4$^{+/+}$ aortas (n=3), and a 13 fold increase after 20 weeks of HFD in the abdominal aortas of ApoE$^{-/-}$Fibulin-4$^{+/R}$ mice (n=5) as compared to ApoE$^{-/-}$Fibulin-4$^{+/+}$ aortas (n=5) as well as compared to ApoE$^{-/-}$Fibulin-4$^{+/R}$ mice after 20 weeks of chow diet (n=5), which had a 1.6 fold increase compared to ApoE$^{-/-}$Fibulin-4$^{+/+}$ aortas (n=3). Horizontal lines depict the level of the diaphragm, indicating the transition of the thoracic into the abdominal part of the aorta.

ApoE$^{-/-}$Fibulin-4$^{+/R}$ aortas display increased thoracic and abdominal aortic diameters

To subsequently determine whether the combination of atherosclerosis and an extracellular matrix defect can result in aortic dilation in ApoE$^{-/-}$Fibulin-4$^{+/R}$ mice, we measured thoracic and abdominal aortic diameters using *in vivo* ultrasound imaging of ApoE$^{-/-}$Fibulin-4$^{+/+}$ and ApoE$^{-/-}$Fibulin-4$^{+/R}$ mice after 10 and 20 weeks of HFD and after 10 or 20 weeks of CFD, which has a similar nutrient composition as HFD, but a lower fat percentage. We also included mice after 20 weeks of chow diet and mice of 9 weeks old (without starting a diet: 0 weeks HFD/CFD) as controls. Interestingly, significantly increased thoracic aortic diameters were observed in ApoE$^{-/-}$Fibulin-4$^{+/R}$ mice after 20 weeks of CFD compared to ApoE$^{-/-}$Fibulin-4$^{+/+}$ mice, but no difference was observed between the two genotypes on HFD or chow diet (Fig. 2A and Supplemental Fig. 1A). The thoracic aortic diameters of the ApoE$^{-/-}$Fibulin-4$^{+/R}$ mice on 20 weeks CFD were also significantly larger compared to ApoE$^{-/-}$Fibulin-4$^{+/R}$ mice on 10 weeks CFD and ApoE$^{-/-}$Fibulin-4$^{+/R}$ mice on 20 weeks chow diet. ApoE$^{-/-}$Fibulin-4$^{+/+}$ and ApoE$^{-/-}$Fibulin-4$^{+/R}$ mice on 10 and 20 weeks of HFD displayed similar distributions with large variations in aortic arch diameters, which seemed to show some dilation in both ApoE$^{-/-}$Fibulin-4$^{+/+}$ and ApoE$^{-/-}$Fibulin-4$^{+/R}$ mice. Since increased aortic arch diameters were also observed in ApoE$^{-/-}$Fibulin-4$^{+/+}$ mice on HFD, this probably indicates that HFD induces aortic arch dilations in both ApoE$^{-/-}$Fibulin-4$^{+/+}$ and ApoE$^{-/-}$Fibulin-4$^{+/R}$ mice. Aortic arch diameter measurements at 0 weeks of diet or after 20 weeks of chow diet, showed no difference between ApoE$^{-/-}$Fibulin-4$^{+/+}$ and ApoE$^{-/-}$Fibulin-4$^{+/R}$ mice. In short, after a subtle increase in fat diet (CFD) ApoE$^{-/-}$Fibulin-4$^{+/R}$ mice developed thoracic aortic dilations compared to ApoE$^{-/-}$Fibulin-4$^{+/+}$ mice, while a diet with even more fat (HFD) results in a large variation in thoracic aortic diameters between animals in both the ApoE$^{-/-}$Fibulin-4$^{+/+}$ and ApoE$^{-/-}$Fibulin-4$^{+/R}$ group.

Additionally, to determine the effect of atherosclerosis on the stiffness of the aortic wall, we performed calculations on the distensibility of the aortic arch, which is an elasticity index of the aorta and inversely correlates with aortic wall stiffness. A slight reduction was already observed in adult Fibulin-4$^{+/R}$ aortas compared to Fibulin-4$^{+/+}$ aortas (Supplemental Fig. 2A). A similar slight reduction was observed in ApoE$^{-/-}$Fibulin-4$^{+/R}$ mice after 10 and 20 weeks of CFD as compared to ApoE$^{-/-}$Fibulin-4$^{+/+}$ mice (data not shown). The same measurements in ApoE$^{-/-}$Fibulin-4$^{+/R}$ mice after 10 and 20 weeks of HFD revealed a further decreased distensibility as compared to ApoE$^{-/-}$Fibulin-4$^{+/+}$ mice (Supplemental Fig. 2B). This decrease was significant after 10 weeks of HFD, whereas after 20 weeks of HFD ApoE$^{-/-}$Fibulin-4$^{+/+}$ aortas also showed a slight decrease in aortic arch distensibility. In conclusion, these results indicate that CFD, probably inducing modest atherosclerosis formation, results in aortic arch dilation in extracellular matrix defective ApoE$^{-/-}$Fibulin-4$^{+/R}$ mice, while a HFD leads to an equal distribution of aortic arch diameters in both ApoE$^{-/-}$Fibulin-4$^{+/R}$ and ApoE$^{-/-}$Fibulin-4$^{+/+}$ mice, (including aortic arch dilations in some of both). This could point to the fact that under the same conditions Fibulin-4$^{+/R}$ animals

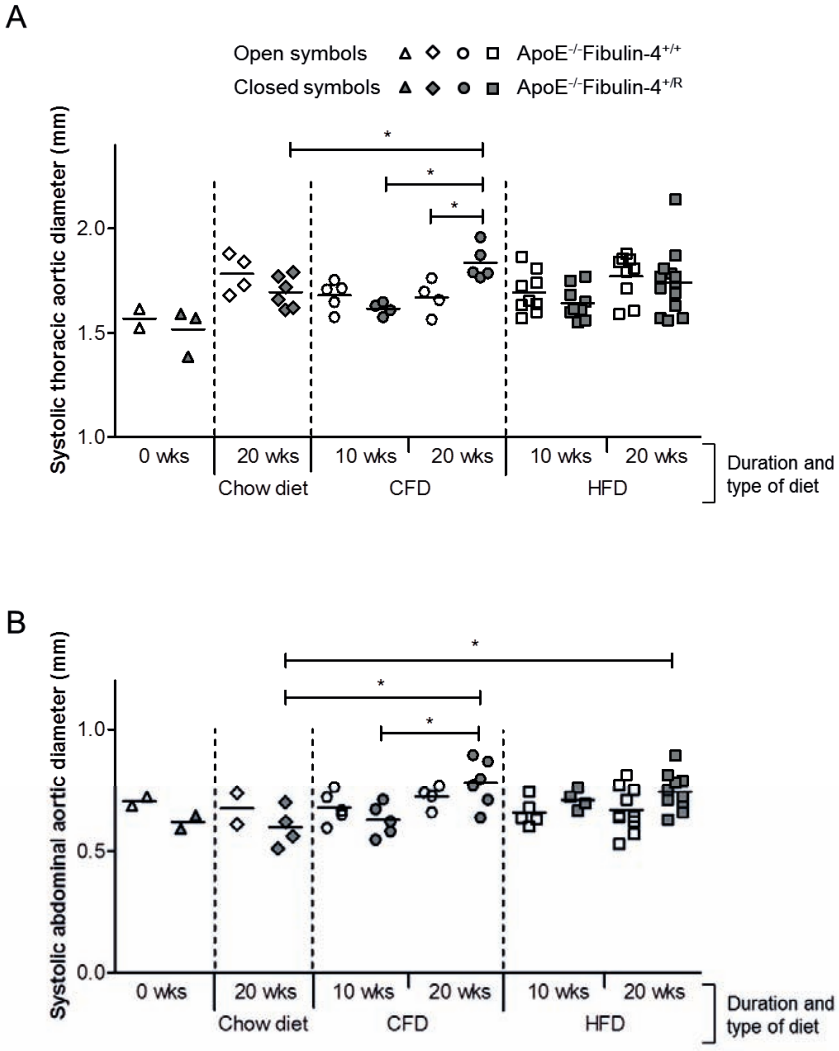

Figure 2. Increased thoracic and abdominal aortic diameters in ApoE$^{-/-}$Fibulin-4$^{+/R}$ mice. (A) Aortic arch diameter measurements by ultrasound imaging in M-mode show significant increased systolic aortic arch diameters in ApoE$^{-/-}$Fibulin-4$^{+/R}$ mice after 20 weeks of CFD (n=5) compared to ApoE$^{-/-}$Fibulin-4$^{+/+}$ mice after 20 weeks of CFD (n=5), ApoE$^{-/-}$Fibulin-4$^{+/R}$ mice after 10 weeks of CFD (n=5), and compared to ApoE$^{-/-}$Fibulin-4$^{+/R}$ mice after 20 weeks of chow diet (n=6). Aortic arch diameters after 10 and 20 weeks HFD appear to be equally distributed in ApoE$^{-/-}$Fibulin-4$^{+/+}$ and ApoE$^{-/-}$Fibulin-4$^{+/R}$ mice, with an increased variation in diameters. No differences are observed in mice fed a chow diet for 0 or 20 weeks. (B) Abdominal aortic measurements at the level of the iliac artery bifurcation also show significantly increased aortic diameters in ApoE$^{-/-}$Fibulin-4$^{+/R}$ mice after 20 weeks of CFD compared to ApoE$^{-/-}$Fibulin-4$^{+/R}$ mice after 10 weeks of CFD and 20 weeks of chow diet. Furthermore, increased abdominal aortic diameters are observed in ApoE$^{-/-}$Fibulin-4$^{+/R}$ mice after 20 weeks of HFD compared to ApoE$^{-/-}$Fibulin-4$^{+/R}$ mice after 20 weeks of chow diet (*$p<0.05$). Open symbols indicate aortic diameters of ApoE$^{-/-}$Fibulin-4$^{+/+}$ mice, closed symbols indicate aortic diameters of ApoE$^{-/-}$Fibulin-4$^{+/R}$ mice.

are more susceptible than Fibulin-$4^{+/+}$ animals to atherosclerosis induction, which is therefore already apparent on a low fat diet. In addition, HFD leads to increased aortic wall stiffness in ApoE$^{-/-}$Fibulin-$4^{+/R}$ mice.

Interestingly, assessment of abdominal aortic diameters at the level of the iliac artery bifurcation showed significantly increased diameters in ApoE$^{-/-}$Fibulin-$4^{+/R}$ mice after 20 weeks on CFD as compared to 10 weeks on CFD, and also compared to ApoE$^{-/-}$Fibulin-$4^{+/R}$ mice after 20 weeks chow diet (Fig. 2B and Supplemental Fig. 1B). Moreover, significantly increased abdominal diameters were observed in ApoE$^{-/-}$Fibulin-$4^{+/R}$ mice on 20 weeks of HFD compared to ApoE$^{-/-}$Fibulin-$4^{+/R}$ mice on 20 weeks of chow diet. Abdominal aortic diameters in ApoE$^{-/-}$Fibulin-$4^{+/+}$ mice were not increased when compared among different diets and diet durations. Altogether, these data suggest that Fibulin-4 deficient ApoE$^{-/-}$ mice already develop thoracic and abdominal aortic dilation on a low fat diet, while in addition HFD induces abdominal aortic dilation in ApoE$^{-/-}$Fibulin-$4^{+/R}$ mice and increases aortic arch stiffness.

ApoE$^{-/-}$Fibulin-$4^{+/R}$ aortas present increased plaque area in the thoracic and abdominal aorta

Next, we investigated the effect of a primary extracellular matrix defect on atherosclerotic plaque formation after 10 or 20 weeks of HFD feeding. Plaque area was quantified on *en face* preparations of Oil-red-O stained aortas. The descending and abdominal aorta of ApoE$^{-/-}$Fibulin-$4^{+/R}$ mice after 10 weeks of HFD showed significantly increased plaque area as compared to ApoE$^{-/-}$Fibulin-$4^{+/+}$ mice (Fig. 3A and C). However, the plaque area in the aortic arch was similar between ApoE$^{-/-}$Fibulin-$4^{+/R}$ and ApoE$^{-/-}$Fibulin-$4^{+/+}$ mice at this age. After 20 weeks of HFD increased plaque area was detected in the aortic arch and abdominal aorta of ApoE$^{-/-}$Fibulin-$4^{+/R}$ mice compared to ApoE$^{-/-}$Fibulin-$4^{+/+}$ mice, but this was not significant due to large variability in plaque area between ApoE$^{-/-}$Fibulin-$4^{+/+}$ mice (Fig. 3B and D). This suggests that Fibulin-4 deficiency accelerates plaque formation such that these are present after 10 weeks of HFD, while plaque occurrence after 20 weeks of HFD also increases in ApoE$^{-/-}$Fibulin-$4^{+/+}$ mice. Interestingly, increased plaque area in individual ApoE$^{-/-}$Fibulin-$4^{+/+}$ mice significantly correlated with increased aortic arch diameter (Fig. 4), while plaque area in ApoE$^{-/-}$Fibulin-$4^{+/R}$ mice did not correlate with aortic arch diameter. These data indicate that the observed dilation in ApoE$^{-/-}$Fibulin-$4^{+/+}$ aortas is due to progression of atherosclerosis. However, in ApoE$^{-/-}$Fibulin-$4^{+/R}$ mice this correlation is absent, which is probably due to the fact that aortic dilation is already present at an earlier stage or with mild atherosclerosis, which means that in these mice the extracellular matrix defect is the underlying cause of the aortic dilation. At the same time, these results together indicate that the extracellular matrix defect in ApoE$^{-/-}$Fibulin-$4^{+/R}$ mice contributes to the increase in plaque area observed in thoracic and abdominal aortas.

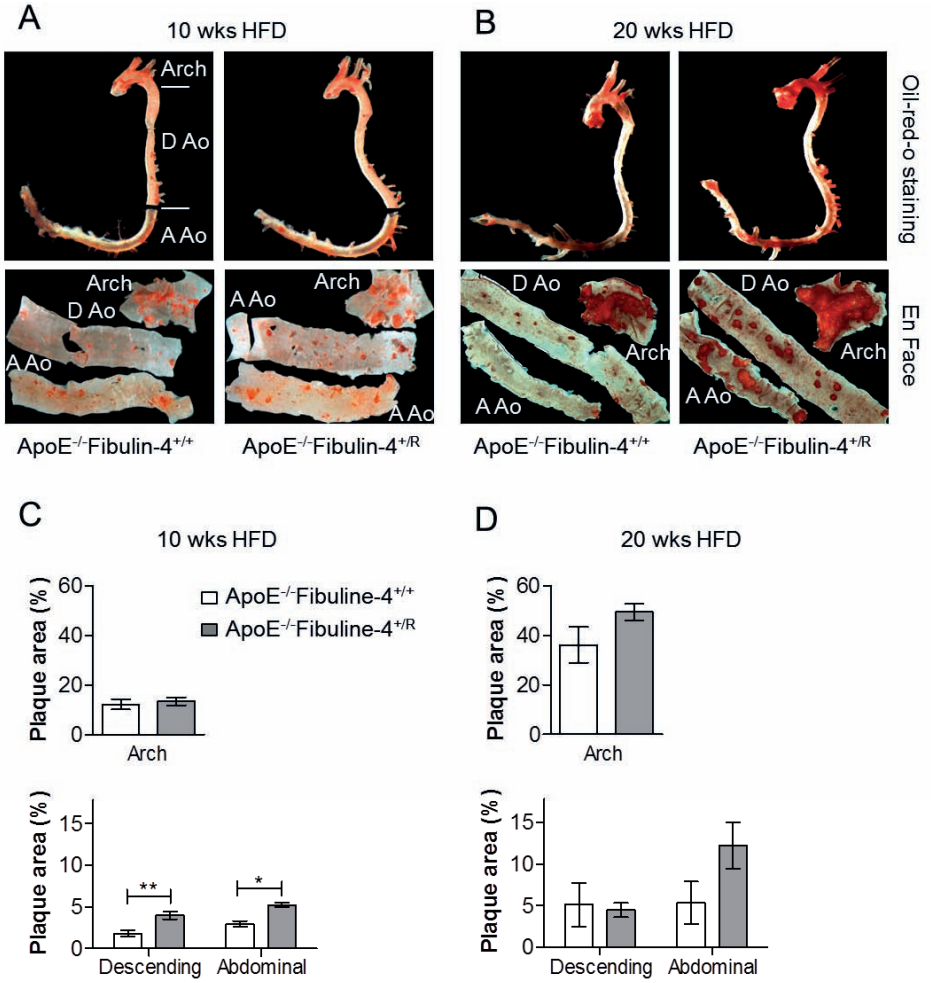

Figure 3. Increased plaque deposition in thoracic and abdominal aortas of ApoE$^{-/-}$Fibulin-4$^{+/R}$ mice. Oil-red-O staining and *en face* preparations of ApoE$^{-/-}$Fibulin-4$^{+/+}$ and ApoE$^{-/-}$Fibulin-4$^{+/R}$ aortas after (A) 10 and (B) 20 weeks of HFD show increased plaque areas in the thoracic and abdominal aortas of ApoE$^{-/-}$Fibulin-4$^{+/R}$ mice. Images in B represent aortas from ApoE$^{-/-}$Fibulin-4$^{+/R}$ mice, which show increased plaque areas as compared to their littermate ApoE$^{-/-}$Fibulin-4$^{+/+}$. Arch= aortic arch, D Ao= descending aorta, A Ao= abdominal aorta. (C) Quantification of the Oil-red-O stained *en face* preparations of ApoE$^{-/-}$Fibulin-4$^{+/R}$ aortas after 10 weeks of HFD (n=5) shows significantly increased plaque areas in the descending and abdominal aortas as compared to ApoE$^{-/-}$Fibulin-4$^{+/+}$ aortas (n=5). (D) After 20 weeks of HFD no significant differences could be observed between ApoE$^{-/-}$Fibulin-4$^{+/R}$ mice (n=10) and ApoE$^{-/-}$Fibulin-4$^{+/+}$ mice (n=5), as some ApoE$^{-/-}$Fibulin-4$^{+/+}$ aortas also displayed an increase in plaque areas (* $p<0.05$, ** $p<0.01$).

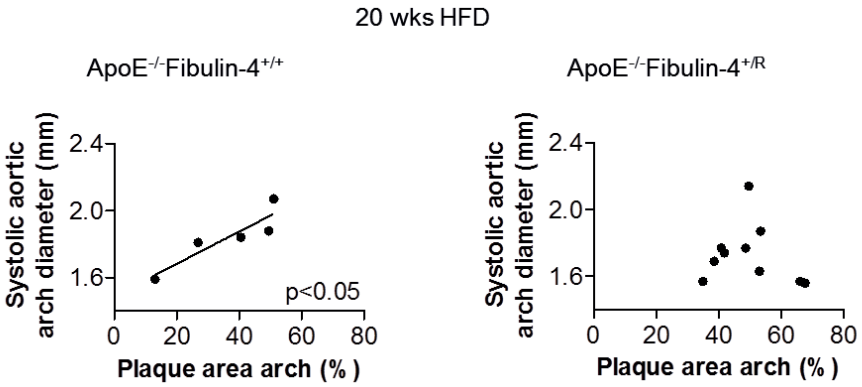

Figure 4. Increased plaque formation correlates with aortic arch dilation in ApoE$^{-/-}$Fibulin-4$^{+/+}$ mice. After 20 weeks of HFD, ApoE$^{-/-}$Fibulin-4$^{+/+}$ mice significantly develop increased aortic arch diameters with increased plaque formation, whereas no such correlation is present in ApoE$^{-/-}$Fibulin-4$^{+/R}$ mice (*p<0.05).

ApoE$^{-/-}$Fibulin-4$^{+/R}$ aortas show altered plaque morphology

Results of the *en face* Oil-red-O staining of the aortic arches were confirmed by quantification of plaque size on haematoxylin-eosin stained sections of the aortic arch, showing no significantly increased plaque size in ApoE$^{-/-}$Fibulin-4$^{+/R}$ animals after 10 and 20 weeks of HFD as compared to ApoE$^{-/-}$Fibulin-4$^{+/+}$ mice. Although a small increase in plaque size and lipid content was observed after 20 weeks of HFD in histological sections of aortic arches of ApoE$^{-/-}$Fibulin-4$^{+/R}$ mice, this increase was not significant due to the low amount of samples (Supplemental Fig. 3). Interestingly, a different plaque morphology was observed in aortic arches of ApoE$^{-/-}$Fibulin-4$^{+/R}$ mice after just 10 weeks of HFD; ApoE$^{-/-}$Fibulin-4$^{+/R}$ aortas showed either 1) partially loose plaques (which will be referred to as disconnected plaques) or 2) plaques grown over existing plaques (which will be referred to as overlying plaques) or 3) a combination of both, in the brachiocephalic artery and in the inner curvature of the aortic arch (Fig. 5A and C). Out of the eight ApoE$^{-/-}$Fibulin-4$^{+/R}$ animals examined, all displayed either disconnected plaques or overlying plaques, or both, in the brachiocephalic artery, whereas one out of eight ApoE$^{-/-}$Fibulin-4$^{+/+}$ mice displayed a disconnected plaque and one an overlying plaque (Table 1). To determine whether this altered plaque morphology is associated with elastin abnormalities due to Fibulin-4 deficiency, we performed histological elastin analysis. This revealed a significantly decreased elastin content in plaques of the brachiocephalic artery of ApoE$^{-/-}$Fibulin-4$^{+/R}$ animals (Fig. 5B). In the inner curvature of the aortic arch, three out of seven ApoE$^{-/-}$Fibulin-4$^{+/R}$ animals had either a disconnected or an overlying plaque, or both, as compared to one out of eight ApoE$^{-/-}$Fibulin-4$^{+/+}$ mice with a disconnected plaque, which is the same animal that showed the disconnected plaque in the brachiocephalic artery (Table 1). Plaques of the inner curvature of the aortic arch of ApoE$^{-/-}$Fibulin-4$^{+/R}$ animals additionally contained a

Table 1. Amount of disconnected and overlying plaques found in the inner curvature of the aortic arch and in the brachiocephalic artery of ApoE$^{-/-}$Fibulin-4$^{+/R}$ mice as compared to ApoE$^{-/-}$Fibulin-4$^{+/+}$

Genotype	Inner curvature			Brachiocephalic artery		
	Disconnected plaque	Overlying plaque	Total	Disconnected plaque	Overlying plaque	Total
ApoE$^{-/-}$Fibulin-4$^{+/R}$	1/8	-/8	1/8	1/8	1/8	2/8
ApoE$^{-/-}$Fibulin-4$^{+/R}$	2/7	3/7	3/7	5/8	6/8	8/8

*One arch could not be analyzed

decrease in elastin content (Fig. 5D). Histological analysis on cross-sections of abdominal aortas showed thickening of the abdominal aortic wall with increased spaces between the elastic laminae in ApoE$^{-/-}$Fibulin-4$^{+/R}$ animals after both 10 and 20 weeks of HFD, which is also observed at sites of plaque formation in the abdominal aorta as compared to

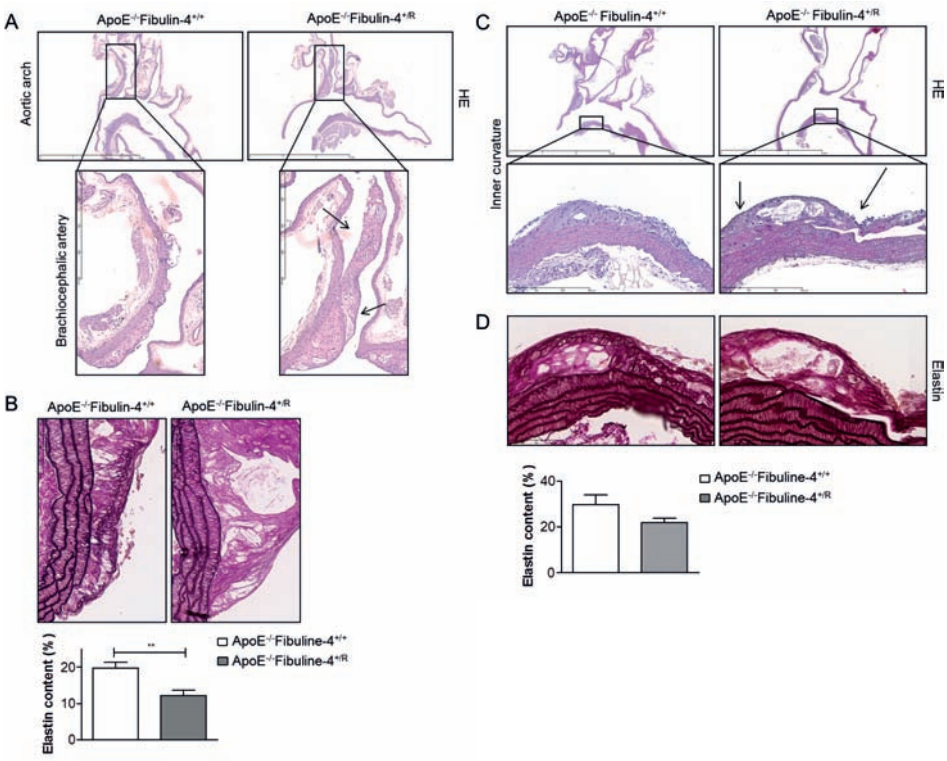

Figure 5. Plaque morphological changes in ApoE$^{-/-}$Fibulin-4$^{+/R}$ aortic arches after 10 weeks of HFD. HE analysis points to more disconnected and overlying plaques in (A) the brachiocephalic artery and (C) inner curvature of the arch of ApoE$^{-/-}$Fibulin-4$^{+/R}$ aortas after 10 weeks of HFD compared to ApoE$^{-/-}$Fibulin-4$^{+/+}$ aortas. (B and D) Elastin staining and quantification of the elastin content in plaques revealed significantly less elastin in plaques in (B) the brachiocephalic artery of ApoE$^{-/-}$Fibulin-4$^{+/R}$ mice. (D) Plaques of the inner curvature of the aortic arch of ApoE$^{-/-}$Fibulin-4$^{+/R}$ mice also show a tendency towards less elastin (*p<0.05).

ApoE$^{-/-}$Fibulin-4$^{+/+}$ animals (Supplemental Fig. 4 and 5). This was also previously observed in the thoracic aortas of homozygous Fibulin-4$^{R/R}$ mice and is associated with degeneration of the aortic wall.[17] No differences in plaque morphology could be observed in the abdominal aorta. Altogether, these results suggest that a deficiency in the extracellular matrix protein Fibulin-4 leads to the formation of morphologically different atherosclerotic plaques in the thoracic aorta.

Decreased survival of atherosclerotic ApoE$^{-/-}$Fibulin-4$^{+/R}$ mice between 20 and 30 weeks of HFD

Interestingly, approximately 30% of ApoE$^{-/-}$Fibulin-4$^{+/R}$ animals that were fed a HFD with the aim to be analyzed at 30 weeks, died suddenly between 20 and 30 weeks on the diet as compared to a 100% survival of ApoE$^{-/-}$Fibulin-4$^{+/+}$ control animals (Fig. 6). Moreover, symptoms of paralysis were observed after handling of 4 out of 16 ApoE$^{-/-}$Fibulin-4$^{+/R}$ animals that survived between 20 and 30 weeks of CFD or HFD, while none of these symptoms were observed in ApoE$^{-/-}$Fibulin-4$^{+/+}$ mice (n=9) (Table 2). These results indicate that atherosclerotic Fibulin-4 deficient ApoE$^{-/-}$Fibulin-4$^{+/R}$ animals display a worsened survival outcome, possibly due to atherosclerosis-induced events, which may cause the paralysis symptoms.

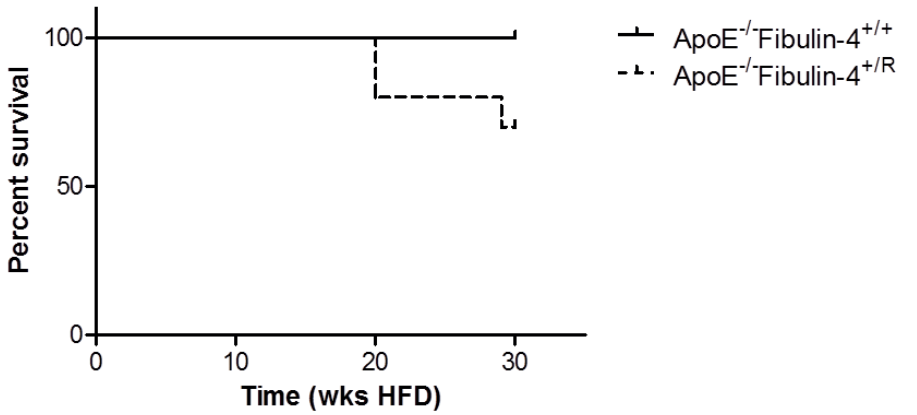

Figure 6. Decreased survival of ApoE$^{-/-}$Fibulin-4$^{+/R}$ mice between 20 and 30 weeks of HFD. After 30 weeks of HFD approximately 30% of ApoE$^{-/-}$Fibulin-4$^{+/R}$ mice (n=10) did not survive as compared to 100% survival of ApoE$^{-/-}$Fibulin-4$^{+/+}$ mice (n=3).

DISCUSSION

In this study we demonstrate that a genetic defect leading to subtle changes in the extracellular matrix structure of the aortic wall, in combination with atherosclerosis, may predispose for thoracic and abdominal aortic disease, including morphologically altered atherosclerotic plaques, and a worsened survival outcome. Atherosclerosis induction in the double mutant ApoE$^{-/-}$Fibulin-4$^{+/R}$ mice results in increased abdominal MMP activity, thoracic and abdominal aortic dilation and increased thoracic and abdominal plaque formation. Furthermore, ApoE$^{-/-}$Fibulin-4$^{+/R}$ mice display altered plaque morphology and have a reduced survival rate after 20 weeks of HFD. These results indicate that an underlying extracellular matrix defect promotes a bidirectional relation between atherosclerotic disease and aortic wall dilation.

On one side, atherosclerosis induction in Fibulin-4 deficient mice leads to enhanced aortic wall degeneration in Fibulin-4 deficient mice. ApoE$^{-/-}$Fibulin-4$^{+/R}$ mice already develop both thoracic and abdominal aortic wall dilations after 20 weeks on CFD. Most probably 20 weeks of CFD induces mild atherosclerosis since ApoE$^{-/-}$ mice spontaneously develop atherosclerosis after 12 weeks on normal chow diet, which has a lower fat percentage and a different nutrient composition compared to CFD.[22-24] Abdominal aortic dilations also occur after 20 weeks of HFD compared to chow diet, indicating that induction of both mild and high atherosclerosis results in increased abdominal aortic dilation in ApoE$^{-/-}$Fibulin-4$^{+/R}$ mice. However, after 20 weeks of HFD both ApoE$^{-/-}$Fibulin-4$^{+/+}$ and ApoE$^{-/-}$Fibulin-4$^{+/R}$ mice have a wide but equal distribution in thoracic aortic arch diameters. This might be explained by highly increased atherosclerotic plaque formation induced by the HFD, which probably overrules the effects of the extracellular matrix degeneration on the aortic wall.

On the other side the aortic wall degeneration in ApoE$^{-/-}$Fibulin-4$^{+/R}$ mice on HFD leads to increased plaque formation and altered plaque morphology. Ten weeks of HFD induces significantly more atherosclerotic plaques in the thoracic and abdominal aorta of ApoE$^{-/-}$Fibulin-4$^{+/R}$ mice, whereas 20 weeks of HFD induces increased plaque formation in both ApoE$^{-/-}$Fibulin-4$^{+/+}$ and ApoE$^{-/-}$Fibulin-4$^{+/R}$ mice. However, a slight increase in plaque formation in the aortic arch and abdominal aorta of ApoE$^{-/-}$Fibulin-4$^{+/R}$ mice after 20 weeks of HFD can be observed. This suggests that Fibulin-4 deficiency leads to enhanced atherosclerosis progression. In ApoE$^{-/-}$Fibulin-4$^{+/+}$ mice the increased plaque formation is associated with the observed increased diameters, which is in concordance with previous reports.[25] However, ApoE$^{-/-}$Fibulin-4$^{+/R}$ mice show increased plaque formation independent of changes in aortic diameters, probably because this dilation already occurs in an earlier stage at a lower percentage of fat. Histological analyses of aortic plaques of ApoE$^{-/-}$Fibulin-4$^{+/R}$ mice after 10 weeks of HFD show more disconnected plaques, more overlying plaques and less elastin content in plaques compared to ApoE$^{-/-}$Fibulin-4$^{+/+}$ aortic plaques. The

reduced elastin content in atherosclerotic plaques of ApoE$^{-/-}$Fibulin-4$^{+/R}$ mice is likely to be a consequence of impaired elastogenesis since Fibulin-4 influences crosslinking of elastic fiber by affecting the recruitment of LOX.[5, 7, 26, 27] A reduction in elastin content can make these plaques less stable. Additionally, ApoE$^{-/-}$Fibulin-4$^{+/R}$ mice show symptoms of paralysis and a reduced survival between 20 and 30 weeks of HFD. The histological observed alterations in plaque morphology together with the observed worsened survival outcome might indicate that Fibulin-4 deficiency increases atherosclerosis-induced events. Whether these events are caused by plaque rupture is unclear. Our data show overlying plaques, disconnected plaques, and plaques with reduced elastin content and high MMP activity in the double mutant ApoE$^{-/-}$Fibulin-4$^{+/R}$ mice. These features coincide with the occurrence of paralysis and reduced survival outcome.

In this respect, it would be interesting to make whole body angiographies of these animals just before they succumb. However, this is complicated due to their unpredictable and sudden death. Strikingly, plaque rupture was observed in another atherosclerotic mouse model with a more severe ECM defect; the ApoE$^{-/-}$Fibrillin-1$^{+/-}$ mouse.[28] Fibrillin-1 is the major structural component of microfibrils, which provide the scaffold for the deposition and crosslinking of elastin. The C1039G mutated Fibrillin-1 mice used in these studies however are different from the Fibulin-4^{R} mice used here, as the Fibrillin-1 mice spontaneously develop thoracic aneurysms thereby also affecting the hemodynamic parameters. Fragmentation of elastic fibers in these double knockout mice leads to increased vascular stiffness and promoted features of multifocal plaque instability. These mouse models with a structural defect in elastic fibers associated proteins provide insight into the role of extracellular matrix degeneration in the susceptibility for altered plaque morphology and its consequences.

The bidirectional interaction between aortic wall degeneration and atherosclerosis formation in our ApoE$^{-/-}$Fibulin-4$^{+/R}$ mice may lead to a vicious circle, in which the observed increased MMP activity could play a prominent role. The MMPsense probe is activated by MMP2, -3, -9 and -13, of which MMP2 and MMP9 are known to play an important role in extracellular matrix degeneration and in aortic aneurysm formation. Increased MMP activity has indeed been observed in Fibulin-4 deficient mice with these probes.[17, 19] Furthermore, MMPs, mainly MMP3, -9, -12 and -13, were shown to be involved in different stages of plaque formation.[20] Therefore, the highly increased MMP activity observed in ApoE$^{-/-}$Fibulin-4$^{+/R}$ mice might be due to aortic wall degeneration as well as increased atherosclerotic plaques, and might contribute to the altered plaque morphology in these mice.

This ApoE$^{-/-}$Fibulin-4$^{+/R}$ mouse model with diet-induced atherosclerosis shows that subtle manifestations of aberrant elastin formation in heterozygous Fibulin-4$^{+/R}$ mice might predispose to thoracic and abdominal aortic disease as well as enhanced atherosclerotic disease. This combined mouse model provides the opportunity to unravel the biological

processes underlying aortic wall degeneration and to identify markers that elucidate key events in the early stages of the pathogenic sequence that might culminate in an aneurysm. In fact, the ApoE$^{-/-}$Fibulin-4 mouse model therefore indicates that a haploinsufficiency for Fibulin-4 leads to a pathogenic outcome in combination with fat diets, and therefore might resemble patients that experience late-onset 'sporadic' and barely detectable forms of aneurysms. Additionally, this model provides insight in the effect of mild extracellular matrix defects, as observed during aging, on the progression of atherosclerosis.

ACKNOWLEDGEMENT

This work was supported by the 'Lijf en Leven' grant (2008): 'Early detection and diagnosis of aneurysms and heart valve abnormalities' (to JE and PvH).

REFERENCES

1. Lindsay ME, Dietz HC. Lessons on the pathogenesis of aneurysm from heritable conditions. *Nature*. 2011;473:308-316
2. Isselbacher EM. Thoracic and abdominal aortic aneurysms. *Circulation*. 2005;111:816-828
3. Agricola E, Slavich M, Tufaro V, Fisicaro A, Oppizzi M, Melissano G, Bertoglio L, Marone E, Civilini E, Margonato A, Chiesa R. Prevalence of thoracic ascending aortic aneurysm in adult patients with known abdominal aortic aneurysm: An echocardiographic study. *Int J Cardiol*. 2013
4. Larsson E, Vishnevskaya L, Kalin B, Granath F, Swedenborg J, Hultgren R. High frequency of thoracic aneurysms in patients with abdominal aortic aneurysms. *Ann Surg*. 2011;253:180-184
5. Lederle FA, Johnson GR, Wilson SE, Chute EP, Littooy FN, Bandyk D, Krupski WC, Barone GW, Acher CW, Ballard DJ. Prevalence and associations of abdominal aortic aneurysm detected through screening. Aneurysm detection and management (adam) veterans affairs cooperative study group. *Ann Intern Med*. 1997;126:441-449
6. Kielty CM, Sherratt MJ, Shuttleworth CA. Elastic fibres. *J Cell Sci*. 2002;115:2817-2828
7. Argraves WS, Greene LM, Cooley MA, Gallagher WM. Fibulins: Physiological and disease perspectives. *EMBO Rep*. 2003;4:1127-1131
8. Chen Q, Zhang T, Roshetsky JF, Ouyang Z, Essers J, Fan C, Wang Q, Hinek A, Plow EF, Dicorleto PE. Fibulin-4 regulates expression of the tropoelastin gene and consequent elastic-fibre formation by human fibroblasts. *Biochem J*. 2009;423:79-89
9. Hoyer J, Kraus C, Hammersen G, Geppert JP, Rauch A. Lethal cutis laxa with contractural arachnodactyly, overgrowth and soft tissue bleeding due to a novel homozygous fibulin-4 gene mutation. *Clin Genet*. 2009;76:276-281
10. Hucthagowder V, Sausgruber N, Kim KH, Angle B, Marmorstein LY, Urban Z. Fibulin-4: A novel gene for an autosomal recessive cutis laxa syndrome. *Am J Hum Genet*. 2006;78:1075-1080

11. Dasouki M, Markova D, Garola R, Sasaki T, Charbonneau NL, Sakai LY, Chu ML. Compound heterozygous mutations in fibulin-4 causing neonatal lethal pulmonary artery occlusion, aortic aneurysm, arachnodactyly, and mild cutis laxa. *Am J Med Genet A*. 2007;143A:2635-2641
12. Renard M, Holm T, Veith R, Callewaert BL, Ades LC, Baspinar O, Pickart A, Dasouki M, Hoyer J, Rauch A, Trapane P, Earing MG, Coucke PJ, Sakai LY, Dietz HC, De Paepe AM, Loeys BL. Altered tgfbeta signaling and cardiovascular manifestations in patients with autosomal recessive cutis laxa type i caused by fibulin-4 deficiency. *Eur J Hum Genet*. 2010;18:895-901
13. Erickson LK, Opitz JM, Zhou H. Lethal osteogenesis imperfecta-like condition with cutis laxa and arterial tortuosity in mz twins due to a homozygous fibulin-4 mutation. *Pediatr Dev Pathol*. 2012;15:137-141
14. Sawyer SL, Dicke F, Kirton A, Rajapkse T, Rebeyka IM, McInnes B, Parboosingh JS, Bernier FP. Longer term survival of a child with autosomal recessive cutis laxa due to a mutation in fbln4. *Am J Med Genet A*. 2013;161A:1148-1153
15. Kappanayil M, Nampoothiri S, Kannan R, Renard M, Coucke P, Malfait F, Menon S, Ravindran HK, Kurup R, Faiyaz-Ul-Haque M, Kumar K, De Paepe A. Characterization of a distinct lethal arteriopathy syndrome in twenty-two infants associated with an identical, novel mutation in fbln4 gene, confirms fibulin-4 as a critical determinant of human vascular elastogenesis. *Orphanet J Rare Dis*. 2012;7:61
16. McLaughlin PJ, Chen Q, Horiguchi M, Starcher BC, Stanton JB, Broekelmann TJ, Marmorstein AD, McKay B, Mecham R, Nakamura T, Marmorstein LY. Targeted disruption of fibulin-4 abolishes elastogenesis and causes perinatal lethality in mice. *Mol Cell Biol*. 2006;26:1700-1709
17. Hanada K, Vermeij M, Garinis GA, de Waard MC, Kunen MG, Myers L, Maas A, Duncker DJ, Meijers C, Dietz HC, Kanaar R, Essers J. Perturbations of vascular homeostasis and aortic valve abnormalities in fibulin-4 deficient mice. *Circ Res*. 2007;100:738-746
18. Huang J, Davis EC, Chapman SL, Budatha M, Marmorstein LY, Word RA, Yanagisawa H. Fibulin-4 deficiency results in ascending aortic aneurysms: A potential link between abnormal smooth muscle cell phenotype and aneurysm progression. *Circ Res*. 2010;106:583-592
19. Kaijzel EL, van Heijningen PM, Wielopolski PA, Vermeij M, Koning GA, van Cappellen WA, Que I, Chan A, Dijkstra J, Ramnath NW, Hawinkels LJ, Bernsen MR, Lowik CW, Essers J. Multimodality imaging reveals a gradual increase in matrix metalloproteinase activity at aneurysmal lesions in live fibulin-4 mice. *Circ Cardiovasc Imaging*. 2010;3:567-577
20. Carmeliet P, Moons L, Lijnen R, Baes M, Lemaitre V, Tipping P, Drew A, Eeckhout Y, Shapiro S, Lupu F, Collen D. Urokinase-generated plasmin activates matrix metalloproteinases during aneurysm formation. *Nat Genet*. 1997;17:439-444
21. Luttun A, Lutgens E, Manderveld A, Maris K, Collen D, Carmeliet P, Moons L. Loss of matrix metalloproteinase-9 or matrix metalloproteinase-12 protects apolipoprotein e-deficient mice against atherosclerotic media destruction but differentially affects plaque growth. *Circulation*. 2004;109:1408-1414
22. Zhang SH, Reddick RL, Piedrahita JA, Maeda N. Spontaneous hypercholesterolemia and arterial lesions in mice lacking apolipoprotein e. *Science*. 1992;258:468-471
23. Breslow JL. Mouse models of atherosclerosis. *Science*. 1996;272:685-688
24. Plump AS, Smith JD, Hayek T, Aalto-Setala K, Walsh A, Verstuyft JG, Rubin EM, Breslow JL. Severe hypercholesterolemia and atherosclerosis in apolipoprotein e-deficient mice created by homologous recombination in es cells. *Cell*. 1992;71:343-353

25. Lutgens E, de Muinck ED, Heeneman S, Daemen MJ. Compensatory enlargement and stenosis develop in apoe(-/-) and apoe*3-leiden transgenic mice. *Arterioscler Thromb Vasc Biol*. 2001;21:1359-1365
26. Doyle JJ, Gerber EE, Dietz HC. Matrix-dependent perturbation of tgfbeta signaling and disease. *FEBS Lett*. 2012;586:2003-2015
27. Choudhury R, McGovern A, Ridley C, Cain SA, Baldwin A, Wang MC, Guo C, Mironov A, Jr., Drymoussi Z, Trump D, Shuttleworth A, Baldock C, Kielty CM. Differential regulation of elastic fiber formation by fibulin-4 and -5. *J Biol Chem*. 2009;284:24553-24567
28. Van Herck JL, De Meyer GR, Martinet W, Van Hove CE, Foubert K, Theunis MH, Apers S, Bult H, Vrints CJ, Herman AG. Impaired fibrillin-1 function promotes features of plaque instability in apolipoprotein e-deficient mice. *Circulation*. 2009;120:2478-2487

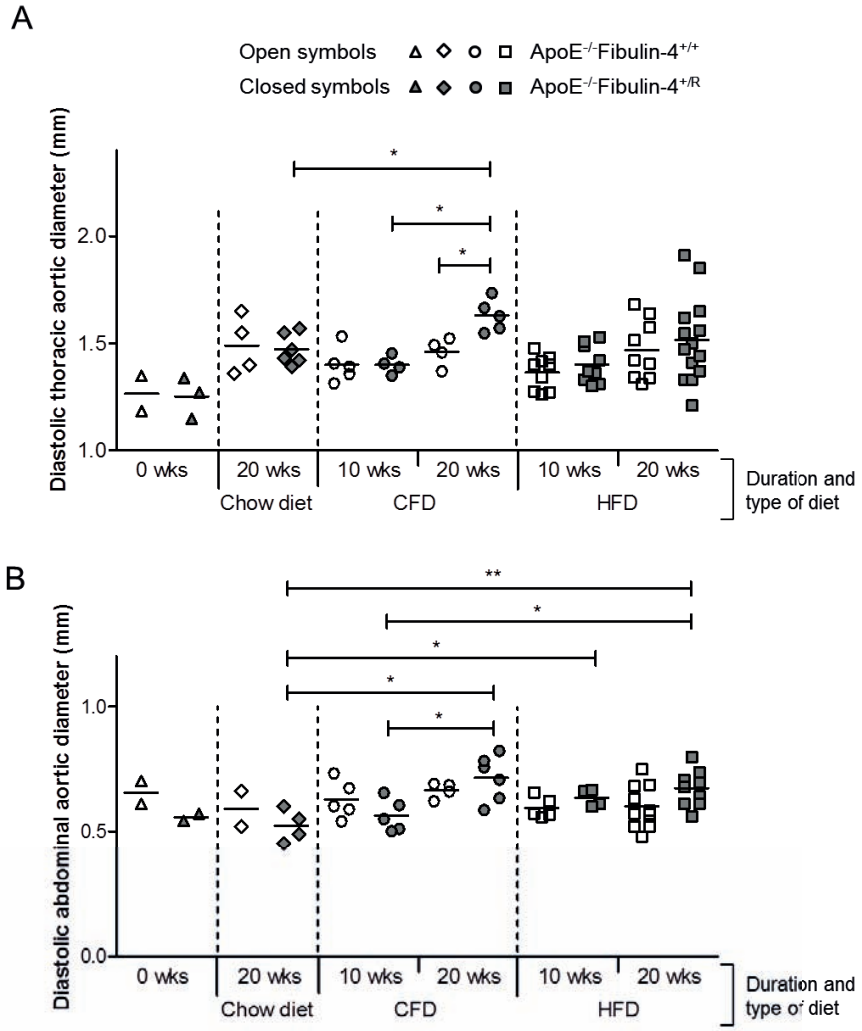

Supplemental Figure 1.Increased diastolic thoracic and abdominal aortic diameters in ApoE$^{-/-}$Fibulin-4$^{+/R}$ mice. (A) M-mode aortic diameter measurements in diastole by ultrasound imaging show significant dilation of the aortic arches of ApoE$^{-/-}$Fibulin-4$^{+/R}$ mice after 20 weeks of CFD (n=5) compared to ApoE$^{-/-}$Fibulin-4$^{+/+}$ mice after 20 weeks of CFD (n=5), ApoE$^{-/-}$Fibulin-4$^{+/R}$ mice after 10 weeks of CFD (n=5) and ApoE$^{-/-}$Fibulin-4$^{+/R}$ mice after 20 weeks of chow diet (n=6). Aortic arch diameters after 10 or 20 weeks of HFD seem to be evenly distributed in ApoE$^{-/-}$Fibulin-4$^{+/+}$ and ApoE$^{-/-}$Fibulin-4$^{+/R}$ mice, with an increased diameter variation. No differences are observed in mice fed a chow diet for 0 or 20 weeks. (B) Abdominal aortic measurements in diastole show significantly increased diameters in ApoE$^{-/-}$Fibulin-4$^{+/R}$ mice after 20 weeks of CFD compared to ApoE$^{-/-}$Fibulin-4$^{+/R}$ mice after 10 weeks of CFD and 20 weeks of chow diet. Furthermore, increased abdominal aortic diameters are observed in ApoE$^{-/-}$Fibulin-4$^{+/R}$ mice after 10 and 20 weeks of HFD compared to ApoE$^{-/-}$Fibulin-4$^{+/R}$ mice after 20 weeks of chow diet, and ApoE$^{-/-}$Fibulin-4$^{+/R}$ mice after 20 weeks of HFD compared to ApoE$^{-/-}$Fibulin-4$^{+/R}$ mice after 10 weeks of CFD (*p<0.05, **p<0.01). Open symbols indicate aortic diameters of ApoE$^{-/-}$Fibulin-4$^{+/+}$ mice, closed symbols indicate aortic diameters of ApoE$^{-/-}$Fibulin-4$^{+/R}$ mice.

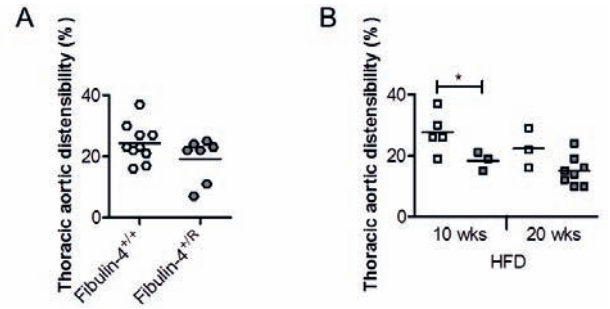

Supplemental Figure 2. Decreased distensibility of aortic arches from ApoE$^{-/-}$Fibulin-4$^{+/R}$ mice. (A) Calculations of aortic wall displacements in M-mode during systole and diastole indicate a slight non-significant reduced distensibility of 15 weeks old Fibulin-4$^{+/R}$ aortas on a chow diet compared to Fibulin-4$^{+/+}$ aortas. (B) A significantly reduced distensibility is observed in calculations of aortic wall displacements in B-mode of ApoE$^{-/-}$Fibulin-4$^{+/R}$ (n=5) aortas after 10 weeks of HFD, which further decreases after 20 weeks (n=10) of HFD compared to ApoE$^{-/-}$Fibulin-4$^{+/+}$ aortas (n=5) (*p<0.05).

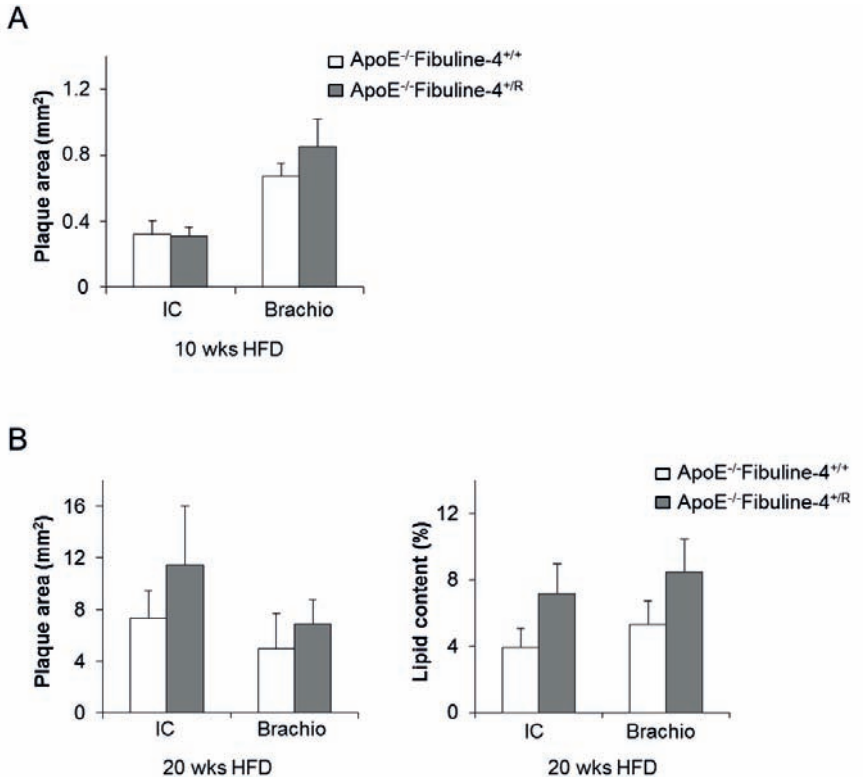

Supplemental Figure 3. Quantification of plaque area on histological sections of ApoE$^{-/-}$Fibulin-4 aortas after 10 and 20 weeks of HFD. (A) Plaque area quantified in the inner curvature of the aortic arch shows no difference between ApoE$^{-/-}$Fibulin-4$^{+/R}$ mice (n=8) and ApoE$^{-/-}$Fibulin-4$^{+/+}$ mice after 10 weeks of HFD (n=8), while a slight increase is observed in the brachiocephalic artery. (B) Quantified plaque area and percentage lipid content in plaques show a slight increase in ApoE$^{-/-}$Fibulin-4$^{+/R}$ mice after 20 weeks of HFD (n=5) compared to ApoE$^{-/-}$Fibulin-4$^{+/R}$ mice (n=3). IC= inner curvature, Brachio= brachiocephalic artery.

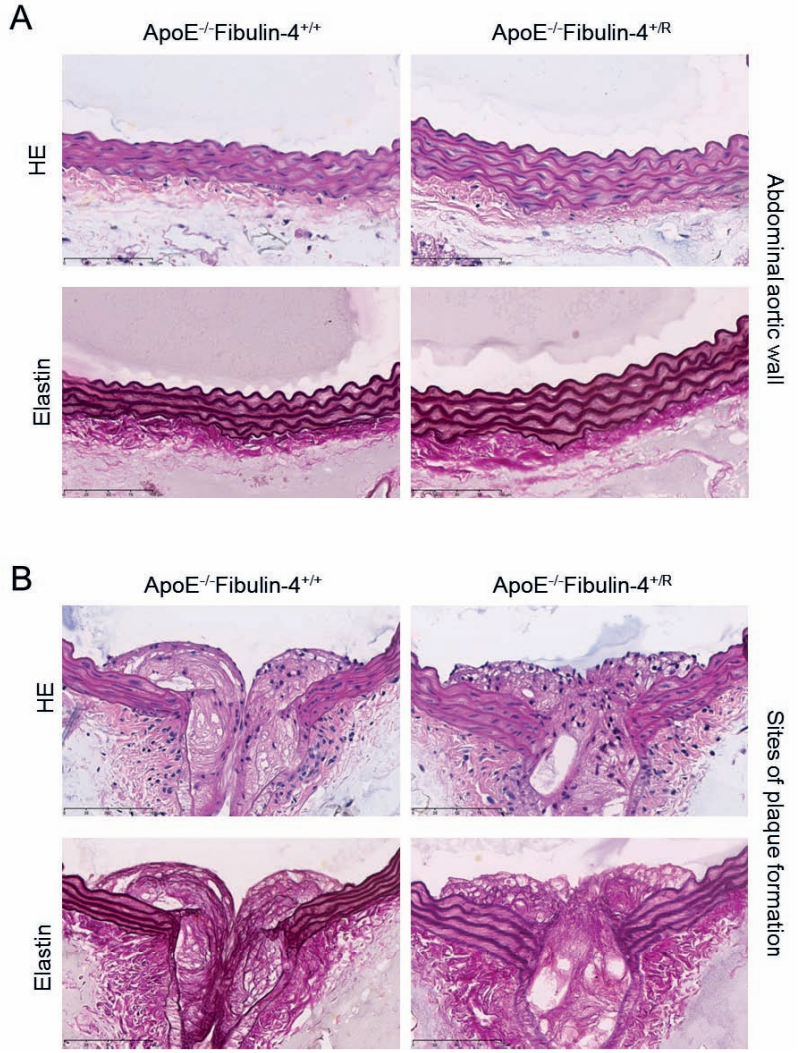

Supplemental Figure 4. Histological analysis of abdominal aortas after 10 weeks of HFD. HE and elastin analysis of the abdominal aorta revealed (A) thickened abdominal aortic wall with increased spaces between the elastic laminae in ApoE$^{-/-}$Fibulin-4$^{+/R}$ mice after 10 weeks of HFD as compared to ApoE$^{-/-}$Fibulin-4$^{+/+}$ mice, (B) which is also observed at sites of plaque formation.

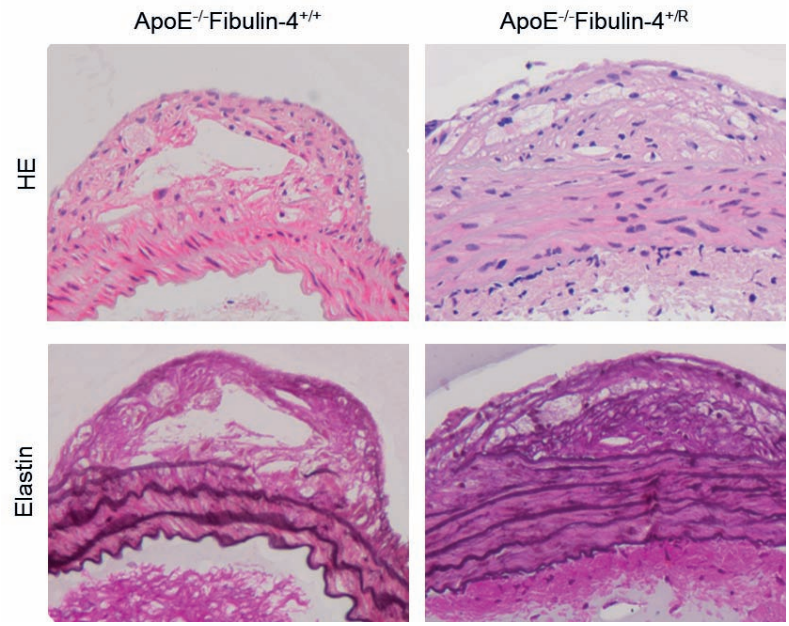

Supplemental Figure 5. Histological analysis of abdominal aortas after 20 weeks of HFD. HE and elastin analysis of the abdominal aorta after 20 weeks of HFD points to a thickened abdominal aortic wall with increased spaces between the elastic laminae in ApoE$^{-/-}$Fibulin-4$^{+/R}$ mice as compared to ApoE$^{-/-}$Fibulin-4$^{+/+}$ mice.

CHAPTER 5

AT1 RECEPTOR BLOCKADE, BUT NOT RENIN INHIBITION, REDUCES ANEURYSM GROWTH AND CARDIAC FAILURE IN FIBULIN-4 MICE

Luuk te Riet[1,2], Elza D. van Deel[3,4], Bibi S. van Thiel[1,2,3], Els Moltzer[1], Nicole van Vliet[3], Yanto Ridwan[3], Richard van Veghel[1], Paula M. van Heijningen[3], Jan Lukas Robertus[5], Ingrid M. Garrelds[1], Marcel Vermeij[5], Ingrid van der Pluijm[2,3], A. H. Jan Danser[1], Jeroen Essers[2,3,6]

[1]Department of Internal Medicine, Division of Pharmacology and Vascular Medicine, [2]Department of Vascular Surgery, [3]Department of Molecular Genetics, Cancer Genomics Center, [4]Department of Cardiology, [5]Department of Pathology, [5]Department of Radiation Oncology, Erasmus MC, Rotterdam, The Netherlands

(Journal of Hypertension 2016 Apr;34(4):654-65)

ABSTRACT

Aims: Increasing evidence supports a role for the angiotensin (Ang) II-AT_1 receptor axis in aneurysm development. Here we studied whether counteracting this axis via stimulation of AT_2 receptors is beneficial. Such stimulation occurs naturally during AT_1 receptor blockade with losartan, but not during renin inhibition with aliskiren.

Methods and Results: Aneurysmal homozygous Fibulin-$4^{R/R}$ mice, displaying a 4-fold reduced fibulin-4 expression, were treated with placebo, losartan, aliskiren, or the β-blocker propranolol from day 35-100. Their phenotype includes cystic media degeneration, aortic regurgitation, left ventricular (LV) dilation, reduced ejection fraction, and fractional shortening. While losartan and aliskiren reduced hemodynamic stress and increased renin similarly, only losartan increased survival. Propranolol had no effect. No drug rescued elastic fiber fragmentation in established aneurysms, although losartan did reduce aneurysm size. Losartan also increased ejection fraction, decreased LV diameter, and reduced cardiac pSmad2 signaling. None of these effects were seen with aliskiren or propranolol. Longitudinal microCT measurements, a novel method in which each mouse serves as its own control, revealed that losartan reduced LV growth more than aneurysm growth, presumably because the heart profits both from the local (cardiac) effects of losartan and its effects on aortic root remodeling.

Conclusions: Losartan, but not aliskiren or propranolol, improved survival in Fibulin-$4^{R/R}$ mice. This most likely relates to its capacity to improve structure and function of both aorta and heart. The absence of this effect during aliskiren treatment, despite a similar degree of blood pressure reduction and renin-angiotensin system blockade, suggests that it might be due to AT_2 receptor stimulation.

INTRODUCTION

Thoracic aorta aneurysms (TAA) show degeneration of the medial layer of the aortic wall, characterized by elastic fiber fragmentation, loss of smooth muscle cells, and the accumulation of amorphous extracellular matrix.[1] Such aortic wall degeneration is often a consequence of inherited connective tissue disorders. The most common inherited TAA disease, Marfan syndrome (MFS), is due to a mutation in the *FBN1* gene, which encodes the extracellular matrix (ECM) glycoprotein fibrillin-1. *FBN1* mutations result in a disorganized ECM assembly in the aortic wall[2], leading to all above described key features of TAA in MFS patients. Mice heterozygous for a cysteine substitution in an epidermal growth factor-like domain of fibrillin-1 (*Fbn1*$^{C1039G/+}$ mice), i.e., a mutation which is prototypical for the *FBN1* mutations in humans, similarly develop TAA.[3]

Another factor in the elastic fiber assembly of the vessel wall, heart valves and myocardial interstitium, is the ECM protein fibulin-4, encoded by the FBLN4 gene.[4, 5] In humans, a mutation in this gene causes cutis laxa syndrome, that besides cutis laxa (loose skin), bone fragility and lung emphysema is characterized by vascular tortuosity and aneurysms similar to those observed in MFS.[6-11] Moreover, mice with a systemic 4-fold reduced fibulin-4 expression (Fibulin-4$^{R/R}$) share similar key features as seen in MFS and cutis laxa syndrome, i.e., cystic media degeneration, aortic regurgitation, and impaired cardiac morphology and function[12, 13], while complete fibulin-4 gene knock-out mice (Fibulin-4$^{-/-}$) die perinatally from aortic rupture.[14]

Recent studies have shown that transforming growth factor (TGF)β signaling is upregulated in TAAs of MFS.[13, 15, 16] While direct regulators of TGFβ signaling include TGFβ and bone morphogenetic protein ligands, indirect stimulation of TGFβ signaling is accomplished by angiotensin (Ang) II, via its type 1 receptor (AT_1R). In support of this concept, both TGFβ-neutralizing antibodies and the AT_1R blocker losartan exerted beneficial effects in rodent TAA models, including Fibulin-4$^{R/R}$ mice when treated prenatally.[13, 15] Yet, clinical studies with losartan in MFS did not yield uniformly positive results.[17, 18] Blocking AT_1R results in a counterregulatory rise in renin, thereby increasing Ang II levels. This Ang II cannot stimulate the blocked AT_1R, but it may still bind to the unoccupied Ang II type 2 receptors (AT_2R), which antagonizes AT_1R-mediated effects.[19, 20] Such AT_2R stimulation is potentially beneficial in TAA[20], and will not occur during other forms of renin-angiotensin system (RAS) blockade, i.e., inhibition of the enzymes that generate Ang I (renin) or Ang II (ACE).

In the present study, we hypothesized that losartan outperforms the renin inhibitor aliskiren in the treatment of Fibulin-4$^{R/R}$ mice, given its additional AT_2R-stimulating effects. Both drugs were compared with placebo and the β-blocker propranolol, a MFS drug that is often used in the clinic because it is expected to reduce heart rate, blood pressure and dP/dt. ACE inhibitors were not included, since such drugs, in addition to suppressing

Ang II, also increase bradykinin, thus introducing interference with yet another hormonal system. Treatment started postnatally at a clinically relevant age: day 35, when the aneurysm is already present, and lasted up to 100 days. Moreover, we used a novel *in-vivo* μCT-technique allowing longitudinal measurement that monitors the therapeutic treatment effects on both aneurysm progression as well as cardiac growth in time simultaneously.

Our data show that losartan, but not aliskiren or propranolol, independently of its blood pressure-lowering effect, improved survival in Fibulin-$4^{R/R}$ mice. The absence of this effect during aliskiren treatment suggests that it might involve AT_2R stimulation.

MATERIAL AND METHODS

Experimental animals

Generation of Fibulin-$4^{R/R}$ mice has been described previously.[12] Heterozygous (Fibulin-$4^{+/R}$) mice in a mixed C57Bl/6x129 background were mated to obtain Fibulin-$4^{+/+}$ (wild-type) and Fibulin-$4^{R/R}$ littermates. Animals were housed in the institutional animal facility. Both males and females were included in the study, and since no apparent sex-related differences were observed, data from both sexes were pooled. All experiments were performed under the regulation and permission of the Animal Care Committee of the Erasmus MC, Rotterdam, The Netherlands (protocol number 139-11-09 and 139-13-11). The investigation conforms to the *Guide for the Care and Use of Laboratory Animals* published by the US National Institutes of Health (NIH Publication, revised 2011).

Treatment

Fibulin-$4^{R/R}$ mice and wild-type mice were treated postnatally from the age of 35 days up to 100 days with placebo, losartan (60 mg/kg p.o. per day; a kind gift of MSD, Haarlem, The Netherlands), aliskiren (62.5 mg/kg p.o. per day; a kind gift of Novartis Pharmaceuticals, Basel, Switzerland), or propranolol (50 mg/kg p.o. per day; Sigma, St. Louis, USA) in drinking water, as described before.[13, 15, 21, 22]

Histology

Mice (age 100 days) were weighed, euthanized by an overdose of CO_2, and necropsied according to standard protocols. Perfusion-fixed aortas and hearts were isolated and paraffin-embedded. Next, 4 μm-aorta sections were haematoxylin and eosin (HE)-stained, stained for elastin (Verhoeff van Gieson), glycosaminoglycans (Alcian Blue) or vascular smooth muscle cells (VSMCs, α-smooth muscle actin). Immunohistochemistry for phosphorylated Smad2 (pSmad2) was performed as described previously[23], using rabbit antiphospho-smad2 antibodies (Cell Signaling Technology, Danvers, USA). Positively stained pSmad2 nuclei were divided by the total number of nuclei to obtain relative

amounts. HE-stained aorta slides were scanned with a nanozoomer (Hamamatsu, Almere, The Netherlands), and subsequently aortic wall diameter and aortic wall area were analyzed with NanoZoomer Digital Pathology view (Hamamatsu). Finally, 5-µm heart sections were stained with Gomori's silver staining to visualize individual cardiomyocytes of the left ventricle (LV).[24] Only transversally cut cells showing a nucleus were used to determine the cardiomyocyte area.

Biochemical measurements

RAS components were measured in kidneys (Ang II) and blood plasma (renin). Blood was collected from the left ventricle immediately prior to euthanization in heparin-coated tubes, centrifuged at 5500 RPM, and plasma was stored at -80°C. Kidneys were removed after the animals had been euthanized, frozen in liquid nitrogen, and stored at -80°C. Tissue Ang II was measured by radioimmunoassay, after SepPak extraction and reversed-phase HPLC separation as previously described.[25, 26] Plasma renin concentration (PRC) was determined by enzyme-kinetic assay in the presence of excess angiotensinogen as described before.[26] Additionally, B-type natriuretic peptide-45 (BNP-45) was measured in plasma, making use of a commercially available enzyme immuno-assay (Phoenix Pharmaceuticals Inc., Karlsruhe, Germany).

Ultrasound and hemodynamic measurements

To evaluate the treatment of the different compounds on aneurysm formation and cardiac function, cardiac geometry, echocardiographic and hemodynamic measurements were performed in 100-days old Fibulin-$4^{+/+}$ (wild type) and Fibulin-$4^{R/R}$ mice. Mice were anesthetized with 2.5% isoflurane and ventilated with 35% O_2. Anesthesia did not affect heart rate (data not shown). Echocardiography of the ascending aorta and LV was performed using a Vevo2100 (VisualSonics Inc., Toronto, Canada). Ascending aorta and LV lumen diameter, aortic distensibility, ejection fraction and fractional shortening were obtained from M-Mode images. Ejection fraction and fractional shortening were defined as the relative differences between end-diastolic and end-systolic volumes and diameter, respectively.[13] Subsequently, a 1.4-Fr microtipped manometer (Millar Instruments, Houston, USA) was inserted into the right carotid artery to measure aortic pressure.[27] Hemodynamic data were recorded and digitized using an online 4-channel data acquisition program (ATCODAS, Dataq Instruments, Akron, USA), analysis was performed with a program written in Matlab.[28] Ten consecutive beats were selected for determination of systolic and diastolic blood pressure, subsequent mean arterial pressures (MAP) were calculated.

Western blot

LV tissue samples were used for immunoblotting of extracellular signal-regulated kinases (ERK1/2), phosphorylated ERK1/2 (pERK1/2), Smad2 and pSmad2 (Cell Signaling Technol-

ogy). Ratios of phosphorylated protein levels to loading control β-actin were calculated and corrected for the ratios in wild-type mice.

Quantitative real-time reverse transcription polymerase chain reaction

Expression of angiotensin II type 1a, type 1b and type 2 receptors ($AT_{1a}R$, $AT_{1b}R$ and AT_2R) was analyzed in LV tissue. Total RNA was isolated using RNeasy Fibrous Tissue Mini Kit (Qiagen, Hilden, Germany) and reverse transcribed using iScript cDNA Synthesis Kit (Bio-Rad, Veenendaal, The Netherlands). cDNA samples were subjected to 40 cycles real-time PCR analysis using SYBR Green qPCR Master Mix 2x (Bio-Rad) and primers; β-actin 5'-AGCCATGTACGTAGCCATCCA-3', 5'-TCTCCGGAGTCCATCACAATG-3'; β_2-microglobin 5'-CTCACACTGAATTCACCCCCA-3', 5'-GTCTCGATCCCAGTAGACGGT-3'; $AT_{1a}R$ 5'-CCCACGTGTCCCTGTTACTAC-3', 5'-TTTGGGGACAGTACAGGTTTC-3'; $AT_{1b}R$ 5'-CTGTGAAATTGCGGACGTAGT-3', 5'-AAGCCATAAAACAGAGGGTTCAG-3'; AT_2R 5'-TACCCGTGACCAAGTCCTGA-3', 5'-TACCCATCCAGGTCAGAGCA-3'. Gene expression was calculated using β-actin and β_2-microglobin as housekeeping genes and the comparative Ct method (ΔΔCt) was used for relative quantification of gene expression.

FMT-CT Imaging

We used vascular Computed Tomography (CT) and fluorescent mediated tomography (FMT)-CT imaging with near-infrared fluorescent protease activatable probes as previously described.[29] In short, mice subjected to FMT-CT were shaved and depilated to remove all hair that otherwise would absorb light and interfere with optical imaging. Mice subjected to vascular CT and FMT-CT mice received 5 mL/kg body weight Exia 160 contrast agent (Binitio Biomedical Inc., Ottawa, Canada) through injection in the tail vein for subsequent CT analysis. Mice only subjected to vascular CT imaging were anesthetized (2.5% isoflurane) and scanned directly with the microCT scanner (Quantum FX system, Perkin Elmer Inc., Akron, USA). The thoracic aorta diameter, thoracic aortic volume and left ventricular volume were analyzed with a rendering program 'microCT Tools by Analyze 11.0 software' (AnalyzeDirect Inc., Overland Park, USA). Fibulin-4 mice which were also subjected to FMT imaging, were scanned with an FMT 2500 system (Perkin Elmer Inc.) at 680 nm excitation and emission wavelengths, at 24 hours after tail vein injection of 5 nmol of MMPSense680™ (Perkin Elmer Inc.). Mice were anesthetized (2.5% isoflurane) and fixed into the portable animal imaging cassette that lightly compressed the anesthetized mouse between optically translucent windows, thereby preventing motion during FMT and CT imaging. After FMT imaging, anesthetized mice were scanned with the microCT scanner to identify heart and aortic root region of the animals. After FMT-CT imaging, complete aortas were harvested and fluorescence was quantified using the FMT 2500 and Odyssey imaging systems (LI-COR Inc.). Near infrared images were obtained in the 680 nm channel.

Data analysis

Normally distributed data are presented as mean±SEM. One-way ANOVA was applied for the analysis between groups, followed by a post-hoc Dunnett's test when appropriate. All statistical tests were two-sided and $P<0.05$ was considered statistically significant.

RESULTS

Losartan increases survival of adult Fibulin-$4^{R/R}$ animals independently of its effect on blood pressure and the degree of RAS blockade

Reduced fibulin-4 expression resulted in severe TAA, cardiac hypertrophy, and diminished survival (Fig. 1A-1B), in full agreement with previous observations.[12, 13] Losartan, but not aliskiren treatment, significantly improved survival (Fig. 1C). Propranolol even tended to diminish survival (P=0.25), and no animal survived up to 100 days with this treatment. As a consequence, blood pressure data could not be obtained in propranolol-treated mice, and in only 3 surviving aliskiren-treated mice versus 5 losartan-treated mice. MAP tended to be diminished in Fibulin-$4^{R/R}$ mice (P=0.17). Both RAS blockers similarly reduced MAP at 100 days (Fig. 1D). PRC and renal Ang II were higher in fibulin-$4^{R/R}$ mice than in wild-type animals (Fig. 1E-1F). Losartan and aliskiren comparably increased PRC versus placebo, suggesting a similar degree of RAS blockade. Losartan, but not aliskiren, additionally suppressed renal Ang II.

Losartan improves aneurysm size and aortic distensibility without affecting structural changes and matrix metalloproteinases (MMPs)

At the age of 100 days, the ascending aortic diameter in Fibulin-$4^{R/R}$ mice was almost 3 times enlarged compared to wild-type mice (Fig. 2A). This widening was accompanied by an approximately 50% decrease in distensibility (Fig. 2B) and an increased wall thickness (Fig. 2C). Losartan improved diameter and distensibility without affecting thoracic aortic wall thickness, whereas aliskiren had no significant effect on any of these parameters (Fig. 2A-2C). For reasons discussed above, similar data could not be obtained for propranolol. Neither losartan nor aliskiren affected the disturbed aortic wall morphology, the severe alterations in elastic fiber organization, or the increased glycosaminoglycan deposition in Fibulin-$4^{R/R}$ mice (Fig. 2D-2F). These drugs also did not significantly improve the reduced VSMC content, or diminish the increased pSmad2-signaling in these animals (Fig. 2G-2H). Non-canonical (pERK) TGFβ signaling was similarly unaffected (data not shown).

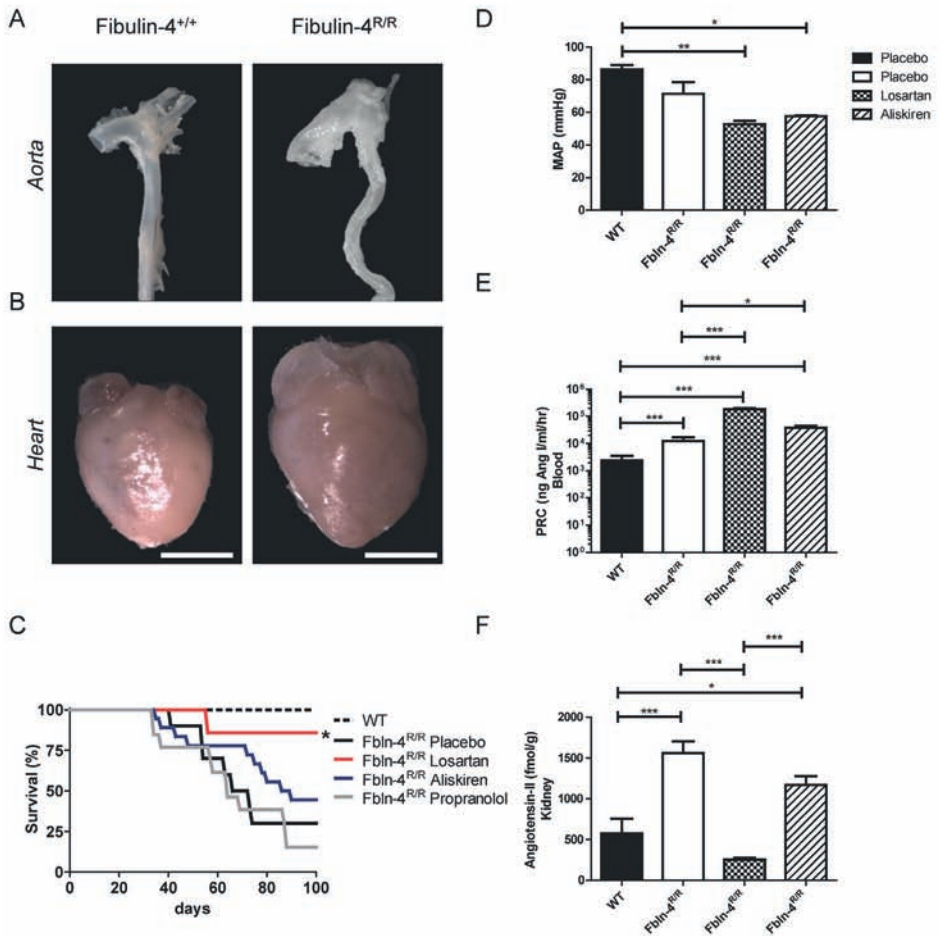

Figure 1. (A-B) Reduced fibulin-4 expression results in thoracic aorta aneurysms and cardiac hypertrophy in 100-day old Fibulin-$4^{R/R}$ mice (white bars represent 4 mm). (C) Kaplan-Meier survival curves of WT and treated Fibulin-$4^{R/R}$ mice (n=7-19). *P<0.05 vs. placebo. (D-F) Mean arterial pressure (MAP; n=3-5), plasma renin concentration (PRC; n=10-18), and renal angiotensin II levels (n=5) in Fibulin-$4^{R/R}$ mice treated for 65 days with placebo, losartan, aliskiren or propranolol vs. untreated age-matched WT mice. Data are mean±SEM. *P<0.05, **P<0.01, ***P<0.001.

In vivo MMP activity, measured by 3D FMT-CT, was undetectable in aortas of wild-type mice, but greatly increased in the aortic arch of placebo- or losartan-treated Fibulin-$4^{R/R}$ mice (Fig. 3A). Abdominal aorta MMP measurements were inaccurate due to the high fluorescent signal from the liver. Removal of the aortas after sacrifice allowed ex-vivo imaging at much great sensitivity (Fig. 3B), and confirmed the in-vivo observations. Losartan did not affect MMP activity as compared to placebo (Fig. 3C). Consequently, MMP activity was not determined in aliskiren-treated mice.

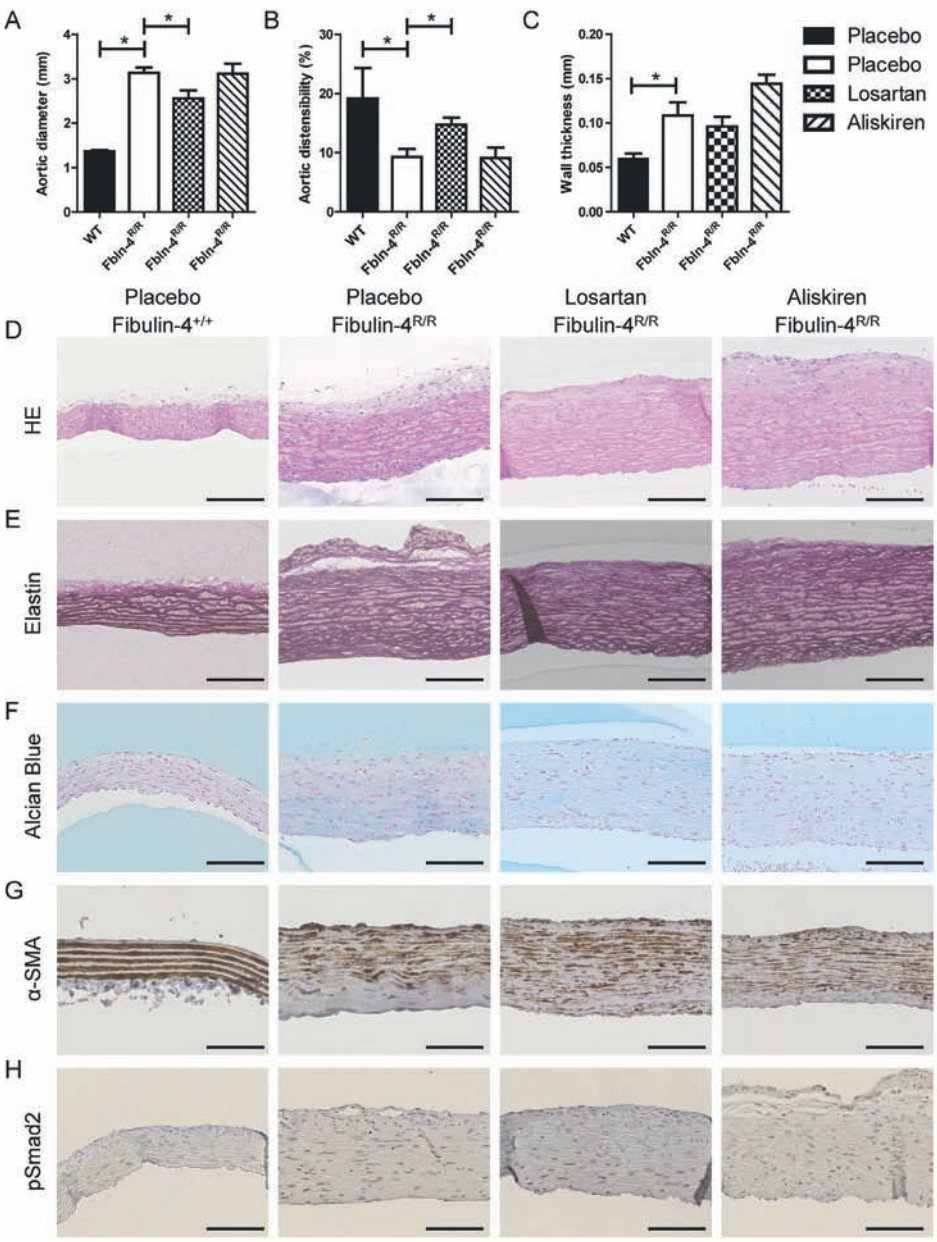

Figure 2. (A-C) Aortic diameter, distensibility and wall diameter in Fibulin-$4^{R/R}$ mice treated for 65 days with placebo, losartan or aliskiren vs. age-matched untreated WT mice (mean±SEM of n=6-10) (black bars represent 100 μm); *P<0.05 vs. placebo. Treatment did not affect aortic wall morphology (D), elastic fiber fragmentation (E), extracellular matrix deposition (Alcian Blue) (F), α-smooth muscle actin (SMA) deposition (G), or pSmad2-signaling (H).

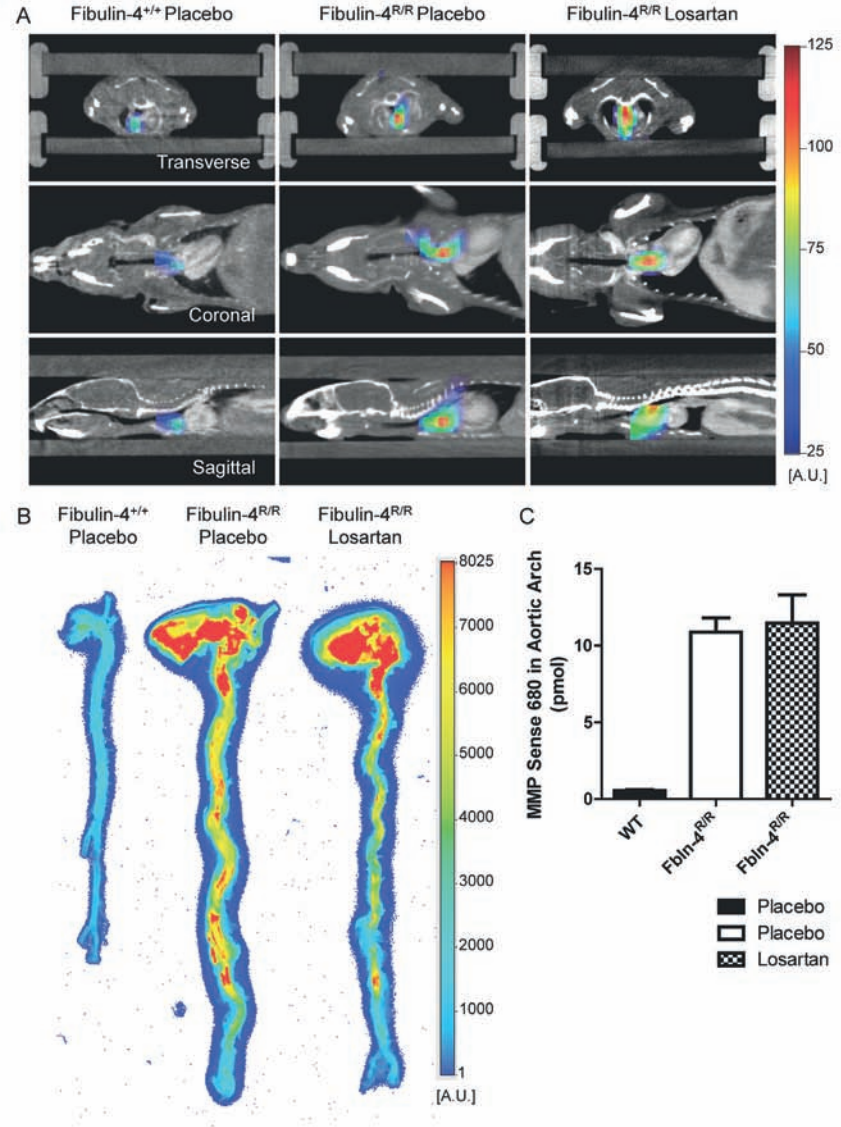

Figure 3. (A) *In-vivo* three-dimensional FMT-CT co-registration of heart and aorta in Fibulin-$4^{R/R}$ mice treated for 65 days with placebo or losartan vs. age-matched untreated WT mice, after injection of MMPSense 680 to determine matrix metalloproteinase (MMP) activity. (B) MMP activity determined *ex vivo* in whole aortas, and (C) its quantification (mean±SEM of n=2).

Losartan improves cardiac morphology and function

Transthoracic echocardiography in placebo-treated Fibulin-$4^{R/R}$ mice revealed a tripling of LV mass and a doubling of LV diameter versus wild-type mice (Fig. 4A-4B) at the age of 100 days. Ejection fraction and fractional shortening were both greatly reduced (Fig.

4C-4D). Losartan improved all parameters, although significance was not reached for LV mass. Aliskiren affected none of these parameters. Data for propranolol in 100-day old mice could not be obtained.

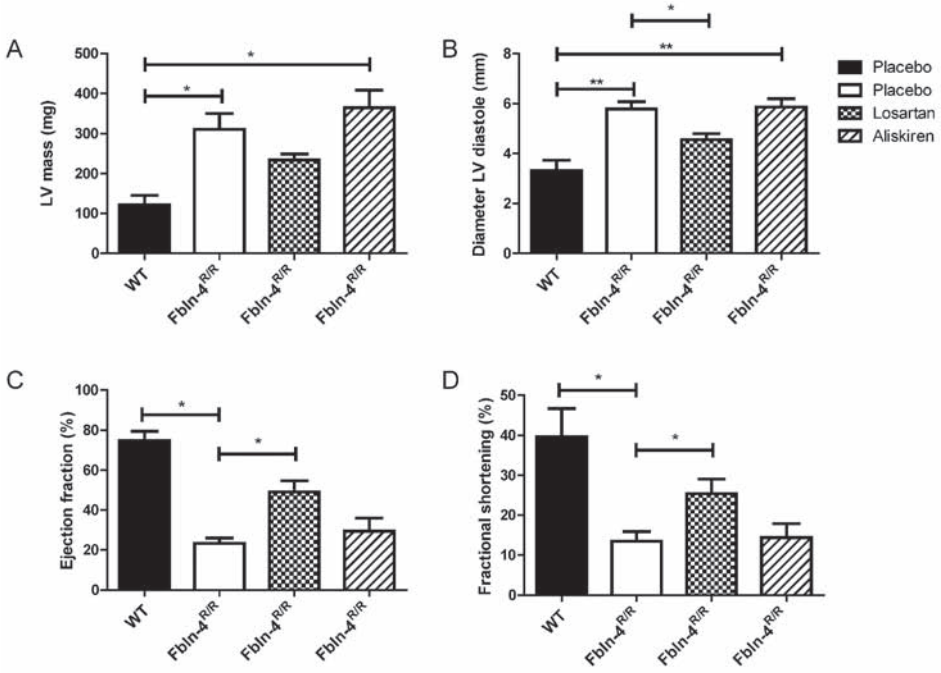

Figure 4. (A-D) Left ventricular (LV) mass, LV diameter, ejection fraction and fractional shortening determined by *in-vivo* transthoracic echocardiography in Fibulin-$4^{R/R}$ mice treated for 65 days with placebo, losartan or aliskiren vs. age-matched untreated WT mice (mean±SEM of n=6-10). *P<0.05, **P<0.01.

Losartan prevents cardiomyocyte hypertrophy and reduces canonical TGFβ signaling

Cardiomyocyte area doubled in Fibulin-$4^{R/R}$ versus wild-type mice, and losartan (but not aliskiren) fully prevented this hypertrophic response (Fig. 5A-5B). As expected, changes in plasma BNP paralleled this pattern, although no significant differences were observed for this parameter (Fig. 5C). Both canonical (pSmad2) and non-canonical (pERK) TGFβ signaling were upregulated in hearts of Fibulin-$4^{R/R}$ mice, but losartan reduced only the former to wild-type levels (Fig. 5D-5E). Smad2 and ERK levels were identical under all conditions (data not shown). LV $AT_{1a}R$ -, $AT_{1b}R$ -, and AT_2R expression were downregulated in Fibulin-$4^{R/R}$ mice versus wild-type mice, and losartan treatment exclusively normalized $AT_{1a}R$ expression (Fig. 5F). Unfortunately, due to scarcity of available tissue, similar data could not be obtained in aliskiren- or propranolol-treated mice.

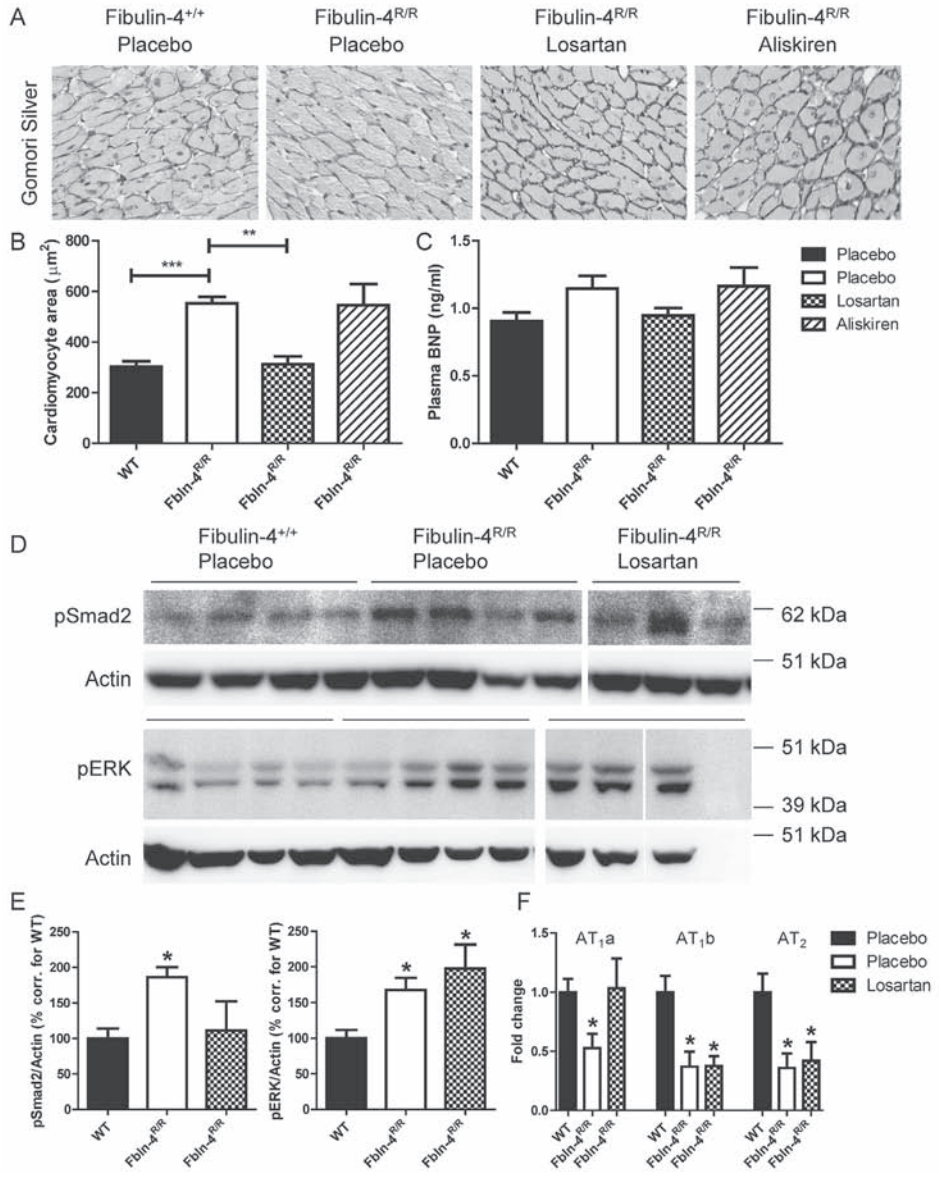

Figure 5. (A-B) Cardiomyocyte area (n=5-12; panel A shows a representative example) and (C) plasma brain natriuretic peptide (BNP; n=10-18) levels in Fibulin-$4^{R/R}$ mice treated for 65 days with placebo, losartan or aliskiren vs. age-matched untreated WT mice. Data are mean±SEM, **P<0.01, ***P<0.001 vs. WT or placebo. (D-E) pSmad2, pERK, and β-actin protein levels in hearts of Fibulin-$4^{R/R}$ mice treated for 65 days with placebo or losartan vs. age-matched untreated WT mice (n=3-4). *P<0.05 vs. WT. (F) Relative gene expression of LV Ang II receptors (n=3-10). *P<0.05 vs. WT.

Losartan prevents LV and aneurysm growth rate

We used a novel microCT method in combination with the vascular contrast agent Exia160, yielding longitudinal 3D data sets in which each animal serves as its own baseline control (Fig. 6A). At the start of treatment, both aortic volume and LV volume were not different in placebo- and losartan-treated Fibulin-$4^{R/R}$ mice (Fig. 6B-6C). Both volumes increased

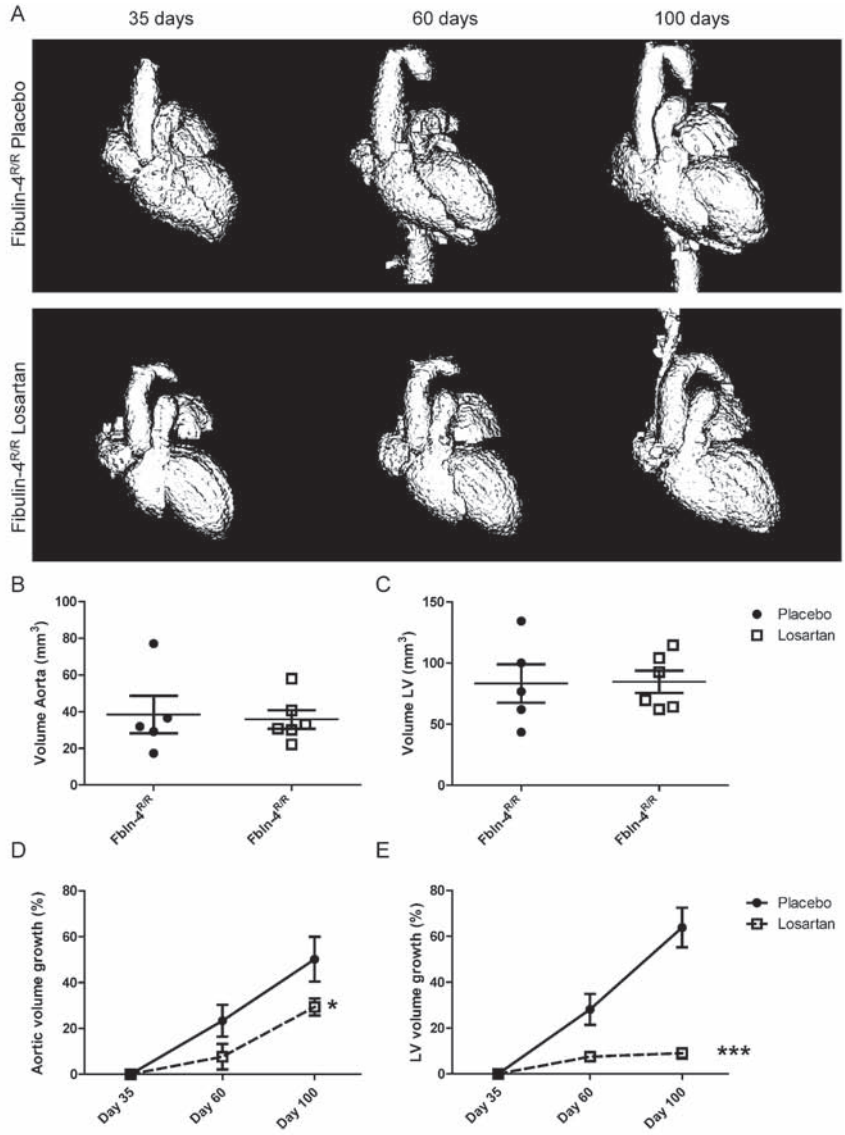

Figure 6. (A) 3D overview of CT-angiography with contrast agent Exia160. (B-C) Aortic and LV volume of placebo and losartan treated Fibulin-$4^{R/R}$ mice at baseline. (D-E) Percentage growth of ascending aortas and left ventricle (LV). Data are mean±SEM of n=4-6. *P<0.05, ***P<0.001 vs. placebo.

by approximately 60% during placebo treatment, and losartan largely (aortic volume), if not completely (LV volume) prevented this (Fig. 6D-6E).

DISCUSSION

The present study shows that losartan, but not aliskiren or propranolol, increased survival in Fibulin-$4^{R/R}$ mice, and that this predominantly related to its capacity to improve cardiac function and structure. Although losartan also stabilized aortic growth, these effects were more modest than its effects on LV growth, and they did not result in any change in aortic wall morphology, TGFβ-signaling, or MMP-activity. Nevertheless, there was an improvement in aortic distensibility. The larger effects on the heart most likely reflect the fact that the heart profits both from the local (cardiac) effects of losartan and its effects on aortic root remodeling. Since none of these effects were seen with aliskiren, despite the fact that this RAS blocker lowered blood pressure and inhibited the RAS to the same degree as losartan, we conclude that they are blood pressure-independent, and that losartan exerts effects beyond blockade of the classical Ang II-AT_1R axis. This most likely concerns its unique capacity to induce AT_2R stimulation. A second possibility would be activation of the angiotensin-(1-7)-Mas receptor axis. However, a study making use of *Fbn1*$^{C1039G/+}$ mice (an alternative, albeit less severe, TAA model) supports the former only, since it observed no effect of an ACE inhibitor, although such a drug, like an AT_1R blocker, activates the angiotensin-(1-7)-Mas receptor axis.[20, 30] Our study is the first to directly compare renin inhibition and AT_1R blockade in a mouse TAA model.

RAS activation, both in the circulation and at the tissue level, is an established characteristic of Fibulin-$4^{R/R}$ mice.[13, 31] Given the low Ang II levels in the aorta and its relatively small size[32], we measured Ang II in renal tissue to confirm the upregulated tissue RAS activity in this model. Increased Ang II levels will facilitate TGFβ-signaling, which is known to be enhanced in patients and mice with MFS.[29, 33-36] In fact, increased serum TGFβ levels correlated directly with aortic root dilation.[33] In agreement with the causative role of Ang II, we showed in an earlier study that prenatal treatment with losartan successfully improved elastic fiber fragmentation and reduced vessel wall thickness in Fibulin-$4^{R/R}$ mice.[13] Moreover, in mice that lack fibulin-4 in VSMCs ($Fbln4^{SMKO}$ mice), aneurysm formation could be prevented completely when RAS blockade was started within a narrow therapeutic window during the first month of life.[31] In this latter study, ACE inhibition with captopril and losartan treatment were equally effective. Yet, in contrast with our study, no cardiac phenotype was reported in $Fbln4^{SMKO}$ mice.

The present study in Fibulin-$4^{R/R}$ mice now evaluated postnatal losartan versus aliskiren treatment, started on day 35, i.e., when aneurysm formation is already present. This is not only more clinically relevant, as treatment in TAA patients usually starts in

the presence of an aneurysm, but also more realistic given the fact that such blockade is contraindicated during pregnancy. Propranolol, a classical MFS drug, was used as a comparator, but exerted no effect, in agreement with its lack of effect at the same dose (50 mg/kg p.o. per day) in *Fbn1*$^{C1039G/+}$ mice.[15] All drugs were given orally, since the fragility of our model, resulting in a very low survival, was not compatible with the operation required to implant osmotic minipumps. Although aliskiren displays a low bioavailability[37], and is highly species-specific[38], it blocks mouse renin at the same concentration range as human renin.[39] Consequently, by applying oral doses that were over 10 times higher than those used in humans (62.5 mg/kg p.o. per day versus 150-300 mg/day in humans), we were able, as in previous studies[21, 22], to achieve a degree of RAS blockade that yielded the same blood pressure-lowering effects as losartan at 60 mg/kg p.o. per day. Importantly, as an indication of RAS blockade, losartan and aliskiren increased circulating renin similarly. Probably as a consequence of this rise in renin release, aliskiren did not significantly decrease renal Ang II. Similar observations were made previously in the rat kidney.[40] Yet, losartan decreased renal Ang II, in agreement with the fact that tissue Ang II largely reflects Ang II that is bound to, or has been internalized via, AT_1R.[41, 42] Therefore, during losartan treatment, the reduction in tissue Ang II is an indication of the degree of AT_1R blockade. Unfortunately, we were unable to obtain comparable data for propranolol-treated mice, since none of these mice survived until the age of 100 days, i.e., the day of sacrifice for our RAS component measurements, at which timepoint blood pressure was measured. Nevertheless, it might be speculated that propranolol, given its modest renin-suppressing effects[43], did reduce Ang II. Long-term treatment with propranolol was feasible in *Fbn1*$^{C1039G/+}$ mice, in which aneurysm formation starts only at the age of 2 months.[3, 44] Propranolol affected blood pressure in *Fbn1*$^{C1039G/+}$ mice to the same extent as losartan.[15] Even if this had also been the case in our model, e.g., based on Ang II reduction, this effect would have resembled that of aliskiren, i.e., it could not have resulted in enhanced AT_2R stimulation. Thus, once TAA are established, both renin suppression with propranolol and renin inhibition with aliskiren lack the beneficial effects of losartan. In contrast, when treatment is started before the onset of TAA, like in the Fbln4^{SMKO} mice model described above[31], captopril yielded the same effects as losartan. Since captopril does not allow AT_2R stimulation, these data suggest that, at a very early stage of TAA, AT_1R are predominant, while at a later stage AT_2R may additionally come into play. This correlates well with the widely accepted phenomenon that AT_2Rs normally display low-to-undetectable levels, which increase only under pathological conditions, e.g., post-myocardial infarction, during hypertension-induced remodeling, and in heart failure.[45-47] Clearly, timing of treatment is of utmost importance, and different ages at the start of treatment (e.g. children/adolescents versus adults) may explain the success (or lack thereof) of different RAS blockers in clinical trials.[17, 18, 48] Moreover, when classifying *FBN1* mutations into 'haploinsufficiency' (decreased amount of normal fibrillin-1), and 'dominant negative' (normal fibrillin-1 abundance with mutant

fibrillin-1 incorporated in the matrix), Franken et al. observed that Marfan patients with haploinsufficient *FBN1* mutations were more responsive to losartan.[49] Since the *Fbn1*$^{C1039G/+}$ and Fibulin-4$^{R/R}$ TAA models closely correspond with the haploinsufficiency situation, it appears that the underlying mutation is an additional determinant of the success of AT_1R blockade in Marfan patients. Taken together, simultaneous AT_2R stimulation may not always offer an additional advantage, and thus selective AT_2R agonists should not by definition be preferred over AT_1R antagonists.

Given the predominant effects of losartan on the heart, we focused on canonical (pSmad2) and non-canonical (pERK) TGFβ signaling in cardiac tissue. Both were upregulated in Fibulin-4$^{R/R}$ mice, comparable to their upregulation in aortic tissue in Fbln4^{SMKO} and *Fbn1*$^{C1039G/+}$ mice.[20, 31] Yet, although losartan suppressed both types of signaling in aortic tissue in these latter models, in the hearts of our mice only the canonical signaling was found to be suppressed after losartan, while no pSmad2 suppression was seen in the aortic wall (Fig. 5E). These findings concur with the heart-specific effect of this AT_1R antagonist in our model, and suggest that the AT_2R stimulatory effects, if occurring, result in reduced canonical TGFβ signaling in the heart. Studies in transgenic animals support the concept that AT_2Rs are antihypertrophic and prevent remodeling.[50, 51] The lack of effect on pERK signaling in our Fibulin-4$^{R/R}$ mice is in agreement with a recent study by Cook et al.[52], who demonstrated that ERK1/2 activation peaks at a very early stage of the disease only, while pSmad2 remains elevated throughout the disease. From this perspective, effects of losartan on pERK1/2 are no longer expected after 100 days, simply because pERK1/2 is not activated anymore at that stage.

Gene expression studies in LV tissue revealed a reduction of all Ang II receptor types in Fibulin-4$^{R/R}$ mice compared to wild type mice. It should be noted that mice, unlike humans, display two AT_1R subtypes, $AT_{1a}R$ and $AT_{1b}R$, and that losartan blocks both AT_1Rs equally well. AT_1R downregulation is also known to occur in heart failure patients.[53] It was not observed in the aortic arch or kidney of our Fibulin-4$^{R/R}$ mice[13], implying that its downregulation was cardiac-specific. Importantly, although the raw Ct values for the $AT_{1b}R$, the AT_2R and the housekeeping genes β-actin and β_2-microglobin were identical in LV tissue and aorta (B.S. van Thiel, data not shown), the raw Ct values for the $AT_{1a}R$ in the LV were approximately 6 cycles lower than in the aorta. This suggests that $AT_{1a}R$ expression in the heart greatly exceeds that in the aorta. Losartan treatment exclusively normalized cardiac $AT_{1a}R$ expression in Fibulin-4$^{R/R}$ mice. Such upregulation is a well-known physiological response to receptor antagonism, once again supporting effective $AT_{1a}R$ blockade by losartan in the heart. Yet, it does not imply that $AT_{1a}R$ activation had now normalized (due to the simultaneous presence of losartan), and thus predominant AT_2R stimulation by the elevated levels of Ang II during losartan treatment is still highly likely.

Our data are the first to show the losartan-induced stabilization of LV growth over time with longitudinal microCT measurements. Using each animal as its own baseline

control, this novel approach enabled us to conclude that the effects of losartan on LV growth exceeded those on aortic growth. Combined with the FMT to co-registrate MMP-activity, this approach allows monitoring of cardiac and aortic remodeling in a unique, non-invasive manner. It would also reduce the required number of animals. Given the major limitation of our animal model, i.e. a complicated breeding scheme and a high death rate resulting in low n-numbers, this is an important advantage.

In conclusion, losartan, but not aliskiren or propranolol, improved survival in Fibulin-$4^{R/R}$ mice, by simultaneously stabilizing aortic growth, reducing aortic distensibility, and improving cardiac function and structure. The absence of these effects during aliskiren treatment, despite a similar reduction in blood pressure and degree of RAS blockade, suggests that it might be due to AT_2R stimulation and/or activation of the angiotensin-(1-7)/Mas receptor axis. Future studies, making use of AT_2R/Mas receptor knockout animals, AT_2R/Mas receptor antagonists (e.g., PD123319 and A779, respectively) or AT_2R/Mas receptor agonists (e.g., C21 and AVE0991, respectively) may help to substantiate this view. However, given the non-specific effects of the latter types of drugs[54, 55], the possibility that AT_2R heterodimerize with Mas receptors[56], and the consequences of AT_2R deletion on cardiac development and remodeling[57], the results of such studies may not be straightforward. In addition, none of these approaches is currently feasible in humans.

ACKNOWLEDGMENT

This work was supported through the use of imaging equipment provided by the Applied Molecular Imaging Erasmus MC facility. We also thank Lambert Speelman for his assistance with the Vevo2100 ultrasound. Funding: This work was supported by a Lijf en Leven grant (2008): 'Early Detection and Diagnosis of Aneurysms and Heart Valve Abnormalities'.

REFERENCES

1. Isselbacher EM. Thoracic and abdominal aortic aneurysms. *Circulation*. 2005;111:816-828
2. Dietz HC, Cutting GR, Pyeritz RE, Maslen CL, Sakai LY, Corson GM, Puffenberger EG, Hamosh A, Nanthakumar EJ, Curristin SM, Stetten G, Meyers DA, Francomano CA. Marfan-syndrome caused by a recurrent denovo missense mutation in the fibrillin gene. *Nature*. 1991;352:337-339
3. Judge DP, Biery NJ, Keene DR, Geubtner J, Myers L, Huso DL, Sakai LY, Dietz HC. Evidence for a critical contribution of haploinsufficiency in the complex pathogenesis of marfan syndrome. *J Clin Invest*. 2004;114:172-181
4. Horiguchi M, Inoue T, Ohbayashi T, Hirai M, Noda K, Marmorstein LY, Yabe D, Takagi K, Akama TO, Kita T, Kimura T, Nakamura T. Fibulin-4 conducts proper elastogenesis via interaction with cross-linking enzyme lysyl oxidase. *Proc Natl Acad Sci U S A*. 2009;106:19029-19034

5. Papke CL, Yanagisawa H. Fibulin-4 and fibulin-5 in elastogenesis and beyond: Insights from mouse and human studies. *Matrix Biol*. 2014
6. Dasouki M, Markova D, Garola R, Sasaki T, Charbonneau NL, Sakai LY, Chu ML. Compound heterozygous mutations in fibulin-4 causing neonatal lethal pulmonary artery occlusion, aortic aneurysm, arachnodactyly, and mild cutis laxa. *Am J Med Genet A*. 2007;143A:2635-2641
7. Hoyer J, Kraus C, Hammersen G, Geppert JP, Rauch A. Lethal cutis laxa with contractural arachnodactyly, overgrowth and soft tissue bleeding due to a novel homozygous fibulin-4 gene mutation. *Clin Genet*. 2009;76:276-281
8. Hucthagowder V, Sausgruber N, Kim KH, Angle B, Marmorstein LY, Urban Z. Fibulin-4: A novel gene for an autosomal recessive cutis laxa syndrome. *Am J Hum Genet*. 2006;78:1075-1080
9. Renard M, Holm T, Veith R, Callewaert BL, Ades LC, Baspinar O, Pickart A, Dasouki M, Hoyer J, Rauch A, Trapane P, Earing MG, Coucke PJ, Sakai LY, Dietz HC, De Paepe AM, Loeys BL. Altered tgfbeta signaling and cardiovascular manifestations in patients with autosomal recessive cutis laxa type i caused by fibulin-4 deficiency. *Eur J Hum Genet*. 2010;18:895-901
10. Roussin I, Sheppard MN, Rubens M, Kaddoura S, Pepper J, Mohiaddin RH. Cardiovascular complications of cutis laxa syndrome: Successful diagnosis and surgical management. *Circulation*. 2011;124:100-102
11. Sawyer SL, Dicke F, Kirton A, Rajapkse T, Rebeyka IM, McInnes B, Parboosingh JS, Bernier FP. Longer term survival of a child with autosomal recessive cutis laxa due to a mutation in fbln4. *Am J Med Genet A*. 2013;161A:1148-1153
12. Hanada K, Vermeij M, Garinis GA, de Waard MC, Kunen MG, Myers L, Maas A, Duncker DJ, Meijers C, Dietz HC, Kanaar R, Essers J. Perturbations of vascular homeostasis and aortic valve abnormalities in fibulin-4 deficient mice. *Circ Res*. 2007;100:738-746
13. Moltzer E, te Riet L, Swagemakers SMA, van Heijningen PM, Vermeij M, van Veghel R, Bouhuizen AM, van Esch JHM, Lankhorst S, Ramnath NWM, de Waard MC, Duncker DJ, van der Spek PJ, Rouwet EV, Danser AHJ, Essers J. Impaired vascular contractility and aortic wall degeneration in fibulin-4 deficient mice: Effect of angiotensin ii type 1 (at(1)) receptor blockade. *Plos One*. 2011;6:e23411
14. McLaughlin PJ, Chen Q, Horiguchi M, Starcher BC, Stanton JB, Broekelmann TJ, Marmorstein AD, McKay B, Mecham R, Nakamura T, Marmorstein LY. Targeted disruption of fibulin-4 abolishes elastogenesis and causes perinatal lethality in mice. *Mol Cell Biol*. 2006;26:1700-1709
15. Habashi JP, Judge DP, Holm TM, Cohn RD, Loeys BL, Cooper TK, Myers L, Klein EC, Liu GS, Calvi C, Podowski M, Neptune ER, Halushka MK, Bedja D, Gabrielson K, Rifkin DB, Carta L, Ramirez F, Huso DL, Dietz HC. Losartan, an at1 antagonist, prevents aortic aneurysm in a mouse model of marfan syndrome. *Science*. 2006;312:117-121
16. Isogai Z, Ono RN, Ushiro S, Keene DR, Chen Y, Mazzieri R, Charbonneau NL, Reinhardt DP, Rifkin DB, Sakai LY. Latent transforming growth factor beta-binding protein 1 interacts with fibrillin and is a microfibril-associated protein. *J Biol Chem*. 2003;278:2750-2757
17. Groenink M, den Hartog AW, Franken R, Radonic T, de Waard V, Timmermans J, Scholte AJ, van den Berg MP, Spijkerboer AM, Marquering HA, Zwinderman AH, Mulder BJ. Losartan reduces aortic dilatation rate in adults with marfan syndrome: A randomized controlled trial. *Eur Heart J*. 2013;34:3491-3500
18. Lacro RV, Dietz HC, Sleeper LA, Yetman AT, Bradley TJ, Colan SD, Pearson GD, Selamet Tierney ES, Levine JC, Atz AM, Benson DW, Braverman AC, Chen S, De Backer J, Gelb BD, Grossfeld PD, Klein GL, Lai WW, Liou A, Loeys BL, Markham LW, Olson AK, Paridon SM,

Pemberton VL, Pierpont ME, Pyeritz RE, Radojewski E, Roman MJ, Sharkey AM, Stylianou MP, Wechsler SB, Young LT, Mahony L, Pediatric Heart Network I. Atenolol versus losartan in children and young adults with marfan's syndrome. *N Engl J Med*. 2014;371:2061-2071

19. Verdonk K, Danser AHJ, van Esch JHM. Angiotensin ii type 2 receptor agonists: Where should they be applied? *Expert Opin Inv Drug*. 2012;21:501-513
20. Habashi JP, Doyle JJ, Holm TM, Aziz H, Schoenhoff F, Bedja D, Chen YC, Modiri AN, Judge DP, Dietz HC. Angiotensin ii type 2 receptor signaling attenuates aortic aneurysm in mice through erk antagonism. *Science*. 2011;332:361-365
21. Ye Y, Qian J, Castillo AC, Perez-Polo JR, Birnbaum Y. Aliskiren and valsartan reduce myocardial at1 receptor expression and limit myocardial infarct size in diabetic mice. *Cardiovasc Drugs Ther*. 2011;25:505-515
22. Weng LQ, Zhang WB, Ye Y, Yin PP, Yuan J, Wang XX, Kang L, Jiang SS, You JY, Wu J, Gong H, Ge JB, Zou YZ. Aliskiren ameliorates pressure overload-induced heart hypertrophy and fibrosis in mice. *Acta Pharmacol Sin*. 2014;35:1005-1014
23. Hawinkels LJ, Verspaget HW, van der Reijden JJ, van der Zon JM, Verheijen JH, Hommes DW, Lamers CB, Sier CF. Active tgf-beta1 correlates with myofibroblasts and malignancy in the colorectal adenoma-carcinoma sequence. *Cancer Sci*. 2009;100:663-670
24. van Kerckhoven R, Saxena PR, Schoemaker RG. Restored capillary density in spared myocardium of infarcted rats improves ischemic tolerance. *J Cardiovasc Pharmacol*. 2002;40:370-380
25. Danser AHJ, van Kats JP, Admiraal PJJ, Derkx FHM, Lamers JMJ, Verdouw PD, Saxena PR, Schalekamp MA. Cardiac renin and angiotensins. Uptake from plasma versus in situ synthesis. *Hypertension*. 1994;24:37-48
26. de Lannoy LM, Danser AHJ, van Kats JP, Schoemaker RG, Saxena PR, Schalekamp MADH. Renin-angiotensin system components in the interstitial fluid of the isolated perfused rat heart. Local production of angiotensin i. *Hypertension*. 1997;29:1240-1251
27. van den Bos EJ, Mees BM, de Waard MC, de Crom R, Duncker DJ. A novel model of cryoinjury-induced myocardial infarction in the mouse: A comparison with coronary artery ligation. *Am J Physiol Heart Circ Physiol*. 2005;289:H1291-1300
28. van Deel ED, de Boer M, Kuster DW, Boontje NM, Holemans P, Sipido KR, van der Velden J, Duncker DJ. Exercise training does not improve cardiac function in compensated or decompensated left ventricular hypertrophy induced by aortic stenosis. *J Mol Cell Cardiol*. 2011;50:1017-1025
29. Kaijzel EL, van Heijningen PM, Wielopolski PA, Vermeij M, Koning GA, van Cappellen WA, Que I, Chan A, Dijkstra J, Ramnath NW, Hawinkels LJ, Bernsen MR, Lowik CW, Essers J. Multimodality imaging reveals a gradual increase in matrix metalloproteinase activity at aneurysmal lesions in live fibulin-4 mice. *Circ Cardiovasc Imaging*. 2010;3:567-577
30. Seva Pessoa B, van der Lubbe N, Verdonk K, Roks AJM, Hoorn EJ, Danser AHJ. Key developments in renin-angiotensin-aldosterone system inhibition. *Nat Rev Nephrol*. 2013;9:26-36
31. Huang JB, Yamashiro Y, Papke CL, Ikeda Y, Lin YL, Patel M, Inagami T, Le VP, Wagenseil JE, Yanagisawa H. Angiotensin-converting enzyme-induced activation of local angiotensin signaling is required for ascending aortic aneurysms in fibulin-4-deficient mice. *Sci Transl Med*. 2013;5
32. Campbell DJ, Kladis A, Duncan AM. Nephrectomy, converting enzyme inhibition, and angiotensin peptides. *Hypertension*. 1993;22:513-522

33. Matt P, Schoenhoff F, Habashi J, Holm T, Van Erp C, Loch D, Carlson OD, Griswold BF, Fu Q, De Backer J, Loeys B, Huso DL, McDonnell NB, Van Eyk JE, Dietz HC, Consortium G. Circulating transforming growth factor-beta in marfan syndrome. *Circulation*. 2009;120:526-532
34. Renard M, Holm T, Veith R, Callewaert BL, Ades LC, Baspinar O, Pickart A, Dasouki M, Hoyer J, Rauch A, Trapane P, Earing MG, Coucke PJ, Sakai LY, Dietz HC, De Paepe AM, Loeys BL. Altered tgf beta signaling and cardiovascular manifestations in patients with autosomal recessive cutis laxa type i caused by fibulin-4 deficiency. *Eur J Hum Genet*. 2010;18:895-901
35. Neptune ER, Frischmeyer PA, Arking DE, Myers L, Bunton TE, Gayraud B, Ramirez F, Sakai LY, Dietz HC. Dysregulation of tgf-beta activation contributes to pathogenesis in marfan syndrome. *Nat Genet*. 2003;33:407-411
36. Chung AWY, Yeung KA, Sandor GGS, Judge DP, Dietz HC, van Breemen C. Loss of elastic fiber integrity and reduction of vascular smooth muscle contraction resulting from the upregulated activities of matrix metalloproteinase-2 and-9 in the thoracic aortic aneurysm in marfan syndrome. *Circ Res*. 2007;101:512-522
37. Wood JM, Schnell CR, Cumin F, Menard J, Webb RL. Aliskiren, a novel, orally effective renin inhibitor, lowers blood pressure in marmosets and spontaneously hypertensive rats. *J Hypertens*. 2005;23:417-426
38. Krop M, van Veghel R, Garrelds IM, de Bruin RJA, van Gool JMG, van den Meiracker AH, Thio M, van Daele PLA, Danser AHJ. Cardiac renin levels are not influenced by the amount of resident mast cells. *Hypertension*. 2009;54:315-321
39. Feldman DL, Jin L, Xuan H, Contrepas A, Zhou Y, Webb RL, Müller DN, Feldt S, Cumin F, Maniara W, Persohn E, Schuetz H, Danser AHJ, Nguyen G. Effects of aliskiren on blood pressure, albuminuria, and (pro)renin receptor expression in diabetic tg(mren-2)-27 rats. *Hypertension*. 2008;52:130-136
40. van Esch JHM, Moltzer E, van Veghel R, Garrelds IM, Leijten F, Bouhuizen AM, Danser AH. Beneficial cardiac effects of the renin inhibitor aliskiren in spontaneously hypertensive rats. *J Hypertens*. 2010;28:2145-2155
41. Mazzolai L, Pedrazzini T, Nicoud F, Gabbiani G, Brunner HR, Nussberger J. Increased cardiac angiotensin ii levels induce right and left ventricular hypertrophy in normotensive mice. *Hypertension*. 2000;35:985-991
42. van Esch JHM, Gembardt F, Sterner-Kock A, Heringer-Walther S, Le T, Lassner D, Stijnen T, Coffman T, Schultheiss H-P, Danser AHJ, Walther T. Cardiac phenotype and angiotensin ii levels in at1a, at1b and at2 receptor single, double and triple knockouts. . *Cardiovasc Res*. 2010;86:401-409
43. Danser AHJ, Derkx FHM, Schalekamp MADH, Hense HW, Riegger GAJ, Schunkert H. Determinants of interindividual variation of renin and prorenin concentrations: Evidence for a sexual dimorphism of (pro)renin levels in humans. *J Hypertens*. 1998;16:853-862
44. Moltzer E, Essers J, van Esch JHM, Roos-Hesselink JW, Danser AHJ. The role of the renin-angiotensin system in thoracic aortic aneurysms: Clinical implications. *Pharmacol Therapeut*. 2011;131:50-60
45. Wagenaar LJ, Voors AA, Buikema H, van Gilst WH. Angiotensin receptors in the cardiovascular system. *Can J Cardiol*. 2002;18:1331-1339
46. Utsunomiya H, Nakamura M, Kakudo K, Inagami T, Tamura M. Angiotensin ii at(2) receptor localization in cardiovascular tissues by its antibody developed in at(2) gene-deleted mice. *Regul Peptides*. 2005;126:155-161

47. Lopez JJ, Lorell BH, Ingelfinger JR, Weinberg EO, Schunkert H, Diamant D, Tang SS. Distribution and function of cardiac angiotensin at(1)-receptor and at(2)-receptor subtypes in hypertrophied rat hearts. *Am J Physiol*. 1994;267:H844-H852
48. Dietz HC. Potential phenotype-genotype correlation in marfan syndrome: When less is more? *Circ Cardiovasc Genet*. 2015;8:256-260
49. Franken R, den Hartog AW, Radonic T, Micha D, Maugeri A, van Dijk FS, Meijers-Heijboer HE, Timmermans J, Scholte AJ, van den Berg MP, Groenink M, Mulder BJM, Zwinderman AH, de Waard V, Pals G. Beneficial outcome of losartan therapy depends on type of fbn1 mutation in marfan syndrome. *Circ-Cardiovasc Gene*. 2015;8:383-388
50. Booz GW, Baker KM. Role of type 1 and type 2 angiotensin receptors in angiotensin ii-induced cardiomyocyte hypertrophy. *Hypertension*. 1996;28:635-640
51. van Kesteren CAM, van Heugten HAA, Lamers JMJ, Saxena PR, Schalekamp MADH, Danser AHJ. Angiotensin ii mediated growth and antigrowth effects in cultured neonatal rat cardiac myocytes and fibroblasts. *J Mol Cell Cardiol*. 1997;29:2147-2157
52. Cook JR, Clayton NP, Carta L, Galatioto J, Chiu E, Smaldone S, Nelson CA, Cheng SH, Wentworth BM, Ramirez F. Dimorphic effects of transforming growth factor-beta signaling during aortic aneurysm progression in mice suggest a combinatorial therapy for marfan syndrome. *Arterioscler Thromb Vasc Biol*. 2015;35:911-917
53. Haywood GA, Gullestad L, Katsuya T, Hutchinson HG, Pratt RE, Horiuchi M, Fowler MB. At1 and at2 angiotensin receptor gene expression in human heart failure. *Circulation*. 1997;95:1201-1206
54. Verdonk K, Durik M, Abd-Alla N, Batenburg WW, van den Bogaerdt AJ, van Veghel R, Roks AJ, Danser AH, van Esch JH. Compound 21 induces vasorelaxation via an endothelium- and angiotensin ii type 2 receptor-independent mechanism. *Hypertension*. 2012;60:722-729
55. Lautner RQ, Villela DC, Fraga-Silva RA, Silva N, Verano-Braga T, Costa-Fraga F, Jankowski J, Jankowski V, Sousa F, Alzamora A, Soares E, Barbosa C, Kjeldsen F, Oliveira A, Braga J, Savergnini S, Maia G, Peluso AB, Passos-Silva D, Ferreira A, Alves F, Martins A, Raizada M, Paula R, Motta-Santos D, Klempin F, Pimenta A, Alenina N, Sinisterra R, Bader M, Campagnole-Santos MJ, Santos RA. Discovery and characterization of alamandine: A novel component of the renin-angiotensin system. *Circ Res*. 2013;112:1104-1111
56. Villela D, Leonhardt J, Patel N, Joseph J, Kirsch S, Hallberg A, Unger T, Bader M, Santos RA, Sumners C, Steckelings UM. Angiotensin type 2 receptor (at2r) and receptor mas: A complex liaison. *Clin Sci (Lond)*. 2015;128:227-234
57. Biermann D, Heilmann A, Didie M, Schlossarek S, Wahab A, Grimm M, Romer M, Reichenspurner H, Sultan KR, Steenpass A, Ergun S, Donzelli S, Carrier L, Ehmke H, Zimmermann WH, Hein L, Boger RH, Benndorf RA. Impact of at2 receptor deficiency on postnatal cardiovascular development. *Plos One*. 2012;7:e47916

PART III

CARDIOVASCULAR AGING

CHAPTER 6

DIETARY RESTRICTION BUT NOT ANGIOTENSIN II TYPE I RECEPTOR BLOCKADE IMPROVES DNA DAMAGE-RELATED VASODILATOR DYSFUNCTION

Haiyan Wu[1,2]*, Bibi S. van Thiel[1,3,4]*, Paula K. Bautista-Niño[1], Erwin Reiling[7], Matej Durik[1,8], Frank P.J. Leijten[1], Yanto Ridwan[3, 5], Renata M.C. Brandt[3], Harry van Steeg[7], Martijn E.T. Dollé[7], Wilbert P. Vermeij[3], Jan H.J. Hoeijmakers[3,9], Jeroen Essers[3,4,6], Ingrid van der Pluijm[3,4], A.H. Jan Danser[1] and Anton J.M. Roks[1]

* Equal contributors

[1]Department of Internal Medicine, Division of Vascular Medicine and Pharmacology, Erasmus University Medical Center Rotterdam, [2]Department of Pharmacology, West China School of Preclinical and Forensic Medicine, Sichuan University, Chengdu, P.R. China, [3]Department of Molecular Genetics, Cancer Genomics Center Netherlands, [4]Department of Vascular Surgery, [5]Department of Radiology and Nuclear Medicine, [6]Department of Radiation Oncology, Erasmus University Medical Center Rotterdam, The Netherlands, [7]Centre for Health Protection, National Institute for Public Health and the Environment (RIVM), Bilthoven, The Netherlands, [8]Department of Pediatric and Adolescent Medicine, Mayo Clinic College of Medicine, Rochester, Minnesota, USA, [9]CECAD Forschungszentrum, Universität zu Köln, Germany.

(Manuscript submitted)

ABSTRACT

DNA damage is an important contributor to endothelial dysfunction and age-related vascular disease. Recently, we demonstrated in a DNA repair-deficient, prematurely aging mouse model (*Ercc1*$^{d/-}$ mice) that dietary restriction (DR) strongly increases life- and health span, including ameliorating endothelial dysfunction, by preserving genomic integrity. In this mouse mutant displaying prominent accelerated, age-dependent endothelial dysfunction we investigated the signaling pathways involved in improved endothelium-mediated vasodilation by DR, and explore the potential role of the renin-angiotensin system. *Ercc1*$^{d/-}$ mice showed increased blood pressure and decreased aortic relaxations to acetylcholine in organ bath experiments. Nitric oxide (NO) signaling was compromised. DR improved relaxations by increasing prostaglandin-mediated responses, and cyclo-oxygenase 1 and decreased phosphodiesterase 4B were identified as potential mechanisms. DR also prevented loss of NO signaling in vascular smooth muscle cells and normalized angiotensin II vasoconstrictions, which were increased in *Ercc1*$^{d/-}$ mice. *Ercc1*$^{d/-}$ mutants showed a loss of Angiotensin II type 2 receptor-mediated counterregulation of Angiotensin II type 1 receptor-induced vasoconstrictions. Chronic losartan treatment effectively decreased blood pressure, but did not improve endothelium-dependent relaxations. This result might relate to the aging-associated loss of treatment efficacy of renin-angiotensin system blockade with respect to endothelial function improvement. In summary, dietary restriction effectively prevents endothelium-dependent vasodilator dysfunction by augmenting prostaglandin-mediated responses, whereas chronic Ang type 1 receptor blockade is ineffective.

INTRODUCTION

Age is a major risk factor for the development of cardiovascular diseases (CVD), independently from traditional risk factors.[1] An important factor that contributes to organismal aging, including vascular aging, is genomic instability.[2, 3] We recently demonstrated that mutation of the DNA repair endonuclease excision repair cross complementing 1 in mice (*Ercc1*$^{d/-}$ mice) accelerates important characteristics of vascular aging-related vasomotor dysfunction.[4, 5] In general, *Ercc1*$^{d/-}$ mice rapidly and faithfully mimic natural human aging compared to aged wild-type (WT) mice.[6] Accordingly, mouse models of accelerated vascular aging due to genomic instability can be used as tools complementary to models representing the impact of classical risk factors, such as hypertension and dyslipidemia.

We demonstrated that dietary restriction (DR, 30% reduced food intake without malnutrition), a universal intervention extending lifespan in numerous species, tripled remaining lifespan and strongly improved health span in *Ercc1*$^{d/-}$ animals, by far exceeding the relative lifespan extension in WT mice. We found that this dramatic anti-accelerated aging effect in the mutant was at least in part due to preserving genomic integrity by reducing DNA damage accumulation.[2] The improvement of health span included prevention of endothelial dysfunction, which in humans is one of the major contributors to morbidity and mortality due to a decline in vascular function.[1] In humans, DR has a beneficial effect on cardiovascular risk, which is attributed to the reduction in diet-related risk factors such as dyslipidemia, high blood pressure (salt intake), and hyperglycemia.[7] This in turn reduces oxidative stress and augments the nitric oxide (NO) – cGMP pathway, an important endothelial signaling axis involved in blood flow, blood pressure and cardiovascular growth regulation.[7] Our results in *Ercc1*$^{d/-}$ mice have added a novel paradigm, namely that DR preserves genomic integrity and thus in this manner protects against vascular aging.

In this new paradigm it is not known which vasodilatory signaling pathway is improved. In our previous studies we have shown that, comparable to human aging, *Ercc1*$^{d/-}$ mice display a reduction of NO – cGMP signaling and increased oxidative stress.[4, 5] Therefore, we here set out to identify which vasodilatory signaling pathway is improved by DR in *Ercc1*$^{d/-}$ mice. In addition, the impact of DR on endothelium-independent relaxation was investigated.

A potential mediator of blood pressure increase and decreased endothelium-dependent relaxation caused by DNA damage is activation of the renin-angiotensin system (RAS). Angiotensin (Ang) II, the main bioactive hormone of this system, is strongly involved in hypertension, arteriosclerosis, vascular DNA damage and cell senescence, inflammation, oxidative stress, longevity and health span.[8] Also, Ang II inhibits eNOS - NO - cGMP signaling.[9] Given that the RAS is sensitive to salt and LDL cholesterol, it may also respond to DR.[10, 11] However, it is not known how genomic instability influences RAS activity, let alone whether RAS activation would mediate its detrimental effects on

the vascular wall. Therefore, we additionally studied the vasoconstrictor responses of the *Ercc1*$^{d/-}$ mouse vasculature to Ang II under *ad libitum* (AL) feeding and DR. Also, we evaluated the effect of chronic AT_1 receptor blockade on endothelial function and blood pressure in AL-fed *Ercc1*$^{d/-}$ mice.

MATERIAL AND METHODS

Animals and interventions

Animal experiments were performed at RIVM and Erasmus MC in accordance with the Principles of Laboratory Animal Care and with the guidelines approved by the Dutch Ethical Committee in full accordance with European legislation.

Dietary restriction studies

Ercc1$^{d/-}$ mice and their wild-type littermates (WT) (Bl6/FVB F1 hybrids) underwent DR intervention from resp. 7 and 11 weeks after birth until sacrifice as described extensively in our previous publication, and in the Methods supplement.[2]

Losartan intervention study

From 5 weeks of age, *Ercc1*$^{d/-}$ and WT mice (Bl6/FVB F1 hybrids) were divided into two groups per strain, which were either treated with losartan (100 mg/kg/day) in drinking water, or drinking water only until the age of 12 weeks when the animals were sacrificed. Blood pressure was measured by tail cuff at the age of 11 weeks. The study rationale and animal numbers are described in the Methods supplement.

Organ bath experiments

Tissue harvesting and preparation procedures, and detailed description of the organ bath experiments can be found in the Methods supplement.

In short, thoracic aorta and iliac arteries were collected and tested in small wire organ bath setups. Vasodilations to cumulative concentrations of acetylcholine (ACh) and sodium nitroprusside (SNP) were measured in vessels preconstricted with U46619 to construct concentration-response curves (CRCs). When sufficient aortic tissue was available, the involvement of nitric oxide (NO) and prostaglandins in ACh responses was investigated by performing the experiments in the presence of the endothelial nitric oxide synthase (eNOS) inhibitor N^G-Methyl-L-Arginine acetate salt (L-NMMA, 10^{-5} mol/L), the cyclo-oxygenase (COX) inhibitor indomethacin (INDO, 10^{-5} mol/L) or both inhibitors. In iliac arteries Ang II (10^{-10}-10^{-7} mol/L) CRCs were constructed. PD123319 (10^{-7} mol/L) was used to test the involvement of Ang II type 2 (AT_2) receptors, and the guanylyl cyclase

inhibitor 1H-(1,2,4)oxadiazolo[4,3-a]quinoxalin-1-one (ODQ, 10^{-5} mol/L) to test the role of NO-cGMP signaling. Inhibitors were added 15 minutes prior to U46619 or Ang II.

Quantitative real-time PCR

Total RNA was isolated and cDNA was prepared, which was amplified by real-time PCR to perform ΔΔCt quantification, either with the use of SYBR green or Taqman analysis. Further details are in the Methods supplement.

Plasma renin concentration

Blood was collected from 12-wk-old WT and *Ercc1*$^{d/-}$ mice by cardiac puncture and transferred to EDTA coagulation vials. Blood samples were centrifuged at 4600 rpm for 10 minutes to collect plasma. Plasma renin concentration was determined by an enzyme-kinetic assay as described previously.[12]

Statistical methods

Data are presented as mean±SEM. SNP-corrected ACh responses were calculated as follows: (response to ACh as % of U46619 preconstriction / response to 10^{-4} mol/L SNP as % of U46619) x 100 (to indicate as a percentage) x -1 (to indicate that it is a relaxation). Statistical testing for differences between single values expressed in bar graphs was performed by t-test or 1-way ANOVA followed by appropriate post-hoc tests. Differences in CRC were tested by general linear model for repeated measures (GLM-RM, sphericity assumed). Differences were considered significant at $p<0.05$.

RESULTS

The effect of DR on acetylcholine responses in WT and *Ercc1*$^{d/-}$ mice

We first investigated the effect of genomic instability and DR on the diminished ACh response at different ages in *Ercc1*$^{d/-}$ and WT mice. As previously reported, AL-fed *Ercc1*$^{d/-}$ mutants showed a lifespan of 19 weeks (median age), which was extended by DR to a median age of 44 weeks.[2] ACh responses in the *Ercc1*$^{d/-}$ aorta of AL-fed animals age-dependently decreased between the age of 7 to 16 weeks (Fig. 1A), and at the latter age were significantly decreased compared to 20-wk old WT. WT aortas did not show any change in ACh response between 11 to 20 weeks (data not shown). To explore if DR would protect against endothelial dysfunction until an age at which AL-fed *Ercc1*$^{d/-}$ mice have already succumbed (predominantly occurring from neurodegeneration), we proceeded to an age of 30 weeks in DR-fed animals. In our initial publication on the effect of DR on general health[2] we demonstrated that DR improved the response to ACh in 16-wk-old *Ercc1*$^{d/-}$ mice. Here we show that the improvement of ACh responses persisted in 30-wk-old

DR-fed *Ercc1*$^{d/-}$ mutants (Fig.1B), well after the AL mice had died. In WT animals DR had no effect on ACh-induced relaxation (Fig. 1B). Thus, *Ercc1*$^{d/-}$ mice showed decreased aortic relaxations to ACh with increasing age, which could partly be prevented by DR.

Endothelial vs. non-endothelial responses

Ercc1$^{d/-}$ aortas displays a pronounced decrease of endothelium-independent responses to NO.[4, 5] We therefore investigated the effect of DR on responses to SNP, which entirely rely on direct release of NO and subsequent cGMP production in vascular smooth muscle cells (VSMC), as evidenced by the complete blockade of this response by the guanylyl cyclase inhibitor ODQ (data not shown). Dilatory responses to 10^{-4} mol/L SNP, which was given on top of ACh, progressively decreased in AL-fed *Ercc1*$^{d/-}$ mice, reaching statistical significance in 16-wk-old mice as compared to 7-wk-old mice (Fig. 1C, $p<0.05$ one-way ANOVA on 7-, 11- and 16-wk AL-fed mice with Dunnett post-hoc test). DR significantly prevented the age-dependent decline in dilator responses in 11- and 16-wk-old mice (Fig. 1C, $p<0.05$, t-test). Even 30-wk-old DR-fed *Ercc1*$^{d/-}$ mutants still displayed a better SNP response as compared to 16-wk AL-fed *Ercc1*$^{d/-}$ mice ($p<0.05$, t-test). In WT animals no age- or diet-related changes were observed (Fig. 1D, 11-wk animals not shown), and SNP responses were similar to those in 7-wk AL-fed and DR-fed *Ercc1*$^{d/-}$ mice, which is expected as WT mice at 20 weeks of age do not (yet) display an aging-phenotype

To exclude any influence of ACh on SNP responses and to explore dose-related effects of SNP, we generated SNP CRCs in 16-wk-old *Ercc1*$^{d/-}$ and in 20-wk-old WT animals (Fig. 1E). The data confirmed that in AL-fed *Ercc1*$^{d/-}$ mice SNP responses were strongly reduced, and that they were fully restored to the level of WT animals by DR. In WT animals no significant changes occurred.

The response to ACh depends on the amount of relaxing factors that is released from the endothelium as well as the responsiveness of the VSMC to these factors. The present observation that responses of VSMC to NO are fully restored by DR (Fig. 1C, E) while the responses to ACh are not (Fig. 1B), suggests that the release of endothelial-derived relaxing factors is compromised. Therefore, we studied the contribution of these factors to vasodilation.

The role of endothelial signaling compounds in genotype- and diet-related effects

Dilations in AL-fed vs. DR-fed WT mice did not differ and results were therefore pooled. ACh responses were almost completely dependent on NO in WT animals since adding the eNOS inhibitor L-NMMA blocked the response to ACh (Fig. 2A). As expected from our previous study[4], NO also mediated a large part of the vasodilation to ACh in AL-fed *Ercc1*$^{d/-}$ mice (Fig. 2B). The residual response suggests the emergence of an endothelium-derived hyperpolarizing factor (EDHF), which did not appear to be COX-dependent, since it was not affected by indomethacin (Fig. 2B). This result, together with the observation that

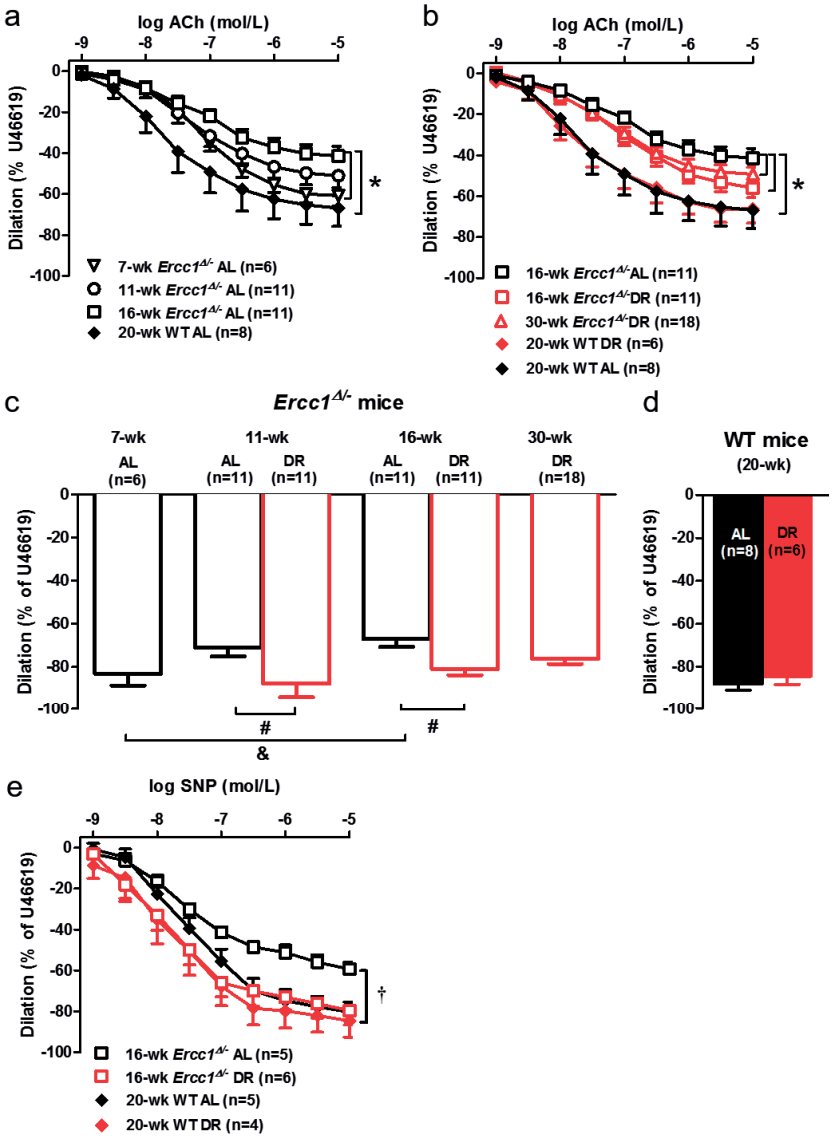

Figure 1. (A) Age-dependent acetylcholine (ACh)-induced vasodilation in aortic segments from *ad libitum* (AL) fed wildtype (WT) and *Ercc1*$^{d/-}$ mice as measured *ex vivo* in small wire organ baths. (B) Effect of diet restrictions (DR) on the ACh responses. (C - E) age-dependent sodium nitroprusside (SNP)-induced vasodilations and the effect of diet restriction (DR). SNP was either given as a bolus concentration of 10^{-4} mol/L SNP after constructing ACh concentration response curves (C, D) or administered in cumulative concentrations immediately after preconstriction (E). Cumulative concentrations of ACh and SNP were applied after preconstriction with the thromboxane analogue U46619. Responses are expressed as % relaxation of the U46619 in panels A-E. Error bars: S.E.M. *:p<0.05, general linear model for repeated measures (GLM-RM). &: p<0.05 16-week (16-wk) vs. 7-week (7-wk) *Ercc1*$^{d/-}$AL, one-way ANOVA, Dunnett post-hoc test, #: p<0.05 t-test, †: p<0.05, 16-wk *Ercc1*$^{d/-}$AL compared to all other groups, GLM-RM.

inhibition of vasodilation by L-NMMA was much more pronounced in WT confirms the specific loss of NO signaling in *Ercc1*$^{d/-}$ aorta's. Remarkably, the DR-induced facilitation of the ACh response in *Ercc1*$^{d/-}$ mice appeared to be due to an upregulation of a vasodilator prostaglandin pathway, since now indomethacin did further reduce the response of ACh on top of L-NMMA, while the effect of L-NMMA alone was unaltered (Fig. 2C).

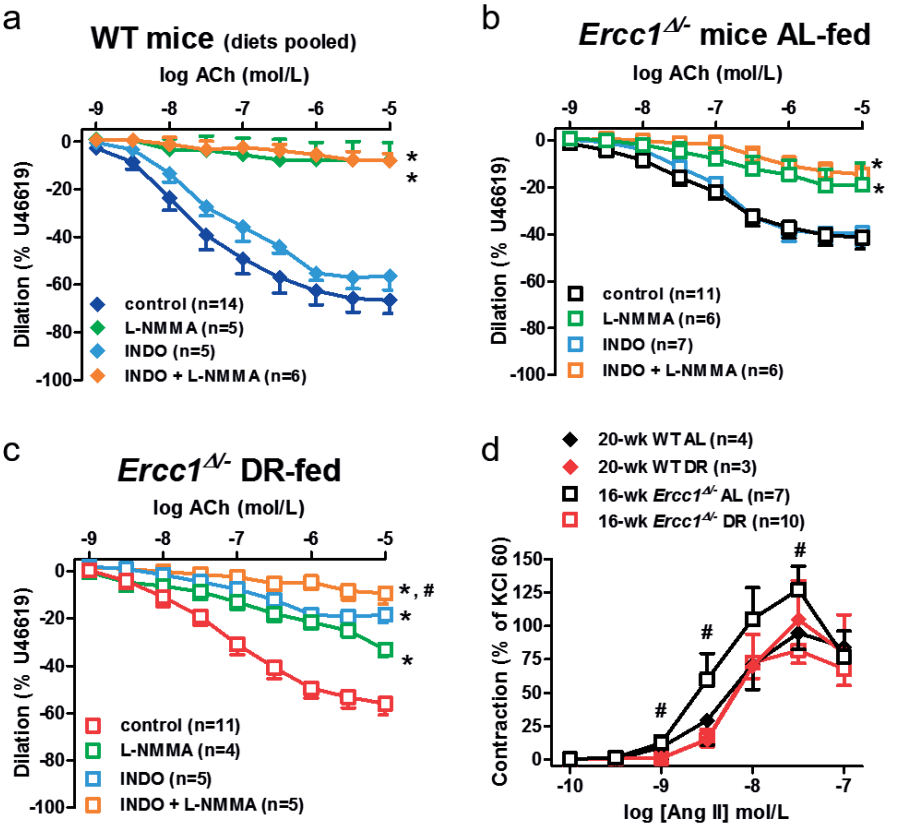

Figure 2. Contribution of nitric oxide (NO) and prostaglandins to ACh-induced vasodilation of aortic segments from 20-wk-old AL- and DR-fed wild-type (WT) (A), and 16-wk-old AL-fed (B) and DR-fed (C) *Ercc1*$^{d/-}$ mice measured in organ baths. L-NMMA (10^{-5} mol/L) and INDO (10^{-5} mol/L) resp. inhibit NO and prostaglandin synthesis, and were added to the organ baths 10 minutes before U46619. Responses are expressed as % relaxation of the U46619 preconstriction. (D) Vasoconstriction to Ang II expressed as % of contraction to 100 mM KCl. Error bars: S.E.M. *:p<0.05 vs. non-pretreated segments. #:p<0.05 vs. L-NMMA-treated segments.

Prostaglandins are produced by COX-1 or 2, and exert their vasodilator effects through the IP receptor using adenylyl cyclase (AC) 5/6 – cAMP signaling as a second messenger system. cAMP is prone to degradation by phosphodiesterase type 4B/D (PDE4).[13-15]

To investigate which of these components could be responsible for the upregulated prostaglandin response we quantified their expression in blood vessel-rich lung tissue. Ct values for the IP receptor, PDE4D and AC6 mRNA levels were on average >34, and therefore we considered these levels too low for reliable detection. COX-1 mRNA showed a trend to increase ($p<0.05$ one-way ANOVA for all 4 groups) after DR in WT and in *Ercc1*$^{d/-}$ mice, and did significantly increase in DR-fed *Ercc1*$^{d/-}$ mice as compared with AL-fed WT mice (Fig. 3A). PDE4B mRNA was decreased in both *Ercc1*$^{d/-}$ mouse groups compared with AL-fed WT mice (Fig. 3A). COX-2 and AC 5/6 mRNA did not show significant changes among the groups. The results suggest that both an increase of prostaglandin production by COX1 and decreased metabolism by PDE4B underlie the improved vasodilation after DR in *Ercc1*$^{d/-}$ mice.

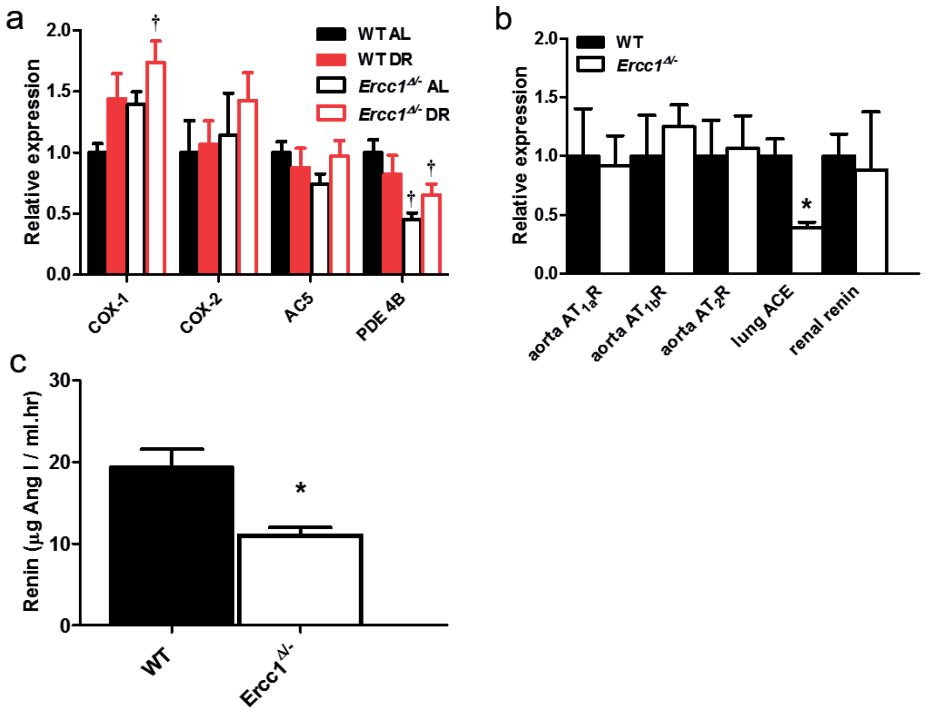

Figure 3. (A) Relative mRNA expression levels in lung tissue of COX-1, COX-2, AC 5/6, and PDE4B in 16-wk-old *Ercc1*$^{d/-}$ mice and 20-wk-old wild-type (WT) littermates from the diet intervention study. (B) Relative mRNA expression levels of AT_{1a}-, AT_{1b}- and AT_2-receptors in abdominal aortic tissue, of ACE in lung tissue and of renin in renal tissue of 12-wk-old *Ercc1*$^{d/-}$ mice and WT littermates from the losartan treatment study. All values are corrected for β-actin and normalized to WT expression levels. Results were similar when corrected for HPRT-1 (data not shown). (C) Plasma renin concentration in *Ercc1*$^{d/-}$ mice and WT littermates from the losartan treatment study. Error bars: S.E.M. †=$P<0.05$ vs. WT-AL (one way- ANOVA followed by Dunnett's post-hoc test vs. WT-AL); *:$p<0.05$ vs. WT, t-test.

Effects of genomic instability and DR on Ang II responses

To explore a possible role of the renin-angiotensin system we first investigated vasoconstriction to Ang II in a subset of the diet intervention mice. Ang II responses were in general highly variable within each strain, and tended to be higher in AL-fed *Ercc1*$^{d/-}$ vs. AL-fed WT mice (Fig. 2D), although this did not reach significance over the entire CRC (GLM-RM). DR-fed *Ercc1*$^{d/-}$ animals showed a trend for a decreased response to Ang II as compared to AL-fed *Ercc1*$^{d/-}$ mutants (GLM-RM, p=0.059). The results suggest a genomic instability-induced upregulation of the Ang II response, which is normalized by DR.

The losartan intervention study

In a separate cohort of *Ercc1*$^{d/-}$ and WT mice we evaluated the effect of chronic AT_1 receptor blockade on blood pressure and vascular function. In agreement with our previous study[4] blood pressure tended to be slightly higher in *Ercc1*$^{d/-}$ mice, mainly reflected by systolic blood pressure (SBP), and to a lesser extent by diastolic blood pressure (DBP) (Fig. 4). The difference reached borderline significance for SBP (p = 0.076, t-test). Chronic AT_1 receptor blockade by losartan significantly lowered SBP and DBP in both mouse strains.

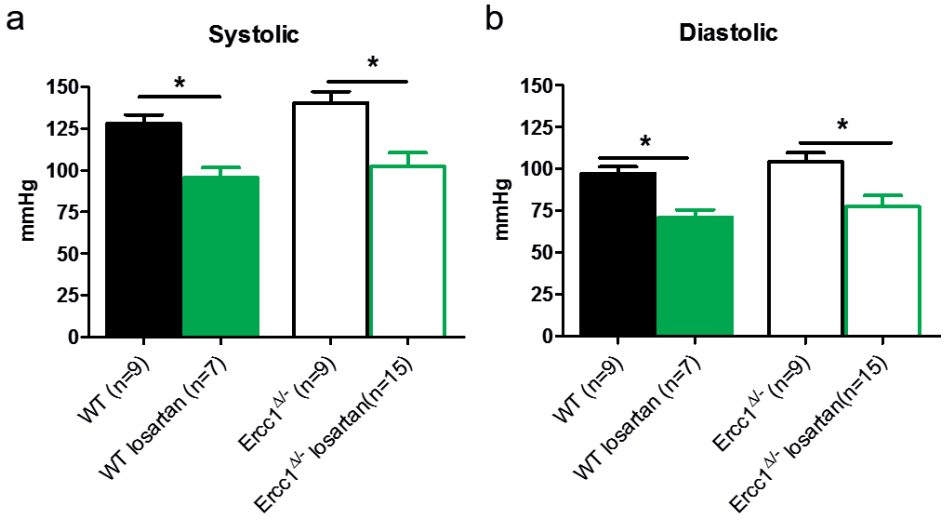

Figure 4. (A) Systolic and (B) diastolic blood pressure in conscious *Ercc1*$^{d/-}$ and wild-type (WT) mice of the losartan intervention study as measured by the tail cuff method. *: p<0.05, t-test

Vasomotor responses to Ang II in the losartan intervention study

In the losartan intervention cohort, *Ercc1*$^{d/-}$ mice displayed an exaggerated response to Ang II as compared to WT mice (Fig. 5A). Vasoconstrictions are mediated by AT_1 receptors and we therefore explored other indicators of increased AT_1 receptor activity such as negative feedback on renin activity and ACE expression. Plasma renin activity was reduced (Fig.

3C). This was not due to a change in mRNA level in the kidney (Fig. 3B). ACE mRNA in the lung was reduced (Fig. 3B). Both findings are in agreement with increased AT_1 receptor activity.

To further explore mechanisms leading to increased Ang II vasoconstrictions we studied vascular AT_1 and AT_2 receptor expression and function. We and others previously reported that AT_2 receptor stimulation counteracts AT_1 receptor-mediated vasoconstriction.[16] To explore the effect of genomic instability on AT_2 receptor activity, Ang II responses in *Ercc1*$^{d/-}$ and WT animals in the presence of AT_2 receptor antagonist PD123319 were compared to those in the absence of this antagonist. PD123319 did not change in *Ercc1*$^{d/-}$ mice, but tended (p=NS) to increase the Ang II response in WT (Fig. 5A). Chronic treatment with losartan, starting from week 5 after birth until the end of week 12, normalized this exaggerated response in the *Ercc1*$^{d/-}$ mice (Fig. 5B), but had no effect on the Ang II response in WT mice (data not shown). Therefore, genomic instability leads to loss of counterregulation of AT_1 receptor-mediated vasoconstriction by AT_2 receptor, and not due changes in receptor expression.

To explore the possible involvement of counterregulation of Ang II-induced constriction by NO-cGMP signaling, which can be the result of endothelial AT_2 receptor stimulation, Ang II responses were studied in the presence of the guanylyl cyclase inhibitor ODQ. This approach, rather than adding an eNOS inhibitor, was chosen because *Ercc1*$^{d/-}$ mice show both changes in endothelial NO production as well as in cGMP responses of VSMC. Although the presence of ODQ tended to increase Ang II responses, the increase was very modest and did not reach significance in *Ercc1*$^{d/-}$ animals (Fig. 5B), nor in WT (not shown). Apparently, the loss of NO-cGMP signaling cannot entirely explain the increase Ang II vasoconstrictions.

Since increased AT_1 receptor signaling is believed to be involved in vascular disease related to endothelial dysfunction, a role that might both provoke as wells as be mediated by increased blood pressure, we tested the effect of chronic losartan treatment on vasodilator function in *Ercc1*$^{d/-}$ mice.

Effect of chronic losartan treatment on accelerated age-related vasodilator dysfunction

In the 12-wk-old *Ercc1*$^{d/-}$ mutants vasodilator responses to ACh were significantly decreased as compared to WT animals (Fig. 5C). The dilation response to a SNP concentration-response curve was also decreased in *Ercc1*$^{d/-}$ mice (Fig. 5D). Chronic AT_1 receptor blockade with losartan *in vivo* did not significantly change any of the responses. Our findings indicate that the observed vasodilator dysfunction (persistent after losartan) was not blood pressure-dependent and that the detrimental effect of genomic instability cannot be opposed by chronic AT_1 receptor blockade with Losartan.

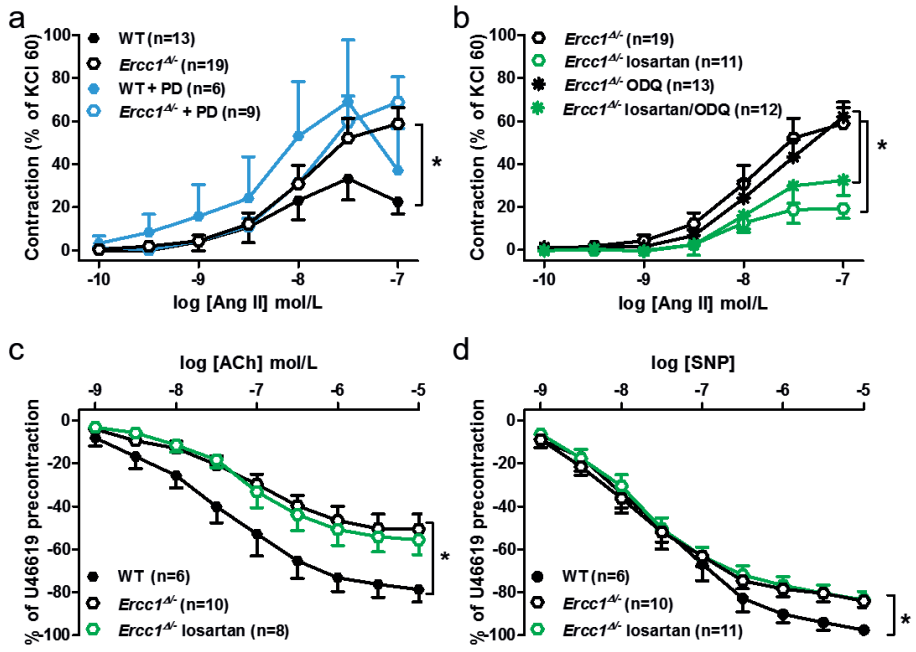

Figure 5. Vasoconstriction to angiotensin II (Ang II) of isolated iliac arteries from mice of the (A) diet intervention study, and (B) the losartan intervention study. (C, D) Vasodilation in isolated aortic tissue of the mice from the losartan intervention study to the endothelium-dependent vasodilator acetylcholine (ACh) and the endothelium-independent vasodilator, NO-donor sodium nitroprusside (SNP). All responses were measured *ex vivo* in small wire organ baths. Aortic tissue used to measure vasodilator responses was preconstricted with thromboxane analogue U46619. Error bars: S.E.M. *:p<0.05, general linear model for repeated measures. #: p<0.05, t-test on individual concentrations of Ang II of *ad libitum* (AL) fed *Ercc1*$^{d/-}$ mice vs. wild-type (WT) littermates.

DISCUSSION

In the present study we explored potential mechanisms that lead to DR-mediated improvement of vasodilator dysfunction caused by DNA damage. Loss of vasodilation was entirely due to loss of NO-cGMP signaling, both as a result of decreased endothelial NO release and decreased VSMC responsiveness to NO. In previous publications we showed that the decreased NO function was due to decreased eNOS expression and activation, increased PDE1 and possibly also PDE5 activity, and for a small part due to increased ROS production.[4, 5] The present results indicate that DR improves vascular dilations up to an age of at least 30 weeks. This is because DR enables aortic tissue to recruit endothelium-derived vasodilatory prostaglandins, which are normally absent. In addition, the responsiveness of VSMC to NO is improved. A possible explanation for the emerging prostaglandin response is the increase in COX-1 combined with a decreased in PDE4B, which together should lead

to improved vasodilator cAMP signaling. We have also explored the possible involvement of Ang II. Although defective DNA repair increased vasoconstrictive responses to Ang II, chronic blockade of AT_1 receptors with losartan did not rescue vasodilator responses. Also, blood pressure is not a driving mechanism in the observed vasodilator dysfunction, since blood pressure-lowering did not affect this dysfunction. Ang II-induced vasoconstriction most likely increased due to the loss of counterregulatory action of AT_1 receptor by AT_2 receptor when *Ercc1*$^{d/-}$ mutants age.

Preservation of endothelium-dependent responses by DR has been previously reported in aging WT rodents, involving nuclear factor erythroid-2-related factor-2 (Nrf2)-mediated upregulation of antioxidants.[17] In various tissues of AL-fed *Ercc1*$^{d/-}$ mice Nrf2-related antioxidants are already increased as a protective mechanism ([2] and unpublished observations), but *ex vivo* aortic vasodilator responses are still improved by the oxygen radical scavenger N-acetylcysteine due to an interaction in VSMC.[2, 4] After DR,Nrf2 is further activated[2] and SNP responses are totally normalized (Fig. 1), establishing the potential role of Nrf2. The present study now demonstrates that DR recruits yet another system to enhance endothelial function, namely vasodilatory prostaglandin signaling, acting through cAMP. To achieve this, COX-1 expression increased in DR-fed *Ercc1*$^{d/-}$ mice, on top of already decreased PDE4B expression in those mice. Potentially, this points at the genoprotective effect of DR improving transcriptional output in *Ercc1*$^{d/-}$, as was demonstrated in our previous publication.[2] Although the fate of COX products in the aging vasculature is certainly not uniform in diverse studies in rodents and humans[18], our results confirm the observation that DR prevents the decline of plasma and renal prostacyclin levels in aging rats.[19, 20] Another study shows rather diverse changes, claiming lower levels of both vasoconstrictive and vasodilatory COX products after DR in the aging rat aorta.[21] Although both findings indicate the participation of COX products in DR-induced changes, this topic has attracted little attention until now. Nevertheless, the combined improvement of VSMC responses to NO-cGMP and increased prostaglandin-cAMP by the endothelium explains the effect of DR.

Ang II responses increased in AL-fed *Ercc1*$^{d/-}$ mice compared to WT, whereas plasma renin activity decreased. The latter result is in agreement with the observation that renin levels decrease with age.[22, 23] Although renin levels start decreasing already when approaching middle age, our present findings indicate that the aging process might contribute to this decrease. With respect to the effect of aging on AT_1 receptor-mediated vasoconstrictions many contrasting findings have been described, depending on the species or the vessels that have been used.[24-28] Nevertheless, our observation is in agreement with findings showing that in older persons blood pressure and blood flow responses to Ang II are elevated, especially in the presence of diabetes or the absence of counterregulation by AT_2 receptors.[26, 29-31] Counterbalancing of AT_1-mediated pathogenesis is the basis for development of AT_2 receptor agonists as clinical drugs against cardiovascular diseases.[32, 33] Conversely,

increased Ang II activity via AT_1 receptors due to a loss of counterregulation by AT_2 receptor is a mechanism observed in various disease models and in aging wild-type rats.[32, 34] The counterbalancing effect by AT_2 receptors is often ascribed to endothelial NO release, or might relate to a change in dimerization of the two Ang II receptor subtypes.[35] Loss of NO signaling clearly does not play a role in *Ercc1*$^{d/-}$ mutants nor their WT littermates given the absence of an effect of ODQ, leaving receptor interaction as the alternative mechanism.

The endothelial dysfunction observed in the present study was clearly not related to Ang II and increased blood pressure. In patients, the effect of chronic AT_1 receptor blockade on preservation of vasodilator function is variable, having either a protective effect or not.[36] It was assumed that this might depend on the underlying disease or the vessel type that is investigated. However, our study suggests that the aging process might explain such variation. Unfortunately, most of the human studies exploring the effect of chronic AT1 receptor blockade focus on patients around 60 and younger, and not on the oldest old. Nevertheless, there are clues that aging affects the effectiveness of AT_1 receptor blockade. It has been shown that losartan becomes gradually less effective in aging rats, especially in the presence of hypertension and after loss of endothelium-independent NO function.[37] Clinical observations show that losartan/antihypertensive treatment can lead to adverse cognitive effects in elderly, which is ascribed to perfusion problems.[38] However, the same study suggests that this perfusion problem is a result of both blood pressure lowering and a persisting vascular dysfunction, at least in the brain. This implicates that vasodilator function is not improved. More dedicated studies in the oldest patients are necessary to resolve this paradox. There are mechanistic explanations available for this paradigm. In patients or in models of heart failure, hypertension, diabetes etc. Ang II blockade largely improves endothelial function due to an acute reduction of ROS formation by NAPH oxidase, increasing NO bioavailability.[9] DNA damage largely lowers NO independently from ROS[4], and apparently this undermines the treatment efficacy of AT_1 antagonists in our mouse model. It is therefore relevant to find tools to investigate this possibility in humans. Suboptimal effectiveness of and treatment response variability to RAS inhibition are well-known phenomena, but remain largely unexplained, and therefore drive studies that attempt to find prediction markers for therapy effectiveness. [39, 40]

CLINICAL PERSPECTIVES

DR is a very efficient intervention to prevent vasodilator dysfunction caused by genomic instability. In this study we set out to identify potential mechanisms that lead to DR-mediated improvement of vasodilator dysfunction caused by DNA damage.

- Improvement of prostaglandin-mediated endothelium-dependent signaling and of VSMC responses to NO were identified as mechanisms. Endothelial dysfunction induced by genomic instability is not reversible with chronic losartan treatment.
- Mouse models of genomic instability appear to represent the RAS blockade-resistant part of aging-related vascular disease, and might be tools to further explore this clinically relevant issue. Further study on the effect of genomic instability might offer a novel source of mechanistic explanations and markers with potential for clinical translation.

AUTHORS CONTRIBUTION

Anton Roks, Jan Danser and Jan Hoeijmakers designed the research. Bibi van Thiel and Paula Bautista-Niño conducted the research, collected data, provided important scientific input and participated in writing of the paper. Haiyan Wu, Erwin Reiling, Matej Durik, Frank Leijten, Yanto Ridwan and Renata Brandt helped in conducting the research and collecting data. Harry van Steeg, Martijn Dolle, Wilbert Vermeij, Jeroen Essers and Ingrid van der Pluijm provided important scientific input. All authors read and approved the final paper. There are no conflicts of interest to disclose.

ACKNOWLEDGEMENT

None

FUNDING

AJMR is sponsored by Dutch Heart foundation Grant # 2015T094. Diet restriction studies and cohort elevations were sponsored in part by National Institutes of Health/National Institute of Aging (P01AG017242). JHJH acknowledges the support from ERC Advanced grant DamAge and the academia professorship of the Royal Academy of Arts and Sciences of the Netherlands.

REFERENCES

1. Lakatta EG, Levy D. Arterial and cardiac aging: Major shareholders in cardiovascular disease enterprises: Part i: Aging arteries: A “set up” for vascular disease. *Circulation*. 2003;107:139-146

2. Vermeij WP, Dolle ME, Reiling E, Jaarsma D, Payan-Gomez C, Bombardieri CR, Wu H, Roks AJ, Botter SM, van der Eerden BC, Youssef SA, Kuiper RV, Nagarajah B, van Oostrom CT, Brandt RM, Barnhoorn S, Imholz S, Pennings JL, de Bruin A, Gyenis A, Pothof J, Vijg J, van Steeg H, Hoeijmakers JH. Restricted diet delays accelerated ageing and genomic stress in DNA-repair-deficient mice. *Nature*. 2016;537:427-431
3. Bautista-Nino PK, Portilla-Fernandez E, Vaughan DE, Danser AH, Roks AJ. DNA damage: A main determinant of vascular aging. *Int J Mol Sci*. 2016;17
4. Durik M, Kavousi M, van der Pluijm I, Isaacs A, Cheng C, Verdonk K, Loot AE, Oeseburg H, Bhaggoe UM, Leijten F, van Veghel R, de Vries R, Rudez G, Brandt R, Ridwan YR, van Deel ED, de Boer M, Tempel D, Fleming I, Mitchell GF, Verwoert GC, Tarasov KV, Uitterlinden AG, Hofman A, Duckers HJ, van Duijn CM, Oostra BA, Witteman JC, Duncker DJ, Danser AH, Hoeijmakers JH, Roks AJ. Nucleotide excision DNA repair is associated with age-related vascular dysfunction. *Circulation*. 2012;126:468-478
5. Bautista Nino PK, Durik M, Danser AH, de Vries R, Musterd-Bhaggoe UM, Meima ME, Kavousi M, Ghanbari M, Hoeijmakers JH, O'Donnell CJ, Franceschini N, Janssen GM, De Mey JG, Liu Y, Shanahan CM, Franco OH, Dehghan A, Roks AJ. Phosphodiesterase 1 regulation is a key mechanism in vascular aging. *Clin Sci (Lond)*. 2015;129:1061-1075
6. Vermeij WP, Hoeijmakers JH, Pothof J. Genome integrity in aging: Human syndromes, mouse models, and therapeutic options. *Annu Rev Pharmacol Toxicol*. 2016;56:427-445
7. Weiss EP, Fontana L. Caloric restriction: Powerful protection for the aging heart and vasculature. *Am J Physiol Heart Circ Physiol*. 2011;301:H1205-1219
8. Williams B. Vascular ageing and interventions: Lessons and learnings. *Ther Adv Cardiovasc Dis*. 2016;10:126-132
9. Brandes RP, Weissmann N, Schroder K. Nadph oxidases in cardiovascular disease. *Free Radic Biol Med*. 2010;49:687-706
10. de Borst MH, Navis G. Sodium intake, raas-blockade and progressive renal disease. *Pharmacol Res*. 2016;107:344-351
11. Nickenig G, Sachinidis A, Michaelsen F, Bohm M, Seewald S, Vetter H. Upregulation of vascular angiotensin ii receptor gene expression by low-density lipoprotein in vascular smooth muscle cells. *Circulation*. 1997;95:473-478
12. Danser AH, van Kesteren CA, Bax WA, Tavenier M, Derkx FH, Saxena PR, Schalekamp MA. Prorenin, renin, angiotensinogen, and angiotensin-converting enzyme in normal and failing human hearts. Evidence for renin binding. *Circulation*. 1997;96:220-226
13. von Hayn K, Werthmann RC, Nikolaev VO, Hommers LG, Lohse MJ, Bunemann M. Gq-mediated ca2+ signals inhibit adenylyl cyclases 5/6 in vascular smooth muscle cells. *Am J Physiol Cell Physiol*. 2010;298:C324-332
14. Lehrke M, Kahles F, Makowska A, Tilstam PV, Diebold S, Marx J, Stohr R, Hess K, Endorf EB, Bruemmer D, Marx N, Findeisen HM. Pde4 inhibition reduces neointima formation and inhibits vcam-1 expression and histone methylation in an epac-dependent manner. *J Mol Cell Cardiol*. 2015;81:23-33
15. Tunaru S, Chennupati R, Nusing RM, Offermanns S. Arachidonic acid metabolite 19(s)-hete induces vasorelaxation and platelet inhibition by activating prostacyclin (ip) receptor. *PLoS One*. 2016;11:e0163633
16. Seva Pessoa B, van der Lubbe N, Verdonk K, Roks AJ, Hoorn EJ, Danser AH. Key developments in renin-angiotensin-aldosterone system inhibition. *Nat Rev Nephrol*. 2013;9:26-36

17. Ungvari Z, Bailey-Downs L, Sosnowska D, Gautam T, Koncz P, Losonczy G, Ballabh P, de Cabo R, Sonntag WE, Csiszar A. Vascular oxidative stress in aging: A homeostatic failure due to dysregulation of nrf2-mediated antioxidant response. *American Journal of Physiology-Heart and Circulatory Physiology*. 2011;301:H363-H372
18. Matz RL, Schott C, Stoclet JC, Andriantsitohaina R. Age-related endothelial dysfunction with respect to nitric oxide, endothelium-derived hyperpolarizing factor and cyclooxygenase products. *Physiological research / Academia Scientiarum Bohemoslovaca*. 2000;49:11-18
19. Choi JH, Yu BP. The effects of dietary restriction on age-related changes in rat serum prostaglandins. *J Nutr Health Aging*. 1998;2:138-142
20. Choi JH, Yu BP. Dietary restriction as a modulator of age-related changes in rat kidney prostaglandin production. *J Nutr Health Aging*. 1998;2:167-171
21. Kim JW, Zou Y, Yoon S, Lee JH, Kim YK, Yu BP, Chung HY. Vascular aging: Molecular modulation of the prostanoid cascade by calorie restriction. *J Gerontol A Biol Sci Med Sci*. 2004;59:B876-885
22. Sealey JE, Atlas SA, Laragh JH. Prorenin and other large molecular weight forms of renin. *Endocr Rev*. 1980;1:365-391
23. Wilson DM, Stevenson DK, Luetscher JA. Plasma prorenin and renin in childhood and adolescence. *Am J Dis Child*. 1988;142:1070-1072
24. Vamos Z, Cseplo P, Ivic I, Matics R, Hamar J, Koller A. Age determines the magnitudes of angiotensin ii-induced contractions, mrna, and protein expression of angiotensin type 1 receptors in rat carotid arteries. *J Gerontol A Biol Sci Med Sci*. 2014;69:519-526
25. Hogikyan RV, Supiano MA. Arterial alpha-adrenergic responsiveness is decreased and sns activity is increased in older humans. *Am J Physiol*. 1994;266:E717-724
26. Cherney DZ, Reich HN, Miller JA, Lai V, Zinman B, Dekker MG, Bradley TJ, Scholey JW, Sochett EB. Age is a determinant of acute hemodynamic responses to hyperglycemia and angiotensin ii in humans with uncomplicated type 1 diabetes mellitus. *Am J Physiol Regul Integr Comp Physiol*. 2010;299:R206-214
27. Batenburg WW, Tom B, Schuijt MP, Danser AH. Angiotensin ii type 2 receptor-mediated vasodilation. Focus on bradykinin, no and endothelium-derived hyperpolarizing factor(s). *Vascul Pharmacol*. 2005;42:109-118
28. van der Heijden-Spek JJ, Staessen JA, Fagard RH, Hoeks AP, Boudier HA, van Bortel LM. Effect of age on brachial artery wall properties differs from the aorta and is gender dependent: A population study. *Hypertension*. 2000;35:637-642
29. Takeda R, Morimoto S, Uchida K, Miyamori I, Hashiba T. Effect of age on plasma aldosterone response to exogenous angiotensin ii in normotensive subjects. *Acta Endocrinol (Copenh)*. 1980;94:552-558
30. Wray DW, Nishiyama SK, Harris RA, Richardson RS. Angiotensin ii in the elderly: Impact of angiotensin ii type 1 receptor sensitivity on peripheral hemodynamics. *Hypertension*. 2008;51:1611-1616
31. Batenburg WW, Garrelds IM, Bernasconi CC, Juillerat-Jeanneret L, van Kats JP, Saxena PR, Danser AH. Angiotensin ii type 2 receptor-mediated vasodilation in human coronary microarteries. *Circulation*. 2004;109:2296-2301
32. Verdonk K, Danser AH, van Esch JH. Angiotensin ii type 2 receptor agonists: Where should they be applied? *Expert opinion on investigational drugs*. 2012;21:501-513

33. Danyel LA, Schmerler P, Paulis L, Unger T, Steckelings UM. Impact of at2-receptor stimulation on vascular biology, kidney function, and blood pressure. *Integr Blood Press Control*. 2013;6:153-161
34. Pinaud F, Bocquet A, Dumont O, Retailleau K, Baufreton C, Andriantsitohaina R, Loufrani L, Henrion D. Paradoxical role of angiotensin ii type 2 receptors in resistance arteries of old rats. *Hypertension*. 2007;50:96-102
35. AbdAlla S, Lother H, Abdel-tawab AM, Quitterer U. The angiotensin ii at2 receptor is an at1 receptor antagonist. *J Biol Chem*. 2001;276:39721-39726
36. Virdis A, Ghiadoni L, Taddei S. Effects of antihypertensive treatment on endothelial function. *Curr Hypertens Rep*. 2011;13:276-281
37. Demirci B, McKeown PP, Bayraktutan U. Blockade of angiotensin ii provides additional benefits in hypertension- and ageing-related cardiac and vascular dysfunctions beyond its blood pressure-lowering effects. *J Hypertens*. 2005;23:2219-2227
38. Mossello E, Pieraccioli M, Nesti N, Bulgaresi M, Lorenzi C, Caleri V, Tonon E, Cavallini MC, Baroncini C, Di Bari M, Baldasseroni S, Cantini C, Biagini CA, Marchionni N, Ungar A. Effects of low blood pressure in cognitively impaired elderly patients treated with antihypertensive drugs. *JAMA Intern Med*. 2015
39. van den Heuvel M, Batenburg WW, Jainandunsing S, Garrelds IM, van Gool JM, Feelders RA, van den Meiracker AH, Danser AH. Urinary renin, but not angiotensinogen or aldosterone, reflects the renal renin-angiotensin-aldosterone system activity and the efficacy of renin-angiotensin-aldosterone system blockade in the kidney. *J Hypertens*. 2011;29:2147-2155
40. Schievink B, de Zeeuw D, Parving HH, Rossing P, Lambers Heerspink HJ. The renal protective effect of angiotensin receptor blockers depends on intra-individual response variation in multiple risk markers. *Br J Clin Pharmacol*. 2015;80:678-686

CHAPTER 7

HYBRID OPTICAL AND CT IMAGING REVEALS INCREASED MATRIX METALLOPROTEASE ACTIVITY AND APOPTOSIS PRECEDING CARDIAC FAILURE IN PROGEROID *ERCC1* MICE

Bibi S. van Thiel[1,2,3], Yanto Ridwan[1,3], Martine de Boer[4], Marion G.J. de Kleijnen[4], Nicole van Vliet[1], Paula M. van Heijningen[1], Wilbert P. Vermeij[1], A.H. Jan Danser[3], Roland Kanaar[1,5], Dirk J. Duncker[4], Ingrid van der Pluijm[1,2], Jeroen Essers[1,2,5]

[1]Department of Molecular Genetics, Cancer Genomics Center Netherlands, [2]Department of Vascular Surgery, [3]Division of Vascular Medicine and Pharmacology, Department of Internal Medicine, [4]Division of Experimental Cardiology, Department of Cardiology, [5]Department of Radiation Oncology, Erasmus Medical Center, Rotterdam, The Netherlands

(Manuscript in preparation)

ABSTRACT

In this study, we tested the use of functional micro-Computed Tomography (microCT) imaging combined with near infrared fluorescent (NIRF) probes to directly report the *in vivo* activity of key biomarkers of age-related cardiac failure using progeroid *Ercc1* mouse models. Mutations in the ERCC1 gene causes diminished DNA damage repair and an accelerated aging phenotype in mice, including cardiovascular aging. We tested the effect and kinetics of diminished DNA damage repair on protease activity and apoptosis and possible subsequent cardiac failure *in vivo*.

Full body *Ercc1*$^{d/-}$, cardiomyocyte-specific *Ercc1*$^{c/-}$ and their *Ercc1*-proficient controls were imaged with contrast enhanced microCT for anatomical reference and to assess cardiac morphology and function. The NIRF probes MMPSense680™ and Annexin-Vivo750™ were used to image matrix metalloprotease activity and apoptosis, respectively. Functional microCT analysis was compared to ultrasound imaging and results were validated by histology.

Ercc1$^{d/-}$ deficiency resulted in changes in left ventricular geometry and functioning at 24 weeks of age; an increase in left ventricular end-diastolic and left ventricular end-systolic volume was observed, thereby leading to an overall decrease in stroke volume and a substantial reduction in left ventricular ejection fraction. *Ercc1*-proficient mice showed relative stable volumes over time. Moreover, *Ercc1*$^{d/-}$ deficiency leads to increased myocardial apoptosis at 12 and 24 weeks of age, and a gradual increase of MMP activity already starting at 6 weeks, suggesting that these processes precede cardiac failure in these progeroid *Ercc1* mice. Cardiomyocyte-specific inactivation of *Ercc1* also led to impaired cardiac functioning and increased myocardial apoptosis and MMP activity, indicating that *Ercc1* deficiency in cardiomyocytes is associated with adverse cardiac remodeling and poor cardiac functioning.

In conclusion, combined microCT and optical imaging allows simultaneous analysis of molecular and functional changes in mouse models for accelerated aging and shows that gradual increases in matrix metalloprotease activity is followed by apoptosis and cardiac functional decline in progeroid *Ercc1* mice.

INTRODUCTION

Cardiovascular diseases (CVDs) persist as one of the leading causes of morbidity and mortality in the elderly population worldwide. The incidence and prevalence of numerous CVDs, including heart failure, myocardial infarction, atherosclerosis and hypertension, increase tremendously after the age of 50 years.[1, 2] Many hypotheses have been proposed to explain the aging process, but neither appears to be fully satisfactory.[3, 4] The accumulation of unrepaired DNA damage over time is regarded as one of the driving forces of accelerated aging and age-related diseases, as exemplified in mice and patients with genetic defects in DNA repair pathways.[5, 6] A variety of these genetically altered mice with affected DNA repair pathways, demonstrate a strict correlation between the severity of the DNA repair defect and the extend of aging pathology and reduced lifespan, suggesting that the load of DNA damage directly relates to the rate of aging.[6] Several lines of evidence, in experimental as well as clinical studies, support the notion that accumulation of DNA damage, secondary to oxidative stress, is involved in the development of age-related CVDs.[7] Yet, the precise role of DNA damage and related aging on the manifestation of CVDs remains elusive and needs further exploration.

One of the most widely studied mouse models of accelerated aging as a consequence of increased DNA damage is the *Ercc1*$^{d/-}$ mouse model. These mice contain one knockout allele of the Excision Repair Cross Complementation group 1 (*ERCC1*) gene, and one protein truncating mutation, in which the last seven amino acids at the C-terminus of the Ercc1 protein are deleted.[8] Due to this effect, these animals are deficient in multiple DNA repair mechanisms including global genome-and transcription-coupled nucleotide excision repair, interstrand crosslink repair and homologous recombination.[9] Consequently, DNA damage accumulation causes these mice to display an accelerated aging phenotype, including growth retardation, neurological degeneration and a shortened lifespan. In addition, *Ercc1*$^{d/-}$ mutants display accelerated age-dependent vasodilator dysfunction, increased vascular stiffness, increased blood pressure and vascular cell senescence.[10] Hence, these mice are useful to explore why DNA damage and aging are crucial components in CVD etiology.

Cardiac aging is a complex process in which many cellular and molecular changes occur in the heart, including increases in cardiomyocyte apoptosis, interstitial fibrosis and cardiomyocyte hypertrophy. At a functional level, aging is associated with an altered left ventricular (LV) diastolic function, diminished LV systolic reserve capacity, decreased blood flow and an increased prevalence of atrial fibrillation, eventually leading to a reduction in cardiac output and ejection fraction.[11] Loss of myocytes, through necrosis and apoptosis, has been demonstrated in the aging heart and is thought to contribute to the progressive loss of cardiac functioning.[12-14] Apoptosis is a tightly regulated cell death process that is an important contributor to the development of the cardiovascular

system as well as to the adaptation of the cardiovascular system to the continuous changing environment.[15, 16] Progressive apoptosis may lead to a dysbalance between cell death and cell renewal, eventually leading to cardiac decline and failure.[12, 13] It has been shown that unrepaired DNA damage is a trigger for a cell to undergo apoptosis, however, how this process contributes to a decline in cardiac performance remains to be elucidated. In addition to apoptosis, matrix metalloproteinases (MMPs) are found to participate in cardiac tissue remodeling in several CVDs, including myocardial infarction, heart failure and development of dilated cardiomyopathy (DCM).[17-20] MMPs are a family of proteolytic enzymes with the capacity to cleave components of the extracellular matrix, including elastin and collagen and thereby promote extracellular matrix turnover and degradation of the myocardial wall.[21] Clinical evidence suggests that MMP-9 has a significant role in LV remodeling and thus can serve as a novel prognostic biomarker for individuals at increased risk for CV mortality.[22-25] In this study, we therefore focused on apoptosis and MMP activity as potential biomarkers of age-related cardiac failure.

The most commonly used modality to evaluate cardiac functioning is echocardiography. However, functional analysis is performed in a 2D-view, and this generates a potential risk of inaccurate measurements of the whole heart, especially in small animals. In addition, assessment of right ventricular volumes and function remains challenging because of the particular shape of the right ventricle wrapped around the LV. This has been shown to be particularly unsatisfying in patients with non-standard ventricular size and anatomy.[26-28] Thus, there is a need for other noninvasive imaging techniques to evaluate CVDs. Contrast enhanced micro-Computed Tomography (microCT) imaging has been shown to be useful to investigate cardiac function and structure in small animals, as it has a high resolution and allows 3D imaging of heart and associated structures, providing reliable information about ventricular structure and function.[29] Moreover, the introduction of *in vivo* multimodality molecular imaging plays an increasingly pivotal role in biomedical and clinical research. MicroCT imaging can be combined with fluorescence molecular tomography (FMT) and near infrared fluorescent (NIRF) probe(s), which not only provides anatomical and functional data but also allows non-invasive studying of molecular targets involved in the development and progression of disease, including CVD, in small animals.[30-33] NIRF optical molecular imaging offers a new approach to evaluate processes involved in cardiac disease and provide valuable insights into different aspect of disease development and progression.

As *Ercc1* plays an important role in several DNA damage responses, we hypothesized that intact DNA repair in cardiomyocytes is critical for maintaining normal cardiac function and that complete or partial loss of *Ercc1* would provoke induced DNA damage, apoptosis and subsequent cardiac aging and failure. Furthermore, we tested the use of functional microCT imaging combined with NIRF probes targeting apoptosis and MMP

activity to directly report on the *in vivo* activity of these markers of age-related cardiac failure.

MATERIAL AND METHODS

Mouse model

All animal procedures were performed in accordance with the Principles of Laboratory Animal Care and Guidelines approved by the Dutch Animal Ethical Committee in full accordance with European legislation. As required by Dutch law, formal permission to generate and use genetically modified animals was obtained from the responsible local and national authorities. Animals were housed in individual ventilated cages under specific pathogen free conditions and maintained in a controlled environment (20-22°C, 12 h light: 12 h dark cycle). They were given *ad libitum* access to food (maintained on either AIN93G synthetic pellets (Research Diet Services B.V.; gross energy content 4.9 kcal/g dry mass, digestible energy 3.97 kcal/g) or standard chow diet) and water.

Male and female animals were used in this experiment. The generation of *Ercc1*$^{d/-}$ and *Ercc1*$^{+/+}$ mice has been described previously.[8] *Ercc1*$^{d/-}$ mutants (15% expression of the mutant Ercc1 allele), and their wild-type *Ercc1*$^{+/+}$ littermates (WT), in an F1 hybrid FVB/NJ x C57BL/6J background, were studied at 6, 12 and 24 weeks of age. Mice with a cardiomyocyte-specific deletion of *ERCC1* (αMHC-*Ercc1*$^{c/-}$) were generated using the *Cre-loxP* technology on a similar mixed background. Briefly, a floxed allele of *Ercc1* was generated by inserting loxP sites in intron 2 and 5, such that Cre recombinase excises exons 3–5 of the *Ercc1* locus.[34-36] Mice harboring two floxed alleles of *Ercc1* were crossed with hemizygous mice expressing Cre-recombinase under the control of the α-myosin heavy chain (αMHC-Cre) promotor. αMHC-*Ercc1*$^{c/-}$ and their control (cre^{-}) littermates were studied at 8 and 16 weeks of age.

In vivo microCT-FMT imaging of MMP activity and apoptosis

Mice were imaged with contrast enhanced Quantum FX Micro-computed Tomography (microCT) (Perkin Elmer Inc., Akron, Ohio, USA) for anatomical reference and to assess cardiac morphology and function. The NIRF probes MMPSense680™ and Annexin-Vivo750™ (Perkin Elmer Inc.) were used to image matrix metalloprotease (MMP) activity and apoptosis, respectively and imaged with the FMT 2500 fluorescence tomography *in vivo* imaging system (Perkin Elmer Inc.). The MMPsense probe is optically silent in a non-active state and becomes highly fluorescent following protease-mediated activation by MMPs, including MMP-2, -3, -9 and -13, whereas Annexin-Vivo binds to phosphatidylserine, which is exposed on the outer leaflet of the cell membrane lipid bilayer during the early stages of apoptosis. Briefly, mice were injected intravenously with MMPSense680™ (2 nmol/25 gram bodyweight in 100µl

PBS) 24 hours before microCT-FMT imaging. Mice were anaesthetized (1.5-2.5% isoflurane, O_2 1 L/min) and depilated to minimize the interference of fur on the fluorescent signal. 2 hours before FMT imaging, mice were injected intravenously with Annexin-Vivo750™. Before microCT imaging (Perkin Elmer Inc.), mice were injected in the tail vein with the iodinated contrast agent eXIA160 (Binitio Biomedical Inc., Ottawa, Canada), positioned in the imaging cassette and restrained to prevent movement during imaging. Mice were scanned using intrinsic cardiac respiratory gating to reduce artifacts caused by breathing or cardiac motion. After microCT imaging, mice remained under anesthesia and the cassette was transferred to the FMT 2500 fluorescent tomography *in vivo* imaging system (Perkin Elmer Inc.). FMT imaging was performed using 680 and 700 nm excitation and emission wavelengths, respectively, 24 hours after injection of MMPSense680™. The multimodal animal cassette facilitates the coregistration of FMT and CT data through fiducial landmarks. FMT and microCT data were merged using the Amide software and *in vivo* fluorescence was quantified. Functional parameters were calculated from the 3D microCT images with the help of the software ANALYZE® 12.0 (AnalyzeDirect Inc., Overland Parks, KS, USA).

Ex vivo fluorescent imaging of excised hearts

After *in vivo* microCT-FMT imaging, mice were euthanized using an overdose of inhalant anesthetic isoflurane. Hearts were excised, emersion fixed in formalin and assessed for *ex vivo* tissue epifluorescence using the FMT system and the Odyssey® CLx imaging system (LI-COR® Biosciences, Lincoln, Nebraska, USA).

Statistical analysis

Data are expressed as the mean±SEM. Differences between groups were evaluated by Student's t-test or ANOVA, and corrected for multiple testing by post-hoc Bonferroni analysis when needed. $P<0.05$ was considered significant. All analyses were performed using IBM SPSS Statistics version 20.0 (SPSS Inc., Chicago, IL, USA).

RESULTS

Ercc1 deficiency results in changes in LV geometry and functioning

As previously described, *Ercc1*$^{d/-}$ mice showed reduced growth, declined body weight and a shortened lifespan (of approximately half a year) compared to their control littermates (Fig. 1a and 1b, and Table 1).[37] To investigate the effect of *Ercc1*$^{d/-}$ deficiency on heart geometry and function, anesthetized mice were injected with an iodinated contrast agent and imaged with the use of microCT. Imaging revealed an enlargement of the heart chambers in *Ercc1*$^{d/-}$ animals at 24 weeks of age compared to *Ercc1*$^{d/-}$ animals at 6 and 12 weeks of age. This was in striking contrast to the relatively stable volumes in the WT group over time, shown by a

volumetric 2D representation of the heart in end-diastole (Fig. 1c). To investigate whether normal cardiac function is maintained in *Ercc1*$^{d/-}$ mice, LV parameters were analyzed. *Ercc1*$^{d/-}$ mice showed an increase in left ventricular end-diastolic (LVED) volume (24-week-old *Ercc1*$^{d/-}$ 33+/-1 mm^3 versus 6-week-old *Ercc1*$^{d/-}$ 27+/-2 mm^3; p<0.05; n=22 and n=6, respectively), suggesting that the LV chamber is 24% dilated in diastole at 24 weeks of age compared to the earlier time points (Fig. 1d and Table 1). In addition, an increase in left ventricular end-

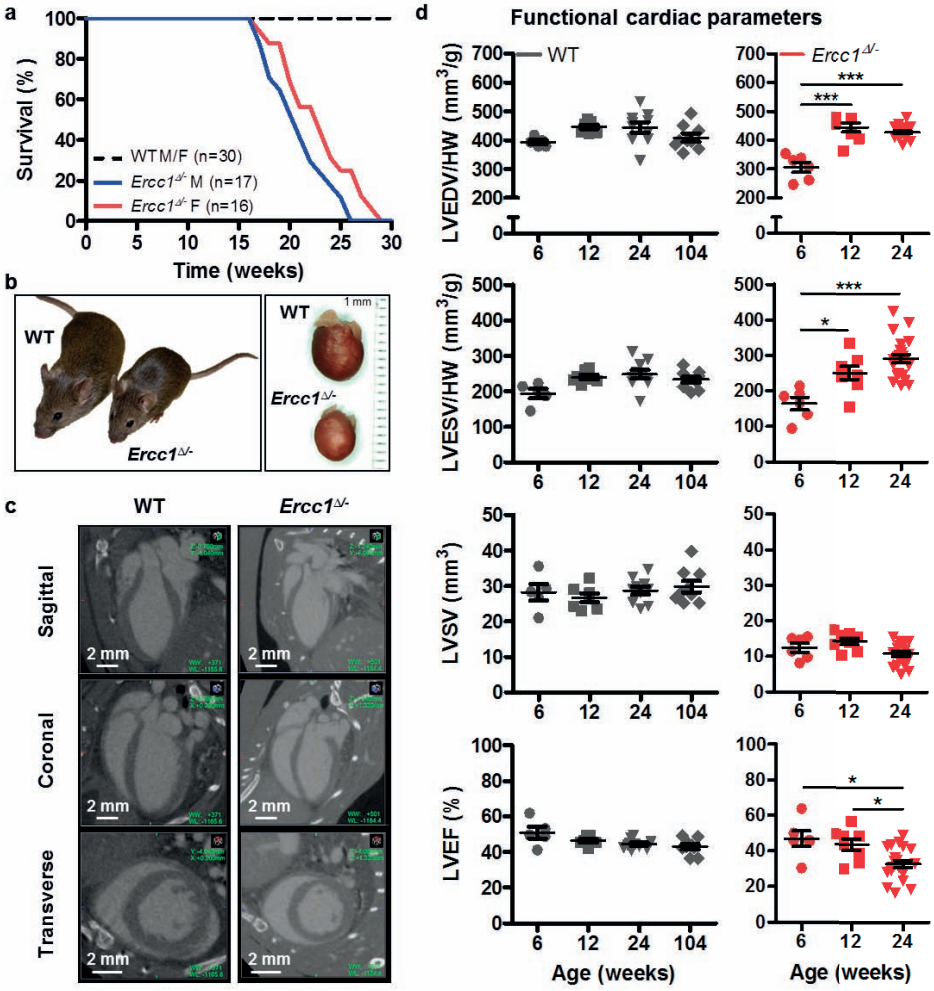

Figure 1. *Ercc1* deficiency results in a shortened lifespan and a deterioration in left ventricular function (LV) at 24 weeks of age. a. Lifespan is reduced in *Ercc1*$^{d/-}$ mice compared to control littermates. b. Representative pictures of WT and *Ercc1*$^{d/-}$ mice and hearts at the age of 24 weeks. c. Representative microCT images of the heart in left ventricular end-diastole from WT and *Ercc1*$^{d/-}$ mice at 24 weeks of age. d. MicroCT functional imaging revealed a deterioration in LV function in *Ercc1*$^{d/-}$ at 24 weeks of age. Data is presented as mean±SEM. Statistical significance *P<0.05 and **P< 0.001.

systolic (LVES) volume was observed, leading to an overall decrease in stroke volume at 24 weeks (24-week-old *Ercc1*$^{d/-}$ 22+/-1 mm^3 versus 6-week-old *Ercc1*$^{d/-}$ 14+/-2 mm^3; p<0.05; n=22 and n=6, respectively). WT mice showed stable volumes over time. Because stroke volume decreased while LVED volume increased in *Ercc1*$^{d/-}$ mice at the age of 24 weeks, there is a substantial reduction in left ventricular ejection fraction (LVEF) (24-week-old *Ercc1*$^{d/-}$ 33%+/-2 versus WT 44%+/-1; p<0.05; n=22 and n=10, respectively).

Table 1. Left ventricular volumes and global functional indices measured in 6- and 24-week-old WT and *Ercc1*$^{d/-}$ mice. Data represents mean±SEM. Statistical significance *P<0.05 and **P< 0.01. LVEDV, left ventricular end-diastolic volume; LVESV, left ventricular end-systolic volume; LVSV, left ventricular stroke volume; LVEF, left ventricular ejection fraction; LVMV, total left ventricular myocardial volume; LVMM, left ventricular myocardial mass; BPM, beats per minute.

	Control WT			Mutant *Ercc1*$^{\Delta/-}$		
	6 weeks	**24 weeks**	**Δ %**	**6 weeks**	**24 weeks**	**Δ %**
Body weight (g)	26.1 ± 1.38 M	43.4 ± 1.01 M	+16	17.3 ± 0.89 M	13.5 ± 0.32 M	-13
	20.7 ± 0.20 F	28.6 ± 1.42 F	-2	13.7 ± 0.50 F	13.3 ± 0.23 F	-10
Heart weight (g)	0.139 ± 0.005	0.148 ± 0.008	+6	0.087 ± 0.003	0.077 ± 0.001	-12
LVEDV (mm^3)	54.69 ± 1.53	64.71 ± 2.27	+18	26.68 ± 1.69	33.00 ± 0.55	+24**
LVESV (mm^3)	26.74 ± 1.50	36.02 ± 1.39	+35	14.25 ± 1.52	22.16 ± 0.80	+55**
LVSV (mm^3)	27.94 ± 2.39	28.69 ± 1.12	+3	12.43 ± 1.26	10.84 ± 0.69	-13
LVEF (%)	50.87 ± 3.35	44.35 ± 0.85	-13	46.82 ± 4.36	32.87 ± 2.10	-30*
LVMV (mm^3)	81.92 ± 3.63	93.62 ± 9.30	+14	49.98 ± 2.59	46.25 ± 1.46	-7
LVMM (mg)	86.02 ± 3.81	93.30 ± 9.76	+14	52.48 ± 2.72	48.56 ± 1.53	-7

Cardiomyocyte-specific deletion of *Ercc1* in the heart leads to impaired cardiac functioning

In order to investigate whether the observed cardiac impairment in the *Ercc1*$^{d/-}$ animals was due to loss of *Ercc1* in the heart or due to overall age-related systemic organ failure, *Ercc1* was deleted specifically in the cardiomyocytes of the heart. These αMHC-*Ercc1*$^{c/-}$ mice exhibited normal growth and body weight, similar to control (Table 2), but subsequently showed a reduced lifespan of about 24 weeks (Fig. 2a). From 16 weeks on an overall decrease in health and survival was observed. Therefore, cardiac size and function were assessed with microCT in 8 and 16-week-old αMHC-*Ercc1*$^{c/-}$ and control mice. At 16 weeks, αMHC-*Ercc1*$^{c/-}$ showed an increase in LVED volume (*Ercc1*$^{c/-}$ 73+/-6 mm^3 versus WT 57+/-3 mm^3; p<0.05; n=4 both groups) as well as an increase in LVES volume (*Ercc1*$^{c/-}$ 51+/-5 mm^3 versus WT 29+/-3 mm^3; p<0.05; n=4 both groups). This suggest that left ventricular dilation and systolic dysfunction were present in αMHC-*Ercc1*$^{c/-}$ at 16 weeks of age (Fig. 2c). The deterioration of LV function in αMHC-*Ercc1*$^{c/-}$ mice preceded signs of heart failure (*Ercc1*$^{c/-}$ 30%+/-1 versus WT 50%+/-2; p<0.05; n=6 both groups) (Fig. 2c). These results indicate that *Ercc1* deficiency in cardiomyocytes is associated with adverse cardiac remodeling and poor cardiac functioning.

Table 2. Left ventricular volumes and global functional indices measured in 8- and 16-week-old control and αMHC-*Ercc1*$^{c/-}$ mice. Data represents mean ± SEM. Statistical significance *P<0.05 and **P< 0.01. LVEDV, left ventricular end-diastolic volume; LVESV, left ventricular end-systolic volume; LVSV, left ventricular stroke volume; LVEF, left ventricular ejection fraction; BPM, beats per minute.

	Control Cre-			aMHC-*Ercc1*$^{c/-}$		
	8 weeks	**16 weeks**	**Δ %**	**8 weeks**	**16 weeks**	**Δ %**
Body weight (g)	22.7 ± 1.2	27.8 ± 3.3	+22	21.3 ± 2.1	24.2 ± 2.2	+14
Heart weight (g)	0.111 ± 0.004	0.136 ± 0.007	+22	0.112 ± 0.008	0.130 ± 0.008	+16
LVEDV (mm^3)	46.91 ± 1.59	57.26 ± 2.98	+22	50.55 ± 3.07	72.48 ± 5.76	+43
LVESV (mm^3)	25.08 ± 1.12	28.85 ± 2.63	+15	29.49 ± 2.25	50.85 ± 4.43	+72
LVSV (mm^3)	21.83 ± 1.47	28.42 ± 1.01	+30	21.06 ± 0.82	21.63 ± 1.18	+3
LVEF (%)	46.46 ± 2.14	50.10 ± 2.29	+8	41.76 ± 0.88	29.97 ± 1.18	-28

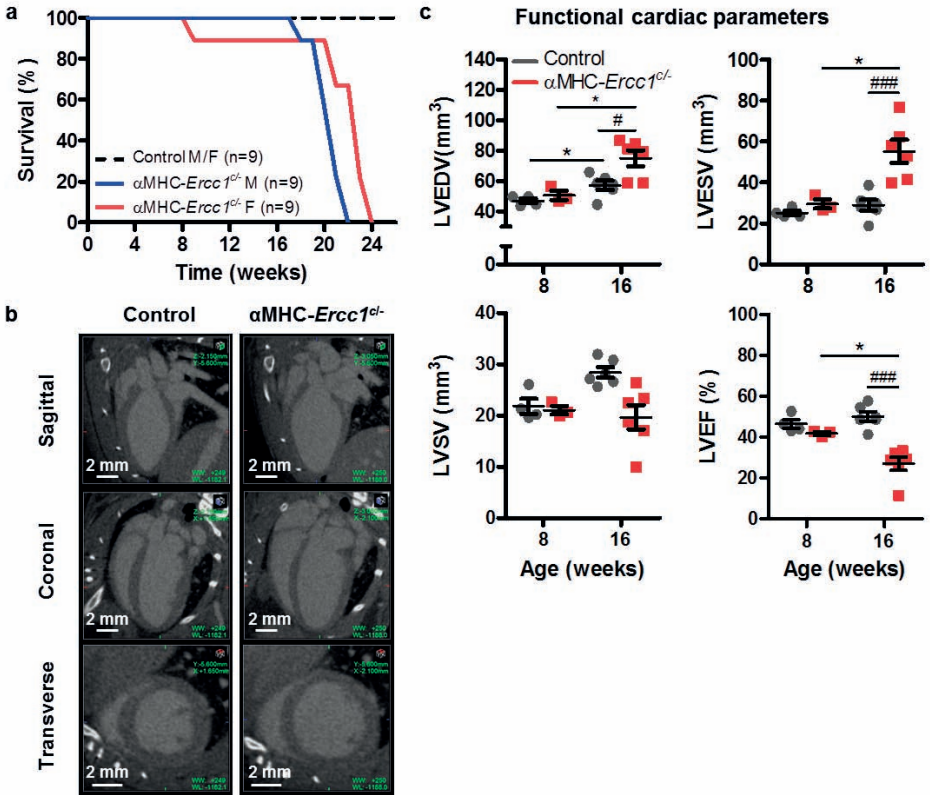

Figure 2. Specific deletion of Ercc1 in cardiomyocytes leads to early onset of left ventricular (LV) dysfunction. a. Specific loss of *Ercc1* in cardiomyocytes (αMHC-*Ercc1*$^{c/-}$) leads to a significant reduction in lifespan compared to littermate controls. b. Representative microCT images of the heart from αMHC-*Ercc1*$^{c/-}$ mouse and control littermates, showing an increase in size of the heart from the mutant animals at the age of 16 weeks. c. MicroCT functional imaging revealed that left ventricular function is impaired in αMHC-*Ercc1*$^{c/-}$ mice. Data is presented as mean±SEM. Statistical significance *P<0.05 and **P< 0.001.

Ercc1 deficiency causes a gradual decrease in LV myocardial mass over time

As a lot of patients diagnosed with heart failure have an underlying type of cardiomyopathy, i.e. disease of the myocardium, we quantified the myocardial wall volume and mass in *Ercc1*$^{d/-}$ hearts of 6, 12 and 24 weeks of age, using the microCT data (as indicated in Fig. 3a). 3D-reconstructed myocardial wall images showed a gradual decrease in myocardial mass in *Ercc1*$^{d/-}$ hearts over time (Fig. 3b). Quantification of the LV wall mass confirmed LV myocardial wall thinning in *Ercc1*$^{d/-}$ hearts at 24 weeks of age compared to 6-week-old *Ercc1*$^{d/-}$ mice, whereas the LV myocardial wall mass of WT mice increased from 6 until 24 weeks of age (Fig. 3c).

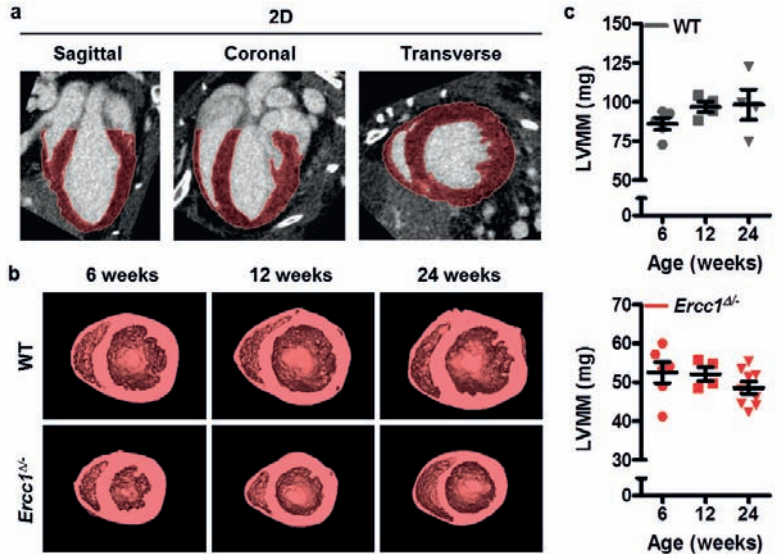

Figure 3. *Ercc1*$^{D/-}$ mice causes a gradual decrease in LV myocardial mass over time. a. Representative microCT images of a WT heart in which the myocardial wall is selected (red) for analysis. b. 3D reconstructed myocardial wall images of WT and *Ercc1*$^{d/-}$hearts over time show a gradual thinning of the myocardial wall in 24-week-old *Ercc1*$^{d/-}$hearts. c. Quantification of the left ventricular (LV) wall mass confirmed a trend in LV myocardial wall thinning in *Ercc1*$^{d/-}$ hearts at 24 weeks of age. Data is presented as mean±SEM. Statistical significance *P<0.05 and **P< 0.001.

Ercc1 deficiency leads to increased myocardial apoptosis and MMP activity

To investigate whether we could, non-invasively, detect apoptotic cells in the aging *Ercc1*$^{d/-}$ hearts, we injected these animals with the NIRF probe Annexin-Vivo750™ that binds to phosphatidylserine which is exposed on the outer leaflet of the cell membrane lipid bilayer during the early stages of apoptosis. MicroCT-FMT-reconstructed 3D images showed an increased intensity of Annexin-Vivo in *Ercc1*$^{d/-}$ compared to WT mice, at 24 weeks of age (Fig. 4a). Quantification of the *in vivo* fluorescent signal revealed significantly increased myocardial apoptosis in *Ercc1*$^{d/-}$ mice at all ages when compared to WT (24 weeks 164+/-25

versus 16+/-3 pmol/g, respectively; p<0.001; n=8 vs n=5) (Fig. 4b). 2D tissue epifluorescence imaging of excised hearts confirmed the increased fluorescence seen noninvasively by FMT in the *Ercc1*$^{d/-}$ mice (Fig. 4c and d). In addition, representative heart sections were

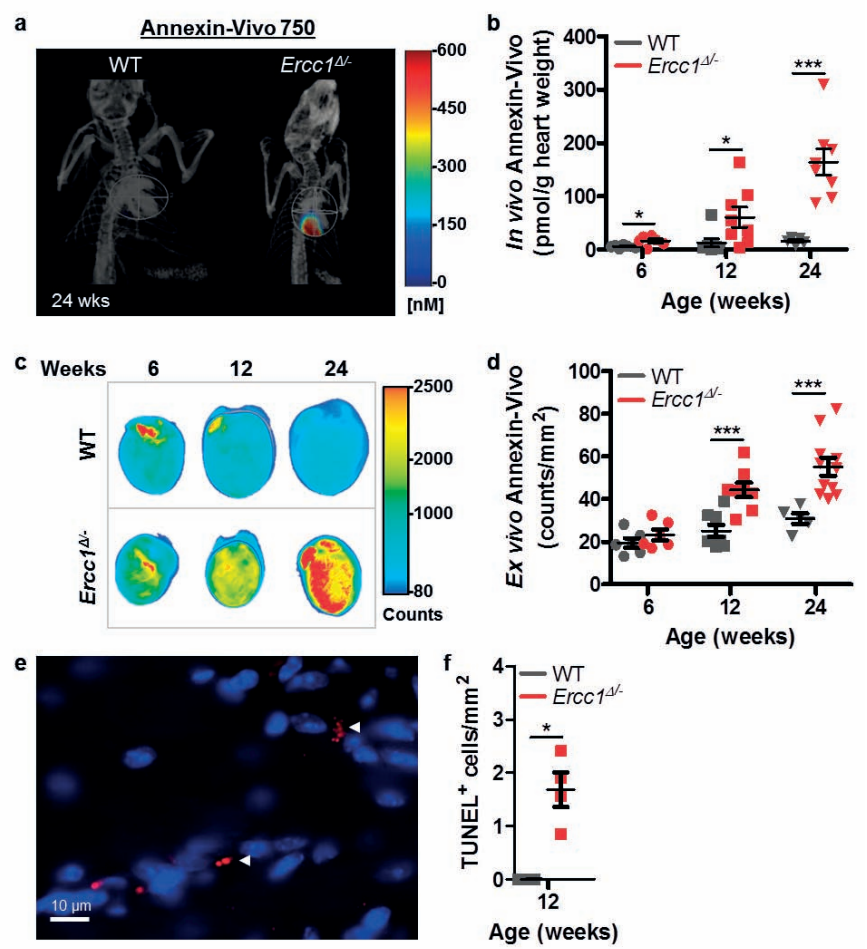

Figure 4. *Ercc1* deficiency leads to increased myocardial apoptosis. a. *In vivo* fluorescent imaging of apoptosis in the heart in *Ercc1*$^{d/-}$ mice compared to WT, at 24 weeks of age. Signal from the other tissues is excluded for clarity. b. *In vivo* quantitative data, by dual fusion of FMT and CT imaging, revealed increased myocardial apoptosis in *Ercc1*$^{d/-}$ mice at 12 and 24 weeks of age. c. Epifluorescence images of the heart, obtained with an odyssey imaging system, show an increase in apoptotic signal at 24 weeks of age in the *Ercc1*$^{d/-}$ mice compared to WT. d. Quantification of 2D tissue epifluorescence imaging of excised hearts confirmed the increased fluorescence in the *Ercc1*$^{d/-}$ mice. e. Representative heart sections showed that the NIRF fluorescence of the injected Annexin-Vivo probe was detected on the membrane of cells. f. Immunohistochemistry confirmed the presence of apoptotic cells in the myocardium of 12 and 18 weeks old *Ercc1*$^{d/-}$ mice. Data is presented as mean±SEM. Statistical significance *P<0.05 and **P< 0.001

examined under a fluorescent microscope, which showed that the NIRF fluorescence of the injected Annexin-Vivo probe was detected on the membrane of cells (Fig. 4e). Immunohistochemistry confirmed the presence of apoptotic cells in the myocardium of 12 weeks old *Ercc1*$^{d/-}$ mice (Fig. 4f). TUNEL staining revealed a greater occurrence of apoptotic myocytes in *Ercc1*$^{d/-}$ hearts, whereas only a few TUNEL-positive cells were detected in WT hearts. Apoptotic cells were located throughout the whole myocardium. As shown in Figure 4f, quantification of cardiomyocyte apoptosis by TUNEL staining demonstrated an approximate 2-fold increase in *Ercc1*$^{d/-}$ hearts compared to WT hearts. Since MMPs participate in cardiac remodeling after acute injury and are involved in the breakdown of the myocardium, we injected the accelerated aging *Ercc1*$^{d/-}$ mice with the MMP-specific activatable NIRF probe MMPSense680™ to detect possibly increased MMP activity in the *Ercc1*$^{d/-}$ hearts. We subsequently determined tissue epifluorescence levels in excised hearts using the Odyssey imaging system. At 6 and 24 weeks of age, *Ercc1*$^{d-}$ hearts showed increased MMP activity compared to WT hearts (Fig. 5a and b).

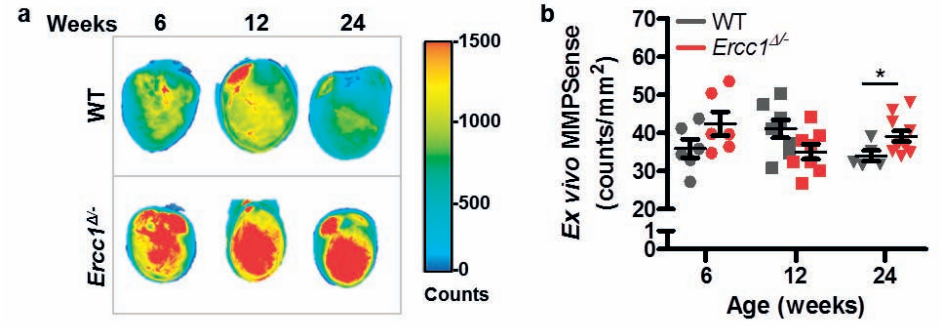

Figure 5. *Ercc1* deficiency results in a gradual increase of MMP activity in the myocardium. a. 2D Tissue epifluorescence imaging of excised hearts using the Odyssey imaging system. b. Quantification of epifluorescence imaging of excised hearts showed a significant gradual increase of MMP activity at 24 weeks of age, in the *Ercc1*$^{d/-}$ mice compared to WT. Data is presented as mean±SEM. Statistical significance *P<0.05 and **P< 0.001.

DISCUSSION

Research focusing on age-related diseases in humans carries unique challenges, because of its complexity as well as the time involved, thus the need remains for preclinical studies based on animal models that resemble the clinical setting of age-related diseases at accelerated pace. During the past few decades, many animal models to study certain aspects of cardiac aging and related disease have emerged, however, the precise role of DNA repair deficiency and related accelerated aging on CVD remains largely elusive.[38, 39] As accumulation of DNA damage is regarded as one of the possible explanations of aging, in this study

we explored the effect of *Ercc1* deficiency, leading to defects in DNA repair, on cardiac function.[4] We evaluated cardiac performance starting at 6 through 24 weeks of age using non-invasive microCT imaging. Additionally, we tested the use of functional microCT imaging combined with NIRF probes to explore whether we could directly report on the *in vivo* activity of MMP and the occurrence of apoptosis in the aging heart, and investigated if these probes can serve as markers for age-related CVD.

In the present study, we demonstrate that *Ercc1* deficiency results in changes in geometry and functioning of the heart with age. Adult *Ercc1*$^{d/-}$ mice exhibited ventricular chamber enlargement and LV myocardial wall thinning, however decreased stroke volume/ejection fraction only occurred at the end of their lifespan (24 weeks). The overall changes in the heart and myocardium of the 24-week-old *Ercc1*$^{d/-}$ mice suggest that *Ercc1* deficiency contributes to the development of features consistent with progressive DCM, a common pathology seen in aged humans.[40] DCM is a disease of the myocardium that is characterized by ventricular chamber enlargement with a reduction in cardiac performance, often accompanied by progressive thinning of the myocardial wall. Several studies have already indicated a link between DNA damage and DCM in humans as well animal models. Patients with DCM, exhibited elevated levels of 8-hydroxy-2-deoxyguanosine (8-OhdG) in their serum and myocardium, suggesting an increase in overall oxidative DNA damage in this type of cardiac disease.[41] Moreover, mitochondrial DNA damage and dysfunction have been shown to activate apoptosis and cause DCM.[42-44] DNA damage and aging are not limited to DCM, but also contribute to other types of CVDs, including heart failure and myocardial infarction.[45-49] In addition, increasing evidence indicates that therapeutic radiation treatment causes various types of DNA damage and consequently can cause cardiovascular complications (reviewed within Ishida et al.).[46]

The *Ercc1*$^{d/-}$ mouse model has been well recognized as a model of accelerated aging, and as such the pathology observed in these animals could be the result of accelerated systemic organ aging and consequent failure.[6, 37] However, as we showed that cardiomyocyte-specific deletion of *Ercc1* identically impaired cardiac functioning, we conclude that *Ercc1* deficiency in the heart results in adverse cardiac remodeling and poor cardiac functioning, independently of overall age-related systemic organ failure. Mice with cardiomyocyte-specific deletion of *Ercc1* had an overall lifespan approximately 20 weeks and likely died due to the decrease in cardiac performance. However, only at 24 weeks of age the Ercc1$^{d/-}$ mice showed a decrease in LVEF. We chose 24 weeks as our end-point because it has been previously reported that *Ercc1*$^{d/-}$mice have an average lifespan of 24-28 weeks, as shown in Figure 1a.[37, 50, 51] During their lifetime, these *Ercc1*$^{d/-}$ animals show numerous accelerated aging features including loss of vision and hearing, dystonia and tremors, kyphosis, ataxia and progressive neurodegeneration.[50, 52, 53] The exact cause of death in these mice is still unknown, but is probably related to the fact that the most vulnerable organ systems fail first, thus preventing information acquisition of the aging phenotype on other organ

systems, including the heart. Nevertheless, the vast amount on functional, histopathological, transcriptional, proteomic, metabolomics and ultrastructural data regarding the *Ercc1*$^{d/-}$ mice support the conclusion that these animals copy normal murine aging, and are a useful model to study the effect of aging and DNA repair defects on disease development and progression (reviewed within Gurkar et al.).[54]

Hybrid imaging optimized for small animals is very important because of the widespread use of genetically engineered mice resembling disease and the need to *in vivo* investigate the functional, anatomical and molecular phenotype of these mice. Imaging of the cardiovascular system, especially the right ventricle and the myocardial wall, has been quite challenging for a long time. The advances in new and existing imaging modalities for small animals, allow more accurate, high resolution, 3D, longitudinal imaging of the cardiovascular system and provides rapid translation of new knowledge to the clinic.[55] MicroCT imaging is frequently used for characterization of cardiac function and structure in small animals, and current systems now provide cardio-respiratory gating, to minimize movement interference.[56, 57] The current study used microCT imaging not only to determine cardiac function but also explore the shape and anatomy of the myocardial wall. We could accurately measure the myocardial wall volume and mass, demonstrating that *Ercc1*$^{d/-}$ mice show myocardial wall thinning at 24 weeks of age. Moreover, representative microCT images of the *Ercc1*$^{d/-}$ hearts suggest that the right ventricle is also affected in these mice, and analysis and quantification thereof should give us more answers regarding the function and geometry of the right ventricle. The microCT is well suited for examination of cardiac disease in small animals.

Fluorescent molecular imaging data presented in this study revealed that cardiac aging and subsequent failure in the progeroid *Ercc1* mice is preceded by a gradual increase in MMP activity and an increase in apoptosis. Aging is linked to increased MMP activity and extracellular matrix turnover, which could lead to myocardial remodeling thereby affecting cardiac performance. Several different types of MMPs are detected in diseased hearts, in which MMP-9, in particular, is found to play a key role.[24, 58, 59] However, the suggestion that MMP-9 can serve as potential plasma markers for cardiac aging might not be correct, as the age-associated increase of circulating MMP-9 in mice is in contrast with the decrease of circulating MMP-9 found in aging humans.[60, 61] This highlights the complexity of the presence and role of MMPs in age-related diseases. The MMPs found in the aging heart might be derived from senescent cells and due to the senescence-associated secretory phenotype.[62] Numerous examples of increased cellular senescence involved in age-related pathology have been reported.[63] DNA damage is a crucial mediator for cells to undergo apoptosis or enter senescence and it was shown that *Ercc1* deficient cells undergo premature cellular senescence.[8] Hence, the increased MMP activity observed in *Ercc1*$^{d/-}$ mice might also be derived from senescent cells, and the use of *in vivo* molecular imaging of MMP activity could help to follow changes in activity over time. Additionally, apoptosis

has been suggested to be responsible for a significant amount of cardiomyocyte death that contributes to the development and progression of heart failure. Indeed, apoptosis has been found in several cardiac diseases.[64-66] However, whether there are increases in apoptotic cells in failing hearts remains controversial.[67] One of the arguments is that the TUNEL technique, which detect apoptosis by identifying *in situ* DNA nicks, is not solely specific for programmed cell death but might also label cells that undergo DNA repair.[68] The apoptosis probe we used in this study, Annexin-Vivo750™, binds to phosphatidylserines exposed on the outside of early apoptotic cells and does not detect DNA nicks, and therefore holds potential for *in vivo* identification of apoptosis. Fluorescent imaging of Annexin-Vivo in the *Ercc1*$^{d/-}$ mice, demonstrated that *Ercc1* deficiency leads to increased myocardial apoptosis already starting at 6 weeks of age before changes in cardiac performance occurred. Accordingly, this probe holds important potential for *in vivo* assessment of apoptosis involved in CVDs and can provide valuable insights into early disease detection. Prevention of cardiovascular disease requires early detection and risk stratification before the manifestation of disease.

In conclusion, this is the first study to show that *Ercc1* deficient accelerated aging mice develop cardiac pathology which starts with an *in vivo* gradual increase in MMP activity followed by apoptosis, leading to progressive ventricular enlargement, LV myocardial wall thinning and reduction in cardiac performance. The use of microCT is a valuable imaging modality to establish cardiac function in small animals as well as explore 3D geometric changes throughout the heart. Moreover, combined CT and optical imaging allows simultaneous analysis of molecular and functional changes in mouse models for accelerated aging and hold important potential for early disease detection, exploring disease progression and the assessment of therapeutic effects.

REFERENCES

1. Benjamin EJ, Blaha MJ, Chiuve SE, Cushman M, Das SR, Deo R, de Ferranti SD, Floyd J, Fornage M, Gillespie C, Isasi CR, Jimenez MC, Jordan LC, Judd SE, Lackland D, Lichtman JH, Lisabeth L, Liu S, Longenecker CT, Mackey RH, Matsushita K, Mozaffarian D, Mussolino ME, Nasir K, Neumar RW, Palaniappan L, Pandey DK, Thiagarajan RR, Reeves MJ, Ritchey M, Rodriguez CJ, Roth GA, Rosamond WD, Sasson C, Towfighi A, Tsao CW, Turner MB, Virani SS, Voeks JH, Willey JZ, Wilkins JT, Wu JH, Alger HM, Wong SS, Muntner P, American Heart Association Statistics C, Stroke Statistics S. Heart disease and stroke statistics-2017 update: A report from the american heart association. *Circulation*. 2017;135:e146-e603
2. Niccoli T, Partridge L. Ageing as a risk factor for disease. *Curr Biol*. 2012;22:R741-752
3. Jin K. Modern biological theories of aging. *Aging Dis*. 2010;1:72-74
4. Lopez-Otin C, Blasco MA, Partridge L, Serrano M, Kroemer G. The hallmarks of aging. *Cell*. 2013;153:1194-1217

5. Garinis GA, van der Horst GT, Vijg J, Hoeijmakers JH. DNA damage and ageing: New-age ideas for an age-old problem. *Nat Cell Biol*. 2008;10:1241-1247
6. Vermeij WP, Hoeijmakers JH, Pothof J. Genome integrity in aging: Human syndromes, mouse models, and therapeutic options. *Annu Rev Pharmacol Toxicol*. 2016;56:427-445
7. De Flora S, Izzotti A. Mutagenesis and cardiovascular diseases molecular mechanisms, risk factors, and protective factors. *Mutat Res*. 2007;621:5-17
8. Weeda G, Donker I, de Wit J, Morreau H, Janssens R, Vissers CJ, Nigg A, van Steeg H, Bootsma D, Hoeijmakers JH. Disruption of mouse ercc1 results in a novel repair syndrome with growth failure, nuclear abnormalities and senescence. *Curr Biol*. 1997;7:427-439
9. Niedernhofer LJ, Garinis GA, Raams A, Lalai AS, Robinson AR, Appeldoorn E, Odijk H, Oostendorp R, Ahmad A, van Leeuwen W, Theil AF, Vermeulen W, van der Horst GT, Meinecke P, Kleijer WJ, Vijg J, Jaspers NG, Hoeijmakers JH. A new progeroid syndrome reveals that genotoxic stress suppresses the somatotroph axis. *Nature*. 2006;444:1038-1043
10. Durik M, Kavousi M, van der Pluijm I, Isaacs A, Cheng C, Verdonk K, Loot AE, Oeseburg H, Bhaggoe UM, Leijten F, van Veghel R, de Vries R, Rudez G, Brandt R, Ridwan YR, van Deel ED, de Boer M, Tempel D, Fleming I, Mitchell GF, Verwoert GC, Tarasov KV, Uitterlinden AG, Hofman A, Duckers HJ, van Duijn CM, Oostra BA, Witteman JC, Duncker DJ, Danser AH, Hoeijmakers JH, Roks AJ. Nucleotide excision DNA repair is associated with age-related vascular dysfunction. *Circulation*. 2012;126:468-478
11. North BJ, Sinclair DA. The intersection between aging and cardiovascular disease. *Circ Res*. 2012;110:1097-1108
12. Foo RS, Mani K, Kitsis RN. Death begets failure in the heart. *J Clin Invest*. 2005;115:565-571
13. Haudek SB, Taffet GE, Schneider MD, Mann DL. Tnf provokes cardiomyocyte apoptosis and cardiac remodeling through activation of multiple cell death pathways. *J Clin Invest*. 2007;117:2692-2701
14. Higami Y, Shimokawa I. Apoptosis in the aging process. *Cell Tissue Res*. 2000;301:125-132
15. van Heerde WL, Robert-Offerman S, Dumont E, Hofstra L, Doevendans PA, Smits JF, Daemen MJ, Reutelingsperger CP. Markers of apoptosis in cardiovascular tissues: Focus on annexin v. *Cardiovasc Res*. 2000;45:549-559
16. Watanabe M, Choudhry A, Berlan M, Singal A, Siwik E, Mohr S, Fisher SA. Developmental remodeling and shortening of the cardiac outflow tract involves myocyte programmed cell death. *Development*. 1998;125:3809-3820
17. Dollery CM, McEwan JR, Henney AM. Matrix metalloproteinases and cardiovascular disease. *Circ Res*. 1995;77:863-868
18. Kim HE, Dalal SS, Young E, Legato MJ, Weisfeldt ML, D'Armiento J. Disruption of the myocardial extracellular matrix leads to cardiac dysfunction. *J Clin Invest*. 2000;106:857-866
19. Spinale FG. Myocardial matrix remodeling and the matrix metalloproteinases: Influence on cardiac form and function. *Physiol Rev*. 2007;87:1285-1342
20. Tyagi SC, Campbell SE, Reddy HK, Tjahja E, Voelker DJ. Matrix metalloproteinase activity expression in infarcted, noninfarcted and dilated cardiomyopathic human hearts. *Mol Cell Biochem*. 1996;155:13-21
21. Nagase H, Woessner JF, Jr. Matrix metalloproteinases. *J Biol Chem*. 1999;274:21491-21494
22. Blankenberg S, Rupprecht HJ, Poirier O, Bickel C, Smieja M, Hafner G, Meyer J, Cambien F, Tiret L, AtheroGene I. Plasma concentrations and genetic variation of matrix metalloproteinase 9 and prognosis of patients with cardiovascular disease. *Circulation*. 2003;107:1579-1585

23. Bonnans C, Chou J, Werb Z. Remodelling the extracellular matrix in development and disease. *Nat Rev Mol Cell Biol*. 2014;15:786-801
24. Chiao YA, Ramirez TA, Zamilpa R, Okoronkwo SM, Dai Q, Zhang J, Jin YF, Lindsey ML. Matrix metalloproteinase-9 deletion attenuates myocardial fibrosis and diastolic dysfunction in ageing mice. *Cardiovasc Res*. 2012;96:444-455
25. Halade GV, Jin YF, Lindsey ML. Matrix metalloproteinase (mmp)-9: A proximal biomarker for cardiac remodeling and a distal biomarker for inflammation. *Pharmacol Ther*. 2013;139:32-40
26. Crean AM, Maredia N, Ballard G, Menezes R, Wharton G, Forster J, Greenwood JP, Thomson JD. 3d echo systematically underestimates right ventricular volumes compared to cardiovascular magnetic resonance in adult congenital heart disease patients with moderate or severe rv dilatation. *J Cardiovasc Magn Reson*. 2011;13:78
27. Ho SY, Nihoyannopoulos P. Anatomy, echocardiography, and normal right ventricular dimensions. *Heart*. 2006;92 Suppl 1:i2-13
28. Orwat S, Diller GP, Baumgartner H. Imaging of congenital heart disease in adults: Choice of modalities. *Eur Heart J Cardiovasc Imaging*. 2014;15:6-17
29. Das NM, Hatsell S, Nannuru K, Huang L, Wen X, Wang L, Wang LH, Idone V, Meganck JA, Murphy A, Economides A, Xie L. In vivo quantitative microcomputed tomographic analysis of vasculature and organs in a normal and diseased mouse model. *PLoS One*. 2016;11:e0150085
30. Jaffer FA, Libby P, Weissleder R. Optical and multimodality molecular imaging: Insights into atherosclerosis. *Arterioscler Thromb Vasc Biol*. 2009;29:1017-1024
31. Kaijzel EL, van Heijningen PM, Wielopolski PA, Vermeij M, Koning GA, van Cappellen WA, Que I, Chan A, Dijkstra J, Ramnath NW, Hawinkels LJ, Bernsen MR, Lowik CW, Essers J. Multimodality imaging reveals a gradual increase in matrix metalloproteinase activity at aneurysmal lesions in live fibulin-4 mice. *Circ Cardiovasc Imaging*. 2010;3:567-577
32. Khamis RY, Woollard KJ, Hyde GD, Boyle JJ, Bicknell C, Chang SH, Malik TH, Hara T, Mauskapf A, Granger DW, Johnson JL, Ntziachristos V, Matthews PM, Jaffer FA, Haskard DO. Near infrared fluorescence (nirf) molecular imaging of oxidized ldl with an autoantibody in experimental atherosclerosis. *Sci Rep*. 2016;6:21785
33. Liang G, Vo D, Nguyen P. Fundamentals of cardiovascular molecular imaging: A review of concepts and strategies. *Curr Cardiovasc Imaging Rep*. 2017;10
34. Agah R, Frenkel PA, French BA, Michael LH, Overbeek PA, Schneider MD. Gene recombination in postmitotic cells. Targeted expression of cre recombinase provokes cardiac-restricted, site-specific rearrangement in adult ventricular muscle in vivo. *J Clin Invest*. 1997;100:169-179
35. Kirschner K, Singh R, Prost S, Melton DW. Characterisation of ercc1 deficiency in the liver and in conditional ercc1-deficient primary hepatocytes in vitro. *DNA Repair (Amst)*. 2007;6:304-316
36. Moore RC, Redhead NJ, Selfridge J, Hope J, Manson JC, Melton DW. Double replacement gene targeting for the production of a series of mouse strains with different prion protein gene alterations. *Biotechnology (N Y)*. 1995;13:999-1004
37. Vermeij WP, Dolle ME, Reiling E, Jaarsma D, Payan-Gomez C, Bombardieri CR, Wu H, Roks AJ, Botter SM, van der Eerden BC, Youssef SA, Kuiper RV, Nagarajah B, van Oostrom CT, Brandt RM, Barnhoorn S, Imholz S, Pennings JL, de Bruin A, Gyenis A, Pothof J, Vijg J, van Steeg H, Hoeijmakers JH. Restricted diet delays accelerated ageing and genomic stress in DNA-repair-deficient mice. *Nature*. 2016;537:427-431
38. Houser SR, Margulies KB, Murphy AM, Spinale FG, Francis GS, Prabhu SD, Rockman HA, Kass DA, Molkentin JD, Sussman MA, Koch WJ, American Heart Association Council on Basic

Cardiovascular Sciences CoCC, Council on Functional G, Translational B. Animal models of heart failure: A scientific statement from the american heart association. *Circ Res*. 2012;111:131-150

39. Mirzaei H, Di Biase S, Longo VD. Dietary interventions, cardiovascular aging, and disease: Animal models and human studies. *Circ Res*. 2016;118:1612-1625
40. Coughlin SS, Tefft MC, Rice JC, Gerone JL, Baughman KL. Epidemiology of idiopathic dilated cardiomyopathy in the elderly: Pooled results from two case-control studies. *Am J Epidemiol*. 1996;143:881-888
41. Kono Y, Nakamura K, Kimura H, Nishii N, Watanabe A, Banba K, Miura A, Nagase S, Sakuragi S, Kusano KF, Matsubara H, Ohe T. Elevated levels of oxidative DNA damage in serum and myocardium of patients with heart failure. *Circ J*. 2006;70:1001-1005
42. Li YY, Hengstenberg C, Maisch B. Whole mitochondrial genome amplification reveals basal level multiple deletions in mtdna of patients with dilated cardiomyopathy. *Biochem Biophys Res Commun*. 1995;210:211-218
43. Wang J, Wilhelmsson H, Graff C, Li H, Oldfors A, Rustin P, Bruning JC, Kahn CR, Clayton DA, Barsh GS, Thoren P, Larsson NG. Dilated cardiomyopathy and atrioventricular conduction blocks induced by heart-specific inactivation of mitochondrial DNA gene expression. *Nat Genet*. 1999;21:133-137
44. Zhang D, Mott JL, Farrar P, Ryerse JS, Chang SW, Stevens M, Denniger G, Zassenhaus HP. Mitochondrial DNA mutations activate the mitochondrial apoptotic pathway and cause dilated cardiomyopathy. *Cardiovasc Res*. 2003;57:147-157
45. Dai DF, Rabinovitch PS, Ungvari Z. Mitochondria and cardiovascular aging. *Circ Res*. 2012;110:1109-1124
46. Ishida T, Ishida M, Tashiro S, Yoshizumi M, Kihara Y. Role of DNA damage in cardiovascular disease. *Circ J*. 2014;78:42-50
47. Mondal NK, Sorensen E, Hiivala N, Feller E, Griffith B, Wu ZJ. Oxidative stress, DNA damage and repair in heart failure patients after implantation of continuous flow left ventricular assist devices. *Int J Med Sci*. 2013;10:883-893
48. Shukla PC, Singh KK, Yanagawa B, Teoh H, Verma S. DNA damage repair and cardiovascular diseases. *Can J Cardiol*. 2010;26 Suppl A:13A-16A
49. Tsutsui H, Ide T, Kinugawa S. Mitochondrial oxidative stress, DNA damage, and heart failure. *Antioxid Redox Signal*. 2006;8:1737-1744
50. Dolle ME, Kuiper RV, Roodbergen M, Robinson J, de Vlugt S, Wijnhoven SW, Beems RB, de la Fonteyne L, de With P, van der Pluijm I, Niedernhofer LJ, Hasty P, Vijg J, Hoeijmakers JH, van Steeg H. Broad segmental progeroid changes in short-lived ercc1(-/delta7) mice. *Pathobiol Aging Age Relat Dis*. 2011;1
51. Gregg SQ, Robinson AR, Niedernhofer LJ. Physiological consequences of defects in ercc1-xpf DNA repair endonuclease. *DNA Repair (Amst)*. 2011;10:781-791
52. de Waard MC, van der Pluijm I, Zuiderveen Borgesius N, Comley LH, Haasdijk ED, Rijksen Y, Ridwan Y, Zondag G, Hoeijmakers JH, Elgersma Y, Gillingwater TH, Jaarsma D. Age-related motor neuron degeneration in DNA repair-deficient ercc1 mice. *Acta Neuropathol*. 2010;120:461-475
53. Spoor M, Nagtegaal AP, Ridwan Y, Borgesius NZ, van Alphen B, van der Pluijm I, Hoeijmakers JH, Frens MA, Borst JG. Accelerated loss of hearing and vision in the DNA-repair deficient ercc1(delta/-) mouse. *Mech Ageing Dev*. 2012;133:59-67

54. Gurkar AU, Niedernhofer LJ. Comparison of mice with accelerated aging caused by distinct mechanisms. *Exp Gerontol*. 2015;68:43-50
55. Tsui BM, Kraitchman DL. Recent advances in small-animal cardiovascular imaging. *J Nucl Med*. 2009;50:667-670
56. Badea CT, Fubara B, Hedlund LW, Johnson GA. 4-d micro-ct of the mouse heart. *Mol Imaging*. 2005;4:110-116
57. Drangova M, Ford NL, Detombe SA, Wheatley AR, Holdsworth DW. Fast retrospectively gated quantitative four-dimensional (4d) cardiac micro computed tomography imaging of free-breathing mice. *Invest Radiol*. 2007;42:85-94
58. Ma Y, Chiao YA, Clark R, Flynn ER, Yabluchanskiy A, Ghasemi O, Zouein F, Lindsey ML, Jin YF. Deriving a cardiac ageing signature to reveal mmp-9-dependent inflammatory signalling in senescence. *Cardiovasc Res*. 2015;106:421-431
59. Yabluchanskiy A, Ma Y, Chiao YA, Lopez EF, Voorhees AP, Toba H, Hall ME, Han HC, Lindsey ML, Jin YF. Cardiac aging is initiated by matrix metalloproteinase-9-mediated endothelial dysfunction. *Am J Physiol Heart Circ Physiol*. 2014;306:H1398-1407
60. Bonnema DD, Webb CS, Pennington WR, Stroud RE, Leonardi AE, Clark LL, McClure CD, Finklea L, Spinale FG, Zile MR. Effects of age on plasma matrix metalloproteinases (mmps) and tissue inhibitor of metalloproteinases (timps). *J Card Fail*. 2007;13:530-540
61. Chiao YA, Dai Q, Zhang J, Lin J, Lopez EF, Ahuja SS, Chou YM, Lindsey ML, Jin YF. Multi-analyte profiling reveals matrix metalloproteinase-9 and monocyte chemotactic protein-1 as plasma biomarkers of cardiac aging. *Circ Cardiovasc Genet*. 2011;4:455-462
62. Campisi J. Aging, cellular senescence, and cancer. *Annu Rev Physiol*. 2013;75:685-705
63. Childs BG, Durik M, Baker DJ, van Deursen JM. Cellular senescence in aging and age-related disease: From mechanisms to therapy. *Nat Med*. 2015;21:1424-1435
64. Koda M, Takemura G, Kanoh M, Hayakawa K, Kawase Y, Maruyama R, Li Y, Minatoguchi S, Fujiwara T, Fujiwara H. Myocytes positive for in situ markers for DNA breaks in human hearts which are hypertrophic, but neither failed nor dilated: A manifestation of cardiac hypertrophy rather than failure. *J Pathol*. 2003;199:229-236
65. Olivetti G, Abbi R, Quaini F, Kajstura J, Cheng W, Nitahara JA, Quaini E, Di Loreto C, Beltrami CA, Krajewski S, Reed JC, Anversa P. Apoptosis in the failing human heart. *N Engl J Med*. 1997;336:1131-1141
66. Saraste A, Pulkki K, Kallajoki M, Heikkila P, Laine P, Mattila S, Nieminen MS, Parvinen M, Voipio-Pulkki LM. Cardiomyocyte apoptosis and progression of heart failure to transplantation. *Eur J Clin Invest*. 1999;29:380-386
67. Takemura G, Kanoh M, Minatoguchi S, Fujiwara H. Cardiomyocyte apoptosis in the failing heart--a critical review from definition and classification of cell death. *Int J Cardiol*. 2013;167:2373-2386
68. Kanoh M, Takemura G, Misao J, Hayakawa Y, Aoyama T, Nishigaki K, Noda T, Fujiwara T, Fukuda K, Minatoguchi S, Fujiwara H. Significance of myocytes with positive DNA in situ nick end-labeling (tunel) in hearts with dilated cardiomyopathy: Not apoptosis but DNA repair. *Circulation*. 1999;99:2757-2764

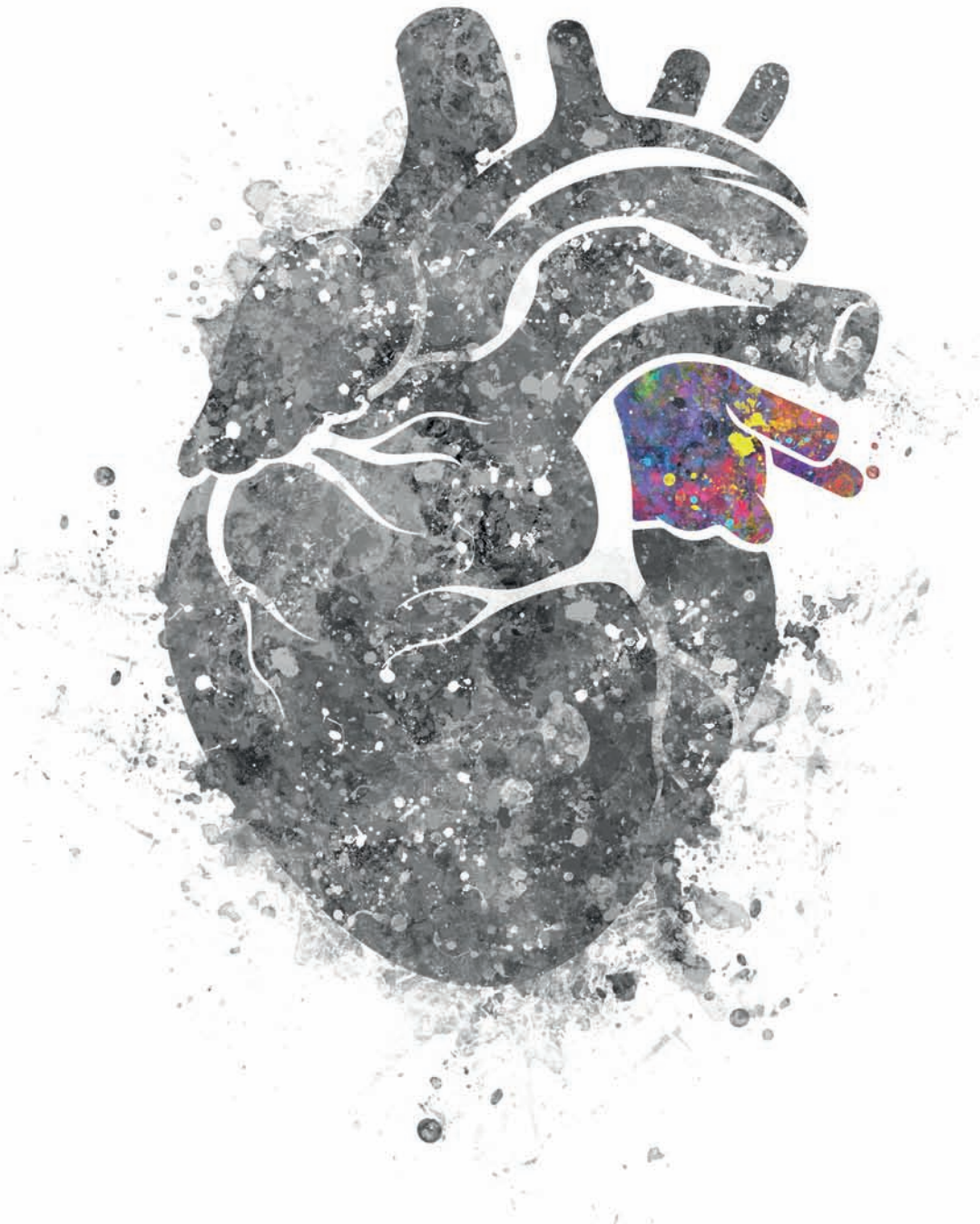

PART IV

THE RENIN-ANGIOTENSIN SYSTEM

CHAPTER 8

IN VIVO RENIN ACTIVITY IMAGING IN THE KIDNEY OF PROGEROID *ERCC1* MUTANT MICE

Bibi S. van Thiel[1,2,3], Yanto Ridwan[1,2], Ingrid. M Garrelds[2], Marcel Vermeij[4], Marian C. Clahsen-van Groningen[4], Fatimunnisa Qadri[6], Natalia Alenina[6,7], Michael Bader[6-10], A. Roks[2], A.H. Jan Danser[2], Jeroen Essers[1,3,5], Ingrid van der Pluijm[1,3]

[1]Department of Molecular Genetics, Cancer Genomics Center Netherlands, [2]Division of Vascular Medicine and Pharmacology, Department of Internal Medicine, [3]Department of Vascular Surgery, [4]Department of Pathology, [5]Department of Radiation Oncology, Erasmus Medical Center, Rotterdam, The Netherlands. [6]Max Delbrück Center, Berlin, Germany; [7]DZHK (German Center for Cardiovascular Research), partner site Berlin, Germany; [8]Berlin Institute of Health (BIH), Berlin, Germany; [9]Charité - University Medicine, Berlin, Germany; [10]Institute for Biology, University of Lübeck, Lübeck, Germany

(Manuscript in preparation)

ABSTRACT

Changes in the renin-angiotensin system, known for its critical role in the regulation of blood pressure and sodium homeostasis, may contribute to aging and age-related diseases. While the systemic renin-angiotensin system is suppressed during aging, little is known about its regulation and activity within tissues. Yet, this knowledge is required to successively treat and/or prevent renal disease in the elderly. In this study, we tested the use of the renin activatable near-infrared fluorescent probe ReninSense680™ to facilitate non-invasive imaging of renin activity *in vivo*. First, we validated the specificity of the probe, by detecting increased intrarenal activity after losartan treatment and the virtual absence of fluorescence in renin knock-out mice. Second, age-related kidney pathology, tubular anisokaryosis, glomerulosclerosis and increased apoptosis was confirmed in kidneys of 12, 18 and 24-week-old *Ercc1*$^{d/-}$ mice, while initial renal development was normal. Next, we examined the *in vivo* renin activity in these *Ercc1*$^{d/-}$ mice. Interestingly, increased intrarenal renin activity was detected by ReninSense in *Ercc1*$^{d/-}$ compared to WT mice, while plasma renin activity was lower. Hence, this study demonstrates that intrarenal RAS activity does not necessarily run in parallel with circulating renin in the aging mouse. In addition, our study supports the use of this probe for longitudinal imaging of altered RAS signaling in aging.

INTRODUCTION

Aging is a natural biological process that is associated with diverse detrimental changes in cells and tissues, ultimately leading to loss of organ function. Progressive deterioration of the renal structure is part of the normal aging process, including loss of renal mass, loss of tubules and increase in the incidence of glomerulosclerosis and tubulointerstitial fibrosis.[1] Besides sclerosis and loss of most of the glomeruli, the remaining glomeruli often exhibit impaired filtration ability. Accordingly, many elderly suffer from a decline in renal function, often shown as a progressive decrease in glomerular filtration rate and renal blood flow. These age-related structural and functional changes may predispose the kidney to acute kidney injury or progressive chronic kidney disease.[2]

The renin-angiotensin system (RAS) has long been recognized for its critical role in the regulation of blood pressure and fluid homeostasis. Changes in the responsiveness and activity of the RAS have been shown to play an important role in aging, as well as in renal disease as it predisposes the elderly to acute kidney injury and chronic kidney disease.[3-7] It is suggested that overexposure to the RAS hormone angiotensin (Ang) II causes DNA damage as well as cellular senescence and/or apoptosis; processes known to play a role in aging and disease.[8, 9] Moreover, interference in the RAS system by using RAS blockers has been proposed to extend lifespan and to prevent age-associated changes.[10] However, not all elderly respond well to RAS blockade and related adverse events include acute kidney injury, hyperkalemia and hypotension.[11, 12] Thus, we need more insight into the regulation of the RAS during aging, in order to successively treat and/or prevent renal disease in the elderly population.

Although Ang II is considered to be the principal effector molecule of the RAS, renin is the rate-limiting enzyme in the cascade and plays an essential role in regulating RAS activity. Several classes of drugs blocking renin activity have been shown to have renoprotective actions.[13] Currently, plasma renin activity is used as the clinical marker for systemic RAS activity, and previous studies have shown that circulating renin is suppressed with advancing age.[7, 14] However, multiple studies reported on the existence of so-called tissue RAS, which may act independently of the systemic RAS.[15] Indeed, RAS components in the kidney did not always change in parallel with RAS components in the circulation.[16] In fact, inappropriate activation of the intrarenal RAS might underlie the pathogenesis of hypertension and renal injury (reviewed within Kobori et al.).[17] Thus, next to systematic plasma renin activity measurements more emphasis should be placed on quantifying tissue RAS activity. As it is difficult to measure tissue RAS components *in vivo*, non-invasive imaging of local renin activity would help to evaluate the possible role of tissue renin activity in disease development and progression. Moreover, the development of new non-invasive imaging methods with the use of near-infrared fluorescent (NIRF) probes could lead to better detection and treatment options in the future.

It has previously been shown that kidneys of the progeroid *Ercc1*$^{d/-}$ mouse model display severe tubular attenuation and degeneration with marked anisokaryosis.[18, 19] Moreover, Schermer et al.[20] showed that age-related transcriptional changes were present in the glomeruli of *Ercc1*$^{d/-}$ mice, thus suggesting that the progeroid *Ercc1*$^{d/-}$ mouse model is a valuable tool to study age-related glomerular pathologies. To investigate age-related changes in the intrarenal RAS *in vivo*, we applied the renin activatable NIRF probe ReninSense680™ allowing non-invasive imaging of renin activity in the progeroid *Ercc1*$^{d/-}$ mouse model.[21]

MATERIAL AND METHODS

All animal experiments were performed under the regulation and permission of the Animal Care Committee, conforming to the Guide for the Care and Use of Laboratory Animals published by the US National Institutes of Health (NIH Publication No. 8523, revised 1985). As required by Dutch law, formal permission to generate and use genetically modified animals was obtained from the responsible local and national authorities (DEC 118-11-05 and DEC 139-12-16).

Experimental animals

Animals used in this study were male and female *Ercc1*$^{d/-}$ mutants and their wild-type *Ercc1*$^{+/+}$ littermates (WT) in an F1 hybrid FVB/N-C57BL/6J background. The generation of nucleotide excision repair-deficient *Ercc1*$^{d/-}$ mice has been previously described.[22] Ren1c homozygous null mice (RenKO; 3 females and 1 male) were generated as described before (C57BL/6J background) and sacrificed at the age of 3-6 months.[23] A separate group of WT mice were divided into two groups, which were either given losartan (100 mg/kg/day) in drinking water, or drinking water only from 5 weeks of age until the age of 12 weeks when the animals were sacrificed.

All mice were housed under standard laboratory conditions (temperature 23±1°C, 12-hour light-dark cycle) and maintained on standard chow (Special Diets Services, Essex, UK) with ad libitum access to water. Since *Ercc1*$^{d/-}$ mice are smaller, water bottles with long nozzles were used and food was administered within the cages from four weeks of age.

In vivo microCT-FMT imaging of renin activity

Ercc1$^{d/-}$ and WT mice, treated with or losartan or placebo, were injected intravenously with ReninSense680™ (2 nmol/100µl per 25 gram bodyweight) (Perkin Elmer Inc., Akron, Ohio, USA) 24 hours post FMT imaging. Mice were anesthetized (1.5-2.5% isoflurane, O_2 1 L/min) and depilated to minimize the interference of fur on the fluorescent signal. To improve detection of intrarenal renin activity, mice were injected with the NIRF probe

Annexin-Vivo750™ (Perkin Elmer Inc.) 2 hours post FMT imaging to visualize the kidneys and/or imaged with the microCT to allow co-registration of anatomical data with the *in vivo* fluorescence. Before FMT imaging, mice were injected in the tail vein with the iodine contrast agent eXIA160 (Binitio Biomedical Inc., Ottawa, Canada) for microCT imaging. Mice were positioned in the animal imaging cassette, restrained to prevent movement during imaging and imaged by using the Quantum FX imaging system (microCT) (Perkin Elmer Inc.). After microCT imaging, mice remained under anesthesia and the cassette was transferred to the FMT 2500 fluorescence tomography *in vivo* imaging system (Perkin Elmer Inc.). FMT imaging was performed using 680 and 700 nm excitation and emission wavelengths, respectively, 24 hours after injection. The multimodal animal imaging cassette facilitates the co-registration of microCT and FMT data through fiducial landmarks. Fusion of microCT and FMT images was done using the TrueQuant 4.0 software (Perkin Elmer Inc.). The position of the kidney was determined by the accumulation of the fluorescence of Annexin-Vivo750™ in the kidney and/or based on the distribution of the iodine contrast visualized with the microCT, which allowed quantification of *in vivo* fluorescence of ReninSense680™.

Tissue collection and *ex vivo* fluorescent imaging of excised kidneys

Mice were euthanized after *in vivo* microCT-FMT imaging by isoflurane overdose. Blood samples were harvested by cardiac puncture, transferred to EDTA coagulation vials and centrifuged at 4600 rpm for 10 minutes to collect plasma. Next, kidneys were excised, emersion fixated in formalin and assessed for *ex vivo* tissue epifluorecence using the FMT system and the Odyssey® CLx imaging system (LI-COR® Biosciences, Lincoln, Nebraska, USA). A separate group of *Ercc1*$^{d/-}$ and WT mice were sacrificed, kidneys were excised, snap frozen in liquid nitrogen and stored at -80°C.

In vitro fluorescent imaging of kidney and plasma renin activity

Activation of ReninSense680™ was determined in plasma (pooled plasma from C57Bl/6J mice, GeneTex, Irvine, CA, USA) and kidney lysates. Frozen kidneys of 2 WT and 4 RenKO mice were homogenised in PBS using mortar-pestle method. Protein concentration was determined using a Pierce BCA Protein Assay kit (Thermo Fisher Scientific, Rockford, IL, USA). Samples were pre-incubated in the presence or absence of different concentrations of the renin inhibitor aliskiren (10^{-11} – 10^{-4} M) at 37°C for 30 minutes. Next, tissue fluorescence was assessed by incubation of plasma or kidney lysates with ReninSense680™ (end concentration 0.2 pmol/µl) at 37°C in a humidified incubator for 30 hours. Fluorescence was measured using the Odyssey® CLx imaging system (excitation settings 700 nm). For background subtraction, kidney lysates of RenKO mice together with denatured kidney and plasma lysates (by heating the sample for 10 min at 70°C) were incubated with and without ReninSense680™.

Plasma renin concentration measured by enzyme-kinetic assay

To determine the plasma renin concentration, Ang I generation was quantified in the presence of excess sheep angiotensinogen.[24, 25]

Histological assessment

Emersion fixated kidneys were embedded in paraffin, sectioned at 5 µm, and mounted on Superfrost Plus slides. Cross-sections of the whole kidney including the cortex and medulla were stained for haematoxylin and eosin (HE), Periodic acid-Schiff stain (PAS), Jones 2 and terminal deoxynucleotidyl transferase-mediated dUTP nick end labelling (TUNEL). The number of TUNEL-positive cells in the kidney was determined using 40x magnification.

Urine measurements relevant to renal function

Urine was collected and urinary protein, creatinine and urea level were measured according to supplier instructions with Pierce BCA Protein Assay kit (Thermo Fisher Scientific, Rockford, IL, USA), QuantiChrome Creatinine Assay Kit (Gentaur, Brussels, Belgium) and QuantiChrome Urea Assay Kit (Gentaur, Brussels, Belgium), respectively.

Statistical analysis

Data are expressed as the mean±SEM. Differences between groups were evaluated by Student's t-test or ANOVA, and corrected for multiple testing by post-hoc Bonferroni analysis when needed. $P<0.05$ was considered significant. All analyses were performed using IBM SPSS Statistics version 20.0 (SPSS Inc., Chicago, IL, USA).

RESULTS

Progeroid *Ercc1*$^{d/-}$ mice display age-related kidney pathology

We first set out to confirm the age-related kidney pathology in *Ercc1*$^{d/-}$ mice, for which we examined kidneys of 12 and 18-week-old mice. Indeed, from 12 weeks onwards *Ercc1*$^{d/-}$ mice display progressive kidney pathology including tubular degeneration and anisokaryosis (Fig. 1a). In addition, they present with signs of kidney aging, shown by reduced proliferation (data not shown) and increased apoptosis (Fig. 1b) already at 12 weeks of age, which was even more pronounced at 18 weeks. Moreover, at 18 weeks of age, hyaline proteinaceous casts were present within the lumen of the tubules in kidneys of *Ercc1*$^{d/-}$ mice. Renal development of *Ercc1*$^{d/-}$ kidneys was found to be normal, as 12-week-old animals had normal kidney architecture including normal numbers of glomeruli (Fig. 1c). To rule out significant renal dysfunction due to the observed pathology, we confirmed that urinary

albumin, creatinine and urea levels were unaltered in *Ercc1*$^{d/-}$ mice compared to WT mice (Fig. 2a-c).

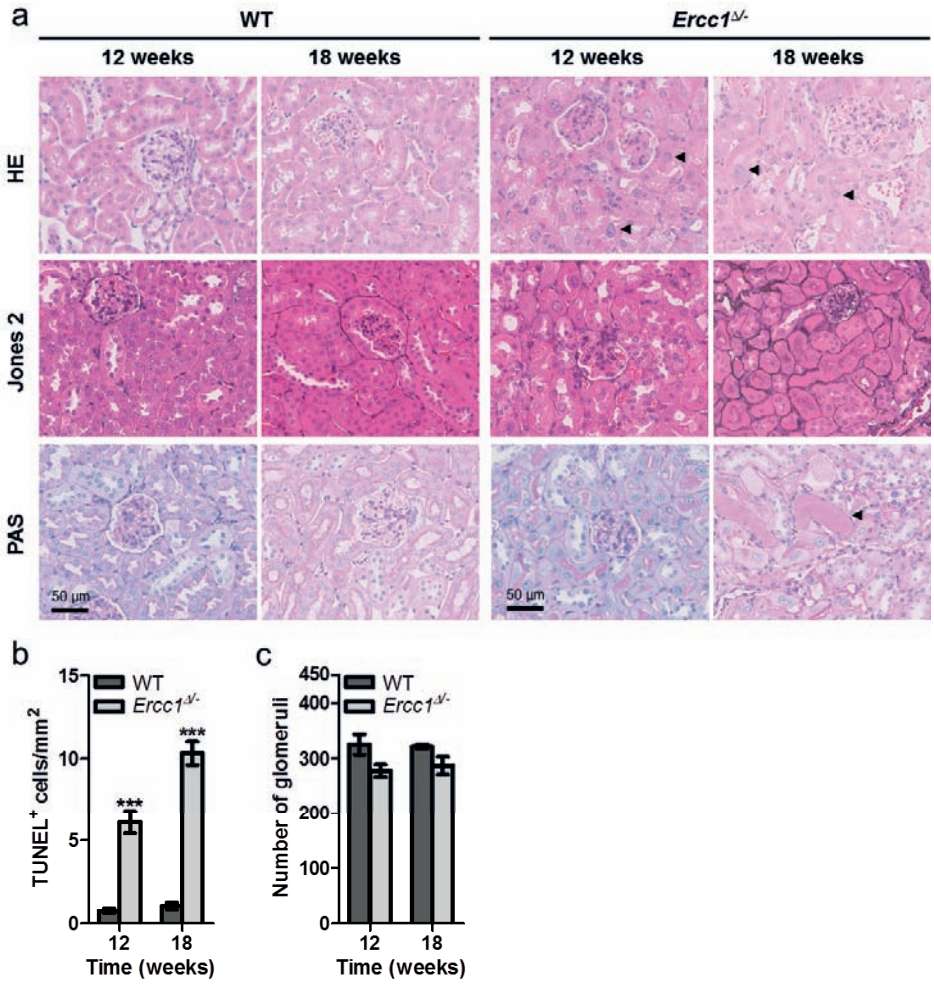

Figure 1. Histopathological changes in the kidney of progeroid *Ercc1*$^{d/-}$ mice. a. Haematoxylin and eosin (HE), Periodic acid-Schiff stain (PAS) and Jones 2 staining of the kidneys of 12 and 18-week-old *Ercc1*$^{d/-}$ mice and their wild-type (WT) littermates. Histological examination showed signs of kidney aging in *Ercc1*$^{d/-}$, including anisokaryosis, tubular degeneration and glomerulosclerosis. Moreover, hyaline proteinaceous casts were found within the lumen of the tubules in kidneys of *Ercc1*$^{d/-}$ mice at 18 weeks of age (indicated by the arrow in PAS staining). In all panels, scale bar = 50µm. b. TUNEL staining indicated increased apoptotic cell death in *Ercc1*$^{d/-}$ kidneys. c. The number of glomeruli confirmed normal kidney development from birth in *Ercc1*$^{d/-}$. $^{***}P<0.01$ vs. WT.

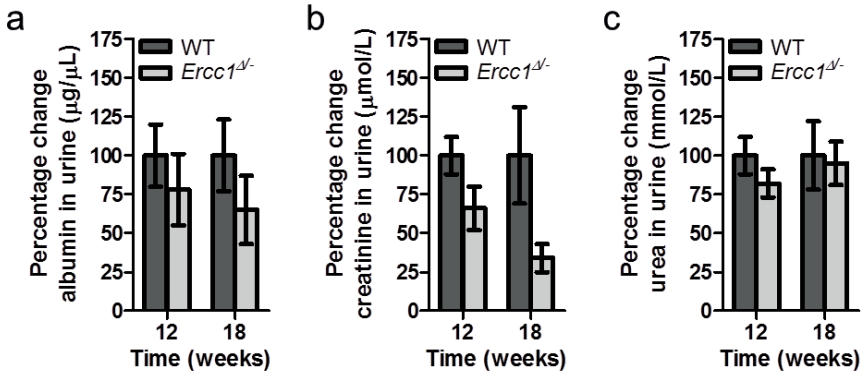

Figure 2. Functional renal changes in progeroid *Ercc1*$^{d/-}$ mice. Urinary albumin (a), creatinine (b) and urea (c) was unaltered in *Ercc1*$^{d/-}$ mice compared to WT mice at 12 and 18 weeks of age.

ReninSense selectively detects renin activity in the kidney *in vitro*

To assess the ability of ReninSense680™ to detect both kidney and plasma renin, activation of ReninSense was tested in kidney lysates and plasma from WT and Ren1c homozygous null (RenKO) mice, with and without co-incubation of the renin inhibitor aliskiren. As expected, ReninSense was rapidly activated in kidney lysates of WT mice assessed by fluorescent measurements with the odyssey system. The microplate kidney extract fluorescent assay showed <5% variation between duplicate wells. Aliskiren blocked ReninSense activation in a concentration-dependent manner by maximally ≈80% (Fig. 3a). The half maximal inhibitory concentration (IC50) for aliskiren in kidney lysates was approximately $10^{-7.7}$ M as measured here with the ReninSense probe (Fig. 3b), i.e. close to the IC50 reported earlier for mouse renin.[26] The remaining fluorescent signal in the presence of the highest concentration of aliskiren was comparable to the fluorescence seen in kidney extracts from RenKO mice and denatured kidneys, indicating that this is the background fluorescent level of the ReninSense probe, in other words the detection limit of this system. When evaluating the ReninSense probe in mouse plasma, fluorescence levels remained in this background range and were unaffected by aliskiren, indicating that the probe cannot be used to measure renin activity in plasma using the odyssey system.

In vivo imaging of renin upregulation shown by ReninSense

To address the ability of ReninSense to be cleaved and used as a readout for *in vivo* renin activity, ReninSense activation was examined in WT mice treated either with vehicle or with the AT_1 receptor antagonist losartan, which is known to increase renin levels. In addition, ReninSense activation was measured in RenKO mice. Animals were imaged tomographically by FMT 2500 24 h after ReninSense injection. To improve detection of intrarenal renin activity, mice were injected with the NIRF probe Annexin-Vivo750™ to visualize the kidneys

and, when possible, also imaged with the microCT to allow co-registration of anatomical data with the *in vivo* fluorescence (Fig. 4a). Losartan-treated mice showed increased *in vivo* (Fig. 4b) and *ex vivo* (Fig. 4c) activation of ReninSense in their kidneys compared to vehicle treated mice. The increase in renin activity after losartan treatment was validated by quantification of the *in vivo* results (Fig. 4d), increased plasma renin activity (Fig. 4e) and increased renin expression levels in the kidney (Fig. 4f). As expected, fluorescence of ReninSense could not be detected *in vivo* or *ex vivo* in RenKO mice, which do not express the renin gene. These results validate the specificity of the ReninSense probe for renin activity.

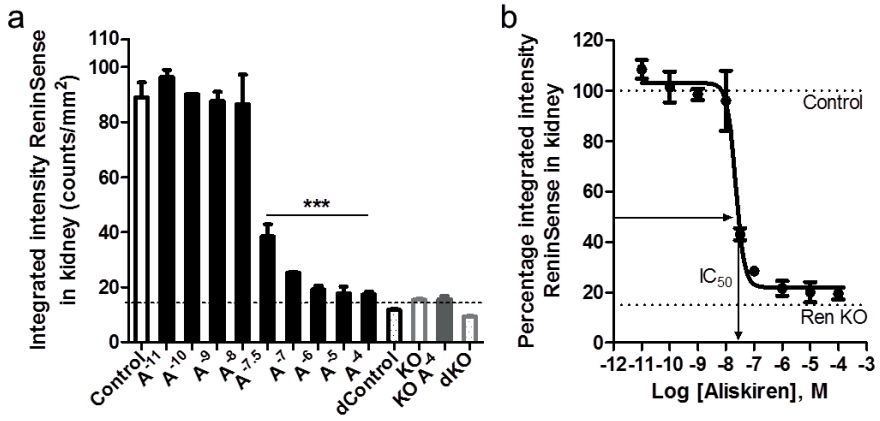

Figure 3. Specific *in vitro* enzymatic activation of ReninSense by kidney and plasma renin. a. ReninSense was rapidly activated by kidney renin in WT mice. Low levels of fluorescence were found in RenKO kidney lysates comparable to autofluorescence of the probe. High concentrations of aliskiren completely blocked ReninSense activation. b. The half maximal inhibitory concentration (IC50) for aliskiren in kidney lysates was $10^{-7.7}$ M. Data are mean±SEM of duplicate samples. $^{***}P<0.01$ vs. control.

8

Increased renin activity in the kidney of progeroid *Ercc1*$^{d/-}$ mice *in vivo*

While it is generally accepted that circulating renin activity is suppressed during aging, little is known about the regulation and activity of renin within tissues with increasing age. In order to investigate *in vivo* kidney renin activity during aging, we injected progeroid *Ercc1*$^{d/-}$ mice and their WT littermates with ReninSense. Combined microCT and FMT imaging of ReninSense showed increased *in vivo* intrarenal renin activity in *Ercc1*$^{d/-}$ mice compared to WT mice already from 12 weeks of age onwards, which was significantly different at 24 weeks of age (Fig. 5a and b). Quantification of the *in vivo* fluorescence (Fig. 5b) and *ex vivo* imaging of the kidneys (Fig. 5c) confirmed these results. We found no differences in *in vivo* renin activity between male and female mice (data not shown). Remarkably, plasma renin activity in the *Ercc1*$^{d/-}$ mice was significantly lower compared to WT mice at 24 weeks of age (Fig. 5d), while normal plasma renin activity levels were found at 6 weeks of age.

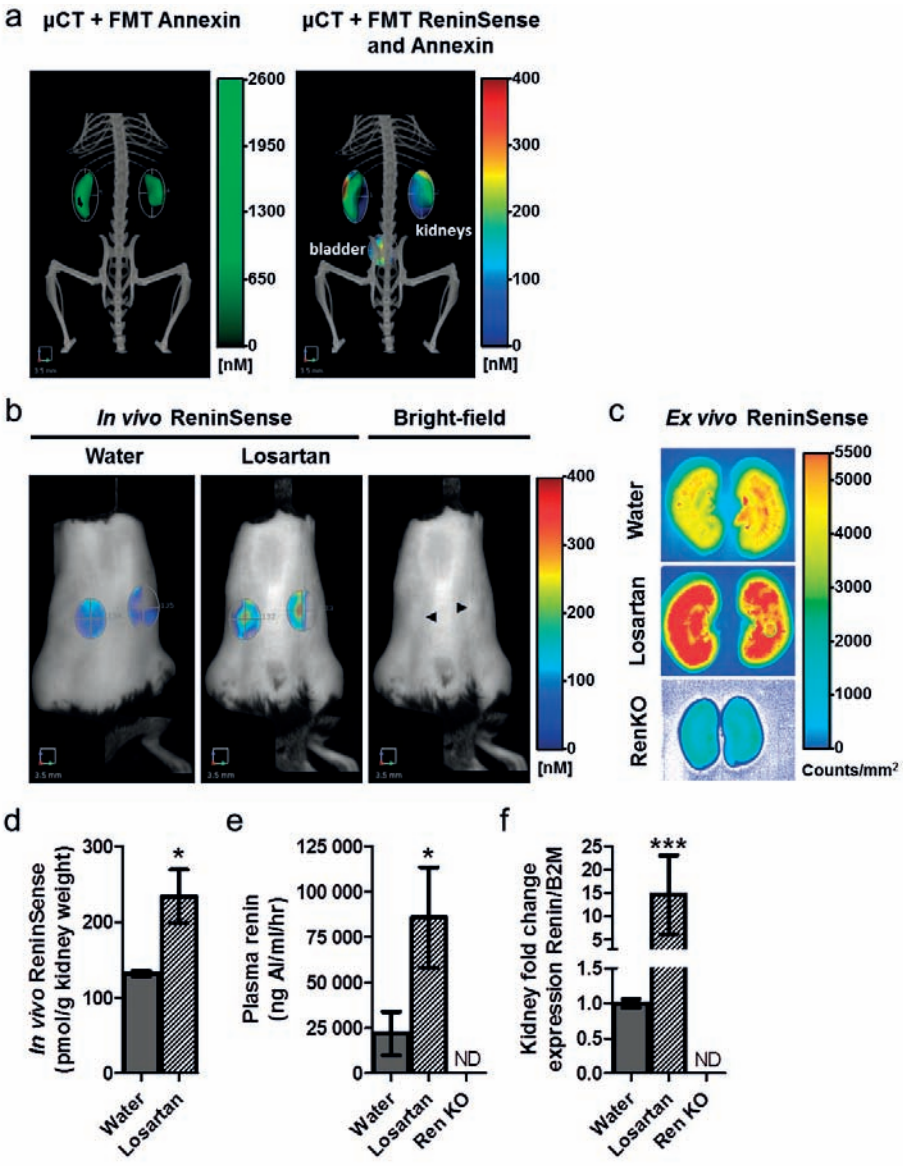

Figure 4. *In vivo* activation of ReninSense in kidneys of WT mice, with and without losartan treatment. a. Mice were imaged tomographically by FMT 2500 and microCT 24 h after ReninSense injection. Micro CT imaging and FMT imaging of Annexin-Vivo allowed accurate localization of the kidneys. Combined microCT and FMT imaging of Annexin-Vivo and ReninSense showed *in vivo* renin activity in the kidneys and bladder (clearance of probe). b. Losartan-treated mice showed increased *in vivo* intrarenal renin activity, which was confirmed by quantification (c). d. *Ex vivo* imaging of the kidneys by the Odyssey® system confirmed activation of the ReninSense probe in losartan-treated mice. Fluorescence of Renin-Sense could not be detected *in vivo* of *ex vivo* in RenKO mice. e. Losartan treatment increased plasma renin activity. f. Increased expression levels of renin in the kidney were found in losartan-treated mice. ND, not detectable. Data are mean±SEM of n=3. $^{*}P<0.05$, $^{***}P<0.01$ vs. WT.

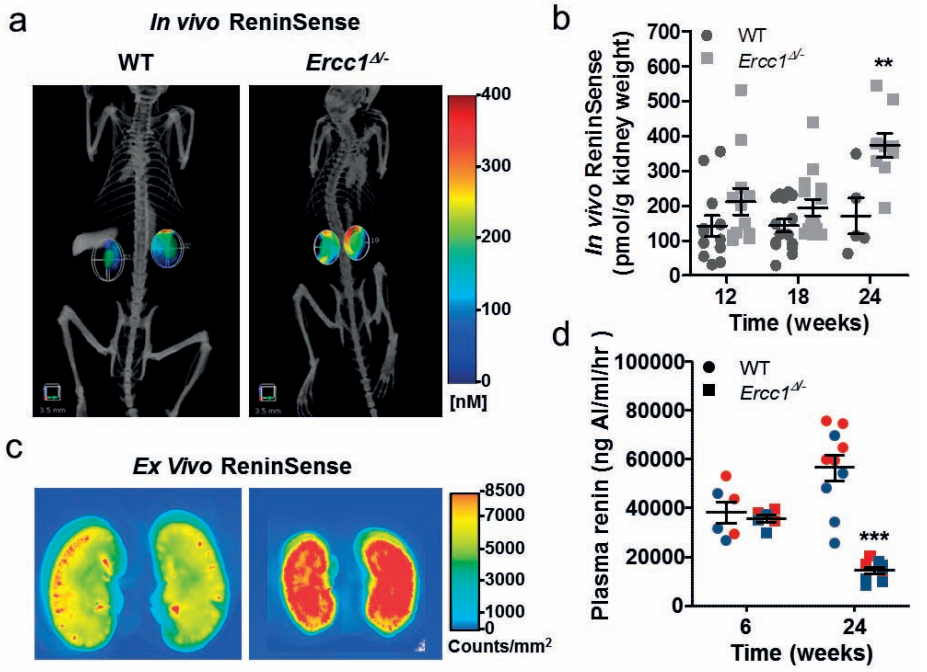

Figure 5. *In vivo* imaging of renin activity by ReninSense in progeroid *Ercc1*$^{d/-}$ mice. a. *Ercc1*$^{d/-}$ mice display activated intrarenal renin activity at 24 weeks of age, as evidenced by increased fluorescence detected with the ReninSense probe when imaged with the microCT and FMT. b. Quantification of the *in vivo* fluorescence of ReninSense confirmed increased renin activity in the kidney which was significantly different at 24 weeks of age. c. These results were further confirmed by *ex vivo* by imaging of the kidneys with the Odyssey® system. d. Plasma renin activity measurements showed that *Ercc1*$^{d/-}$ mice (squares) tended to have lower plasma renin activity levels compared to WT mice (circles), which was significantly lower at 24 weeks of age. No difference in *in vivo* renin activity was observed between male (blue) and female (red) mice. Data are mean±SEM of n=6-12. Differences were assessed by one-way ANOVA, followed by correction for multiple testing by post-hoc Bonferroni analysis. $^{**}P<0.01$, $^{***}P<0.01$ vs. WT.

DISCUSSION

Changes in the RAS are associated with the pathophysiology of various cardiovascular and renal diseases, and therefore targeting the RAS seems a logical therapeutic approach in treatment of these diseases. Indeed, pharmacological RAS blockade has been shown to effectively slow down the progression of renal disease. However, it is important to note that not all patients, e.g. elderly, respond well to RAS blockade. While the systemic RAS is suppressed with advancing age, the regulation and activity of tissue RAS during aging is not well defined. As such, previous reports showed that although the circulating RAS is suppressed during normal aging, some components of the intrarenal RAS are elevated.[3, 16, 17, 27-29] Varying tissue RAS activity might, at least in part, explain why elderly respond

unpredictable to RAS blockade. Therefore, in this study we aimed to evaluate the use of the renin activatable near-infrared fluorescent probe ReninSense to facilitate non-invasive imaging of renin activity *in vivo*. In addition, we investigated the activity of plasma as well as intrarenal renin in progeroid *Ercc1*$^{d/-}$ mice with accompanying age-related kidney pathology. First, we showed that ReninSense specifically detects renin activity, as fluorescence of the probe was increased after losartan treatment, while virtually no fluorescence could be detected in RenKO mice. Secondly, this study demonstrated that intrarenal renin activity does not necessarily run in parallel with circulating renin in the progeroid aging *Ercc1*$^{d/-}$ mice.

It is important to note that most of the clinical studies supporting the beneficial effects of RAS inhibition do not include participants older than 75 years of age or elderly patients that are frail with a high comorbidity burden.[30, 31] Not all elderly respond well to RAS blockade, and related adverse events include acute kidney injury, hyperkalemia, hypotension and a further decline in glomerular filtration rate.[3, 11, 12, 32, 33] Additionally, combination therapy with ACE inhibitors and angiotensin receptor blockers in patients with cardiovascular complications is linked to an increased risk of adverse renal outcomes with higher rates of hyperkalemia, hypotension, renal dysfunction and no observed benefit with respect to overall mortality.[34-37] The occurrence of these side effects might be worse in the elderly population, as they are prone to develop acute kidney injury and hyperkalemia due to the risk of complete RAS inhibition as they already have low plasma renin levels. Therefore, caution and close monitoring are recommended when using these drugs in elderly patients with kidney dysfunction and the optimal RAS inhibition with respect to end organ protection has yet to be determined in the elderly.[38] In this respect, it would be interesting to see how RAS inhibition would affect the aging kidney alone. In other words, study the effect of RAS inhibition in kidney-specific *Ercc1* mutant mice, which would represent a healthy mouse with aging kidneys. This might answer important questions on how the RAS is regulated in the aging kidney, and whether this is a systemic effect or not.

Controversy remains as to whether all RAS components that are required to generate Ang II locally are produced locally, or are taken up from the circulation.[15, 39, 40] In the present study, the opposing findings on intrarenal and plasma renin in progeroid *Ercc1*$^{d/-}$ mice supports an independent upregulation of intrarenal RAS. This might be very similar in the elderly as their circulating renin is lower with increasing age.[7, 14] It remains to be seen whether kidney renin levels are increased with age in the elderly population. Interestingly, low plasma renin levels with increased kidney renin levels have also been found in diabetic patients.[13, 41] Animal models of early diabetic nephropathy identically showed decreased plasma renin activity and increases in kidney renin.[42-45] Epidemiologic studies showed that with age, the incidence and susceptibility of abnormal glucose levels and diabetic disease increases, however the mechanisms linking aging and diabetes are not well understood.[46, 47] It is suggested that increased intrarenal renin is responsible for the

development and progression of nephropathy in diabetes, through increased intrarenal AT_1 receptor signaling.[17, 42] Therefore, it would be interesting to investigate whether diabetes is responsible for this increased intrarenal renin and accompanying kidney injury, or rather that this increased intrarenal RAS, like diabetes, is in fact an concomitant result of the aging process.[41]

As the circulating RAS does not necessarily reveal the responsiveness of the RAS within tissues, there is a need for reliable methods to assess the RAS within tissues. Whether urinary angiotensinogen reflects intrarenal RAS activity is doubtful.[48-50] In addition, renal plasma flow responses to infused Ang II are used as an indirect measure of intrarenal RAS activation in humans, as it correlates inversely with endogenous RAS activity.[51-55] However, all these methods are indirect measurements of intrarenal RAS activity and currently there is no method to directly assess intrarenal RAS activity in humans. Thus, non-invasive imaging of the ReninSense probe holds considerable promise to improve the detection and localization of local renin activity, including intrarenal renin. Determining local renin activity would help to evaluate the complexity of RAS biology and the possible role of local renin activity in disease development and progression. Moreover, this method enables longitudinal imaging of altered RAS signaling, consequently, disease progression can be monitored over time and the effect of (new) interventions can be studied non-invasively.
In the present study, the fluorescence levels of the ReninSense probe in mouse plasma remained in the background range and were unaffected by aliskiren, indicating that the probe cannot be used to measure renin activity with the odyssey system. These results are consistent with the results demonstrated by Zhang et al., as ReninSense fluorescence in mouse plasma in their hands was also unaffected by renin inhibition.[21] Only when mice were treated with low salt diet, ReninSense fluorescence increased over time and L-810 treatment in these mice reduced the fluorescence to a level similar to the fluorescence levels in untreated mouse plasma, indicating that these measured fluorescence in normal mouse plasma actually represented background. We did however, observe that ReninSense was rapidly activated in kidney lysates of WT mice and that aliskiren blocked ReninSense activation by maximally ≈80%. The remaining fluorescent signal in the presence of the highest concentration of aliskiren was comparable to the fluorescence seen in kidney extracts from RenKO mice and denatured kidneys. This implies that the remaining fluorescent signal either represents the background fluorescent level of the ReninSense probe, or represents activation of the probe ReninSense by renin-like enzyme (e.g. cathepsins), which might also be capable of reacting with the angiotensinogen sequence of the probe. Nevertheless, when comparing *in vivo* and *ex vivo* kidney activation of ReninSense in RenKO mice, fluorescence did not reach the threshold value an thus could not be detected, while losartan significantly increased kidney fluorescence levels *in vivo* as well as *ex vivo*, verifying the specificity of the probe to measure renin activity in the kidneys of small animals.

In conclusion, we have demonstrated that the NIRF probe ReninSense can be used to non-invasively visualize and measure intrarenal renin activity. By using this method to identify local RAS activity, we might gain important insights into the changes in the RAS that occur with age as well as in other (age-related) diseases. Although further study is warranted, our observations in the progeroid *Ercc1*$^{d/-}$ mouse model provide evidence that circulating RAS activity does not necessarily run in parallel with intrarenal RAS activity during aging, which has important clinical consequences. As this increased intrarenal RAS activity, might contribute to the disturbed kidney pathology observed in these mice, future investigations should examine the effect of the observed age-dependent changes in intrarenal renin activity on kidney deterioration.

REFERENCES

1. Zhou XJ, Rakheja D, Yu X, Saxena R, Vaziri ND, Silva FG. The aging kidney. *Kidney Int*. 2008;74:710-720
2. Weinstein JR, Anderson S. The aging kidney: Physiological changes. *Adv Chronic Kidney Dis*. 2010;17:302-307
3. Anderson S. Ageing and the renin-angiotensin system. *Nephrol Dial Transplant*. 1997;12:1093-1094
4. Conti S, Cassis P, Benigni A. Aging and the renin-angiotensin system. *Hypertension*. 2012;60:878-883
5. Remuzzi G, Perico N, Macia M, Ruggenenti P. The role of renin-angiotensin-aldosterone system in the progression of chronic kidney disease. *Kidney Int Suppl*. 2005:S57-65
6. Rodriguez-Romo R, Benitez K, Barrera-Chimal J, Perez-Villalva R, Gomez A, Aguilar-Leon D, Rangel-Santiago JF, Huerta S, Gamba G, Uribe N, Bobadilla NA. At1 receptor antagonism before ischemia prevents the transition of acute kidney injury to chronic kidney disease. *Kidney International*. 2016;89:363-373
7. Weidmann P, De Myttenaere-Bursztein S, Maxwell MH, de Lima J. Effect on aging on plasma renin and aldosterone in normal man. *Kidney Int*. 1975;8:325-333
8. Dimmeler S, Rippmann V, Weiland U, Haendeler J, Zeiher AM. Angiotensin ii induces apoptosis of human endothelial cells. Protective effect of nitric oxide. *Circ Res*. 1997;81:970-976
9. Herbert KE, Mistry Y, Hastings R, Poolman T, Niklason L, Williams B. Angiotensin ii-mediated oxidative DNA damage accelerates cellular senescence in cultured human vascular smooth muscle cells via telomere-dependent and independent pathways. *Circ Res*. 2008;102:201-208
10. de Cavanagh EM, Piotrkowski B, Basso N, Stella I, Inserra F, Ferder L, Fraga CG. Enalapril and losartan attenuate mitochondrial dysfunction in aged rats. *FASEB J*. 2003;17:1096-1098
11. Turgut F, Balogun RA, Abdel-Rahman EM. Renin-angiotensin-aldosterone system blockade effects on the kidney in the elderly: Benefits and limitations. *Clin J Am Soc Nephrol*. 2010;5:1330-1339
12. Yoon HE, Choi BS. The renin-angiotensin system and aging in the kidney. *Korean J Intern Med*. 2014;29:291-295

13. Hollenberg NK, Fisher ND, Nussberger J, Moukarbel GV, Barkoudah E, Danser AH. Renal responses to three types of renin-angiotensin system blockers in patients with diabetes mellitus on a high-salt diet: A need for higher doses in diabetic patients? *J Hypertens*. 2011;29:2454-2461
14. Messerli FH, Sundgaard-Riise K, Ventura HO, Dunn FG, Glade LB, Frohlich ED. Essential hypertension in the elderly: Haemodynamics, intravascular volume, plasma renin activity, and circulating catecholamine levels. *Lancet*. 1983;2:983-986
15. Gibbons GH. The pathophysiology of hypertension: The importance of angiotensin ii in cardiovascular remodeling. *Am J Hypertens*. 1998;11:177S-181S
16. Navar LG, Imig JD, Zou L, Wang CT. Intrarenal production of angiotensin ii. *Semin Nephrol*. 1997;17:412-422
17. Kobori H, Nangaku M, Navar LG, Nishiyama A. The intrarenal renin-angiotensin system: From physiology to the pathobiology of hypertension and kidney disease. *Pharmacol Rev*. 2007;59:251-287
18. Vermeij WP, Hoeijmakers JH, Pothof J. Genome integrity in aging: Human syndromes, mouse models, and therapeutic options. *Annu Rev Pharmacol Toxicol*. 2016;56:427-445
19. Dolle ME, Kuiper RV, Roodbergen M, Robinson J, de Vlugt S, Wijnhoven SW, Beems RB, de la Fonteyne L, de With P, van der Pluijm I, Niedernhofer LJ, Hasty P, Vijg J, Hoeijmakers JH, van Steeg H. Broad segmental progeroid changes in short-lived ercc1(-/delta7) mice. *Pathobiol Aging Age Relat Dis*. 2011;1
20. Schermer B, Bartels V, Frommolt P, Habermann B, Braun F, Schultze JL, Roodbergen M, Hoeijmakers JH, Schumacher B, Nurnberg P, Dolle ME, Benzing T, Muller RU, Kurschat CE. Transcriptional profiling reveals progeroid ercc1(-/delta) mice as a model system for glomerular aging. *BMC Genomics*. 2013;14:559
21. Zhang J, Preda DV, Vasquez KO, Morin J, Delaney J, Bao B, Percival MD, Xu D, McKay D, Klimas M, Bednar B, Sur C, Gao DZ, Madden K, Yared W, Rajopadhye M, Peterson JD. A fluorogenic near-infrared imaging agent for quantifying plasma and local tissue renin activity in vivo and ex vivo. *Am J Physiol Renal Physiol*. 2012;303:F593-603
22. Weeda G, Donker I, de Wit J, Morreau H, Janssens R, Vissers CJ, Nigg A, van Steeg H, Bootsma D, Hoeijmakers JH. Disruption of mouse ercc1 results in a novel repair syndrome with growth failure, nuclear abnormalities and senescence. *Curr Biol*. 1997;7:427-439
23. Takahashi N, Lopez ML, Cowhig JE, Jr., Taylor MA, Hatada T, Riggs E, Lee G, Gomez RA, Kim HS, Smithies O. Ren1c homozygous null mice are hypotensive and polyuric, but heterozygotes are indistinguishable from wild-type. *J Am Soc Nephrol*. 2005;16:125-132
24. Danser AH, van Kesteren CA, Bax WA, Tavenier M, Derkx FH, Saxena PR, Schalekamp MA. Prorenin, renin, angiotensinogen, and angiotensin-converting enzyme in normal and failing human hearts. Evidence for renin binding. *Circulation*. 1997;96:220-226
25. Fraune C, Lange S, Krebs C, Holzel A, Baucke J, Divac N, Schwedhelm E, Streichert T, Velden J, Garrelds IM, Danser AH, Frenay AR, van Goor H, Jankowski V, Stahl R, Nguyen G, Wenzel UO. At1 antagonism and renin inhibition in mice: Pivotal role of targeting angiotensin ii in chronic kidney disease. *Am J Physiol Renal Physiol*. 2012;303:F1037-1048
26. Feldman DL, Jin L, Xuan H, Contrepas A, Zhou Y, Webb RL, Mueller DN, Feldt S, Cumin F, Maniara W, Persohn E, Schuetz H, Jan Danser AH, Nguyen G. Effects of aliskiren on blood pressure, albuminuria, and (pro)renin receptor expression in diabetic tg(mren-2)27 rats. *Hypertension*. 2008;52:130-136
27. Campbell DJ, Lawrence AC, Towrie A, Kladis A, Valentijn AJ. Differential regulation of angiotensin peptide levels in plasma and kidney of the rat. *Hypertension*. 1991;18:763-773

28. Gilliam-Davis S, Payne VS, Kasper SO, Tommasi EN, Robbins ME, Diz DI. Long-term at1 receptor blockade improves metabolic function and provides renoprotection in fischer-344 rats. *Am J Physiol Heart Circ Physiol*. 2007;293:H1327-1333
29. Thompson MM, Oyama TT, Kelly FJ, Kennefick TM, Anderson S. Activity and responsiveness of the renin-angiotensin system in the aging rat. *Am J Physiol Regul Integr Comp Physiol*. 2000;279:R1787-1794
30. Sarafidis PA, Bakris GL. Does evidence support renin-angiotensin system blockade for slowing nephropathy progression in elderly persons? *Ann Intern Med*. 2009;150:731-733
31. Suzuki H, Kikuta T, Inoue T, Hamada U. Time to re-evaluate effects of renin-angiotensin system inhibitors on renal and cardiovascular outcomes in diabetic nephropathy. *World J Nephrol*. 2015;4:118-126
32. Ahmed AK, Kamath NS, El Kossi M, El Nahas AM. The impact of stopping inhibitors of the renin-angiotensin system in patients with advanced chronic kidney disease. *Nephrol Dial Transplant*. 2010;25:3977-3982
33. Chaumont M, Pourcelet A, van Nuffelen M, Racape J, Leeman M, Hougardy JM. Acute kidney injury in elderly patients with chronic kidney disease: Do angiotensin-converting enzyme inhibitors carry a risk? *J Clin Hypertens (Greenwich)*. 2016;18:514-521
34. Kuenzli A, Bucher HC, Anand I, Arutiunov G, Kum LC, McKelvie R, Afzal R, White M, Nordmann AJ. Meta-analysis of combined therapy with angiotensin receptor antagonists versus ace inhibitors alone in patients with heart failure. *PLoS One*. 2010;5:e9946
35. Mallat SG. Dual renin-angiotensin system inhibition for prevention of renal and cardiovascular events: Do the latest trials challenge existing evidence? *Cardiovasc Diabetol*. 2013;12:108
36. McAlister FA, Zhang J, Tonelli M, Klarenbach S, Manns BJ, Hemmelgarn BR, Alberta Kidney Disease N. The safety of combining angiotensin-converting-enzyme inhibitors with angiotensin-receptor blockers in elderly patients: A population-based longitudinal analysis. *CMAJ*. 2011;183:655-662
37. Phillips CO, Kashani A, Ko DK, Francis G, Krumholz HM. Adverse effects of combination angiotensin ii receptor blockers plus angiotensin-converting enzyme inhibitors for left ventricular dysfunction: A quantitative review of data from randomized clinical trials. *Arch Intern Med*. 2007;167:1930-1936
38. Aronow WS, Fleg JL, Pepine CJ, Artinian NT, Bakris G, Brown AS, Ferdinand KC, Forciea MA, Frishman WH, Jaigobin C, Kostis JB, Mancia G, Oparil S, Ortiz E, Reisin E, Rich MW, Schocken DD, Weber MA, Wesley DJ, Harrington RA, Force AT. Accf/aha 2011 expert consensus document on hypertension in the elderly: A report of the american college of cardiology foundation task force on clinical expert consensus documents. *Circulation*. 2011;123:2434-2506
39. Bader M, Ganten D. Update on tissue renin-angiotensin systems. *J Mol Med (Berl)*. 2008;86:615-621
40. Te Riet L, van Esch JH, Roks AJ, van den Meiracker AH, Danser AH. Hypertension: Renin-angiotensin-aldosterone system alterations. *Circ Res*. 2015;116:960-975
41. Hollenberg NK, Price DA, Fisher ND, Lansang MC, Perkins B, Gordon MS, Williams GH, Laffel LM. Glomerular hemodynamics and the renin-angiotensin system in patients with type 1 diabetes mellitus. *Kidney Int*. 2003;63:172-178
42. Carey RM, Siragy HM. The intrarenal renin-angiotensin system and diabetic nephropathy. *Trends Endocrinol Metab*. 2003;14:274-281
43. Correa-Rotter R, Hostetter TH, Rosenberg ME. Renin and angiotensinogen gene expression in experimental diabetes mellitus. *Kidney Int*. 1992;41:796-804

44. Jaffa AA, Chai KX, Chao J, Chao L, Mayfield RK. Effects of diabetes and insulin on expression of kallikrein and renin genes in the kidney. *Kidney Int*. 1992;41:789-795
45. Zimpelmann J, Kumar D, Levine DZ, Wehbi G, Imig JD, Navar LG, Burns KD. Early diabetes mellitus stimulates proximal tubule renin mrna expression in the rat. *Kidney Int*. 2000;58:2320-2330
46. Cowie CC, Rust KF, Ford ES, Eberhardt MS, Byrd-Holt DD, Li C, Williams DE, Gregg EW, Bainbridge KE, Saydah SH, Geiss LS. Full accounting of diabetes and pre-diabetes in the u.S. Population in 1988-1994 and 2005-2006. *Diabetes Care*. 2009;32:287-294
47. Kalyani RR, Egan JM. Diabetes and altered glucose metabolism with aging. *Endocrinol Metab Clin North Am*. 2013;42:333-347
48. Roksnoer LC, Heijnen BF, Nakano D, Peti-Peterdi J, Walsh SB, Garrelds IM, van Gool JM, Zietse R, Struijker-Boudier HA, Hoorn EJ, Danser AH. On the origin of urinary renin: A translational approach. *Hypertension*. 2016;67:927-933
49. Roksnoer LC, Verdonk K, van den Meiracker AH, Hoorn EJ, Zietse R, Danser AH. Urinary markers of intrarenal renin-angiotensin system activity in vivo. *Curr Hypertens Rep*. 2013;15:81-88
50. van den Heuvel M, Batenburg WW, Jainandunsing S, Garrelds IM, van Gool JM, Feelders RA, van den Meiracker AH, Danser AH. Urinary renin, but not angiotensinogen or aldosterone, reflects the renal renin-angiotensin-aldosterone system activity and the efficacy of renin-angiotensin-aldosterone system blockade in the kidney. *J Hypertens*. 2011;29:2147-2155
51. Fisher ND, Price DA, Litchfield WR, Williams GH, Hollenberg NK. Renal response to captopril reflects state of local renin system in healthy humans. *Kidney Int*. 1999;56:635-641
52. Hollenberg NK, Chenitz WR, Adams DF, Williams GH. Reciprocal influence of salt intake on adrenal glomerulosa and renal vascular responses to angiotensin ii in normal man. *J Clin Invest*. 1974;54:34-42
53. Hollenberg NK, Williams GH, Burger B, Chenitz W, Hoosmand I, Adams DF. Renal blood flow and its response to angiotensin ii. An interaction between oral contraceptive agents, sodium intake, and the renin-angiotensin system in healthy young women. *Circ Res*. 1976;38:35-40
54. Hollenberg NK, Williams GH, Taub KJ, Ishikawa I, Brown C, Adams DF. Renal vascular response to interruption of the renin-angiotensin system in normal man. *Kidney Int*. 1977;12:285-293
55. Shoback DM, Williams GH, Moore TJ, Dluhy RG, Podolsky S, Hollenberg NK. Defect in the sodium-modulated tissue responsiveness to angiotensin ii in essential hypertension. *J Clin Invest*. 1983;72:2115-2124

CHAPTER 9

BRAIN RENIN-ANGIOTENSIN SYSTEM: DOES IT EXIST?

Bibi S. van Thiel[1,2,3], Alexandre Góes Martini[1], Luuk te Riet[1,2], David Severs[1,4], Estrellita Uijl[1,4], Ingrid M. Garrelds[1], Frank P.J. Leijten[1], Ingrid van der Pluijm[2,3], Jeroen Essers[2,3,5], Fatimunnisa Qadri[6], Natalia Alenina[6,7], Michael Bader[6-10], Ludovit Paulis[11,12], Romana Rajkovicova[11], Oliver Domenig[13,14], Marko Poglitsch[13] and A.H. Jan Danser[1]

[1]Division of Vascular Medicine and Pharmacology, Department of Internal Medicine; [2]Department of Vascular Surgery; [3]Department of Molecular Genetics; Cancer Genomics Center Netherlands [4]Division of Nephrology and Transplantation, Department of Internal Medicine; [5]Department of Radiation Oncology, Erasmus MC, Rotterdam, The Netherlands; [6]Max Delbrück Center, Berlin, Germany; [7]DZHK (German Center for Cardiovascular Research), partner site Berlin, Germany; [8]Berlin Institute of Health (BIH), Berlin, Germany; [9]Charité - University Medicine, Berlin, Germany; [10]Institute for Biology, University of Lübeck, Lübeck, Germany; [11]Institute of Pathophysiology, Faculty of Medicine, Comenius University; [12]Institute of Normal and Pathophysiological Physiology, Slovak Academy of Sciences, Bratislava, Slovak Republic; [13]Attoquant Diagnostics and [14]Department of Internal Medicine III, Medical University of Vienna, Vienna, Austria

(Hypertension 2017 Jun;69:1136-1144)

ABSTRACT

Because of the presence of the blood-brain barrier, brain renin-angiotensin system activity should depend on local (pro)renin synthesis. Indeed, an intracellular form of renin has been described in the brain, but whether it displays angiotensin (Ang) I-generating activity (AGA) is unknown. Here, we quantified brain (pro)renin, before and after buffer perfusion of the brain, in wild-type mice, renin knockout mice, deoxycorticosterone acetate salt-treated mice, and Ang II-infused mice. Brain regions were homogenized and incubated with excess angiotensinogen to detect AGA, before and after prorenin activation, using a renin inhibitor to correct for nonrenin-mediated AGA. Renin-dependent AGA was readily detectable in brain regions, the highest AGA being present in brain stem (>thalamus=cerebellum=striatum=midbrain>hippocampus=cortex). Brain AGA increased marginally after prorenin activation, suggesting that brain prorenin is low. Buffer perfusion reduced AGA in all brain areas by >60%. Plasma renin (per mL) was 40x to 800x higher than brain renin (per gram). Renin was undetectable in plasma and brain of renin knockout mice. Deoxycorticosterone acetate salt and Ang II suppressed plasma renin and brain renin in parallel, without upregulating brain prorenin. Finally, Ang I was undetectable in brains of spontaneously hypertensive rats, while their brain/plasma Ang II concentration ratio decreased by 80% after Ang I type 1 receptor blockade. In conclusion, brain renin levels (per gram) correspond with the amount of renin present in 1 to 20 μL plasma. Brain renin disappears after buffer perfusion, and varies in association with plasma renin. This indicates that brain renin represents trapped plasma renin. Brain Ang II represents Ang II taken up from blood rather than locally synthesized Ang II.

INTRODUCTION

Since the discovery of renin in the brain nearly 50 years ago,[1] numerous studies have proposed that a so-called brain renin-angiotensin system (RAS) exists. Given the presence of the blood-brain barrier, brain RAS activity should depend on the local synthesis of renin or prorenin (together denoted as (pro)renin) in the brain rather than uptake from blood. In support of this concept, an intracellular, nonsecreted form of renin (icREN) has been shown to occur exclusively in the brain. This renin isoform is derived from an alternative transcript of the renin gene, lacking the signal peptide and part of the prosegment.[2, 3] To what degree this truncated prorenin truly generates angiotensin (Ang) I remains elusive. Lee-Kirsch et al[2] detected low Ang I-generating activity (AGA) levels in cell lysates of AtT20 cells transfected with icREN during incubation with excess angiotensinogen, but failed to demonstrate to what degree this AGA was renin-mediated (eg, by making use of a renin inhibitor). Peters et al[4] showed increased AGA in cardiac homogenates of transgenic rats overexpressing icREN and were able to block this with the renin inhibitor CH732. Yet, unexpectedly, the AGA increase was observed only after prosegment removal with trypsin, in disagreement with the fact that truncated prorenin does not require prosegment removal to display activity.[5] Moreover, icREN overexpression in the heart, if anything, resulted in effects that were unrelated to angiotensin formation.[6]

Deoxycorticosterone acetate (DOCA) salt treatment is widely believed to stimulate brain RAS activity. Confusingly, it lowers icREN expression, but increases the expression of the classical, secreted form of renin in brain tissue (sREN),[7] possibly because, icREN, via an unknown mechanism, inhibits sREN expression.[8] Li et al[9, 10] proposed that DOCA-salt selectively increases brain prorenin, which, in the absence of a prosegment-cleaving enzyme in the brain, requires interaction with the (pro)renin receptor to allow Ang I generation locally. The underlying assumption of this concept is that prorenin binding to the (pro)renin receptor results in a conformational change in the prorenin molecule, allowing it to display enzymatic activity without prosegment cleavage.[11] Yet, the low (nanomolar) affinity of the (pro)renin receptor implies that high prorenin levels are required for receptor binding,[11] for which there currently is no evidence.[10]

Given these uncertainties, in the present study, we set out to re-evaluate the occurrence of (pro)renin in the brain. We quantified brain (pro)renin in a wide variety of brain regions, derived from control mice, mice exposed to DOCA salt or Ang II, and renin-deficient mice. Under all conditions, a comparison was made with plasma (pro)renin, and the renin inhibitor aliskiren was applied in the assay to evaluate whether AGA was truly renin mediated. Mice were studied given the fact that their (pro)renin levels are several orders of magnitude higher than those in humans or rats, thereby facilitating the detection of renin-dependent AGA, even in areas with low (pro)renin levels. To obtain a more complete understanding of the brain RAS, we also quantified brain angiotensinogen, and

we studied the changes in brain angiotensin generation making use of brain stem tissue obtained from control spontaneously hypertensive rats (SHR) and SHR treated with the Ang II type 1 (AT_1) receptor blocker olmesartan or the angiotensin-converting enzyme inhibitor lisinopril for 4 weeks.

MATERIAL AND METHODS

Mouse and rat studies

Renin, prorenin and angiotensinogen were measured in plasma and brain regions (cerebellum, brain stem, cortex, hippocampus, midbrain, striatum, and thalamus) obtained from wild-type mice, mice treated with deoxycorticosterone acetate (DOCA)-salt or angiotensin II, and renin-deficient mice ($Ren1c^{-/-}$), either without and with transcardial perfusion with PBS to wash away blood from the brain vasculature. Renin expression in brain tissue was also explored by using Ingenuity Pathway Analysis, and angiotensinogen synthesis was additionally studied in rat primary cortical astrocytes. Angiotensins were measured in plasma and brain stem tissue obtained from SHR treated with vehicle, lisinopril or olmesartan. For further details, see the Methods section in the online-only Data Supplement.

Statistical Analysis

Data are expressed as mean±SEM. Univariate linear associations between plasma and brain renin levels were assessed by calculation of Pearson's coefficient of correlation. Differences between groups were evaluated by Student's *t* test or analysis of variance and corrected for multiple testing by post hoc Bonferroni analysis when needed. $P<0.05$ was considered significant.

RESULTS

Aliskiren Inhibits AGA in the Mouse Brain

Aliskiren identically inhibited AGA in mouse plasma (n=2), mouse kidney homogenate (n=2) and mouse brain homogenate (n=3: Fig.1). The half maximal inhibitory concentration (IC50) was in the nanomolar range, as has been reported before for mouse renin.[12, 13] These data suggest that AGA in mouse brain homogenates is caused by renin. All subsequent AGA measurements were performed both in the absence and presence of 10 μmol/L aliskiren to correct for nonrenin (ie, nonaliskiren-inhibitable) AGA.

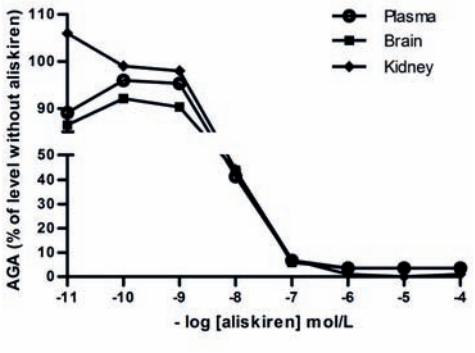

Figure 1. Concentration-dependent inhibition of angiotensin I-generating activity (AGA) by aliskiren in mouse plasma (n=2), mouse kidney homogenate (n=2) and mouse brain homogenate (n=3, representing pooled brain stem, cortex, and midbrain regions, respectively, from 3 to 4 mice each).

Buffer Perfusion Reduces Mouse Brain Renin by >60%

Renin-dependent (ie, aliskiren-inhibitable) AGA was readily detectable in brain regions, the highest AGA being present in brain stem (>thalamus=cerebellum=striatum=midb rain >hippocampus=cortex: Fig.2; n=5/group). AGA increased in each individual brain region after prorenin activation, but only when analyzing all brain regions together by multivariate analysis of variance did this increase reach significance (P<0.05). Applying the prorenin activation procedure to 3 mouse brain homogenates (cortex, midbrain, and brain stem, respectively) to which recombinant human prorenin had been added yielded values in a renin immunoradiometric assay (IRMA; 211±12 pg/mL) that were similar to those when activating the same amount of recombinant human prorenin in buffer with aliskiren[14] (169±6 pg/mL). This confirms that our prorenin activation procedure was appropriate. PBS perfusion of the mouse brain reduced AGA in all brain areas by >60% (Fig. 2; P<0.01) and diminished the percentage of AGA that could be blocked by aliskiren (Table S2). These data suggest that blood removal predominantly washes away renin, but not

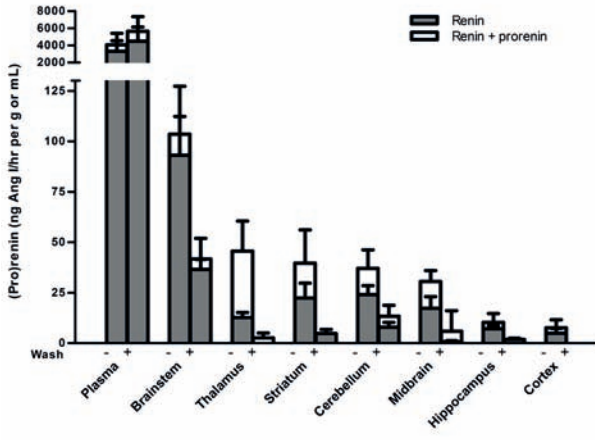

Figure 2. Renin and total renin (=renin+prorenin) levels in plasma and brain regions of mice before and after buffer perfusion (wash) of the brain. Data are mean±SEM of n=5. Multivariate analysis of variance (ANOVA) showed that total renin levels were higher than renin levels (P<0.05) and that buffer perfusion reduced renin by >60% in all regions (P<0.01).

nonrenin enzymes that are also capable of reacting with angiotensinogen. Plasma renin (expressed per milliliter of plasma) was 40x to 800x higher than brain renin (expressed per gram of tissue), and, as expected, identical in mice that were exposed to buffer perfusion. Plasma prorenin levels were of the same order of magnitude as plasma renin levels, as demonstrated earlier in mice.[15]

Comparable Reductions in Brain and Plasma (Pro)Renin after DOCA Salt Treatment, Ang II infusion, and Renin Deficiency

DOCA salt (n=6) and Ang II (n=7) suppressed plasma renin versus wild-type (n=6) mice, and parallel decreases were observed for brain stem, midbrain, and cortex renin (Fig. 3), although significance was not reached in all cases. Nevertheless, brain renin levels (expressed per gram of tissue) correlated significantly with plasma renin levels (expressed per milliliter of plasma) in all 3 brain regions (Fig. 4). The different slopes may reflect the different blood content of each brain region. Plasma prorenin levels were comparable to plasma renin levels, and prorenin activation in brain regions nonsignificantly increased brain AGA. Plasma renin and prorenin were undetectable in Ren1c$^{-/-}$ mice (n=4), and renin (ie, aliskiren-inhibitable AGA) was also undetectable in the 3 brain regions obtained from Ren1c$^{-/-}$ mice. However, low levels of aliskiren-inhibitable AGA were present in brain stem (1 out of 4), midbrain (3 out of 4), and cortex (2 out of 4) after prorenin activation in the Ren1c$^{-/-}$ mice. Because this cannot represent prorenin, these data imply that our prorenin activation procedure occasionally activated a renin-like enzyme, capable of reacting with angiotensinogen, the activity of which can be blocked by 10 μmol/L aliskiren.

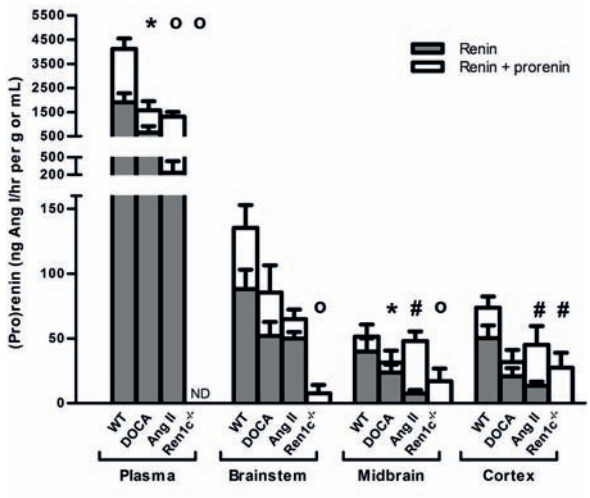

Figure 3. Renin and total renin (=renin+prorenin) levels in plasma and brain regions of untreated mice (wild-type [WT]), mice treated with deoxycorticosterone acetate (DOCA) salt, mice infused with Ang II, and Ren1c$^{-/-}$ mice. Data are mean±SEM of n=4 to 7. Differences in renin levels were assessed by 1-way analysis of variance (ANOVA), followed by correction for multiple testing by post hoc Bonferroni analysis. *P<0.05, $^{\#}P$<0.01, $^{\circ}P$<0.001 vs WT.

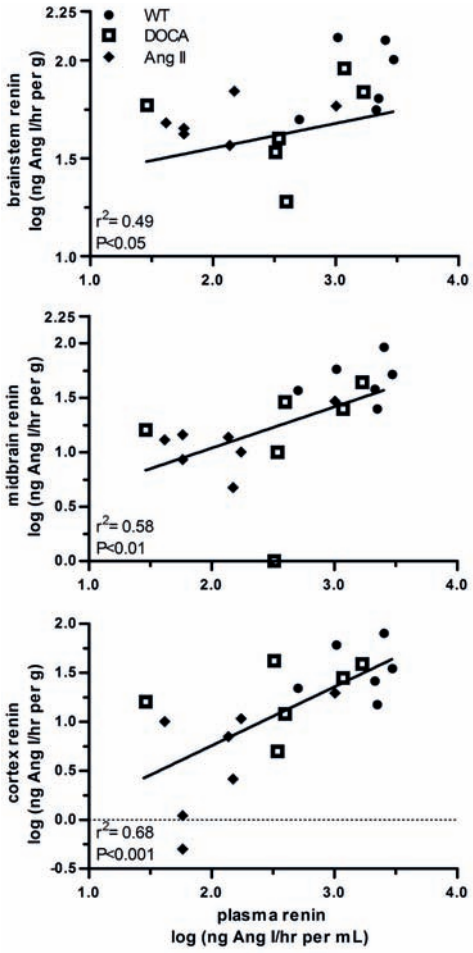

Figure 4. Relationship between renin in plasma and renin in 3 different brain regions in untreated mice (wild-type [WT], n=6), mice treated with deoxycorticosterone acetate (DOCA) salt (n=6), and mice infused with angiotensin (Ang) II (n=7).

9

Renin Expression in the Brain

Renin (secreted+intracellular), sREN, or icREN mRNA expression levels were undetectable in all brain regions in wild-type, DOCA salt-treated, and Ang II-infused mice. Primer specificity for renin (secreted+intracellular) and sREN was validated by measuring renal renin expression in Ren1c$^{-/-}$ mice (Fig. S1B). In the Ingenuity Pathway Analysis tissue expression data sets, renin expression was found in cerebellum, hypothalamus, and pituitary, but only in 3 out of 9 different datasets examined (data not shown).

Despite Angiotensinogen Expression, Angiotensinogen Protein is Undetectable in Mouse Brain and Rat Astrocytes

Mouse plasma contained detectable levels of angiotensinogen (28±5 pmol/mL). Angiotensinogen mRNA expression was observed in different brain regions (Fig. 5), at C_t values

of 23 (cerebellum), 22 (thalamus), 25 (hippocampus), and 27 (striatum) versus ≈18 in the liver. Brain expression levels changed inconsistently after DOCA salt, Ang II, and renin deficiency: an increase was observed in the thalamus after DOCA salt (P<0.05), while decreases occurred in the cerebellum after DOCA salt (P<0.05), and in the hippocampus after Ang II (P<0.05). Yet, angiotensinogen protein was undetectable (<1 pmol/g) in mouse cortex and brain stem (n=4 of each). Angiotensinogen was also undetectable in the medium of cultured rat astrocytes (<0.3 pmol/mL), cultured for 24, 48, 72 or 96 hours (n=4 for each condition), or the accompanying cell lysates (<0.3 pmol/mg protein).

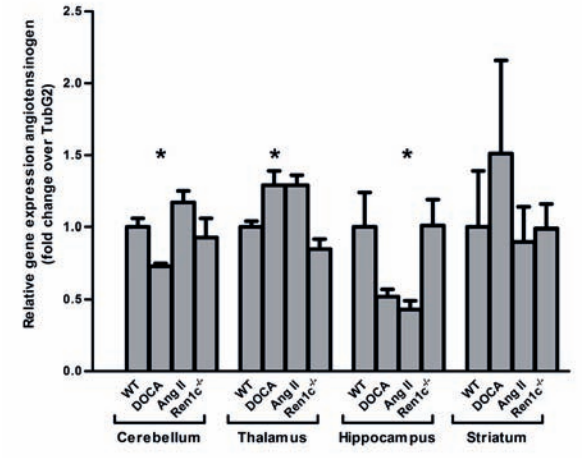

Figure 5. Angiotensinogen mRNA expression in different brain regions in untreated mice (wild-type [WT]), mice treated with deoxycorticosterone acetate (DOCA) salt, mice infused with angiotensin (Ang) II, and Ren1c$^{-/-}$ mice. Data, presented as fold change over TubG2 relative to WT levels, are mean±SEM of n=3-6. Differences were assessed by 1-way analysis of variance (ANOVA), followed by correction for multiple testing by post hoc Bonferroni analysis. *P<0.05 vs WT.

Angiotensins in the SHR brain with and without RAS blockade

Ang I, Ang-(1-7), and Ang-(2-8) were below detection limit in brain tissue of untreated SHR (n=6), while Ang II could be detected in the rat brain at levels corresponding with ≈25% of the Ang II levels in blood plasma (Table S3; Fig. 6). Ang I and Ang-(2-8), but not Ang-(1-7), were detectable in plasma in untreated SHR. Brain Ang-(1-7) and Ang-(2-8) remained undetectable after olmesartan (n=6) or lisinopril (n=4), while Ang I became detectable in the rat brain after both types of RAS blockade (P<0.001 for both). Because plasma Ang I increased ≈20-fold after olmesartan and lisinopril (P<0.001 for both), it could be calculated that during both types of RAS blockade, brain Ang I levels corresponded with ≈1% of the Ang I levels in plasma. Olmesartan increased brain Ang II ≈5-fold (P<0.001) and plasma Ang II ≈25-fold (P<0.001), so that after AT_1 receptor blockade, the brain/plasma ratio of Ang II decreased by ≈80% (P<0.05). Lisinopril decreased plasma Ang II by >90% (P<0.001), and diminished brain Ang II to undetectable levels (P<0.001). Lisinopril also decreased plasma Ang-(2-8) to undetectable levels and greatly increased plasma Ang-(1-7), while olmesartan increased both plasma Ang-(2-8) and plasma Ang-(1-7). Taken together, given that brain Ang I levels correspond with ≈1% of the circulating

Ang I levels, 10 μL plasma per gram brain tissue is sufficient to explain the entire brain Ang I content. Brain Ang II levels, relative to plasma Ang II levels, are higher, suggesting either local synthesis or an active uptake mechanism. The massive decrease in the Ang II brain/plasma ratio after olmesartan supports the latter.

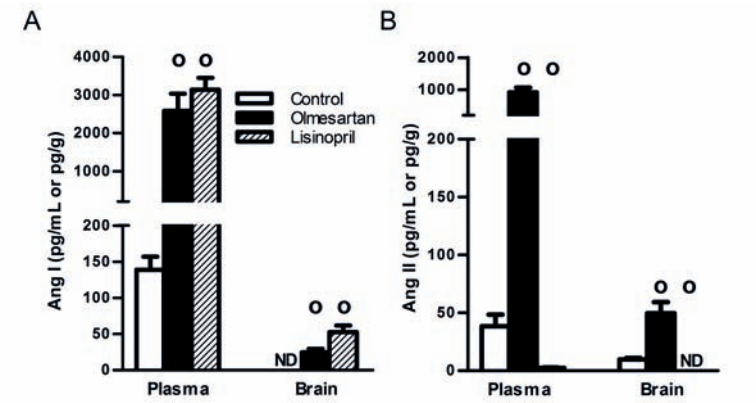

Figure 6. Angiotensin (Ang) I and II levels in plasma and brain of SHR treated with vehicle (control), olmesartan, or lisinopril. Data are mean±SEM of n=4 to 6. Differences were assessed by 1-way analysis of variance (ANOVA), followed by correction for multiple testing by post hoc Bonferroni analysis. °P<0.001 vs control. ND indicates not detectable.

DISCUSSION

The present study confirms that renin-dependent AGA can be detected in virtually every region of the mouse brain. Yet, as compared with plasma, brain renin levels were low, corresponding with the amount of renin in 1 to 25 μL blood plasma per gram brain tissue (≈0.1%-2.5% [v/v]). This volume mimics the amount of blood plasma in various brain regions determined with tritiated inulin or Evans blue dye.[16, 17] Moreover, perfusing the brain with PBS prior to the collection of the various regions reduced brain renin uniformly by >60%. Had local renin synthesis occurred in one or more specific brain regions, the washout percentage should have been much lower in these regions, similar to the fact that in the kidney one cannot wash away stored renin,[18, 19] while this does happen in nonrenin producing organs like the heart.[20] Furthermore, DOCA salt, like Ang II, reduced circulating renin and, contrary to our expectations, did not increase brain prorenin. In fact, if anything, both DOCA-salt and Ang II lowered brain renin in parallel with plasma renin. Aliskiren-inhibitable AGA was entirely absent in the brain of Ren1c$^{-/-}$ mice, supporting the validity of our brain renin measurement. Taken together, our data do not support the presence of kidney-independent (pro)renin synthesis in the brain, nor the concept that this occurs particularly in the DOCA salt model. In fact, brain renin levels are so low that the

accumulation of renin at brain tissue sites outside the blood compartment seems unlikely. This greatly differs from other organs (eg, the heart), where renin diffuses freely into the interstitium and/or binds to a receptor, thereby reaching tissue levels that are, on a gram basis, at least as high as the renin levels in blood plasma (on an mL basis).[20-22] Clearly, the presence of the blood-brain barrier prevents such distribution.

Prorenin activation resulted in modest AGA increases in all brain regions, and significance for this increase was only obtained by analyzing all regions together. Applying recombinant human prorenin to brain homogenates prior to the prorenin activation procedure (on the basis of acid activation[22]) confirmed that this procedure resulted in complete prorenin activation. However, small rises in aliskiren-inhibitable AGA were also observed in brain homogenates from Ren1c$^{-/-}$ mice after their exposure to acid. Because Ren1c$^{-/-}$ mouse brain tissue cannot contain prorenin, this implies that the brain contains a nonrenin proenzyme, which is activated by acid exposure, and which is capable of cleaving Ang I from angiotensinogen in an aliskiren-inhibitable manner. A possible candidate is procathepsin D. Indeed, renin inhibitors, at high micromolar concentrations, do inhibit cathepsin D.[23] Our difficulty to demonstrate prorenin in the brain is reminiscent of earlier studies in organs not synthesizing prorenin themselves, like the heart.[22] Obviously, blood plasma contains prorenin, and thus some prorenin should be detected in the blood-containing homogenates derived from such tissues. Yet only under conditions where circulating prorenin levels were greatly elevated, like in heart failure in humans, did we reliably detect prorenin in cardiac tissue.[24] In mice, in contrast to humans, circulating prorenin levels are relatively low (versus renin), making it even more difficult to show a rise in AGA on top of already low renin-mediated AGA. A further complicating factor is that tissue homogenization per se may result in (partial) prorenin activation. In summary, given the presence of prorenin in blood plasma, brain homogenates should minimally contain the amount of prorenin present in a few microliter of blood. The rises in AGA after prorenin activation are consistent with this view, but should still be interpreted with caution given the fact that nonrenin enzymes also came into play after acid activation. Brain-selective prorenin rises, for example, after DOCA salt, were not observed. This implies that prorenin-(pro)renin receptor interaction is unlikely to occur in the mouse brain, particularly after DOCA salt (which lowers brain (pro)renin), although it may obviously occur after intracerebroventricular infusion of pharmacological prorenin doses into the brain.[10]

Most, if not all, studies on brain renin relied on the detection of renin mRNA in the brain, either under normal conditions or after deleting/overexpressing sREN or icREN. Deleting sREN in neurons or glia did not affect blood pressure, heart rate, water intake, or metabolic rate,[25] while preservation of icREN did not compensate for the consequences of whole-body sREN deficiency (hypotension, renal defects, and lethality).[26] Surprisingly, brain-selective deletion of icREN even caused neurogenic hypertension, possibly because

icREN inhibits sREN.[8] These data seem to argue against icREN as an Ang I-generating enzyme. Yet, overexpressing either human icREN or sREN in astrocytes, if combined with human angiotensinogen, resulted in Ang II-dependent hypertension and an increase in drinking volume.[27] Because icREN under the latter conditions was not detectable in cerebrospinal fluid, it was concluded that this phenomenon involved intracellular Ang II formation. We attempted to detect renin mRNA, using either specific assays for sREN or icREN or a nonspecific assay that detects both sREN and icREN. Under no condition were we able to show renin (secreted+intracellular), sREN, or icREN gene expression in any of the different regions of the brain: the expression level was below the detection threshold of the reverse transcriptase polymerase chain reaction assay, even with the use of the highly sensitive Taqman probes. The specificity of our renin primers was validated by making use of the kidneys of Ren1c$^{-/-}$ mice. Of course, poor renin expression in the brain has been noted before.[28-30] Because of the technical limitations inherent in any reverse transcriptase polymerase chain reaction assay, we could not load > 100 ng of total RNA. Our results, therefore, indicate that if renin is expressed in the brain, its expression is >2^{18}-fold lower than that in the kidney (no signal after 40 cycles, with renin detection in the kidney at C_t=22). The Ingenuity Pathway Analysis expression data sets confirm this view. Yet, Kubo et al[31] observed a blood pressure drop after intraventricular renin antisense injection in SHR. In their hands only 1 of 3 tested antisense oligonucleotides acted hypotensive, and this response was accompanied by a 20% drop in renin mRNA (detected after 45 cycles of reverse transcriptase polymerase chain reaction). These authors did not measure renin levels in brain or plasma and were unable to rule out antisense leakage to the kidney. Therefore, these data cannot be taken as definitive proof for the existence of an independent brain RAS.

The mouse RAS differs from the human RAS, in that the circulating renin levels in mice are ≤1000-fold higher (on a nanogram Ang I/mL hour basis) than in humans. As a consequence, circulating angiotensinogen levels in mice are far below K_m range, as confirmed in the present study. Nevertheless, despite these differences, mouse angiotensin levels in blood and tissue are comparable to those in humans, rats and pigs.[32-35] We attempted to measure angiotensinogen in the mouse brain, both at the mRNA and protein level. Although we did observe angiotensinogen mRNA expression in different regions of the brain, in full agreement with previous work,[36, 37] expression was ≤500-fold lower than in the liver. Under no condition were we able to detect angiotensinogen protein in the brain. Given the detection limit of our assay (1 pmol/g), this implies that brain angiotensinogen, if present, occurs at levels (per gram of tissue) that are <3% of the levels in plasma (per milliliter of plasma). Such low levels have been reported before in the rat brain, as well as in human and rat cerebrospinal fluid,[16, 38-40] and thus, our data entirely agree with the literature. Clearly, mice, given their low angiotensinogen levels, are not the optimal species to study brain angiotensinogen. As astrocytes are assumed to be the source of brain

angiotensinogen,[41, 42] we additionally studied angiotensinogen synthesis by rat primary cortical astrocytes, but again failed to detect any angiotensinogen. Nevertheless, data from Schink et al.[40] do support the functional presence of angiotensinogen in the rat brain. These authors artificially elevated renin in the brain by either intracerebroventricular renin infusion (in Sprague-Dawley rats) or by making use of transgenic hypertensive rats overexpressing mouse Ren2. The responses to both approaches (drinking and blood pressure reduction, respectively) were greatly diminished after lowering brain angiotensinogen by brain-selective expression of an antisense RNA against angiotensinogen mRNA.

Finally, given our observation that brain renin is confined to the plasma compartment, while brain angiotensinogen is extremely low (if not also confined to the plasma compartment), an urging question is what degree local angiotensin generation truly occurs in the brain. We, therefore, collected brain stem tissue (ie, the brain region with the highest renin level) from SHR under control conditions and during RAS blockade with olmesartan or lisinopril. Rats rather than mice were used here, because at identical angiotensin levels in both species, the larger rat brain stem would allow a more reliable quantification of angiotensins. Without treatment, brain Ang I was undetectable, while Ang II occurred at levels that were ≈25% of the levels in plasma (per gram tissue weight). This contrasts with other organs where Ang II is usually much higher than in plasma, while Ang I is easily detectable.[43-46] RAS blockade induced the usual rise in Ang I levels in plasma, and now brain Ang I became detectable, however, at only 1% (v/v) of its plasma levels. It seems reasonable to assume that also in the untreated animals, brain Ang I levels were in the 1% range of plasma Ang I and, therefore, too low to be detected with our assays. If so, this implies that under all conditions, brain Ang I at most represented the amount of Ang I that is inherently present in brain tissue because it contains a small amount (≈1%) of blood.[16] Lisinopril decreased brain Ang II to undetectable levels, while olmesartan reduced the brain/plasma Ang II ratio by >80%. The latter finding suggests that, normally, circulating Ang II accumulates in brain tissue via binding to AT_1 receptors. Such uptake occurs in multiple organs[47] and facilitates the intracellular accumulation of Ang II.[48] Without receptors (ie, in AT receptor-deficient mice), tissue Ang II levels drop dramatically,[49] suggesting that tissue Ang II levels do not originate intracellularly. If Ang II binding to AT_1 receptors is the only source of Ang II in the brain, one would expect angiotensin metabolites that do not (or only with low affinity) bind to this receptor to be undetectable in the brain. This is indeed what we observed for both Ang-(2-8) and Ang-(1-7). An olmesartan-induced reduction in brain Ang II levels was also observed in Dahl-sensitive hypertensive rats, albeit in the absence of an effect on blood pressure.[50] Clearly, therefore, the changes observed in brain Ang II are blood pressure independent.

PERSPECTIVES

The absence of renin-dependent AGA in the brain outside the blood compartment implies that angiotensin generation in the brain, if occurring, does not involve renin. Brain prorenin levels, if anything, were even lower than brain renin levels and, therefore, like renin, at most represented the amount of prorenin expected in brain tissue based on its blood content. Selective brain prorenin upregulation, for example, after DOCA salt, could not be observed, arguing against the concept that DOCA salt-induced neurogenic hypertension involves prorenin-(pro)renin receptor interaction. Finally, the absence of Ang I in brain tissue outside the blood compartment (which contrasts sharply with the presence of Ang I in every other organ of the body) strongly suggests that there is no local Ang I generation in the brain. Apparently, therefore, nonrenin enzymes do not compensate for the absence of renin, assuming at least that brain angiotensinogen levels are of sufficient magnitude to allow independent Ang I generation at all. Only *ex vivo*, after prohormone-activating procedures, did we occasionally obtain evidence for a modest contribution of such nonrenin enzymes, but the *in vivo* relevance of these findings is questionable. Brain Ang II, therefore, seems to originate in the blood compartment. Of course, circulating Ang II will bind to brain AT receptors that are outside the blood-brain barrier (eg, in the circumventricular organ). Yet, it may also gain access to brain areas behind this barrier, for example, under conditions where blood-brain barrier permeability is compromised, like in (DOCA salt) hypertension.[51, 52] In fact, Ang II itself may be responsible for disturbing the blood-brain barrier, thus, facilitating its own access to critical brain areas like the hypothalamus and brain stem. From this perspective, the brain RAS in reality represents circulating Ang II that accumulates in brain nuclei, possibly after it has (partially) broken down the blood-brain barrier. This Ang II subsequently activates sympatho-neurohumoral outflow, for instance, by upregulating reactive oxygen species.[52, 53] This is entirely different from other organs like heart, kidney, and vascular wall, where renin and angiotensinogen diffuse freely into the interstitial space, allowing local production of Ang I to occur.[20, 54, 55] Blocking AT_1 receptors or enhancing Ang II degradation (eg, by angiotensin-converting enzyme 2) will prevent the effects of circulating Ang II in the brain, thereby explaining the success of intracerebroventricular application of losartan or brain-selective angiotensin-converting enzyme 2 overexpression in DOCA salt hypertension.[56]

SOURCES OF FUNDING

This study was supported by the 'Lijf en Leven' grant (2011): 'Dilating versus stenosing arterial disease (DIVERS)' (B.S. van Thiel, I. van der Pluijm, and J. Essers) and Scientific Research Agency grant VEGA 1/0380/14 (M. Poglitsch).

DISCLOSURES

None.

NOVELTY AND SIGNIFICANCE

What is new?

- Brain renin levels parallel plasma renin levels in a variety of hypertension models and in fact are as high as can be expected on the basis of the presence of blood in brain tissue.
- Because the latter was also true for brain prorenin, this implies that neither renin nor prorenin contributes to angiotensin I production in the brain.

What is relevant?

- Brain angiotensin II originates in the circulation, and the brain renin-angiotensin system activation that has been claimed to occur under pathological conditions (hypertension, deoxycorticosterone acetate salt) most likely represents a compromised blood-brain barrier, allowing circulating angiotensin II access to brain regions behind the blood-brain barrier.

Summary

Quantifying brain (pro)renin in wild-type mice, renin-deficient mice, deoxycorticosterone acetate salt-treated mice, and angiotensin II-infused mice, revealed that changes in brain renin paralleled those in plasma renin, that brain renin disappeared after buffer perfusion of the brain, and that brain renin and prorenin levels were as high as expected based on the presence of (pro)renin in blood in brain tissue. Angiotensin I was undetectable in the brain, while angiotensin II type 1 receptor blockade reduced the brain/plasma angiotensin II concentration ratio by 80%. In conclusion, (pro)renin-mediated angiotensin I production in the brain is unlikely, and brain angiotensin II therefore represents angiotensin II sequestered from blood via angiotensin II type 1 receptor binding.

REFERENCES

1. Ganten D, Minnich JL, Granger P, Hayduk K, Brecht HM, Barbeau A, Boucher R, Genest J. Angiotensin-forming enzyme in brain tissue. *Science*. 1971;173:64-65
2. Lee-Kirsch MA, Gaudet F, Cardoso MC, Lindpaintner K. Distinct renin isoforms generated by tissue-specific transcription initiation and alternative splicing. *Circ Res*. 1999;84:240-246.

3. Mercure C, Thibault G, Lussier-Cacan S, Davignon J, Schiffrin EL, Reudelhuber TL. Molecular analysis of human prorenin prosegment variants in vitro and in vivo. *J Biol Chem*. 1995;270:16355-16359
4. Peters J. Secretory and cytosolic (pro)renin in kidney, heart, and adrenal gland. *J Mol Med (Berl)*. 2008;86:711-714
5. Grobe JL, Xu D, Sigmund CD. An intracellular renin-angiotensin system in neurons: Fact, hypothesis, or fantasy. *Physiology (Bethesda)*. 2008;23:187-193
6. Wanka H, Staar D, Lutze P, Peters B, Hildebrandt J, Beck T, Baumgen I, Albers A, Krieg T, Zimmermann K, Sczodrok J, Schafer S, Hoffmann S, Peters J. Anti-necrotic and cardioprotective effects of a cytosolic renin isoform under ischemia-related conditions. *J Mol Med (Berl)*. 2016;94:61-69
7. Grobe JL, Rahmouni K, Liu X, Sigmund CD. Metabolic rate regulation by the renin-angiotensin system: Brain vs. Body. *Pflugers Arch*. 2013;465:167-175
8. Shinohara K, Liu X, Morgan DA, Davis DR, Sequeira-Lopez ML, Cassell MD, Grobe JL, Rahmouni K, Sigmund CD. Selective deletion of the brain-specific isoform of renin causes neurogenic hypertension. *Hypertension*. 2016;68:1385-1392
9. Li W, Sullivan MN, Zhang S, Worker CJ, Xiong Z, Speth RC, Feng Y. Intracerebroventricular infusion of the (pro)renin receptor antagonist pro20 attenuates deoxycorticosterone acetate-salt-induced hypertension. *Hypertension*. 2015;65:352-361
10. Li W, Peng H, Mehaffey EP, Kimball CD, Grobe JL, van Gool JMG, Sullivan MN, Earley S, Danser AHJ, Ichihara A, Feng Y. Neuron-specific (pro)renin receptor knockout prevents the development of salt-sensitive hypertension. *Hypertension*. 2014;63:316-323
11. Batenburg WW, Lu X, Leijten F, Maschke U, Müller DN, Danser AHJ. Renin- and prorenin-induced effects in rat vascular smooth muscle cells overexpressing the human (pro)renin receptor: Does (pro)renin-(pro)renin receptor interaction actually occur? *Hypertension*. 2011;58:1111-1119
12. Wood JM, Maibaum J, Rahuel J, Grutter MG, Cohen NC, Rasetti V, Ruger H, Goschke R, Stutz S, Fuhrer W, Schilling W, Rigollier P, Yamaguchi Y, Cumin F, Baum HP, Schnell CR, Herold P, Mah R, Jensen C, O'Brien E, Stanton A, Bedigian MP. Structure-based design of aliskiren, a novel orally effective renin inhibitor. *Biochem Biophys Res Commun*. 2003;308:698-705
13. Lu H, Rateri DL, Feldman DL, Jr RJ, Fukamizu A, Ishida J, Oesterling EG, Cassis LA, Daugherty A. Renin inhibition reduces hypercholesterolemia-induced atherosclerosis in mice. *J Clin Invest*. 2008;118:984-993
14. Batenburg WW, de Bruin RJA, van Gool JM, Müller DN, Bader M, Nguyen G, Danser AHJ. Aliskiren-binding increases the half life of renin and prorenin in rat aortic vascular smooth muscle cells. *Arterioscler Thromb Vasc Biol*. 2008;28:1151-1157
15. Mercure C, Prescott G, Lacombe MJ, Silversides DW, Reudelhuber TL. Chronic increases in circulating prorenin are not associated with renal or cardiac pathologies. *Hypertension*. 2009;53:1062-1069
16. Gregory TJ, Wallis CJ, Printz MP. Regional changes in rat brain angiotensinogen following bilateral nephrectomy. *Hypertension*. 1982;4:827-838
17. Migliarini S, Pacini G, Pelosi B, Lunardi G, Pasqualetti M. Lack of brain serotonin affects postnatal development and serotonergic neuronal circuitry formation. *Mol Psychiatry*. 2013;18:1106-1118
18. Fraune C, Lange S, Krebs C, Holzel A, Baucke J, Divac N, Schwedhelm E, Streichert T, Velden J, Garrelds IM, Danser AHJ, Frenay AR, van Goor H, Jankowski V, Stahl R, Nguyen G, Wenzel

UO. At1 antagonism and renin inhibition in mice: Pivotal role of targeting angiotensin ii in chronic kidney disease. *Am J Physiol Renal Physiol*. 2012;303:F1037-F1048

19. Lange S, Fraune C, Alenina N, Bader M, Danser AHJ, Frenay AR, van Goor H, Stahl R, Nguyen G, Schwedhelm E, Wenzel UO. Aliskiren accumulation in the kidney: No major role for binding to renin or prorenin. *J Hypertens*. 2013;31:713-719
20. de Lannoy LM, Danser AHJ, van Kats JP, Schoemaker RG, Saxena PR, Schalekamp MADH. Renin-angiotensin system components in the interstitial fluid of the isolated perfused rat heart. Local production of angiotensin i. *Hypertension*. 1997;29:1240-1251.
21. Heller LJ, Opsahl JA, Wernsing SE, Saxena R, Katz SA. Myocardial and plasma renin-angiotensinogen dynamics during pressure-induced cardiac hypertrophy. *Am J Physiol*. 1998;274:R849-R856.
22. Danser AHJ, van Kats JP, Admiraal PJJ, Derkx FHM, Lamers JMJ, Verdouw PD, Saxena PR, Schalekamp MADH. Cardiac renin and angiotensins. Uptake from plasma versus in situ synthesis. *Hypertension*. 1994;24:37-48
23. Deinum J, Derkx FHM, Danser AHJ, Schalekamp MADH. Identification and quantification of renin and prorenin in the bovine eye. *Endocrinology*. 1990;126:1673-1682
24. Danser AHJ, van Kesteren CAM, Bax WA, Tavenier M, Derkx FHM, Saxena PR, Schalekamp MADH. Prorenin, renin, angiotensinogen, and angiotensin-converting enzyme in normal and failing human hearts. Evidence for renin binding. *Circulation*. 1997;96:220-226
25. Xu D, Borges GR, Davis DR, Agassandian K, Sequeira Lopez ML, Gomez RA, Cassell MD, Grobe JL, Sigmund CD. Neuron- or glial-specific ablation of secreted renin does not affect renal renin, baseline arterial pressure, or metabolism. *Physiol Genomics*. 2011;43:286-294
26. Xu D, Borges GR, Grobe JL, Pelham CJ, Yang B, Sigmund CD. Preservation of intracellular renin expression is insufficient to compensate for genetic loss of secreted renin. *Hypertension*. 2009;54:1240-1247
27. Lavoie JL, Liu X, Bianco RA, Beltz TG, Johnson AK, Sigmund CD. Evidence supporting a functional role for intracellular renin in the brain. *Hypertension*. 2006;47:461-466
28. Bader M, Ganten D. It's renin in the brain: Transgenic animals elucidate the brain renin angiotensin system. *Circ Res*. 2002;90:8-10
29. Lippoldt A, Fuxe K, Luft FC. A view of renin in the brain. *J Mol Med (Berl)*. 2001;79:71-73
30. Saavedra JM. Brain angiotensin ii: New developments, unanswered questions and therapeutic opportunities. *Cell Mol Neurobiol*. 2005;25:485-512
31. Kubo T, Ikezawa A, Kambe T, Hagiwara Y, Fukumori R. Renin antisense injected intraventricularly decreases blood pressure in spontaneously hypertensive rats. *Brain Res Bull*. 2001;56:23-28
32. Roksnoer LCW, van Veghel R, de Vries R, Garrelds IM, Bhaggoe UM, Friesema ECH, Leijten FPJ, Poglitsch M, Domenig O, Clahsen-van Groningen MC, Hoorn EJ, Danser AHJ, Batenburg WW. Optimum at1 receptor-neprilysin inhibition has superior cardioprotective effects compared with at1 receptor receptor blockade alone in hypertensive rats. *Kidney International*. 2015;88:109-120
33. Campbell DJ, Duncan AM, Kladis A. Angiotensin-converting enzyme inhibition modifies angiotensin but not kinin peptide levels in human atrial tissue. *Hypertension*. 1999;34:171-175
34. van Kats JP, Danser AHJ, van Meegen JR, Sassen LM, Verdouw PD, Schalekamp MADH. Angiotensin production by the heart: A quantitative study in pigs with the use of radiolabeled angiotensin infusions. *Circulation*. 1998;98:73-81

35. Klotz S, Burkhoff D, Garrelds IM, Boomsma F, Danser AHJ. The impact of left ventricular assist device-induced left ventricular unloading on the myocardial renin-angiotensin-aldosterone system: Therapeutic consequences? *Eur Heart J*. 2009;30:805-812
36. Davisson RL, Yang G, Beltz TG, Cassell MD, Johnson AK, Sigmund CD. The brain renin-angiotensin system contributes to the hypertension in mice containing both the human renin and human angiotensinogen transgenes. *Circ Res*. 1998;83:1047-1058
37. Thomas WG, Sernia C. Immunocytochemical localization of angiotensinogen in the rat brain. *Neuroscience*. 1988;25:319-341
38. Ito T, Eggena P, Barrett JD, Katz D, Metter J, Sambhi MP. Studies on angiotensinogen of plasma and cerebrospinal fluid in normal and hypertensive human subjects. *Hypertension*. 1980;2:432-436
39. Schelling P, Muller S, Clauser E. Regulation of angiotensinogen in cerebrospinal fluid and plasma of rats. *Am J Physiol*. 1983;244:R466-471
40. Schinke M, Baltatu O, Bohm M, Peters J, Rascher W, Bricca G, Lippoldt A, Ganten D, Bader M. Blood pressure reduction and diabetes insipidus in transgenic rats deficient in brain angiotensinogen. *Proc Natl Acad Sci U S A*. 1999;96:3975-3980
41. Intebi AD, Flaxman MS, Ganong WF, Deschepper CF. Angiotensinogen production by rat astroglial cells in vitro and in vivo. *Neuroscience*. 1990;34:545-554
42. Milsted A, Barna BP, Ransohoff RM, Brosnihan KB, Ferrario CM. Astrocyte cultures derived from human brain tissue express angiotensinogen mrna. *Proc Natl Acad Sci U S A*. 1990;87:5720-5723
43. van Kats JP, Chai W, Duncker DJ, Schalekamp MADH, Danser AHJ. Adrenal angiotensin. Origin and site of generation. *Am J Hypertens*. 2005;18:1045-1051
44. van Kats JP, Schalekamp MADH, Verdouw PD, Duncker DJ, Danser AHJ. Intrarenal angiotensin ii: Interstitial and cellular levels and site of production. *Kidney Int*. 2001;60:2311-2317
45. Campbell DJ, Kladis A, Duncan AM. Nephrectomy, converting enzyme inhibition, and angiotensin peptides. *Hypertension*. 1993;22:513-522
46. Campbell DJ, Kladis A, Duncan AM. Effects of converting enzyme inhibitors on angiotensin and bradykinin peptides. *Hypertension*. 1994;23:439-449.
47. van Kats JP, de Lannoy LM, Danser AHJ, van Meegen JR, Verdouw PD, Schalekamp MADH. Angiotensin ii type 1 (at1) receptor-mediated accumulation of angiotensin ii in tissues and its intracellular half-life in vivo. *Hypertension*. 1997;30:42-49
48. van Kats JP, van Meegen JR, Verdouw PD, Duncker DJ, Schalekamp MADH, Danser AHJ. Subcellular localization of angiotensin ii in kidney and adrenal. *J Hypertens*. 2001;19:583-589
49. van Esch JHM, Gembardt F, Sterner-Kock A, Heringer-Walther S, Le T, Lassner D, Stijnen T, Coffman T, Schultheiss H-P, Danser AHJ, Walther T. Cardiac phenotype and angiotensin ii levels in at1a, at1b and at2 receptor single, double and triple knockouts *Cardiovasc Res*. 2010;86:401-409
50. Pelisch N, Hosomi N, Ueno M, Nakano D, Hitomi H, Mogi M, Shimada K, Kobori H, Horiuchi M, Sakamoto H, Matsumoto M, Kohno M, Nishiyama A. Blockade of at1 receptors protects the blood-brain barrier and improves cognition in dahl salt-sensitive hypertensive rats. *Am J Hypertens*. 2011;24:362-368
51. Biancardi VC, Son SJ, Ahmadi S, Filosa JA, Stern JE. Circulating angiotensin ii gains access to the hypothalamus and brain stem during hypertension via breakdown of the blood-brain barrier. *Hypertension*. 2014;63:572-579

52. Biancardi VC, Stern JE. Compromised blood-brain barrier permeability: Novel mechanism by which circulating angiotensin ii signals to sympathoexcitatory centres during hypertension. *J Physiol*. 2016;594:1591-1600
53. Wang HW, Huang BS, White RA, Chen A, Ahmad M, Leenen FH. Mineralocorticoid and angiotensin ii type 1 receptors in the subfornical organ mediate angiotensin ii - induced hypothalamic reactive oxygen species and hypertension. *Neuroscience*. 2016;329:112-121
54. de Lannoy LM, Danser AHJ, Bouhuizen AMB, Saxena PR, Schalekamp MADH. Localization and production of angiotensin ii in the isolated perfused rat heart. *Hypertension*. 1998;31:1111-1117.
55. Schalekamp MADH, Danser AHJ. Angiotensin ii production and distribution in the kidney: I. A kinetic model. *Kidney Int*. 2006;69:1543-1552
56. Xia H, de Queiroz TM, Sriramula S, Feng Y, Johnson T, Mungrue IN, Lazartigues E. Brain ace2 overexpression reduces doca-salt hypertension independently of endoplasmic reticulum stress. *Am J Physiol Regul Integr Comp Physiol*. 2015;308:R370-378

SUPPLEMENTAL INFORMATION

METHODS

All animal experiments were performed under the regulation and permission of the Animal Care Committee, conforming to the Guide for the Care and Use of Laboratory Animals published by the US National Institutes of Health (NIH Publication No. 8523, revised 1985).

Brain renin, prorenin and angiotensinogen levels in wild-type mice, mice treated with DOCA-salt or angiotensin II, and renin-deficient mice

Male and female C57BL/6J mice (wild-type, WT) were obtained by in-house breeding or purchased from Charles River (Sulzfeld, Germany). Mice (age 3-4 months) were either untreated, treated with deoxycorticosterone acetate (DOCA)-salt (150 mg, 60-day release pellet [Innovative Research of America, Sarasota, USA]) for 4 weeks, or infused with Ang II (490 ng/kg/min by osmotic minipump [Alzet, model 2004, DURECT, Cupertino, USA][1]) for 2 weeks. Ren1c homozygous null mice ($Ren1c^{-/-}$; 3 females and 1 male) were generated as described before (C57BL/6J background)[2] and sacrificed at the age of 3-6 months. All mice were housed under standard laboratory conditions (temperature 23±1°C, 12-hour light-dark cycle) and maintained on standard chow (Special Diets Services, Essex, UK) with ad libitum access to tap water. DOCA-salt-treated mice had ad libitum access to 0.15 mol/L (0.9%) NaCl solution. At the end of the treatment period, mice were sacrificed with an overdose of isoflurane and blood was collected by cardiac puncture into EDTA-coated tubes. Blood was centrifuged at 4600 rpm for 10 minutes and plasma was stored at -80ºC until analysis. Five untreated mice were perfused transcardially with PBS to wash away blood from the brain vasculature. Brains were rapidly removed from all mice and

the desired regions (cerebellum, brainstem, cortex, hippocampus, midbrain, striatum and thalamus) were dissected, frozen in liquid nitrogen, and stored at -80°C until analysis.

Brain and plasma angiotensin levels in spontaneously hypertensive rats

Male 10-week old SHR (Janvier Labs, Le Genest St. Isle, France) were treated with either vehicle (tap water), the ACE inhibitor lisinopril (15 mg/kg body weight; Sigma-Aldrich, Darmstadt, Germany) or the AT_1 receptor blocker olmesartan (10 mg/kg body weight, Daiichi Sankyo Co., Ltd., Japan) once daily per gavage for four weeks. Animals were housed under standard laboratory conditions (temperature 23±1°C, 12-hour light-dark cycle), they were fed a standard pellet diet (1.8% NaCl; Velaz, Prague, Czech Republic), and drank tap water ad libitum. At the end of treatment period, the animals were sacrificed in terminal isoflurane anesthesia (2-3%) by being bled out. Blood was collected in the presence of an inhibitor cocktail containing ethylenediaminetetraacetic acid (EDTA), pepstatin A, p-hydroxymercuribenzoic acid, phenanthroline and specific inhibitors for renin and aminopeptidases to a final concentration of 5% v/v (Attoquant Diagnostics, Vienna, Austria) and immediately cooled on ice.[3] Plasma was isolated by centrifugation at 4°C and frozen at -80°C until analysis. Brains were sampled via scull trepanation followed by removal of the hemispheres and cerebellum. The brainstem was isolated, rapidly frozen in liquid nitrogen and preserved at -80°C until analysis.

Angiotensinogen synthesis by rat primary cortical astrocytes

Rat primary cortical astrocytes (Invitrogen, Thermo Fisher, Waltham, USA) were grown in 6-well plates (Corning Incorporated, Corning, USA) in DMEM medium (85% Dulbecco's Modified Eagle Medium containing high glucose 4.5 g/L, 15% FCS (Gibco, Thermo Fisher) and L-glutamine (600 mg/L; Flow Lab, UK)) in an incubator at 37°C and 5% CO_2 until confluency. Medium and cells were collected after 24, 48, 72 or 96 hours. For the determination of angiotensinogen, the culture medium was removed and stored at -80°C, while cells were gently washed with PBS, lysed with RIPA buffer (50 mmol/L Tris-HCl, 150 mmol/L NaCl, 1% Triton x-100, 0.5% sodium deoxylcholate, 0.1% SDS, 1 mmol/L EDTA), and frozen at -80°C until analysis.

Measurement of renin, prorenin and angiotensinogen

Mouse plasma renin and prorenin were measured as described before.[4] Brain tissue was homogenized in 0.01 mol/L phosphate buffer, pH 7.4, containing 0.15 mol/L NaCl, and the homogenates were used to measure renin, total renin (i.e., renin plus prorenin), and angiotensinogen. AGA was measured by enzyme-kinetic assay in the presence of excess sheep angiotensinogen, both without and with the renin inhibitor aliskiren (10 pmol/L-10 μmol/L).[5] Total renin was measured identically after conversion of prorenin to renin by acidification.[5] Angiotensinogen was measured in mouse plasma, mouse brain homog-

enate, rat astrocyte cell culture medium and astrocyte cell lysate (after its centrifugation at 8000 x g for 10 min) as the maximum quantity of Ang I that was generated during incubation with excess recombinant rat renin.[6]

LC-MS/MS based quantification of angiotensin metabolites

Plasma was thawed on ice, and samples were spiked with 200 pg of stable isotope-labeled internal standards for Ang I, Ang II, Ang-(1-7) and Ang-(2-8). Following C18-based solid-phase-extraction, samples were subjected to LC-MS/MS analysis using a reversed-phase analytical column (Acquity UPLC® C18, Waters, Milford, USA) operating in line with a XEVO TQ-S triple quadrupole mass spectrometer (Waters) in MRM mode. Internal standards were used to correct for peptide recovery of the sample preparation procedure for each angiotensin metabolite in each individual sample. Angiotensin peptide concentrations were calculated considering the corresponding response factors determined in matrix calibration curves, on condition that integrated signals exceeded a signal-to-noise ratio of 10. Brain tissue samples were grinded under liquid nitrogen (pestle and mortar) and the resulting frozen tissue powder was rapidly dissolved in ice cold 6 mol/L guanidine hydrochloride supplemented with 1 % (v/v) TFA at a concentration of 100 mg tissue/mL.[7] Resulting homogenates were spiked with 200 pg of stable isotope-labelled internal standard for each angiotensin metabolite analyzed and subjected to solid phase based peptide extraction and subsequent LC-MS/MS analysis. The lower limits of quantification for Ang I, Ang II, Ang-(1-7) and Ang-(2-8) in plasma were 2.1, 0.9, 1.9 and 1.1 pg/mL, and in brain 8.1, 6.7, 12.7 and 8.0 pg/g tissue, respectively.

Renin and angiotensinogen expression

Total RNA was isolated from kidney and liver tissue, using Tri Reagent (Sigma-Aldrich, Darmstadt, Germany), and from brain tissue (cerebellum, brainstem, cortex, hippocampus, midbrain, striatum and thalamus), using the RNeasy Lipid kit (Qiagen, Venlo, The Netherlands). RNA concentration was quantified using micro-spectrophotometry (NanoDrop Technologies, Wilmington, USA). Single stranded complementary DNA was synthesized using the genomic DNA-free total RNA using the Quantitect Reverse Transcription kit (Qiagen) according to the manufacturer's protocol. Quantitative real-time PCRs were conducted in 10 µL and 100 ng of cDNA, using the CFX384 Touch™ Real-time PCR detection system (BioRad, Hercules, USA), followed by measurement using either IQ™ SYBR® Green Supermix (BioRad) or Taqman probes (IDT, Coralville, USA). The exon-exon junction spanning oligonucleotide primers for qPCR were designed with NCBI (Primer-BLAST). Primer sequences and GenBank accession numbers for the sequences used to design the primers are listed in Table S1. Regarding mouse renin, primers were designed to selectively detect sREN and icREN, as well as to detect renin independently of its signal peptide and prosegment ('secreted + intracellular renin'; Figure S1A). The following

cycling conditions were used [95°C for 3 min, (95°C for 3 sec, 60°C for 25 sec) × 40 cycles] for the KAPA SYBR ® FAST qPCR Master Mix, [95°C for 5 min, (95°C for 10 sec, 59-72°C for 40 sec) × 40 cycles] for the IQ™ SYBR® Green Supermix, and [95°C for 3 min, (95°C for 15 sec, 60°C for 1 min) × 45 cycles] for the Taqman assay. Expression levels in kidney, liver and brain tissue were normalised to the housekeeping genes B2M and TubG2, respectively. The $2-\Delta\Delta C_t$ method was used for relative quantification of gene expression.

Renin expression in brain tissue was also explored by using Ingenuity Pathway Analysis (IPA). In IPA, tissue expression datasets were created based on expression annotations from the GNF Body Atlas (expression calls were made from microarray data from dissection of healthy, adult, untreated C57/BL6 mouse tissues). Data was also available in Gene Expression Omnibus (http://www.ncbi.nlm.nih.gov/geo/query/acc.cgi?acc=GSE1133). Published[8] cases where a gene was marked "Present" in a particular tissue (based upon the Affymetrix MAS5 Absence/ Presence call) were used as evidence of mRNA expression, and were incorporated into the tissue expression dataset for that particular tissue. The criteria used to define a gene as expressed in the body atlas data in IPA correspond to an average concentration of 3 transcripts per cell (10 transcripts per million). Additional mRNA expression calls were derived from findings in the Ingenuity Knowledge Base that describes observations of mRNA expression in normal, healthy, adult mammalian tissue (human, mouse, rat and mammalian orthologs). Only findings where high quality mRNA detection methods were used (e.g. Northern Blots, quantitative RT-PCR, etc.) were included. Additional information is provided at the following link: http://ingenuity.force.com/ipa/IPA Tutorials?id=kA250000000TN5CCAW.

Statistical analysis

Data are expressed as mean±SEM. To determine the minimum number of animals needed for this study, we reasoned that, if renin is synthesized locally in certain brain areas, the majority of this renin (>50%) should not be washed away by buffer perfusion. Moreover, Grobe et al.[9] have suggested that brain sREN expression doubles after DOCA-salt. On the basis of these 2-fold changes, at an SD of 40% (as observed in brainstem, see Results), with $\alpha = 0.05$ and $\beta = 80\%$, the minimum n-number is 3. Univariate linear associations between plasma and brain renin levels were assessed by calculation of Pearson's coefficient of correlation. Differences between groups were evaluated by Student's t-test or ANOVA, and corrected for multiple testing by post-hoc Bonferroni analysis when needed. $P<0.05$ was considered significant. Statistical analysis was performed with IBM SPSS Statistics version 21.0 (IBM, Armonk, New York, USA).

REFERENCES

1. Batenburg WW, van den Heuvel M, van Esch JHM, van Veghel R, Garrelds IM, Leijten F, Danser AHJ. The (pro)renin receptor blocker handle region peptide upregulates endothelium-derived contractile factors in aliskiren-treated diabetic transgenic (mREN2)27 rats. J Hypertens. 2013;31:292-302.
2. Takahashi N, Lopez ML, Cowhig JE, Jr., Taylor MA, Hatada T, Riggs E, Lee G, Gomez RA, Kim HS, Smithies O. Ren1c homozygous null mice are hypotensive and polyuric, but heterozygotes are indistinguishable from wild-type. J Am Soc Nephrol. 2005;16:125-132.
3. Roksnoer LCW, van Veghel R, de Vries R, Garrelds IM, Bhaggoe UM, Friesema ECH, Leijten FPJ, Poglitsch M, Domenig O, Clahsen-van Groningen MC, Hoorn EJ, Danser AHJ, Batenburg WW. Optimum AT1 receptor-neprilysin inhibition has superior cardioprotective effects compared with AT1 receptor receptor blockade alone in hypertensive rats. Kidney International. 2015;88:109-120.
4. Fraune C, Lange S, Krebs C, Holzel A, Baucke J, Divac N, Schwedhelm E, Streichert T, Velden J, Garrelds IM, Danser AHJ, Frenay AR, van Goor H, Jankowski V, Stahl R, Nguyen G, Wenzel UO. AT1 antagonism and renin inhibition in mice: pivotal role of targeting angiotensin II in chronic kidney disease. Am J Physiol Renal Physiol. 2012;303:F1037-F1048.
5. Danser AHJ, van Kesteren CAM, Bax WA, Tavenier M, Derkx FHM, Saxena PR, Schalekamp MADH. Prorenin, renin, angiotensinogen, and angiotensin-converting enzyme in normal and failing human hearts. Evidence for renin binding. Circulation. 1997;96:220-226.
6. Batenburg WW, Lu X, Leijten F, Maschke U, Müller DN, Danser AHJ. Renin- and prorenin-induced effects in rat vascular smooth muscle cells overexpressing the human (pro)renin receptor: does (pro)renin-(pro)renin receptor interaction actually occur? Hypertension. 2011;58:1111-1119.
7. Campbell DJ, Kladis A, Duncan AM. Nephrectomy, converting enzyme inhibition, and angiotensin peptides. Hypertension. 1993;22:513-522.
8. Su AI, Wiltshire T, Batalov S, Lapp H, Ching KA, Block D, Zhang J, Soden R, Hayakawa M, Kreiman G, Cooke MP, Walker JR, Hogenesch JB. A gene atlas of the mouse and human protein-encoding transcriptomes. Proc Natl Acad Sci U S A. 2004;101:6062-6067.
9. Grobe JL, Rahmouni K, Liu X, Sigmund CD. Metabolic rate regulation by the renin-angiotensin system: brain vs. body. Pflugers Arch. 2013;465:167-175.
10. Grobe JL, Xu D, Sigmund CD. An intracellular renin-angiotensin system in neurons: fact, hypothesis, or fantasy. Physiology (Bethesda). 2008;23:187-193.

Table S1. Primer sequences and GenBank accession numbers.

Kidney and brain tissue (Mus musculus)		
SYBR green assay		
Beta-2 microglobulin (B2M)	CTCACACTGAATTCACCCCCA GTCTCGATCCCAGTAGACGGT	>NM_009735.3
Tubulin gamma-2 chain (TubG2)	CAGACCAACCACTGCTACAT AGGGAATGAAGTTGGCCAGT	>NM_134028.2
Renin (secreted + intracellular)	AGCTACATGGAGAACGGGTC TTCCACCCACAGTCACCGAG	>NM_031192.3
Secreted renin (sRen)	GCACCTTCAGTCTCCCAACAC TCCCGGACAGAAGGCATTTTC	>NM_031192.3
Intracellular renin (icRen)	CCGGCTGCTTTGAAGATTTGAT ATGCCAATCTCGCCGTAGTA	-
Angiotensinogen (Agt)	ACCCCCGAGTGGGAGAGGTTC GCCAGGCTGCTGGACAGACG	>NM_007428.3
Taqman assay		
Beta-2 microglobulin (B2M)	Assay ID-Mm.PT.58.10497647 (IDT) NM_009735(1)	
Tubulin gamma-2 chain (TubG2)	Assay ID-Mm.PT.58.41559687 (IDT) NM_134028(1)	
Renin (secreted + intracellular)	FW: TCAGCAAGACTGACTCCTGGC Rev: GCACAGCCTTCTTCACATAGC Probe: TCACGATGAAGGGGGTGTCTGTGGG	
Secreted renin (sRen)	FW: GCACCTTCAGTCTCCCAACAC Rev: TCCCGGACAGAAGGCATTTTC Probe: CCTTTGAACGAATCCC	
Intracellular renin (icRen)	FW: CCGGCTGCTTTGAAGATTTGAT Rev: CAGGTAGTTGGTGAGGACCAC Probe: TCACAAAGAGGCCTTCCTTGACCA	

Table S2. Percent inhibition of angiotensin I-generating activity by aliskiren in brain nucleus homogenates before and after buffer perfusion. Data are mean±SEM of n=5.

Brain nucleus	**Before Buffer Perfusion**		**After Buffer Perfusion**	
	Renin	**Total Renin**	**Renin**	**Total renin**
Brainstem	96±1	91±3	92±3	87±3
Thalamus	81±6	81±9	18±20	28±19
Cerebellum	86±4	92±2	73±12	54±18
Striatum	71±2	60±18	51±16	34±20
Midbrain	83±10	84±6	37±19	30±19
Hippocampus	49±6	48±22	47±15	13±13
Cortex	50±23	36±17	15±17	0±0

Table S3. Angiotensin (Ang) metabolites in SHR plasma and brain during treatment with placebo, olmesartan or lisinopril. Data are mean±SEM of n=4-6, and if undetectable, were based on the detection limit.

	Ang I (pg/mL or g)	Ang II (pg/mL or g)	Ang-(2-8) (pg/mL or g)	Ang-(1-7) (pg/mL or g)
Plasma				
Placebo	139±20	39±11	8±2	<2±0
Olmesartan	2579±497	911±171	223±57	9±2
Lisinopril	3142±362	2±1	<1±0	58±14
Brain				
Placebo	<8±1	9±2	<9±0	<13±1
Olmesartan	25±5	50±11	<8±0	<13±1
Lisinopril	53±10	<7±1	<8±0	<13±1

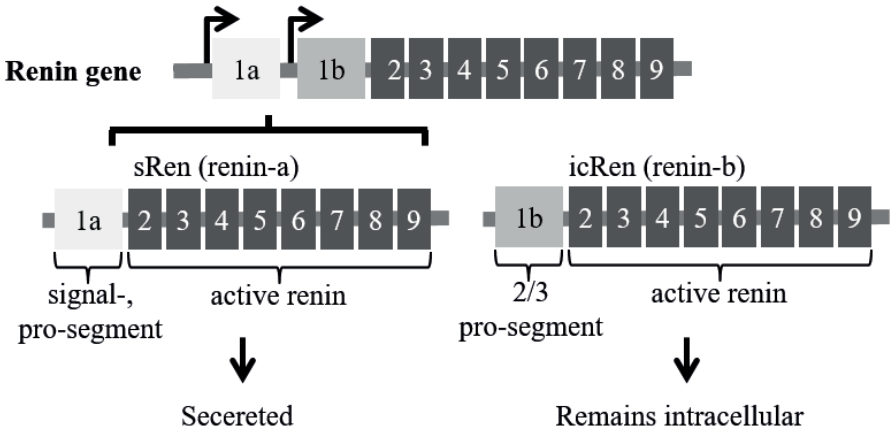

Figure S1A. Proposed pathway for secreted renin and intracellular renin. It is hypothesized that in the brain, a different mRNA, renin-b, is transcribed that result in a novel transcript lacking exon 1a. This renin isoform lacks the signal peptide and part of the prosegment, and is believed to remain intracellular. Adapted from Grobe et al..[10]

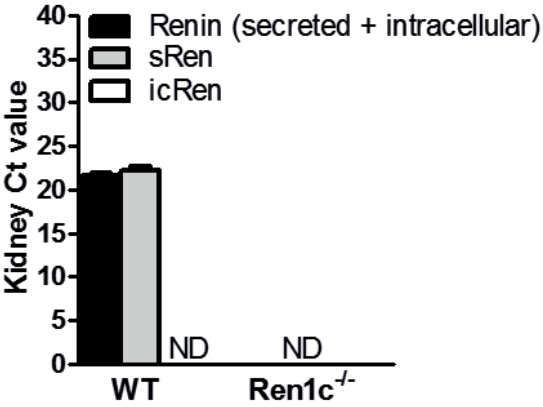

Figure S1B. Renin (secreted or intracellular), sRen and icRen mRNA expression in kidneys of wild-type (WT, n=6) and Ren1c$^{-/-}$ mice (n=4). icRen was undetectable under all conditions, while renin (secreted + intracellular) and sRen were undetectable in kidneys of Ren1c$^{-/-}$ mice. C_t values were generated with the SYBR Green assay.

CHAPTER 10

MAXIMUM RENAL RESPONSES TO RENIN INHIBITION IN HEALTHY SUBJECTS: VTP-27999 VERSUS ALISKIREN

Ebrahim Barkoudah[1], Bibi S. van Thiel[3], Naomi D.L. Fisher[1], Richard A. Gregg[4], A.H. Jan Danser[3], George V. Moukarbel[5] and Norman K. Hollenberg[1,2]

Departments of Medicine[1] and Radiology [2], Brigham and Women's Hospital and Harvard Medical School, Boston, MA, USA; [3]Division of Vascular Medicine and Pharmacology, Department of Internal Medicine, Erasmus MC, Rotterdam, The Netherlands; [4]Vitae Pharmaceuticals Inc., Fort Washington, PA, USA and [5]Department of Internal Medicine, University of Toledo, Toledo, OH, USA

(Journal of Hypertension 2016 May;34(5):935-41)

ABSTRACT

Background: Renin inhibition with aliskiren induced the largest increases in renal plasma flow (RPF) in salt-depleted healthy volunteers of all renin-angiotensin system (RAS) blockers. However, given its side effects at doses >300 mg, no maximum effect of renin inhibition could be established. We hypothesized that VTP-27999, a novel renin inhibitor without major side effects at high doses, would allow us to establish this.

Methods and Results: The effects of escalating VTP-27999 doses (75-600 mg) on RPF, glomerular filtration rate (GFR), and plasma RAS components were compared with those of 300 mg aliskiren in 22 normal volunteers on a low-sodium diet. VTP-27999 dose-dependently increased RPF and GFR; its effects on both parameters at 600 mg (increases of 18±4% and 20±4%, respectively) were equivalent to those at 300 mg, indicating that a maximum had been reached. The effects of 300 mg aliskiren (increases of +13±5% and +8±6%, respectively; $P<0.01$ versus 300 and 600 mg VTP-27999) resembled those of 150 mg VTP-27999. VTP-27999 dose-dependently increased renin, and lowered plasma renin activity and angiotensin II to detection limit levels. The effects of aliskiren on RAS components were best comparable to those of 150 mg VTP-27999.

Conclusion: Maximum renal renin blockade in healthy, salt-depleted volunteers, requires aliskiren doses >300 mg, but can be established with 300 mg VTP-27999. To what degree such maximal effects (exceeding those of ACE inhibitors and AT_1 receptor blockers) are required in patients with renal disease, given the potential detrimental effects of excessive RAS blockade, remains to be determined.

INTRODUCTION

The effects of renin-angiotensin system (RAS) blockers in the kidney, i.e., with regard to renal hemodynamics, albuminuria and renal function, require higher doses than their blood pressure effects.[1-3] This most likely reflects the fact that renin, angiotensin-converting enzyme (ACE) and angiotensin (Ang) II type 1 (AT_1) receptors in the kidney are less easily accessible to drugs taken orally than in blood or the vascular wall.[4-10] In addition, their levels at renal tissue sites, in particular those of renin, are much higher than in blood[9, 11], therefore requiring even higher doses to obtain sufficient blockade. A well-known model to test the efficacy of blockade of RAS activity in the kidney is to measure the renal vasodilator responses to RAS blockade in subjects in whom the RAS has been activated by restriction of sodium intake.[12-14] We have wide experience with this model, both in healthy volunteers and in (diabetic) patients under carefully standardized conditions (e.g., receiving a fixed sodium diet) during a multiple day-stay in our clinical research center.

Remarkably, when using this model, we observed that the renal plasma flow (RPF) responses to aliskiren exceeded those seen with ACE inhibitors or AT_1 receptor blockers.[13] Doses of 300 mg and 600 mg aliskiren were tested, and the effects of 600 mg were ≈20% larger than those of 300 mg. Unfortunately, 600 mg of aliskiren leads to diarrhea; therefore, aliskiren is clinically used at a maximum dose of 300 mg/day. Consequently, at this stage, we do not know to what degree the effects of 600 mg aliskiren, which were twice as large as those observed with captopril (25 mg), and 40% larger than those observed with AT_1 receptor blockers (300 mg irbesartan, 16 mg candesartan, or 600 mg eprosartan)[12, 14, 15], resembled the maximum effects of RAS blockade in the kidney.

A new renin inhibitor, VTP-27999, has recently been compared with aliskiren in healthy volunteers.[16] The drug was safe and well tolerated. Since VTP-27999 is a potent renin inhibitor with an oral bioavailability that is about 10-fold higher than that of aliskiren[17, 18], we hypothesized that, with the help of this new and well-tolerated renin inhibitor, we would be able to establish the maximum effect of renin inhibition in the kidney. Therefore, in the present study, we compared the acute renal effects of escalating VTP-27999 doses (75-600 mg) with those of 300 mg aliskiren in healthy, salt-depleted volunteers.

MATERIAL AND METHODS

Study protocol

This single-center, prospective randomized, double-blinded, placebo-controlled study was performed in healthy volunteers between the age of 18 and 75 years of both sexes. Ethical approval was obtained by expedited review through the Brigham and Women's

Hospital/Partner Healthcare Human Research Committee. Female subjects were required to be postmenopausal or surgically sterilized to participate. Subjects were free of hypertension, diabetes, or any significant medical condition. After an outpatient evaluation, which included history, physical examination, screening chemistry, and hematology laboratory tests, all subjects were studied during a 7-day admission to a metabolic ward, at the Brigham and Women's Hospital General Clinical Research Center (GCRC) (see Table S1). Written informed consent was obtained from each subject, and the protocol was approved by the Human Subjects Committee of the institution. Subjects were placed on a controlled low sodium diet (10 mmol sodium daily, the first several days as outpatient) and randomly assigned to 2 groups. The diet did not affect blood pressure (126±5/76±4 mm Hg versus 120±5/73±3 mm Hg in group 1, and 125±4/75±3 mm Hg versus 116±4/71±2 mm Hg in group 2; P=NS for both). The first group received 75 mg VTP-27999, placebo, and 300 mg aliskiren, respectively. The second group received VTP-27999 in 3 doses, 150 mg, 300 mg, and 600 mg. All drugs were given in single doses on separate study days.

Twenty four-hour urine samples were collected daily; when urinary sodium matched sodium intake (usually on day 5), the first study was initiated. Each subject was tested on three separate study days (Monday, Wednesday, and Friday), separated by a rest interval of 48 hours; drug/placebo was only administered on study days. Phlebotomy limitations prevented subjects from undergoing more than three studies each. Studies began at 6 AM. Subjects had been recumbent and fasting overnight and remained recumbent throughout the study. RPF was measured by the clearance of paraaminohippurate (PAH; Clinalfa, Laufelfingen, Switzerland) and glomerular filtration rate (GFR) by the clearance of inulin (Inutest Polyfructosan, Fresenius Pharma, Linz, Austria) by autoanalyzer methods described previously.[19]

After a 60-minute control period to establish basal RPF, placebo/drug was dosed by mouth. Over the next four (treatment day 2) or five (treatment days 1 and 3) hours, blood pressure was checked every 15 minutes by an automatic recording device (Dinamap, Critikon Inc, Tampa, FL, USA) or as deemed necessary by study staff. Blood samples were collected on ice at the start of the PAH infusion, at 60-minute intervals throughout, and at the end of each study (after five hours). Due to limited PAH stock, on treatment day 2, the PAH clearance measurements stopped at four hours. Samples were spun immediately, and plasma was stored at -80°C until the time of assay.

Biochemical measurements

PRA was determined by measuring Ang I generation during incubation of plasma at 37°C and pH 7.4 using an in-house assay.[16] PRC was measured with an immunoradiometric kit (Renin III, Cisbio, Gif-sur-Yvette, France).[13] Plasma prorenin was measured with a direct prorenin enzyme-linked immunosorbent assay (Molecular Innovations, Novi, MI, USA).[20]

Plasma Ang II was measured by radioimmunoassay after SepPak extraction as described before.[21]

Statistical analysis

RPF and GFR are presented as percent change from baseline on each respective study day. An F-test was applied to the mean percent change of each group to assess overall significance of the linear mixed model. In this analysis, we assumed non-independence of observations across the protocol assignment and the intervention dosings. All other parameters are presented as absolute values or changes (mean±SEM), and have been analyzed by Student's t-test or one-way ANOVA, followed by post-hoc evaluation according to Bonferroni. $P<0.05$ was considered statistically significant. All authors had full access to and take responsibility for the data.

RESULTS

Baseline characteristics of the two groups of healthy volunteers that participated in this study were equivalent (Table 1), and thus all subjects were evaluated together. VTP-27999 dose-dependently increased RPF (Fig. 1A&B), its maximum effect reached at a dose of 300

Table 1. Baseline characteristics (mean±SEM) of the 2 treatment groups under low-sodium conditions. Group 1 received 75 mg VTP-27999, 300 mg aliskiren, and placebo, respectively. Group 2 received VTP-27999 in 3 doses, 150 mg, 300 mg, and 600 mg. BMI, body mass index; SBP, DBP, systolic, diastolic blood pressure; PRA, plasma renin activity; Ang, angiotensin.

Parameter	Group 1 (n=10)	Group 2 (n=12)
Age (years)	48±5	43±5
Male, %	70%	100%
Race (Caucasian/Hispanic), %	90/10%	92/8%
BMI (kg/m^2)	25±1	28±1
SBP (mm Hg)	126±5	125±4
DBP (mm Hg)	76±4	75±3
Heart rate	73±5	72±3
Hematocrit (%)	44±0.9	45±1.0
Serum glucose (mg/dL)	79±4	81±4
Blood urea nitrogen (mg/dL)	14±1	16±1
Serum creatinine (mg/dL)	1.0±0.1	1.0±0.0
Serum Sodium (mmol/L)	140±0	140±1
Serum Potassium (mmol/L)	4.3±0.2	4.3±0.1
Plasma renin (ng/L)	26±5	31±3
Plasma prorenin (ng/L)	82±16	85±10
PRA (nmol Ang I/L.hr)	2.36±0.49	3.12±0.30
Plasma Ang II (pmol/L)	7.6±1.1	8.9±0.8
Renal plasma flow (mL/min.1.73 m^2)	432±17	436±18

mg, given the fact that the effects observed at 600 mg were equivalent to those at 300 mg. Aliskiren 300 mg effects on RPF were similar to those obtained with 150 mg VTP-27999, and significantly lower than those obtained at 300 and 600 mg VTP-27999 (P<0.01). Renin inhibitor-induced GFR changes paralleled this pattern (Fig. 1C&D), although significant increases in fact only occurred at the highest VTP-27999 dose (P<0.05 versus placebo). Both renin inhibitors induced small, non-significant decreases in blood pressure (Table 2). No serious adverse effects were observed (Table S2).

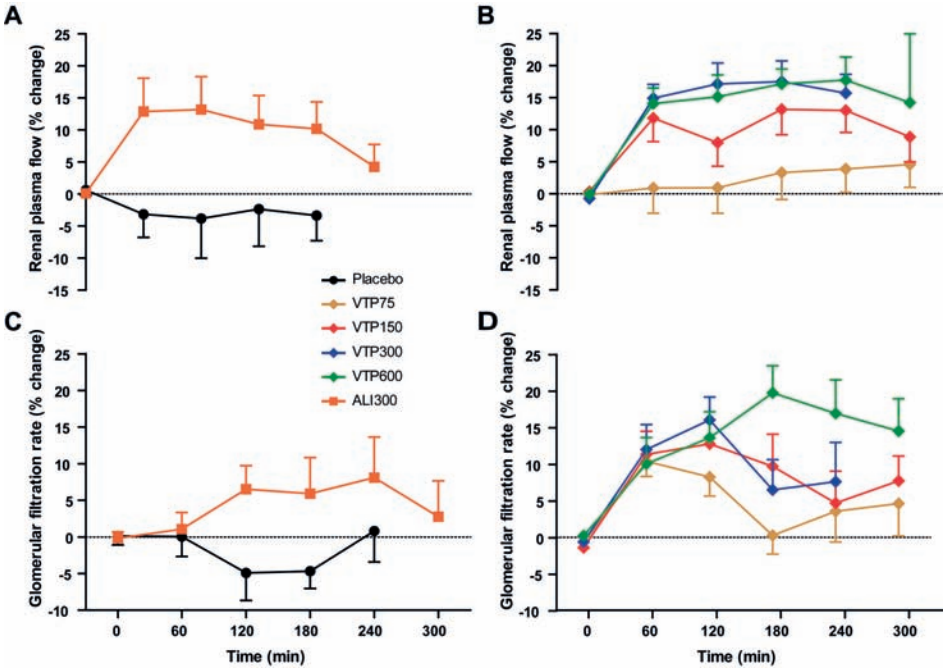

Figure 1. Percent change in renal plasma flow (panels A&B) and glomerular filtration rate (panels C&D) in healthy, salt-depleted volunteers over a 5-hour period following oral intake of placebo, VTP-27999 (VTP; 75, 150, 300 or 600 mg) or 300 mg aliskiren (ALI). Data are mean±SEM of n=9-12. See text for statistical analysis.

Table 2. Change in systolic blood pressure (SBP) and mean arterial pressure (MAP) at 5 hours after placebo/drug intake. Data are mean±SEM of n=9-12. No significant changes vs. placebo were noted.

Treatment	Δ SBP (mm Hg)	MAP (mm Hg)
Placebo	4.1±4.3	112±4
VTP-27999 75 mg	-5.9±3.3	110±4
VTP-27999 150 mg	0.0±3.6	114±2
VTP-27999 300 mg	-5.2±4.1	108±3
VTP-27999 600 mg	-5.0±4.4	112±2
Aliskiren 300 mg	-4.8±4.1	100±5

VTP-27999 dose-dependently increased renin, and lowered PRA and Ang II at 5 hours after dosing (P<0.01 for all renin inhibitor groups versus placebo), without significantly affecting prorenin (Fig. 2A-D). The effects of aliskiren on RAS components again were best comparable to those of 150 mg VTP-27999.

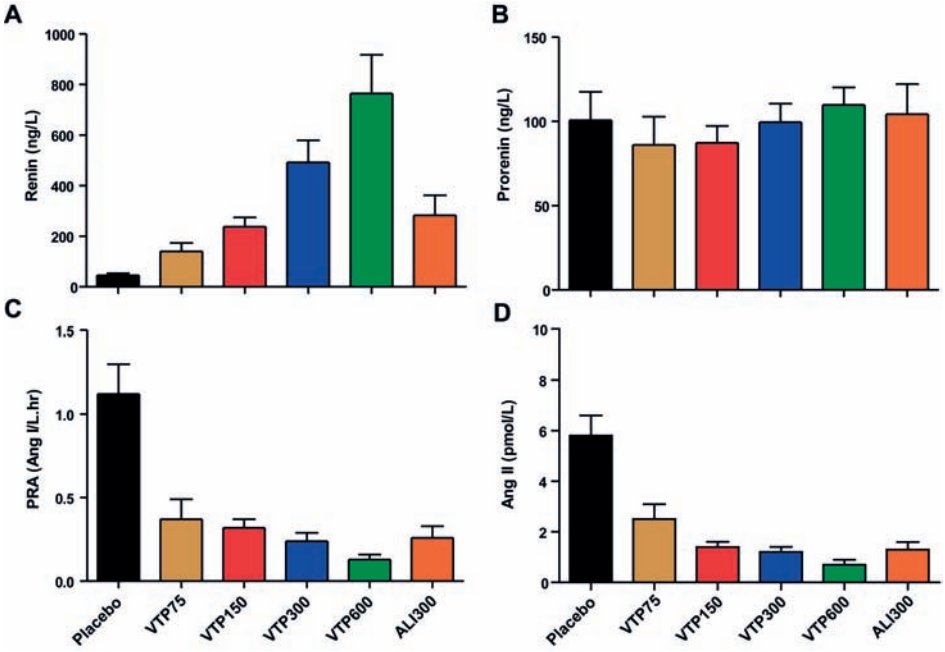

Figure 2. Plasma levels of renin (A) and prorenin (B), plasma renin activity (C) and the plasma level of angiotensin (Ang) II (D) in healthy, salt-depleted volunteers at 5 hours after oral intake of placebo, VTP-27999 (VTP; 75, 150, 300 or 600 mg) or 300 mg aliskiren (ALI). Data are mean±SEM of n=9-12. See text for statistical analysis.

Importantly, when determining RPF, renin, and Ang II at t=0 on each specific treatment day, it became clear that RPF and Ang II, but not renin, at 48 hours after the previous treatment day had returned to baseline (pre-treatment) levels. Baseline renin levels in group 1, receiving 75 mg VTP-27999, placebo and 300 mg aliskiren on Monday, Wednesday and Friday, respectively, were 27±5, 70±14 (P<0.05 versus Monday) and 57±13 pg/mL (P<0.05 versus Monday), while in group 2, receiving 150, 300 and 600 mg VTP-27999 on Monday, Wednesday and Friday, respectively, they were 31±3, 130±15 (P<0.01 versus Monday), and 238±28 pg/mL (P<0.01 versus Monday). For RPF, these values were 432±17, 442±16 and 442±26 versus 436±18, 448±19 and 456±23 mL/min.1.73 m^2, respectively, and for Ang II 7.6±1.1, 9.0±1.3 and 9.4±1.5 versus 8.9±0.8, 8.7±0.8 and 7.9±0.9 pmol/L, respectively. These data demonstrate that not all drug had been washed away at 48 hours, but that the original state of renal hemodynamics and RAS activity had been restored at that time point due to

the rise in renin. This observation has been made before[13], and is in full agreement with the fact that the half life of both aliskiren and VTP-27999 is ≈24 hours.[16]

DISCUSSION

This study revealed a maximum effect of oral renin inhibition on RPF and GFR, which was reached at VTP-27999 doses of 300 mg and higher, but not at an aliskiren dose of 300 mg. The maximum effect of VTP-27999 was roughly 30% higher than the effect of 300 mg aliskiren. This difference is close to the ≈20% larger effect observed with 600 mg aliskiren versus 300 mg aliskiren in our previous study.[13] Therefore, retrospectively, the effects of 600 mg aliskiren most likely did resemble the maximum effects that can be established with renin inhibition. Yet, such high aliskiren doses are not clinically recommended, and only now, with VTP-27999, could we establish that indeed larger RPF increases cannot be accomplished with renin inhibition.

In the current acute study we did not make a comparison with other RAS blockers. Selected comparisons have been made in the past, and, taken together, suggested that the maximum effects of renin inhibition with aliskiren are double those of captopril (25 mg), and 40% larger than those observed with the AT_1 receptor blockers eprosartan (600 mg), irbesartan (300 mg) and candesartan (16 mg).[12-15, 22] Yet, since none of these studies titrated the doses of all three types of RAS blockers up to a maximum effect in a parallel fashion, it is still likely that similar maximal renal effects can be achieved with all types of RAS blockade. Therefore, our data at most indicate that maximum renal effects of renin inhibition are reached at doses that are in or slightly above the normal clinical range, whereas for the other types of RAS blockers much higher doses are required to induce maximum renal effects.[1-3] A likely explanation of this observation is that renin inhibitors, and VTP-27999 in particular, more easily accumulate in the kidney.[23-26] Although it seems logical to attribute this to the fact that renin is abundantly present and stored in the kidney, studies in renin knockout animals showed that this accumulation is in fact unrelated to the presence of renin.[25] However, since accumulation was selective for the kidney, it must involve a kidney-specific uptake system, possibly the organic anion-transporting polypeptide 2B1 (OATP2B1).[27] Interestingly, due to its accumulation at renal tissue sites, the renin inhibitor can still be demonstrated in renal tissue several weeks after stopping treatment.[24, 28] Yet, as a consequence, particularly following treatment with very high doses of VTP-27999, renal RAS inhibition may exceed RAS inhibition in the circulation after stopping drug intake. This will paradoxically cause a rise in circulating Ang II and aldosterone, due to the fact that renal RAS inhibition continues to stimulate renin release, while after stopping drug intake the VTP-27999 levels in plasma are no longer sufficient to block this renin.[16]

In the present study, volunteers received placebo, aliskiren or VTP-27999 on 3 different treatment days with a 48-hour rest interval in between. Clearly, given the half life of aliskiren and VTP-27999 (≈24 hours for both)[16], not all drug will have been washed away on each subsequent treatment day. Indeed, renin levels were still elevated at 48 hours following a dose of either aliskiren or VTP-27999, like in our previous study.[13] Nevertheless, Ang II and RPF at that time had returned to pre-drug baseline values, suggesting that the renin rise was sufficient to overcome the blocking effects of any remaining renin inhibitor still being present. Importantly therefore, baseline hemodynamics and RAS activity were identical at each occasion. Moreover, changes in RPF and GFR have been expressed as a percentage of the baseline value on each respective study day, to correct for any carry-over effect.

RAS inhibitor-induced RPF changes reflect renal vascular function, and may thus serve as an indication of the efficacy on renal vasculature of these drugs. Obviously, the observed acute physiologic response is only a surrogate of the acute drug effect on the kidney that does not by definition indicate meaningful clinical responses in the real world in terms of the drug benefit, when the drug is given on a continuous basis. For instance, under the latter condition, multiple compensatory mechanisms may come into play, which may alter the net effect of renin inhibition. The most important of these is the rise in renin release. Nevertheless, given our current and earlier findings, it seems that maximum beneficial effects of RAS blockade in the kidney may be achieved more easily with a renin inhibitor (i.e., at relatively low doses) than with other types of RAS blockers. Importantly, to obtain beneficial effects, renin inhibitors should be dosed optimally rather than maximally.[29] The combination of a renin inhibitor with other RAS blockers might rapidly tip the balance (i.e., induce too much RAS blockade), as has become apparent in the ALTITUDE trial.[30] Other trials investigating dual or triple RAS blockade[31] also yielded the typical consequences of RAS annihilation: hypotension, renal dysfunction and hyperkalaemia.

Consequently, the optimal dose of VTP-27999 is not necessarily 600 mg, but rather 150-300 mg/day.[16] In the present study, the renal and hormonal effects of VTP-27999 at a dose of 150 mg most closely resembled those of 300 mg aliskiren. Neither of the two renin inhibitors affected prorenin, due to the fact that changes in prorenin require de novo synthesis, because prorenin, unlike renin, is not stored in the kidney. Only VTP-27999, at its highest dose, significantly increased GFR. Since changes in GFR, at least in healthy volunteers, directly correlate with changes in RPF[32], this simply reflects the larger effects of VTP-27999 on RPF. The mechanism underlying this phenomenon involves a change in intravascular oncotic pressure along the glomerular capillary, resulting in greater surface area available for filtration.[32] No significant effects on blood pressure were observed. This is most likely related to the fact that this is an acute study, evaluating a single dose only in a small number of healthy subjects. Similarly, in our previous study, evaluating different

aliskiren doses in healthy, salt-depleted volunteers, we also did not detect significant decreases in blood pressure.[13] Certainly, when dosing repetitively, blood pressure decreases are more likely to occur – particularly in patients with an activated RAS, since such activation will limit their compensatory capacity. Indeed, blood pressure responses to RAS blockers are generally the highest in patients with the highest degree of RAS activation.[33]

In conclusion, of all RAS blockers, renin inhibitors require relatively the lowest doses to inhibit renal RAS activity completely. This may relate to their capacity to selectively accumulate in the kidney. It may also reflect the fact that renin inhibition is the most efficient way to block the RAS, hampered the least by counteracting mechanisms (PRA rise, ACE upregulation) and/or the appearance of multiple angiotensin metabolites acting on non-AT_1 receptors.[34] On the one hand, this implies that maximal beneficial renal effects can be achieved easily with a single RAS blocker, i.e., a renin inhibitor, instead of combining 2 or more alternative RAS blockers at varying (and often high!) doses. However, selective renal accumulation also implies that the degree of renal RAS blockade may rapidly become too high. Therefore, studies are warranted to carefully determine the renin inhibitor dose required for optimal rather than maximal renal RAS blockade. Ultimately, the effects of these doses will need to be tested in large clinical trials specifically in patients with diabetes and nephropathy, where there is a large unmet need.

Unfortunately, an extensive preclinical comparison of the 3 types of RAS blockers is virtually impossible because (human) renin inhibitors are highly species-specific and do not act in rodents, except at high doses.[35] The only model that is available for this purpose is the so-called double transgenic rat, a hypertensive rat model expressing both human renin and human angiotensinogen.[36] Yet, whether this artificial model truly mimics all aspects of hypertension is questionable to date. Furthermore, animal models may also help to shed light on the contribution of the (pro)renin receptor, if at all, to the beneficial effects of RAS blockers. This receptor binds and activates prorenin at high concentrations *in vitro*.[37] However, recent studies questioned the physiological relevance of these findings, since in reality, prorenin concentrations are many orders of magnitude below the levels that are required to interact with this receptor, even during treatment with RAS blockers.[38] Indeed, the (pro)renin receptor has now also been linked to functions beyond the RAS.[39] To what degree its concentrations vary in relation with salt intake still needs to be investigated further.

Finally, an important aspect of future trials might be whether the effects of RAS blockade are sex-specific. Currently, there are no sex-specific recommendations for RAS blocker therapy, given the lack of strong evidence that men and women may respond differentially to RAS blockers.[40, 41] Animal studies do, however, support the existence of such differences.[42] Moreover, men display higher renin levels than women[43], and thus there is a reason to believe that men and women may respond differently, e.g., with regard to renal effects, when exposed to renin inhibitors.

DISCLOSURES

Drs. Barkoudah, Danser, Moukarbel and Hollenberg received research grant support from Vitae Pharmaceuticals, Inc.. Dr. Gregg is an employee of Vitae Pharmaceuticals. Collection, analysis, and presentation of data were performed by the scientific investigators at the Brigham and Women's Hospital, Harvard Catalyst/ the Harvard Clinical and Translational Science Center/ Harvard University and Erasmus Medical Center independently of the sponsor.

ACKNOWLEDGEMENT

The authors wish to thank the study volunteers and the staff at the GCRC at Brigham and Women's Hospital.

REFERENCES

1. Sarafidis PA, Ruilope LM. Aggressive blood pressure reduction and renin-angiotensin system blockade in chronic kidney disease: Time for re-evaluation? *Kidney Int*. 2014;85:536-546
2. Lambers Heerspink HJ, de Borst MH, Bakker SJ, Navis GJ. Improving the efficacy of raas blockade in patients with chronic kidney disease. *Nat Rev Nephrol*. 2013;9:112-121
3. Cerezo C, Ruilope LM, Segura J, Garcia-Donaire JA, de la Cruz JJ, Banegas JR, Waeber B, Rabelink TJ, Messerli FH. Microalbuminuria breakthrough under chronic renin-angiotensin-aldosterone system suppression. *J Hypertens*. 2012;30:204-209
4. Campbell DJ, Duncan AM, Kladis A. Angiotensin-converting enzyme inhibition modifies angiotensin but not kinin peptide levels in human atrial tissue. *Hypertension*. 1999;34:171-175
5. Campbell DJ, Kladis A, Duncan AM. Nephrectomy, converting enzyme inhibition, and angiotensin peptides. *Hypertension*. 1993;22:513-522
6. van Kats JP, Chai W, Duncker DJ, Schalekamp MADH, Danser AHJ. Adrenal angiotensin. Origin and site of generation. *Am J Hypertens*. 2005;18:1045-1051
7. van Kats JP, Danser AHJ, van Meegen JR, Sassen LM, Verdouw PD, Schalekamp MADH. Angiotensin production by the heart: A quantitative study in pigs with the use of radiolabeled angiotensin infusions. *Circulation*. 1998;98:73-81
8. van Kats JP, Schalekamp MADH, Verdouw PD, Duncker DJ, Danser AHJ. Intrarenal angiotensin ii: Interstitial and cellular levels and site of production. *Kidney Int*. 2001;60:2311-2317
9. Schalekamp MADH, Danser AHJ. Angiotensin ii production and distribution in the kidney: I. A kinetic model. *Kidney Int*. 2006;69:1543-1552
10. Nussberger J. Circulating versus tissue angiotensin ii, in: Angiotensin ii receptor antagonists, edited by epstein m, brunner hr, philadelphia, hanley & belfus, inc., pp. 69-78. 2000
11. Fraune C, Lange S, Krebs C, Holzel A, Baucke J, Divac N, Schwedhelm E, Streichert T, Velden J, Garrelds IM, Danser AHJ, Frenay AR, van Goor H, Jankowski V, Stahl R, Nguyen G, Wenzel

UO. At1 antagonism and renin inhibition in mice: Pivotal role of targeting angiotensin ii in chronic kidney disease. *Am J Physiol Renal Physiol*. 2012;303:F1037-F1048

12. Hollenberg NK, Fisher ND, Nussberger J, Moukarbel GV, Barkoudah E, Danser AHJ. Renal responses to three types of renin-angiotensin system blockers in patients with diabetes mellitus on a high-salt diet: A need for higher doses in diabetic patients? *J Hypertens*. 2011;29:2454-2461
13. Fisher NDL, Danser AHJ, Nussberger J, Dole WP, Hollenberg NK. Renal and hormonal responses to direct renin inhibition with aliskiren in healthy humans. *Circulation*. 2008;117:3199-3205
14. Lansang MC, Price DA, Laffel LM, Osei SY, Fisher NDL, Erani D, Hollenberg NK. Renal vascular responses to captopril and to candesartan in patients with type 1 diabetes mellitus. *Kidney Int*. 2001;59:1432-1438
15. Osei SY, Price DA, Laffel LM, Lansang MC, Hollenberg NK. Effect of angiotensin ii antagonist eprosartan on hyperglycemia-induced activation of intrarenal renin-angiotensin system in healthy humans. *Hypertension*. 2000;36:122-126
16. Balcarek J, Sevá Pessôa B, Bryson C, Azizi M, Ménard J, Garrelds IM, McGeehan G, Reeves RA, Griffith SG, Danser AHJ, Gregg R. Multiple ascending dose study with the new renin inhibitor vtp-27999: Nephrocentric consequences of too much renin inhibition. *Hypertension*. 2014;63:942-950
17. Jia L, Simpson RD, Yuan J, Xu Z, Zhao W, Cacatian S, Tice CM, Guo J, Ishchenko A, Singh SB, Wu Z, McKeever BM, Bukhtiyarov Y, Johnson JA, Doe CP, Harrison RK, McGeehan GM, Dillard LW, Baldwin JJ, Claremon DA. Discovery of vtp-27999, an alkyl amine renin inhibitor with potential for clinical utility. *ACS Med Chem Lett*. 2011;2:747-751
18. Krop M, Lu X, Verdonk K, Schalekamp MADH, van Gool JM, McKeever BM, Gregg R, Danser AHJ. New renin inhibitor vtp-27999 alters renin immunoreactivity and does not unfold prorenin. *Hypertension*. 2013;61:1075-1082
19. Fisher NDL, Allan D, Kifor I, Gaboury CL, Williams GH, Moore TJ, Hollenberg NK. Responses to converting enzyme and renin inhibition. Role of angiotensin ii in humans. *Hypertension*. 1994;23:44-51
20. Krop M, van Gool JM, Day D, Hollenberg NK, Danser AHJ. Evaluation of a direct prorenin assay making use of a monoclonal antibody directed against residues 32-39 of the prosegment. *J Hypertens*. 2011;29:2138-2146
21. Klotz S, Burkhoff D, Garrelds IM, Boomsma F, Danser AHJ. The impact of left ventricular assist device-induced left ventricular unloading on the myocardial renin-angiotensin-aldosterone system: Therapeutic consequences? *Eur Heart J*. 2009;30:805-812
22. Price DA, De'Oliveira JM, Fisher ND, Hollenberg NK. Renal hemodynamic response to an angiotensin ii antagonist, eprosartan, in healthy men. *Hypertension*. 1997;30:240-246
23. Lu X, Krop M, Batenburg WW, Musterd-Bhaggoe UM, Garrelds IM, Danser AH. Renin inhibitor vtp-27999 differs from aliskiren: Focus on their intracellular accumulation and the (pro) renin receptor. *J Hypertens*. 2014;32:1255-1263
24. Feldman DL, Jin L, Xuan H, Contrepas A, Zhou Y, Webb RL, Müller DN, Feldt S, Cumin F, Maniara W, Persohn E, Schuetz H, Danser AHJ, Nguyen G. Effects of aliskiren on blood pressure, albuminuria, and (pro)renin receptor expression in diabetic tg(mren-2)-27 rats. *Hypertension*. 2008;52:130-136
25. Lange S, Fraune C, Alenina N, Bader M, Danser AHJ, Frenay AR, van Goor H, Stahl R, Nguyen G, Schwedhelm E, Wenzel UO. Aliskiren accumulation in the kidney: No major role for binding to renin or prorenin. *J Hypertens*. 2013;31:713-719

26. Krop M, Garrelds IM, de Bruin RJA, van Gool JMG, Fisher NDL, Hollenberg NK, Danser AHJ. Aliskiren accumulates in renin secretory granules and binds plasma prorenin. *Hypertension*. 2008;52:1076-1083
27. Tapaninen T, Neuvonen PJ, Niemi M. Orange and apple juice greatly reduce the plasma concentrations of the oatp2b1 substrate aliskiren. *Br J Clin Pharmacol*. 2011;71:718-726
28. Feldman DL, Jin L, Xuan H, Persohn E, Zhou W, Schuetz H, Park JK, Müller DN, Luft FC. The direct renin inhibitor aliskiren localizes and persists in rat kidneys. *Am J Physiol Renal Physiol*. 2013;305:F1593-F1602
29. Nussberger J, Bohlender J. Pharmacotherapy: Optimal blockade of the renin-angiotensin-aldosterone system. *Nat Rev Cardiol*. 2013;10:183-184
30. Parving HH, Brenner BM, McMurray JJ, de Zeeuw D, Haffner SM, Solomon SD, Chaturvedi N, Persson F, Desai AS, Nicolaides M, Richard A, Xiang Z, Brunel P, Pfeffer MA, Investigators A. Cardiorenal end points in a trial of aliskiren for type 2 diabetes. *N Engl J Med*. 2012;367:2204-2213
31. Sakata Y, Shiba N, Takahashi J, Miyata S, Nochioka K, Miura M, Takada T, Saga C, Shinozaki T, Sugi M, Nakagawa M, Sekiguchi N, Komaru T, Kato A, Fukuchi M, Nozaki E, Hiramoto T, Inoue K, Goto T, Ohe M, Tamaki K, Ibayashi S, Ishide N, Maruyama Y, Tsuji I, Shimokawa H, on Behalf of the STI. Clinical impacts of additive use of olmesartan in hypertensive patients with chronic heart failure: The supplemental benefit of an angiotensin receptor blocker in hypertensive patients with stable heart failure using olmesartan (support) trial. *Eur Heart J*. 2015;36:915-923
32. Splenser AE, Fisher ND, Danser AHJ, Hollenberg NK. Renal plasma flow: Glomerular filtration rate relationships in man during direct renin inhibition with aliskiren. *J Am Soc Hypertens*. 2009;3:315-320
33. Schilders JE, Wu H, Boomsma F, van den Meiracker AH, Danser AHJ. Renin-angiotensin system phenotyping as a guidance toward personalized medicine for ace inhibitors: Can the response to ace inhibition be predicted on the basis of plasma renin or ace? *Cardiovasc Drugs Ther*. 2014;28:335-345
34. Danser AHJ. Novel drugs targeting hypertension: Renin inhibitors. *J Cardiovasc Pharmacol*. 2007;50:105-111
35. van Esch JHM, Moltzer E, van Veghel R, Garrelds IM, Leijten F, Bouhuizen AM, Danser AHJ. Beneficial cardiac effects of the renin inhibitor aliskiren in spontaneously hypertensive rats. *J Hypertens*. 2010;28:2145-2155
36. Pilz B, Shagdarsuren E, Wellner M, Fiebeler A, Dechend R, Gratze P, Meiners S, Feldman DL, Webb RL, Garrelds IM, Jan Danser AH, Luft FC, Muller DN. Aliskiren, a human renin inhibitor, ameliorates cardiac and renal damage in double-transgenic rats. *Hypertension*. 2005;46:569-576
37. Batenburg WW, Lu X, Leijten F, Maschke U, Müller DN, Danser AHJ. Renin- and prorenin-induced effects in rat vascular smooth muscle cells overexpressing the human (pro)renin receptor: Does (pro)renin-(pro)renin receptor interaction actually occur? *Hypertension*. 2011;58:1111-1119
38. Batenburg WW, Danser AHJ. (pro)renin and its receptors: Pathophysiological implications. *Clin Sci (Lond)*. 2012;123:121-133
39. Lu X, Meima ME, Nelson JK, Sorrentino V, Loregger A, Scheij S, Dekkers DH, Mulder MT, Demmers JA, Dallinga-Thie GM, Zelcer N, Danser AHJ. Identification of the (pro)renin receptor as a novel regulator of low-density lipoprotein metabolism. *Circ Res*. 2015;118:in press

40. te Riet L, van Esch JHM, Roks AJM, van den Meiracker AH, Danser AHJ. Hypertension: Renin-angiotensin-aldosterone system alterations. *Circulation Research*. 2015;116:960-975
41. Turnbull F, Woodward M, Neal B, Barzi F, Ninomiya T, Chalmers J, Perkovic V, Li N, MacMahon S, Blood Pressure Lowering Treatment Trialists C. Do men and women respond differently to blood pressure-lowering treatment? Results of prospectively designed overviews of randomized trials. *Eur Heart J*. 2008;29:2669-2680
42. Sevá Pessôa B, Slump DE, Ibrahimi K, Grefhorst A, van Veghel R, Garrelds IM, Roks AJM, Kushner SA, Danser AHJ, van Esch JHM. Angiotensin ii type 2 receptor- and acetylcholine-mediated relaxation: Essential contribution of female sex hormones and chromosomes. *Hypertension*. 2015;66:396-402
43. Danser AHJ, Derkx FHM, Schalekamp MADH, Hense HW, Riegger GAJ, Schunkert H. Determinants of interindividual variation of renin and prorenin concentrations: Evidence for a sexual dimorphism of (pro)renin levels in humans. *J Hypertens*. 1998;16:853-862

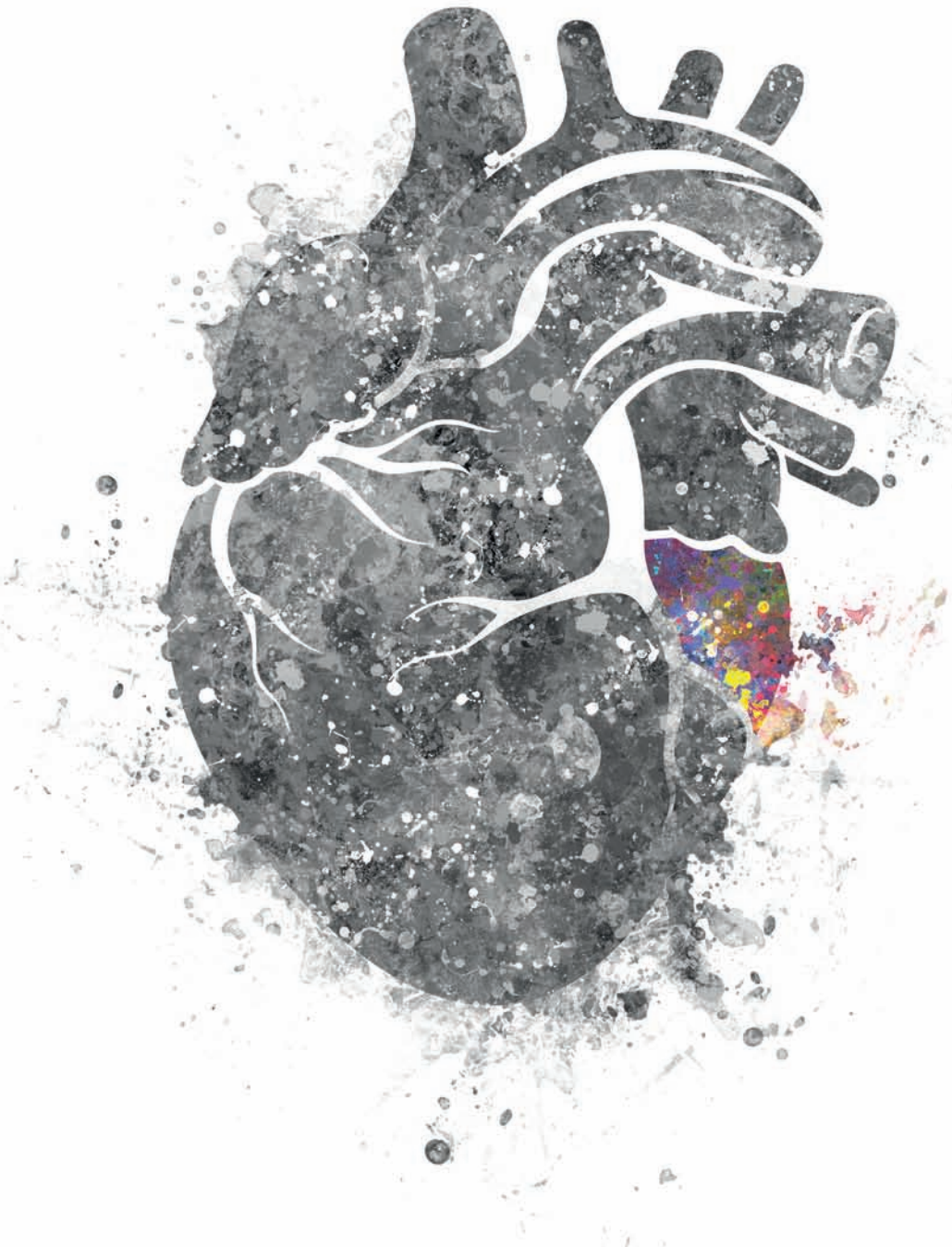

PART V

SUMMARY AND FUTURE PERSPECTIVES

SUMMARY AND PERSPECTIVES

Cardiovascular disease is an umbrella term for any type of disorder that affects the heart and/or circulation. Despite improvements in knowledge and treatment options over the last decades, it remains one of the leading causes of disability and death. The underlying mechanisms vary depending on the disease in question. Most often there is not one cause for cardiovascular disease, but instead several risk factors are involved that increase the risk of development and progression of disease. Some of these risk factors can be avoided, controlled, treated or modified such as high cholesterol, high blood pressure and obesity. While others, such as family history and gender, cannot be avoided and their emphasis lies on monitoring and treatment. In this thesis, different mouse models were used to examine the role of DNA damage, atherosclerosis and the renin angiotensin system (RAS) on cardiovascular disease development and progression. Moreover, the present studies explored the effect of nutritional and therapeutic interventions.

This chapter describes the main findings of this thesis and concludes each part with suggestions for future research.

Part I Introduction

Chapter 2 provides an overview of the general structure and cell biology of the vessel wall. The vessel wall consists of three different layers termed tunica intima, tunica media and tunica adventitia. The main components of these layers include endothelial cells, vascular smooth muscle cells, cytoskeleton proteins and extracellular matrix proteins. Interaction between the components of these different layers determines the biological and physical properties of the blood vessel. Changes and damage to these components and cellular constituents contribute to the pathogenesis and progression of several vascular diseases, as well as to ageing of the vasculature.

In **Chapter 3**, the role of the RAS in the pathogenesis of vascular disease is reviewed. Activity of the RAS affects factors that contribute to the development and progression of vascular disease; i.e. extracellular matrix defects, atherosclerosis and ageing. Oxidative stress seems to be related to all of these components, subsequently contributing to the onset of vascular disease. Though, the precise mechanisms by which these components induce vascular damage is not entirely clear. RAS inhibiting therapies seem to have beneficial effects in treating cardiovascular disease, however, they are not 100 percent effective in all patients and occasionally even give rise to adverse side effects, including hypotension and hyperkalemia. Yet, when an angiotensin receptor blockade is used simultaneous with a neprilysin inhibition ('ARNI'), a much stronger favorable effect was found when compared to angiotensin receptor blockade only, without any extra associated negative side effects.[1, 2] However, insight into the mechanism of action of ARNI is still needed. Thus,

future research should explore optimal strategies of (combined) RAS blockade to prevent or stop the progression of vascular disease. Moreover, it would be particularly interesting to test the efficacy of combined RAS/reactive oxygen species suppressing therapy in animal models of cardiovascular disease, as it might give further beneficial effects on the vasculature.

Part II Aortic aneurysms

In part II, the effect of two risk factors, atherosclerosis and increased RAS signaling, on the development and progression of aortic aneurysms was studied. In **Chapter 4**, the relation between atherosclerosis and aortic aneurysms formation was investigated. In order to get a more representative physiological situation as observed in humans, aneurysmal susceptible heterozygous Fibulin-4 deficient mice (Fibulin-$4^{+/R}$) were combined with the atherosclerotic ApoE knockout mouse model. Our study showed that subtle thoracic aortic wall defects, such as increased elastic fiber fragmentation, induce increased atherosclerotic plaques formation and changes in plaque composition, including decreased elastin content, in ApoE$^{-/-}$Fibulin-$4^{+/R}$ mice after 10 weeks of high fat diet. Moreover, ApoE$^{-/-}$Fibulin-$4^{+/R}$ mice already showed relatively small thoracic dilatations when exposed to 20 weeks of low-fat diet. Interestingly, between 20 and 30 weeks of age, some of these ApoE$^{-/-}$Fibulin-$4^{+/R}$ mice developed symptoms of paralysis and 30% did not survive. These results indicate that subtle thoracic aortic wall defects in association with atherosclerosis, predisposes for development of aortic dilatations and altered plaque morphology. Whole body angiographs might help to further study the cause of paralysis and death observed in the ApoE$^{-/-}$Fibulin-$4^{+/R}$ mice. This will be a challenge since their death is quite sudden and unpredictable. Moreover, preliminary mouse RNA sequencing data suggests a difference in expression of genes involved in mitochondrial dysfunction and the immune system between atherosclerosis and aneurysm formation. Human RNA expression analysis similarly showed differences in immune pathway regulation between abdominal aneurysms and aortic occlusion (AAA vs AOD). Therefore, further analysis of specific immune factors in plasma of both mouse and human might shed light on the observed differences. It is evident that external factors such as diet have an enormous influence on aortic dilatations, especially abdominal. With this ApoE$^{-/-}$Fibulin-$4^{+/R}$ mouse model, we can now study the effect of high- and normal fat diet in a controlled manner, and elucidate the mechanisms that play a role in abdominal aneurysm formation and progression next to genetic factors.

Chapter 5 evaluated whether treating Fibulin-$4^{R/R}$ mice with the angiotensin II type 1 (AT_1) receptor antagonist losartan outperforms the effect of the renin inhibitor aliskiren or the effect of the β-blocker propranolol on aneurysm progression. Although both types of RAS blockers (losartan and aliskiren) identically lowered hemodynamic stress, only losartan increased survival, reduced aneurysm size and improved aortic wall distensibility. Moreover, losartan increased ejection fraction, decreased left ventricular diameter and

reduced cardiac TGF-β signaling, while the other drugs did not have these effects. None of the drugs examined here affected aortic wall morphology. To explain the beneficial effect of losartan compared to aliskiren, we reasoned that losartan offers an additional advantage, possibly by simulation of angiotensin II (AT_2) type receptors and/or activation of the angiotensin-(1-7)/Mas receptor axis. It still remains unclear whether RAS inhibition is effective in the prevention or reduction of aortic root dilations.[3, 4] Most clinical studies have a heterogeneous patient population in which they do not make a distinction between different underlying mutations, which makes it more difficult to draw firm conclusions. In addition, these clinical studies all start at different ages with their treatment, e.g. children, adolescent, adults and elderly. The strength of our study is the fact that these mice have the same genetic mutation, are treated from the same starting point, and accurate monitoring of aneurysm progression is followed within the same animal over time. Moreover, in this present study mice were treated postnatally, when aneurysm formation has already started, which is more clinically relevant as treatment of aneurysmal patients usually starts in the presence of an aneurysm. Timing of treatment as well as the underlying mutation are of utmost importance, as they may explain the success, or lack thereof, of different RAS blockers in clinical trials.[4, 6] Thus, future research should follow the same patient and/or animal over time, and should make a distinction between the underlying mutations of disease causing genes.

Part III Cardiovascular aging

In part III, the effect of defective DNA repair and the consequential aging process on the development of cardiovascular damage was examined. Previous studies have shown that the well-established premature aging *Ercc1*$^{d/-}$ mouse model shows signs of accelerated age-dependent vasodilator dysfunction, accompanied by increased blood pressure, vascular stiffness and vascular senescence. In **Chapter 6**, it was examined whether this accelerated age-dependent vasodilator dysfunction could be prevented by either treating the mice with the chronic AT_1 receptor blocker losartan, a well-known antihypertensive drug, or exposing them to dietary restriction, known to induce an anti-aging response. This study shows that dietary restriction is a very efficient intervention to prevent vasodilator dysfunction caused by genomic instability. Improvement of prostaglandin-mediated endothelium-dependent signaling and better vascular smooth muscle cell responses to nitric oxide were identified as mechanisms. Conversely, endothelial dysfunction was not reversible with chronic losartan treatment. These results suggest that this aging mouse model appears to represent the RAS blockade-resistant part of aging-related vascular disease. Accordingly, future research should use progeroid mouse models to further explore the underlying mechanism leading to age-related vascular disease and test the efficacy of drugs targeting vascular disease in order to extrapolate the results to the elderly population. A possible explanation for the lack of effect of losartan might be that vascular dys-

function in *Ercc1*$^{d/-}$ mice is largely ROS-independent, while often part of the detrimental effects of Ang II involve ROS formation. Additionally, *Ercc1*$^{d/-}$ mice show an upregulation of anti-oxidant and detoxification defense genes as part of a so-called survival response that aims to extend their lifespan.[7, 8] Research efforts should therefore also continue to fully elucidate the role of ROS in age-related vascular dysfunction.

In **Chapter 7**, the effect of aging on the heart was characterized and the use of fluorescent molecular markers for the early detection of cardiovascular disease was tested. MicroCT imaging showed that premature aging *Ercc1*$^{d/-}$ mice at 24 weeks of age display changes in left ventricular geometry and functioning, e.g. increased ventricular volumes and reduced ejection fraction. Results were similar when compared to functional analysis by echocardiography. Moreover, specific loss of *Ercc1* in cardiomyocytes, comparably showed adverse cardiac remodeling and poor cardiac functioning, suggesting the direct involvement of *Ercc1* in the heart. Furthermore, the combination of microCT and optical imaging allowed simultaneous analysis of molecular and functional changes in these mouse models for accelerated aging. Our study showed that a temporal increase in matrix metalloprotease activity and apoptosis precede cardiac functional decline in progeroid *Ercc1* mice. It would be interesting to investigate whether the increase in matrix metalloprotease activity is derived from senescent cells. In addition, this study did not investigate the direct causal effect of DNA damage on the development of heart failure; therefore, future research should be aimed at elucidating this question, for examples by measuring DNA damage markers in the hearts of the *Ercc1* mice, as well as inducing DNA damage by radiation and examining the effect on cardiac function. Furthermore, extensive analysis of mutations in DNA damage and repair genes leading to cardiovascular diseases is needed to expand our comprehension on how DNA damaging factors increase the susceptibility to cardiovascular event.

Part IV The renin-angiotensin system

In part IV, the role of the RAS was investigated. In **Chapter 8**, the use of the NIRF probe ReninSense680™ was tested to study renin activity *in vivo* and characterize renin activity in progeroid *Ercc1*$^{\Delta/-}$ mice which have premature age-related kidney pathology due to a defective nucleotide excision repair gene. Our study confirmed that *Ercc1*$^{d/-}$ kidneys display severe tubular attenuation and degeneration with marked anisokaryosis, which was shown previously.[9-11] In addition, we demonstrated that non-invasive imaging, using the NIRF probe ReninSense680™, enables imaging of altered renin activity in the kidney over time. The increased intrarenal activity detected with the ReninSense680™ probe after losartan treatment, is in full agreement with the literature, and thus not only validates the specificity of this probe, but also supports its use for longitudinal imaging of altered RAS signaling in aging. Moreover, our observations in the premature aging *Ercc1*$^{d/-}$ mouse model provides evidence that intrarenal renin activity does not necessarily run in parallel

with circulating renin. This observation was also seen in animal models of early diabetic nephropathy and patients with diabetes mellitus.[12-16] Hence, it would be interesting to further explore the association between aging and diabetes mellitus on the development of renal injury as well as the implications for future therapies; should we aim at locally lowering the intrarenal RAS in these models? Moreover, in several of the diabetic animal studies it was suggested that altered renin release from the kidney, and not reduced production, is responsible for the low circulating renin levels (reviewed within Price et al.)[14]. Future research should investigate the release and production of renin and other RAS components in aging mouse models.

In **Chapter 9**, our study re-evaluated the occurrence of (pro)renin in the brain, as the concept of a brain RAS has been controversial and this controversy continues to this day. It was found that buffer perfusion reduced mouse brain renin by approximately 60% and although renin-dependent Ang I-generating activity (AGA) could be detected in virtually every region, plasma renin was 40-800x higher than brain renin. Furthermore, deoxycorticosterone acetate (DOCA) salt, like Ang II, reduced circulating renin, and, contrary to our expectations did not increase brain prorenin. In fact, both DOCA-salt and Ang II lowered brain renin in parallel with plasma renin. Aliskiren-inhibitable AGA was entirely absent in the brain of Ren1c$^{-/-}$ mice, supporting the validity of our brain renin measurement. Thus, our data do not support the presence of locally synthesized, kidney-independent renin in the brain and we conclude that brain renin must represent renin that is taken up from blood. Moreover, the absence of Ang I in brain tissue outside the blood compartment strongly suggests that there is no local Ang I generation in the brain, and it appears that brain Ang II therefore originates from the blood compartment. Thus, it would be interesting to explore how this Ang II enters the blood-brain barrier, for instance by binding to brain angiotensin type-receptors that are outside the blood-brain barrier or rather by entering at sites where the blood-brain barrier permeability is compromised. In addition, the ReninSense probe holds considerable promise to localize and detect renin activity in tissues, and future studies should address the possibilities of assessing renin activity in other tissues than the kidney.

In **Chapter 10**, the use of VTP-27999, a novel renin inhibitor -without major side-effects at high doses- was examined in order to establish the maximum effect of renin inhibition in the kidney. The effect of VTP-27999 was compared to the clinically used renin-inhibitor aliskiren in 22 healthy volunteers on a low-sodium diet. A maximum effect of renin inhibition on renal plasma flow (RPF) and glomerular filtration rate (GFR) was found at VTP-27999 doses of 300 mg and higher, while a maximum effect was not reached with aliskiren at a dose of 300 mg. The maximum effect of VTP-27999 was approximately 30% higher than the effect of aliskiren at the same dose. The maximum effect of VTP-27999 can most likely be reached with 600 mg of aliskiren, however such high doses of aliskiren are clinically not recommended because of its side effects. With this study,

we could establish that maximum RPF increases cannot be established with aliskiren at clinically relevant doses. As our study only included healthy patients, future research in patients with diabetes, hypertension and/or kidney disease is necessary to confirm these results, as the use of RAS blockers increases the risk of adverse events, including hyperkalemia, in this population. In addition, it would be interesting to test the effect of VTP-27999 in an aging mouse model, as they may have an altered RAS activity resulting in a different responsiveness. Moreover, in this study we did not compare males and females, thus further research should distinguish between males and females to determine whether or not the effect is similar in both genders.

REFERENCES

11. Tummala R, Bhadra R, Gupta A, Ghosh RK. Combined neprilysin and ras inhibition in cardiovascular diseases: A review of clinical studies. J Cardiovasc Pharmacol. 2016;68:183-190
12. Uijl E, Roksnoer LC, Hoorn EJ, Danser AH. From arb to arni in cardiovascular control. Curr Hypertens Rep. 2016;18:86
13. Brooke BS, Habashi JP, Judge DP, Patel N, Loeys B, Dietz HC, 3rd. Angiotensin ii blockade and aortic-root dilation in marfan's syndrome. N Engl J Med. 2008;358:2787-2795
14. Lacro RV, Dietz HC, Sleeper LA, Yetman AT, Bradley TJ, Colan SD, Pearson GD, Selamet Tierney ES, Levine JC, Atz AM, Benson DW, Braverman AC, Chen S, De Backer J, Gelb BD, Grossfeld PD, Klein GL, Lai WW, Liou A, Loeys BL, Markham LW, Olson AK, Paridon SM, Pemberton VL, Pierpont ME, Pyeritz RE, Radojewski E, Roman MJ, Sharkey AM, Stylianou MP, Wechsler SB, Young LT, Mahony L, Pediatric Heart Network I. Atenolol versus losartan in children and young adults with marfan's syndrome. N Engl J Med. 2014;371:2061-2071
15. Dietz HC. Potential phenotype-genotype correlation in marfan syndrome: When less is more? Circ Cardiovasc Genet. 2015;8:256-260
16. Groenink M, den Hartog AW, Franken R, Radonic T, de Waard V, Timmermans J, Scholte AJ, van den Berg MP, Spijkerboer AM, Marquering HA, Zwinderman AH, Mulder BJ. Losartan reduces aortic dilatation rate in adults with marfan syndrome: A randomized controlled trial. Eur Heart J. 2013;34:3491-3500
17. Niedernhofer LJ, Garinis GA, Raams A, Lalai AS, Robinson AR, Appeldoorn E, Odijk H, Oostendorp R, Ahmad A, van Leeuwen W, Theil AF, Vermeulen W, van der Horst GT, Meinecke P, Kleijer WJ, Vijg J, Jaspers NG, Hoeijmakers JH. A new progeroid syndrome reveals that genotoxic stress suppresses the somatotroph axis. Nature. 2006;444:1038-1043
18. Schumacher B, van der Pluijm I, Moorhouse MJ, Kosteas T, Robinson AR, Suh Y, Breit TM, van Steeg H, Niedernhofer LJ, van Ijcken W, Bartke A, Spindler SR, Hoeijmakers JH, van der Horst GT, Garinis GA. Delayed and accelerated aging share common longevity assurance mechanisms. PLoS Genet. 2008;4:e1000161
19. Dolle ME, Kuiper RV, Roodbergen M, Robinson J, de Vlugt S, Wijnhoven SW, Beems RB, de la Fonteyne L, de With P, van der Pluijm I, Niedernhofer LJ, Hasty P, Vijg J, Hoeijmakers JH, van Steeg H. Broad segmental progeroid changes in short-lived ercc1(-/delta7) mice. Pathobiol Aging Age Relat Dis. 2011;1

20. Schermer B, Bartels V, Frommolt P, Habermann B, Braun F, Schultze JL, Roodbergen M, Hoeijmakers JH, Schumacher B, Nurnberg P, Dolle ME, Benzing T, Muller RU, Kurschat CE. Transcriptional profiling reveals progeroid ercc1(-/delta) mice as a model system for glomerular aging. BMC Genomics. 2013;14:559
21. Vermeij WP, Dolle ME, Reiling E, Jaarsma D, Payan-Gomez C, Bombardieri CR, Wu H, Roks AJ, Botter SM, van der Eerden BC, Youssef SA, Kuiper RV, Nagarajah B, van Oostrom CT, Brandt RM, Barnhoorn S, Imholz S, Pennings JL, de Bruin A, Gyenis A, Pothof J, Vijg J, van Steeg H, Hoeijmakers JH. Restricted diet delays accelerated ageing and genomic stress in DNA-repair-deficient mice. Nature. 2016;537:427-431
22. Hollenberg NK, Fisher ND, Nussberger J, Moukarbel GV, Barkoudah E, Danser AH. Renal responses to three types of renin-angiotensin system blockers in patients with diabetes mellitus on a high-salt diet: A need for higher doses in diabetic patients? J Hypertens. 2011;29:2454-2461
23. Zimpelmann J, Kumar D, Levine DZ, Wehbi G, Imig JD, Navar LG, Burns KD. Early diabetes mellitus stimulates proximal tubule renin mrna expression in the rat. Kidney Int. 2000;58:2320-2330
24. Price DA, Porter LE, Gordon M, Fisher ND, De'Oliveira JM, Laffel LM, Passan DR, Williams GH, Hollenberg NK. The paradox of the low-renin state in diabetic nephropathy. J Am Soc Nephrol. 1999;10:2382-2391
25. Jaffa AA, Chai KX, Chao J, Chao L, Mayfield RK. Effects of diabetes and insulin on expression of kallikrein and renin genes in the kidney. Kidney Int. 1992;41:789-795
26. Correa-Rotter R, Hostetter TH, Rosenberg ME. Renin and angiotensinogen gene expression in experimental diabetes mellitus. Kidney Int. 1992;41:796-804

APPENDICES

NEDERLANDSE SAMENVATTING

Hart- en vaatziekten is een overkoepelende term voor elk type aandoening die het hart en/of de bloedsomloop beïnvloedt. Ondanks verbeteringen omtrent de kennis en behandel opties in de afgelopen decennia, blijft het een van de belangrijkste oorzaken van overlijden en invaliditeit. De mechanismen variëren naargelang de desbetreffende ziekte. Meestal is er niet één oorzaak voor de ziekte, maar zijn er verschillende risicofactoren betrokken die de kans op ontwikkeling en progressie van de ziekte verhogen. Een aantal van deze risicofactoren kunnen worden vermeden, gecontroleerd, behandeld of zelfs verandert zoals hoog cholesterol, hoge bloeddruk en obesitas. Terwijl anderen, zoals familiegeschiedenis en geslacht, niet vermeden kunnen worden en de nadruk ligt hier dan ook op de controle en behandeling. In dit proefschrift, hebben we aan de hand van verschillende muismodellen onderzocht wat de rol van DNA schade, aderverkalking (atherosclerose) en het renine-angiotensine systeem (RAS) is op de ontwikkeling en progressie van hart- en vaatziekten. Daarnaast hebben we het effect van voedings- en therapeutische interventies onderzocht.

Dit hoofdstuk beschrijft de belangrijkste bevindingen van dit proefschrift en concludeert elk deel met een aantal suggesties voor toekomstig onderzoek.

Deel I Introductie

Hoofdstuk 2 geeft een overzicht van de algemene structuur en celbiologie van de vaatwand. De vaatwand bestaat uit drie verschillende lagen genaamd: tunica intima, tunica media en tunica adventitia. De belangrijkste componenten van deze lagen zijn endotheelcellen, gladde spiercellen, eiwitten van het cytoskelet en extracellulaire matrix eiwitten. Interactie tussen de componenten van deze verschillende lagen bepaalt de biologische en fysische eigenschappen van het bloedvat. Veranderingen en beschadiging van deze onderdelen en cel bestanddelen draagt bij aan het ontstaan en de progressie van verschillende vaatziekten, evenals aan veroudering van het vaatstelsel.

In **hoofdstuk 3**, wordt de rol van het RAS in de pathogenese van vasculaire ziekte beoordeeld. Activiteit van het RAS beïnvloed factoren die bijdragen aan de ontwikkeling en progressie van vaatziekten; o.a. extracellulaire matrix defecten, atherosclerose en veroudering. Oxidatieve stress lijkt gerelateerd te zijn aan al deze onderdelen, en draagt daarmee bij aan het ontstaan van vaatziekten. Echter, de precieze mechanismen waarmee deze componenten bijdragen aan het induceren van vaatschade is niet geheel duidelijk. RAS-remmende therapieën lijken effectief bij het behandelen van hart- en vaatziekten, maar ze zijn niet 100 procent effectief bij alle patiënten en hebben soms zelfs nadelige neveneffecten zoals hypotensie en hyperkaliëmie (verhoogd kalium gehalte in plasma). Echter, wanneer een angiotensine receptor remmer gelijktijdig wordt gebruikt met neprilysine remming (zogenaamde 'ARNI '), heeft dit een veel sterker positief effect in vergeli-

jking met slechts angiotensine receptor remming, zonder extra bijbehorende negatieve effecten. Echter meer inzicht in het werkingsmechanisme van ARNI is nog steeds nodig. Daarom is het belangrijk dat toekomstig onderzoek zich richt op het vinden van optimale strategieën met betrekking tot (gecombineerde) RAS remming, om zo verdere progressie van vaatziekten te voorkomen of zelfs te stoppen. Bovendien is het heel interessant om de werkzaamheid van gecombineerde RAS/zuurstofradicalen onderdrukkende therapie te testen in diermodellen die leiden aan hart- en vaatziekten, omdat dit misschien additionele gunstige effecten heeft op de vaten.

Deel II Aorta aneurysmata

In deel II, wordt het effect van twee risicofactoren, zijnde atherosclerose en verhoogde RAS signalering, bestudeerd op de ontwikkeling en progressie van aorta aneurysmata. In **hoofdstuk 4** is de relatie tussen atherosclerose en aorta aneurysma vorming onderzocht. Om een representatieve fysiologische toestand te krijgen die wordt waargenomen bij mensen, werden aneurysma gevoelige heterozygote Fibuline-4 deficiënte (Fibuline-$4^{+/R}$) muizen gekruist met een muismodel voor atherosclerose; de ApoE knockout muis. Onze studie toonde aan dat een subtiele afwijkingen in de thoracale aorta wand, zoals verhoogde elastische vezels fragmentatie, een verhoogde vorming van atherosclerotische plaques veroorzaakt en veranderingen in plaque samenstelling teweeg brengt, inclusief verminderde elastine aanwezigheid, in ApoE$^{-/-}$Fibuline-$4^{+/R}$ muizen na 10 weken hoog vet dieet. Bovendien toonde de ApoE$^{-/-}$Fibuline-$4^{+/R}$ al relatief kleine thoracale verwijdingen van de aorta bij blootstelling aan een 20 weken vetarm dieet. Een interessante observatie is dat sommige van deze ApoE$^{-/-}$Fibuline-$4^{+/R}$ muizen tussen de 20 en 30 weken dieet, verlammingsverschijnselen ontwikkelden en zelfs 30% van de muizen vroegtijdig overlijden. Deze resultaten geven aan dat subtiele thoracale aorta wand afwijkingen in combinatie met atherosclerose, de mens vatbaar maken voor de ontwikkeling van aorta verwijdingen en veranderde plaque morfologie. Angiografie van het hele lichaam, zou kunnen helpen om de oorzaak van de verlamming en de waargenomen vroegtijdige dood in de ApoE$^{-/-}$Fibuline-$4^{+/R}$ muizen te achterhalen. Echter, dit zal een uitdaging zijn omdat hun dood heel plotseling en onvoorspelbaar is. Verder suggereert preliminaire muis RNA sequentie data dat er een verschil is in de expressie van genen betrokken bij mitochondriële dysfunctie en het immuunsysteem wanneer atherosclerose en aneurysmavorming worden vergeleken. Humane RNA-expressie analyse toonde vergelijkbare verschillen in immunologische regulering tussen abdominale aneurysmata en aorta occlusie (AAA vs AOD). Verdere analyse van specifieke immune factoren in plasma van zowel muis als mens zou meer kennis kunnen geven over de waargenomen verschillen. Het is duidelijk dat externe factoren zoals dieet een enorme invloed heeft op de aorta verwijdingen, in het bijzonder in de buik. Dit ApoE$^{-/-}$Fibuline-$4^{+/R}$ muismodel helpt ons enerzijds om het effect van hoog-vet en normaal dieet te bestuderen op een gecontroleerde manier, en anderzijds

bij het in beeld brengen van mechanismen, die naast de genetische factoren, een rol spelen in de vorming en progressie van abdominale aorta aneurysmata.

In **hoofdstuk 5** evalueerden we of het behandelen van Fibuline-$4^{R/R}$ muizen met de angiotensine I (AT_1) receptor antagonist losartan beter werkt in het tegengaan van aneurysma progressie dan de renine-inhibitor aliskiren of het effect van de β-blokker propranolol. Hoewel beide typen RAS blokkers (losartan en aliskiren) identiek de bloeddruk verlagen, zien we dat alleen losartan zorgde voor een betere overleving, verminderde aneurysma groei en een verbeterde aortawand flexibiliteit. Bovendien zorgde losartan behandeling voor een toegenomen ejectiefractie, een verkleining in linker ventrikel diameter en een verlaging in TGF-β signalering in het hart, terwijl de andere geneesmiddelen geen effect hadden. Geen van deze geneesmiddelen beïnvloed de aortawand morfologie. Om het gunstige effect van losartan ten opzichte van aliskiren te verklaren, redeneren wij dat losartan een extra voordeel biedt, mogelijk door stimulatie van de angiotensine II (AT_2) type receptoren en/of activering van de angiotensine-(1-7)/Mas receptor as. Het is nog onduidelijk of remming van het RAS effectief is in het voorkomen of verminderen van aortawortel verwijdingen. De meeste klinische studies hebben een heterogene patiëntenpopulatie waarin zij geen onderscheid maken tussen verschillende onderliggende mutaties, waardoor het moeilijker is om harde conclusies te trekken. Bovendien starten deze klinische studies vaak op verschillende leeftijden met de behandeling van patiënten, zoals kinderen, adolescenten, volwassenen en ouderen. De kracht van onze studie is dat deze muizen dezelfde genetische mutatie hebben, worden behandeld vanaf hetzelfde beginpunt en dat aneurysma progressie over tijd nauwkeurig wordt gevolgd in hetzelfde dier. Daarnaast hebben wij in onze studie de muizen postnataal behandeld, wanneer de vorming van het aneurysma al is ontstaan, zodat het meer klinisch relevant is omdat behandeling van aneurysma patiënten meestal begint als een aneurysma al aanwezig is. Juiste timing van de behandeling, evenals de onderliggende mutatie zijn van groot belang, omdat zij het succes kunnen verklaren, of het gebrek daaraan, van verschillende RAS-blokkers gebruikt in de klinische studies. Toekomstig onderzoek zou daarom dezelfde patiënt en/of dier moeten volgen over tijd, daarbij onderscheid makende tussen de onderliggende mutaties van genen die betrokken zijn bij ziekte.

Deel III Hart- en vaat veroudering

In deel III, onderzochten we het effect van defect DNA herstel en het daaruit voortvloeiende verouderingsproces op de ontwikkeling van cardiovasculaire schade. Eerdere studies hebben aangetoond dat het bekende muismodel voor vroegtijdige veroudering, het *Ercc1*$^{\Delta/-}$ muismodel, tekenen heeft van versnelde, leeftijdsafhankelijke vaatverwijdende dysfunctie, wat vergezeld wordt door verhoogde bloeddruk, vasculaire stijfheid en vasculaire veroudering. In **hoofdstuk 6** onderzochten we of deze versnelde, leeftijdsafhankelijke vaatverwijdende dysfunctie kan worden voorkomen door hetzij behandeling

van de muizen met chronische AT_1 receptor blokker losartan, (een bekende antihypertensivum) of behandeling met dieet restrictie (DR), bekend voor het induceren van een anti-veroudering response. Onze studie toont aan dat DR een zeer efficiënte interventie is tegen vaatverwijdende dysfunctie die veroorzaakt wordt door genomische instabiliteit. Verbetering van de prostaglandine gemedieerde endotheel-afhankelijke signalering en van vaat-gerelateerde spiercel reacties op NO werden geïdentificeerd als mechanismen. Endotheel dysfunctie was niet omkeerbaar met chronische losartan behandeling. Deze resultaten suggereren dat dit snel verouderende muismodel het RAS blokkade-bestendige gedeelte van leeftijdsgerelateerde vaatziekten vertegenwoordigd. Toekomstig onderzoek zou daarom zulke snel verouderende muismodellen moeten gebruiken om het onderliggende mechanisme dat leidt tot leeftijdgerelateerde vaatziekten verder te onderzoeken, evenals gebruiken bij het testen van de werkzaamheid van geneesmiddelen gericht tegen vaatziekte, zodat deze geëxtrapoleerd kunnen worden naar de oudere bevolking. Een mogelijke verklaring voor het gebrek aan effect van losartan is dat de vaatdysfunctie bij *Ercc1*$^{d/-}$ muizen grotendeels ROS onafhankelijk is, terwijl Ang II vaak ROS vorming als nadelige effect heeft. Bovendien vertonen deze *Ercc1*$^{d/-}$ muizen een opregulatie van antioxidant en detox verdedigingsgenen als onderdeel van een zogenaamde overlevingsreactie met als doel het verlengen van de levensduur. Toekomstig onderzoek zou de rol van ROS in leeftijdsgerelateerde vaatziekten moeten ophelderen.

In **hoofdstuk 7**, karakteriseerden we het effect van veroudering op het hart en testen we het gebruik van fluorescente moleculaire markers voor de vroege detectie van hart- en vaatziekte. Met het gebruik van microCT, vonden we dat vroegtijdige verouderende *Ercc1*$^{d/-}$ muizen van 24 weken oud een verandering in linker ventrikel (LV) geometrie en werking laten zien, zoals vergrootte ventriculaire volumes en een verminderde ejectiefractie. De resultaten waren vergelijkbaar met een functionele analyse door middel van echocardiografie. Daarnaast lieten we zien dat specifiek verlies van *Ercc1* in hartspiercellen, vergelijkbare remodellering van het hart vertoonde met een verslechterde hartfunctie, wat de directe betrokkenheid van *Ercc1* in het hart suggereert. Bovendien toonden we aan dat combinatie van microCT en optische beeldvorming gelijktijdige analyse van moleculaire en functionele veranderingen mogelijk maakt in muismodellen voor versnelde veroudering. Onze studie laat zien dat een tijdelijke verhoging van matrix metalloproteinase activiteit en apoptose gevolgd wordt door functionele achteruitgang van het hart in deze snel verouderende *Ercc1*$^{d/-}$ muizen. Het is interessant om te onderzoeken of deze verhoging van matrix metalloproteinase activiteit afkomstig is van senescent cellen. Daarnaast heeft deze studie niet het direct causale effect van DNA-schade op de ontwikkeling van hartfalen onderzocht; daarom zou toekomstig onderzoek gericht moeten zijn op het ophelderen van deze vraag, bijvoorbeeld door het meten van DNA-schade markers in het hart van de (cardiospecifieke) *Ercc1* muizen, evenals het induceren van DNA schade door straling

en het onderzoeken van het effect op de hartfunctie. Uitgebreide analyse van mutaties in DNA-schade en herstel genen die leiden tot hart- en vaatziekten is bovendien nodig om te begrijpen hoe DNA-beschadigende factoren de gevoeligheid op het ontstaan van cardiovasculaire gebeurtenissen vergroten.

Deel IV Het renine-angiotensine systeem

In deel IV, onderzochten we de rol van het RAS. In **hoofdstuk 8** evalueerden we het gebruik van de NIRF probe ReninSense680™ om *in vivo* renine activiteit te bestuderen en daarnaast onderzochten we de renine activiteit in muizen met een vroegtijdige, leeftijdsgebonden nier pathologie als gevolg van een defect in het nucleotide excisie herstel mechanisme (*Ercc1*$^{d/-}$ muizen). Als eerste hebben we bevestigd dat de nieren van de vroegtijdige verouderende *Ercc1*$^{d/-}$ muizen ernstige tubulaire degeneratie vertonen met uitgesproken anisokaryosis, zoals eerder werd aangetoond. Daarnaast lieten we zien dat niet-invasieve beeldvorming met behulp van de NIRF probe ReninSense680™, beeldvorming van veranderde renine activiteit in de nieren in de tijd mogelijk maakt. De verhoogde intrarenale activiteit gedetecteerd met de ReninSense680™ probe na losartan behandeling, is in volledige overeenstemming met de literatuur, en valideert niet alleen de specificiteit van deze probe maar ondersteunt ook het gebruik ervan voor longitudinale beeldvorming van veranderde RAS signalering tijdens veroudering. Bovendien toonden onze observaties in het vroegtijdig verouderende *Ercc1*$^{d/-}$ muismodel dat intrarenale renine activiteit niet noodzakelijkerwijs parallel loopt met het circulerende renine. Deze waarneming werd ook gedaan in diermodellen van vroege diabetische nefropathie en patiënten met diabetes mellitus. Het is dus interessant om het verband tussen veroudering en diabetes mellitus verder te onderzoeken met betrekking op de ontwikkeling van nierschade alswel de gevolgen voor de toekomstige therapieën; moeten we streven naar het lokaal verlagen van het intrarenale RAS in deze modellen? Bovendien werd er in een van de diabetische dierstudies gesuggereerd dat veranderde renine afgifte uit de nier verantwoordelijk is voor de lage circulerende renine niveaus, en niet de verminderde productie (besproken in Price et al., 1999). Toekomstig onderzoek zou dan ook de afgifte en de productie van renine en andere RAS componenten in verouderende muismodellen moeten onderzoeken.

Onze studie, in **hoofdstuk 9**, heronderzocht of (pro) renine zich in de hersenen bevindt, omdat het concept van een brein RAS altijd al controversieel is geweest en momenteel nog steeds heerst. Onze studie toonde aan dat buffer perfusie het muizen hersenrenine met ongeveer 60% verminderde en dat hoewel renine-afhankelijk gegenereerde-Ang I activiteit (AGA) in vrijwel alle regio's kon worden gedetecteerd, plasma renine altijd nog 40-800 keer hoger was dan hersen-renine. Verder, zagen wij dat deoxycorticosteronacetaat (DOCA) zout, zoals Ang II, circulerende renine verminderde, en, in tegenstelling tot onze verwachtingen niet leidde tot verhoging van hersen-prorenine. In feite, zowel DOCA-zout en Ang II verlaagde hersen-renine parallel aan plasma-renine. Aliskiren-geremde AGA was

geheel afwezig in de hersenen van Ren1c$^{-/-}$ muizen, wat de validiteit van onze hersen-renine meting ondersteunt. Onze data biedt dus geen ondersteuning aan het concept van lokaal gesynthetiseerd, nier-onafhankelijke renine aanwezigheid in de hersenen, en we concluderen dan ook dat hersen-renine, eigenlijk renine vertegenwoordigd dat wordt opgenomen uit het bloed. Bovendien suggereert het ontbreken van Ang I in hersenweefsel buiten het bloedcompartiment, dat er geen lokale Ang I productie is in de hersenen, en het lijkt er dus op dat hersen-Ang II afkomstig is van het bloedcompartiment. Het is interessant om te onderzoeken hoe deze Ang II de bloed-hersenbarrière passeert, bijvoorbeeld door binding aan de hersen-angiotensine type-receptoren buiten de bloed-hersenbarrière of door het binnentreden van de hersenen op plaatsen waar de bloed-hersenbarrière permeabiliteit is aangetast. De ReninSense probe biedt daarnaast de mogelijkheid renine activiteit in weefsels te lokaliseren en detecteren, en toekomstige studies zouden de mogelijkheid moeten onderzoeken of renine-activiteit kan worden beoordeelt in andere weefsels dan de nieren.

In **hoofdstuk 10** werd het gebruik van VTP-27999, een nieuwe renine-remmer (zonder belangrijke bijwerkingen bij hoge doses) onderzocht bij de vaststelling van het maximale effect van renine-remming in de nier. Het effect van VTP-27999 werd vergeleken met de veelgebruikte renine-inhibitor aliskiren in 22 gezonde vrijwilligers op een zoutarm dieet. Een maximaal effect van renine remming op de renale plasmastroom (RPF) en de glomerulaire filtratiesnelheid (GFR) werd gevonden bij VTP-27999 doses van 300 mg en hoger, terwijl dit maximale effect niet bereikt werd met aliskiren in een dosis van 300 mg. Het maximale effect van VTP-27999 was ongeveer 30% groter dan het effect van aliskiren bij dezelfde dosis. Het maximale effect zoals gezien bij VTP-27999 kan waarschijnlijk worden bereikt met 600 mg aliskiren, echter zijn zulke hoge doses aliskiren klinisch niet aanbevolen vanwege de bijwerkingen. Met deze studie, konden we vaststellen dat de maximale RPF verhogingen niet kan worden vastgesteld met klinisch relevante doseringen van aliskiren. Aangezien onze studie alleen uit gezonde patiënten bestaat, is het noodzakelijk dat deze resultaten worden bevestigd in patiënten met diabetes, hoge bloeddruk en/of nierfalen omdat het gebruik van RAS blokkers de kans op bijwerkingen in deze populatie verhoogt, waaronder hyperkaliëmie. Bovendien zou het interessant zijn om het effect van VTP-27999 te testen in een snel verouderend muismodel, aangezien deze muizen mogelijk een veranderde RAS activiteit hebben die resulteert in een andere respons. Ook hebben we in deze studie geen onderscheid gemaakt tussen mannen en vrouwen, en zou verder onderzoek dit onderscheid wel moeten maken om te bepalen of het effect vergelijkbaar is in beide geslachten.

CURRICULUM VITAE

Personal details

Full Name:	Bibi Sherise van Thiel
Date of birth:	September 21th 1986
Place of birth:	Rotterdam, The Netherlands
Nationality:	Dutch

Research experience

2012 - 2017	PhD Student Erasmus Medical Centre – Rotterdam, The Netherlands Department of Vascular Surgery, Molecular Genetics, and Internal Medicine, division of Pharmacology and Vascular Medicine 'Multimodality ImAging of Cardiovascular Dysfunction; risk factors, diagnostics and treatment options'
2011	Major Research Internship Erasmus Medical Centre – Rotterdam, The Netherlands Thoraxcenter, Department of Biomedical Engineering 'In vivo imaging of plaque composition and vulnerability in an atherosclerotic mouse model'
2010	Minor Research Internship VU medical centre Amsterdam – Amsterdam, The Netherlands ICaR-VU, Department of Physiology and Lung disease 'Right ventricular hypoxia is related to ^{18}FAZA uptake and HIF-1α staining in pulmonary hypertensive hearts'
2008 - 2009	Bachelor internship VU medical center Amsterdam – Amsterdam, The Netherlands Cancer Center Amsterdam (CCA), Department of Pathology, Epstein-Barr Virus Group 'Development of a physiological co-culture system to study internalization of secreted exosomes by recipient cells in real-time'

Education

2012-2017	Doctor of Philosophy (PhD), Cardiovascular Research School (COEUR) Doctor of Philosophy (PhD), Medical-Genetics Centre (MGC) Erasmus Medical Centre Rotterdam
2009-2012	MSc Top Master Cardiovascular Research VU Medical Centre Amsterdam, Amsterdam, The Netherlands
2006-2010	BSc Biomedical Sciences Vrije Universiteit van Amsterdam, Amsterdam, The Netherlands

LIST OF PUBLICATIONS

- **van Thiel BS**, Ridwan Y, Garrelds IM, Vermeij M, Clahsen-van Groningen MC, Quadri F, Alenina N, Bader M, Danser AHJ, Essers J, van der Pluijm I. *In vivo* renin activity imaging in the kidney of progeroid *Ercc1* mutant mice. *In preparation.*
- **van Thiel BS**, Ridwan Y, de Boer M, de Kleijnen MGJ, van Vliet N, van Heijningen PM, Vermeij WP, Danser AHJ, Kanaar R, Duncker DJ, van der Pluijm I, Essers J. Hybrid Optical and CT Imaging reveals increased matrix metalloprotease activity and apoptosis preceding cardiac failure in progeroid *Ercc1* mice. *In preparation.*
- **van Thiel BS***, Ramnath NWM[*], Van der Heiden K[*], Speelman L, Ridwan Y, Heijningen PM, Vermeij M, Rouwet EV, Kanaar R, van der Pluijm I, Essers J. Fibulin-4 Deficiency induces Thoracic and Abdominal Aortic Wall Dilation and Altered Plaque Morphology in Apolipoprotein E Deficient Mice. [*] Equal contributors. *In preparation.*
- **van Thiel BS***, Wu H*, Bautista Niño P, Reiling E, Durik M, Leijten FPJ, Ridwan Y, Brandt RMC, van Steeg H, Dollé MET, Vermeij WP, Hoeijmakers JH, Essers J, van der Pluijm I, Danser AHJ, Roks AJM. Dietary restriction but not angiotensin II type 1 receptor blockade improves DNA damage-related vasodilator dysfunction.* Equal contributors. *Submitted.*
- **van Thiel BS**, Martini AG, te Riet L, Severs D, Uijl E, Garrelds IM, Leijten FPJ, van der Pluijm I, Essers J, Qadri F, Alenina N, Bader M, Paulis L, Rajkovicova R, Domenig O, Poglitsch M, Danser AHJ. Brain renin-angiotensin system: does it exist? *Hypertension* 2017 Jun;69:1136-1144.
- te Riet L, van Deel ED, **van Thiel BS**, Moltzer E, van Vliet N, Ridwan Y, van Veghel R, van Heijningen PM, Robertus JL, Garrelds IM, Vermeij M, Ingrid van der Pluijm I, Danser AHJ., Essers J. AT1-receptor blockade, but not renin inhibition, reduces aneurysm growth and cardiac failure in fibulin-4 mice. *J Hypertens*. 2016 Apr;34(4):654-65.
- Barkoudah E, **van Thiel BS**, Fisher NDL, Gregg RA, Danser AHJ, Moukarbel GV, Hollenberg NK. Maximum renal responses to renin inhibition in healthy subjects: VTP-27999 versus aliskiren. *J Hypertens.* 2016 May;34(5):935-41.
- **van Thiel BS**, van der Pluijm I, te Riet L, Essers J, Danser AHJ. The renin-angiotensin system and its involvement in vascular disease. *Eur J Pharmacol.* 2015 Sep 15;763(Pt A):3-14.
- **van Thiel BS**, van der Pluijm I, Kanaar R, Danser AHJ, Essers J. (2017) ESC Textbook of Vascular Biology. Oxford. Oxford University Press.
  Chapter 1: Structure and cell biology of the vascular wall.

Publications on other topics

- van der Pluijm I, van Vliet N, von der Thusen JH, Robertus JL, Ridwan Y, van Heijningen PM, **van Thiel BS**, Vermeij M, Hoeks SE, Buijs-Offerman RM, Verhagen HJ, Kanaar R,

Bertoli-Avella AM, Essers J. Defective Connective Tissue Remodeling in Smad3 Mice Leads to Accelerated Aneurysmal Growth Through Disturbed Downstream TGF-β Signaling. *EBioMedicine*. 2016 Sep 10. pii: S2352-3964(16)30413-3.

- Ramnath NW, van de Luijtgaarden KM, van der Pluijm I, van Nimwegen M, van Heijningen PM, Swagemakers SM, **van Thiel BS**, Ridwan RY, van Vliet N, Vermeij M, Hawinkels LJ, de Munck A, Dzyubachyk O, Meijering E, van der Spek P, Rottier R, Yanagisawa H, Hendriks RW, Kanaar R, Rouwet EV, Kleinjan A, Essers J. Extracellular matrix defects in aneurysmal Fibulin-4 mice predispose to lung emphysema. *PLoS One*. 2014 Sep 25;9(9):e106054.
- Winkel LCJ, Groen HC, **van Thiel BS**, Muller C, van der Steen AFW, Wentzel JJ, de Jong M, Van der Heiden K. Folate receptor-targeted SPECT/CT to detect activated macrophages in atherosclerosis; can it distinguish vulnerable from stable atherosclerotic plaques? *Mol Imaging*. 2014;13.

PHD PORTFOLIO

Summary of PhD training and teaching

Name PhD Student:	Bibi S. van Thiel
Erasmus MC Department:	Vascular surgery Molecular Genetics, Internal medicine, division of Pharmacology and Vascular Medicine
Research School:	Cardiovascular Research School (COEUR) and Medical Genetics Center (MGC)
Promotor:	Prof.dr. R. Kanaar and Prof.dr. A.H.J. Danser
Copromotor:	Dr. J. Essers and Dr. I. van der Pluijm
PhD period:	2012-2017

1. PhD training

General academic skills (2.5 ECTS)	Year
• Safe Laboratory Techniques – MGC	2012
• Technology Facilities-Imaging – Boerhaave CME (LUMC)	2013

In-depth courses (17.5 ECTS)	Year
• Cell and Developmental Biology – MGC	2012
• Genetics – MGC	2012
• Biochemistry and Biophysics – MGC	2012
• Vascular Biology – Dutch Heart Foundation (DHF)	2012
• Vascular Clinical Epidemiology – Coeur	2012
• Cardiovascular Pharmacology – Coeur	2013
• Translational Imaging Workshop by AMIE:	2013

From mouse to man – MolMed	
• CPO, Patient Orientated Research – Erasmus MC	2015
• Basiscursus Regelgeving en Organisatie voor Klinisch Onderzoekers (BROK) – Erasmus MC	2015

Research Seminars and lectures (3.5 ECTS)	Year
Various – COEUR, MGC and Biomedical Science cluster	2012-2017

Symposia and conferences (22 ECTS)	Year
Oral Presentations	
• Coeur PhD Day NAI, Rotterdam, the Netherlands	2013
• Wetenschapsdag Vascular Surgery, Rotterdam, the Netherlands	2014
• Wetenschapsdagen Internal Medicine, Antwerp, Belgium	2015
• ESH 25th European Meeting – Hypertension and Cardiovascular Protection, Milan, Italy	2015
• FIGON Dutch medicines days 2015, Ede, The Netherlands	2015
• North American Vascular Biology Organization (NAVBO) – Vascular Biology 2015; Hyannis, Massachusetts, USA	2015
• DNA Repair Group Meeting, Rotterdam, The Netherlands	2015
• Coeur PhD Day NAI, Rotterdam, The Netherlands	2016
• Sector meetings, work discussions and journal clubs	2012-2017
Poster Presentations	
• 7th European Society of Molecular Imaging Winter Conference TOPIM – Imaging the hallmarks of cancer, Les Houches, France	2013
• Wetenschapsdagen Internal Medicine, Antwerp, Belgium	2013
• 20th MGC PhD Workshop, Luxembourg, Luxembourg	2013
• Wetenschapsdagen Internal Medicine, Antwerp, Belgium	2014
• NVF Spring Meeting – (Epi)Genetics in Pharmacology, Nijmegen, The Netherlands	2015
• Gordon research conference and seminar – Angiotensin (2 posters) Lucca (Barga), Italy	2016
Attendance	
• Coeur PhD Day NAI, Rotterdam, The Netherlands	2012
• 19th MGC PhD Workshop, Dusseldorf, Germany	2012
• 22nd, 23rd and 24th MGC Symposium, Leiden/Rotterdam, The Netherlands	2012-2014
• Perkin Elmer Preclinical Imaging User Group Meeting	2014
Grants & prices	
• 3RD prize PhD student competition, FIGON Dutch Medicines Days	2015
• Accommodation grant, 25th ESH meeting	2015
• Trustfonds Travel grant, NAVBO meeting	2015
• Travel award, NAVBO meeting	2015
• Poster prize, Gordon research conference	2016

2. Teaching activities

Teaching (0.5 ECTS)	Year
Bsc Nanobiology - PCR practicum	2013
MSc Molecular Medicine -	2014
Keuze onderwijs: 'Ever thought of doing research?'	

Supervision students (0.5 ECTS)	Year
Partial supervision of master student	2013
Partial supervision of bachelor student	2013-2014

Total 2012-2017 (46.5 ECTS)

ACKNOWLEDGEMENT (DANKWOORD)

Het is zover, mijn proefschrift is klaar!
Met het schrijven van dit dankwoord sluit ik een hele belangrijke fase in mijn leven af. In deze periode heb ik veel geleerd, niet alleen op onderzoeksgebied maar ook op persoonlijk vlak. Graag wil ik een ieder (en dit is in geheel willekeurige volgorde) bedanken die heeft bijgedragen aan deze mooie, inspirerende maar toch zeker ook pittige periode.

Allereerst mijn copromotor, Dr. Jeroen Essers. Beste Jeroen, bedankt voor jouw vertrouwen in mij en de kans die je mij geboden hebt om deel uit te mogen maken van de Fibuline-4 groep. Jouw enthousiasme, kennis en altijd aanwezige optimisme waren voor mij van grote waarde. Mijn promotietraject ging gepaard met enkele hobbels, ik wil je graag bedanken voor alle steun en motivatie die je mij geboden hebt tijdens deze periode. Jouw supervisie en sturing hebben mij geholpen dit proefschrift te maken tot wat het nu is.

Dr. Ingrid van de Pluijm, beste Ingrid, bedankt voor jouw intensieve en onmisbare begeleiding, motivatie en wijsheden. Wanneer ik de kritische kant soms iets teveel toeliet, bleef jij optimistisch, dank voor alle suggesties en inzet bij het samenstellen van de artikelen! Daarnaast wil ik je graag ook nog even bedanken voor jouw onmisbare input in de hoeveelheid vrouwvriendelijke figuren in dit boekje en mocht zich de gelegenheid ooit eens voordoen, dan ben ik graag een keer je tegenstander met sumo worstelen.

Mijn promotoren, prof. dr. Jan Danser en prof. dr. Roland Kanaar. Graag wil ik jullie bedanken voor de fijne begeleiding en discussie in de afgelopen jaren. Bedankt dat jullie beide, ondanks jullie drukke tijdschema, eigenlijk altijd binnen een dag, soms zelfs enkele uren, mijn manuscripten hebben voorzien van commentaar. Beste Jan, jij hebt altijd oog voor zowel de grote lijnen als de details. Bedankt voor je kritische kijk op mijn artikelen, dit heeft mij zeker geholpen de resultaten beter te begrijpen en onder woorden te brengen. Beste Roland, bedankt voor het vertrouwen en de prettige samenwerking. Jouw input tijdens de werkbesprekingen en bij het nakijken van mijn manuscripten zorgde ervoor dat het niveau stukken hoger werd en de relevantie significant duidelijker. Ik wil jullie beiden bedanken dat deur altijd open stond.

Graag bedank ik ook de leden van de grote en kleine commissie: prof.dr. Verhagen, prof.dr. Duncker prof.dr. Schalkwijk, prof.dr. Hoeijmakers, prof.dr. Roos-Hesselink en Dr. Merkus, voor het kritisch beoordelen van mijn proefschrift en hun bereidheid zitting te nemen in mijn promotiecommissie.

Plezier hebben in je werk is niet alleen afhankelijk van de werkzaamheden op het lab maar wordt zeker ook bepaald door de sfeer op de afdeling. Lieve collega's, dank voor de leuke tijd op het lab, de vele gezellige borrels en wetenschappelijke discussies.

Beste Fibuline-4 groep, bedankt voor al jullie hulp op het lab, achter de barriere en in het Amie! Ik heb altijd veel gehad aan jullie input tijdens de werkdiscussies en heb vooral ook veel lol met jullie gehad tijdens het werk en daarbuiten. Nicole, als ik ooit nog eens hulp nodig heb bij het verzinnen van Sinterklaas rijmpjes, pas dan maar op, dan kom ik je namelijk stalken. Natuurlijk zorg ik dan voor de chocolade! Joyce, ik vind het ongelofelijk fijn hoe wij samen kunnen sparren over werk maar ook prive dingen. Heel veel succes met je promotieonderzoek! En ik wil jullie toch nog even meegeven dat als er ooit nog een (amateurs)inzending nodig is voor het songfestival, dan geef ik ons op! Paula, ladiesrun, ikea tripjes, hardlopen in het Kralingse bos, lachen, huilen, noem maar op. Bedankt dat ik zowel plezier als leed met je kan delen, snel maar weer eens een bakkie doen! Nathalie, ik wil je heel veel succes wensen met je PhD, laat je niet gek maken! Luuk en Natasja, jullie zijn al even weg, maar ik waardeer jullie hulp tijdens mijn projecten en daarna ook bij het zoeken van een nieuwe baan. Ik wens jullie veel succes en geluk in jullie verdere carriere. Yanto, jij komt verderop nog aan bod.

Lieve Nathalie en Kishan, bedankt voor alle goede gesprekken en de mogelijkheid die jullie mij gaven om mijn blijheden maar zeker ook frustraties eruit te gooien. Beide heel veel succes met jullie verdere carriere en ik hopelijk komen we elkaar nog weer eens tegen!

All other (former) colleagues from the Molecular Genetics department: Inger, Cecile, Nicole, Anja, Hanny, Titia, Whenhao, Julie, Charlie, Alex, Claire, Joao, Dejan, Gosia, Maarten, Arshdeep, Marcel, Koos, Dik, Joyce L, Laura, Giorgia en Natasa. I really enjoyed the cocktail parties, poker parties, karaoke nights and all other borrels. Ook lab 734-738 met name Sander, Renata, Wilbert, Yvette, Yvonne en Peter, bedankt. Bedankt voor alle hulp, de gezellige tijd in het kleine muizenlabje en de borrels op vrijdag(avond).

Daarnaast wil ik graag mijn collega's en oud-collega's van de Farmacologie afdeling bedanken. Beste Richard, Ingrid, Jeanette, Usha, Frank, Birgitte, Antoinette, Ton, Lodi, Madhi, Arthur, Katie, Khatera, Kristian, Alejandro, Eliana, Eric (Xifeng), Bruno, Koen, Joep, Wendy, Kayi, Matej, Charles, Sieneke, Edith, Alexandre, Haiyan en Paula, bedankt voor de aangename samenwerking, gezellige congressen, heerlijke sushi avonden, borrels en praatjes. Anton, bedankt voor fijne en leerzame samenwerking. David, Estrellita, Langeza en Dominique, bedankt voor de plezierige samenwerking, de etentjes en ontzettend gezellige uitgaans/dansavonden.

Natuurlijk gaat mijn dank ook uit naar alle co-auteurs. Mede door jullie bijdrage en fijne samenwerking zijn er mooie publicaties tot stand gekomen. Lieve Biomedical Engineering

groep (Kim, Lambert, Kim(metje), Jolanda, Frank, Ali, Jelle, Ruoyu, Merih, Marianna, Leah, en Bahar) bedankt voor de leerzame en fijne stage maar ook de overige gezellige lunch en koffie momentjes tijdens de afgelopen 6 jaar. Ook de samenwerking met de cardiologie afdeling, Martine en Marion, stel ik zeer op prijs. Bedankt voor de samenwerking, ik denk dat met trots kunnen zeggen dat er straks mooie publicaties uit voort zullen komen.

Lieve Paranimfen, ik voel mij gesterkt wetende dat jullie tijdens mijn verdediging naast mij staan!

Stephanie, vanaf het begin wist ik eigenlijk meteen al dat ik jou als paranimf wilde vragen, no questions asked. Je was niet alleen mijn collega bij de farmacologie, maar ik ben heel blij jou al ruim 11 jaar als vriendin te mogen hebben. Bedankt dat je mij altijd hebt bijgestaan en gesteund, ook op momenten waarbij ik zelf te eigenwijs was en dacht dat ik geen hulp nodig had, stond je voor mij klaar. Ik heb je de afgelopen maanden veel te weinig gezien, dus ik vind dat we samen snel maar eens die vaak besproken citytrip moeten gaan boeken. We gaan zeker nog veel mooie momenten samen meemaken.

Yanto, toen ik als PhD student meteen onder jouw vleugels werd meegenomen in de wereld van het imaging, heb ik eerst even moeten wennen aan je ochtenritueel tijdens onze vooral vroege maar ook lange imaging dagen (lees: eindeloze stiltes met ontelbaar veel koppen koffie, en zo hier en dan een winegum om je blij te maken). Maar meteen merkte ik al dat jouw soort humor en kijk op het leven niet alleen zorgde voor een ontspannen werksfeer, maar jou tot een waardevolle vriend voor het leven maakt. Bedankt voor jouw enorme inzet tijdens de afgelopen jaren, dit boekje was er zonder jou daadwerkelijk niet geweest. Snel weer een keertje aan de mezcal!

Lieve familie Commijs, Karin, Ronald, Laura, Ferdi en natuurlijk Erwin & Roef. Bedankt voor alle liefde, betrokkenheid, geduld en steun tijdens een belangrijk deel van mijn leven. Ook de andere leden van de familie Commijs, Beuker en Stoffer, hartelijk dank voor de gezellige momenten.

Lieve familie, ouders, broertjes, opa en oma's. Alhoewel het voor jullie niet altijd duidelijk was wat mijn onderzoek allemaal inhield en er tijdens deze drukke periodes vaak wat minder contact was, hadden jullie altijd interesse in mijn werk en boden jullie een luisterend oor voor mijn verhalen. Ik weet niet of ik altijd goed heb kunnen uitleggen waar ik eigenlijk mee bezig was, maar dit is in ieder geval het eindresultaat. En tijdens de afgelopen jaren heb ik leren waarderen dat jullie trots op mij zijn. Familie Roobol, veel dank voor de steun en tips tijdens de laatste fase van mijn proefschrift.

Lieve Stefan, heel veel dank voor je liefde, vertrouwen, steun maar zo nu en dan ook die schop onder mijn achterwerk! Onze reis is eigenlijk nog maar net begonnen maar ik kan niet wachten om met jou, en Ony, nieuwe avonturen tegemoet te gaan. Ik zie u graag!
Heel belangrijk in mijn leven zijn mijn ontzettend leuke en lieve vrienden. Vrienden die gedurende de jaren steeds maar weer enthousiast bleven vragen naar de vorderingen van mijn proefschrift. Mijn lieve RSG granny's, OBL vrienden, VU consortium met aanhang, Power Girls, Rotterdamse all together groep en alle kleine donderstenen, ik durf niemand bij naam te noemen, veel te bang dat ik iemand vergeet (en het zijn er gewoonweg teveel). Bedankt voor alle mooie tripjes, reizen, borrels, filmavonden, theetjes, dansjes, bootcamp en yoga lessen, slap geouwehoer, biernees, shop uitjes, sushi avonden en alle andere plezierigheden. De afgelopen tijd heb ik het ontzettend druk gehad en hebben we elkaar niet zo veel gezien, daarom hoop ik vanaf nu weer volop met jullie te genieten van alle leuke en mooie dingen die het leven te bieden heeft.

Ook wil ik een ieder bedanken die ik eventueel vergeten ben. Zoals velen voor mij al schreven; een proefschrift schrijven doe je niet alleen, wat ik zeker kan beamen. Tot slot:

'I'm glad that I did it, certainly because it was well worth it, but chiefly because I shall never have to do it again.'

(adapted from Mark Twain)

Multimodality ImAging of Cardiovascular Dysfunction

Risk factors, diagnostics and treatment options

Cardiovascular diseases are a major cause of mortality worldwide, and includes all diseases of the heart and circulation. Despite improvements in knowledge and treatment options over the last decades, it remains one of the leading causes of disability and death. The underlying mechanisms vary depending on the disease in question. Some of these risk factors can be avoided, controlled, treated or modified such as high cholesterol, high blood pressure and obesity. While others, such as family history and gender, cannot be avoided and their emphasis lies on monitoring and treatment. In this thesis, the role of DNA damage, atherosclerosis and the renin angiotensin system, factors that modulate cardiovascular damage and disease, are investigated and discussed. Additionally, the effect of nutritional and therapeutic interventions is explored.